Holocene tsunami events in the Eastern Ionian Sea – Geoscientific evidence from Cefalonia and the western Peloponnese (Greece)

Dissertation
zur Erlangung des Grades
„Doktor
der Naturwissenschaften“
im Promotionsfach Geographie

am Fachbereich Chemie, Pharmazie und Geowissenschaften
der Johannes Gutenberg-Universität
in Mainz

Timo Willershäuser
geb. in Marburg

Mainz, 2014

Berichterstatter:
1. Gutachter:
2. Gutachter:
Tag der mündlichen Prüfung: 07.02.2014

Summary

This study presents geo-scientific evidence for Holocene tsunami impact along the shores of the Eastern Ionian Sea. Cefalonia Island, the Gulf of Kyparissia and the Gialova Lagoon were subject of detailed geo-scientific investigations. It is well known that the coasts of the eastern Mediterranean were hit by the destructive influence of tsunamis in the past. The seismically highly active Hellenic Trench is considered as the most significant tsunami source in the Eastern Ionian Sea. This study focuses on the reconstruction and detection of sedimentary signatures of palaeotsunami events and their influence on the Holocene palaeogeographical evolution. The results of fine grained near coast geo-archives are discussed and interpreted in detail to differentiate between tsunami, storm and sea level highstands as sedimentation processes.

A multi-method approach was applied using geomorphological, sedimentological, geochemical, geophysical and microfaunal analyses to detect Holocene tsunamigenic impact. Chronological data were based on radiocarbondatings and archaeological age estimations to reconstruct local geo-chronostratigraphies and to correlate them on supra-regional scales.

Distinct sedimentary signatures of 5 generations of tsunami impact were found along the coasts of Cefalonia in the Livadi coastal plain. The results show that the overall coastal evolution was influenced by tsunamigenic impact that occured around 5700 cal BC (I), 4250 cal BC (II), at the beginning of the 2nd millennium cal BC (III), in the 1st millennium cal BC (IV) and posterior to 780 cal AD (V). Sea level reconstructions and the palaeogeographical evolution show that the local Holocene sea level has never been higher than at present.

At the former Mouria Lagoon along the Gulf of Kyparissia almost four allochtonous layers of tsunamigenic origin were identified. The stratigraphical record and palaeogeographical reconstructions show that major environmental coastal changes were linked to these extreme events. At the southern end of the Agoulenitsa Lagoon at modern Kato Samikon high-energy traces were found more than 2 km inland and upt ot 9 m above present sea level. The geo-chronological framework deciphered tsunami landfall for the 5th millennium cal BC (I), mid to late 2nd mill. BC (II), Roman times (1st cent. BC to early 4th cent. AD) (III) and most possible one of the historically well-known 365 AD or 521/551 AD tsunamis (IV).

Coarse-grained allochthonous sediments of marine origin were found intersecting muddy deposits of the quisecent sediments of the Gialova Lagoon on the southwestern Peloponnese. Radiocarbondatings suggest 6 generations of major tsunami impact. Tsunami generations were dated to around 3300 cal BC (I), around the end of 4th and the beginning of 3rd millennium BC (II), after around 1100 cal BC (III), after the 4th to 2nd cent. BC (IV), between the 8th and early 15th cent. AD (V) and between the mid 14th to beginning of 15th cent. AD (VI). Palaeogeographical and morphological characteristics in the environs of the Gialova Lagoon were controlled by high-energy influence.

Sedimentary findings in all study areas are in good accordance to traces of tsunami events found all over the Ionian Sea. The correlation of geo-chronological data fits very well to coastal Akarnania, the western Peloponnese and finding along the coasts of southern Italy and the Aegean. Supra-regional influence of tsunamigenic impact significant for the investigated sites. The palaeogeographical evolution and palaeo-geomorphological setting of the each study area was strongly affected by tsunamigenic impact.

The selected geo-archives represent extraordinary sediment traps for the reconstruction of Holocene coastal evolution. Our result therefore give new insight to the exceptional high tsunami risk in the eastern Mediterranean and emphasize the underestimation of the overall tsunami hazard.

Table of Contents

List of Figures

List of Tables

1 Introduction

1.1 Coastal changes, vulnerability and tsunami risk in the Mediterranean

Coasts underwent large environmental changes in the last millennia (Bird 2005). The late Pleistocene and the early- to mid-Holocene are characterized by an extensive global eustatic sea level rise and coastal regions were subjected to a major trangression (e.g. Fairbanks 1989). Since the mid-Holocene, a significant decline of the sea level rise marks a reversal in global coastal evolution. Terrestrial morphodynamics were able to progradate into the littoral system which results in the geomorphologic formation of fluvial deltas, coastal lowlands and various coastal accretions. From a geomorphological point of view, the recent coastlines are relatively young structures which are still under control of long-term and short-term coastal changes. Sediment supply, short- and long-term sea level fluctuations and tectonic mechanisms are the major control factors of coastal changes (e.g. Woodroffe 2003, Bird 2008, Kelletat 2013).

Coasts all over the world are exposed to high vulnerabilities and hazards (e.g Scheffers & Kelletat 2003, Gornitz 2005, Nicholls & Hoozemanns 2005, Satake & Atwater 2007, Schielein 2007, Okal 2011). The effects of marine and coastal processes on human population were demonstrated by extreme events such as the Indian Ocean Tsunami 2004 (e.g. Jankaew et al. 2008, Goto et al. 2007, 2010a), the Chilean Tsunami 2010 (e.g. Bahlburg & Spiske 2012) and the Tohoku-oki Tsunami of Japan 2011 (e.g. Goto et al. 2011) or Hurricane Ivan 2004 & Hurricane Kathrina 2005 at the Caribbean (e.g. Wang et al. 2005, Horton et al. 2009). The devasting influence of tsunami hazard in the last decade initiated an imposing change in public awareness and scientific research on coastal hazards and coastal changes (Goff et al. 2012).

The devasting influence of tsunami hazard in the last decade initiated an imposing change in worldwide public awareness and scientific research on coastal hazards and coastal changes (e.g. Dawson 1996, Dawson & Shi 2000, Gelfenbaum & Jaffe 2003, Scheffers & Kelletat 2003, Switzer et al. 2005, Kelletat et al. 2007, Shiki et al. 2008, Richmond et al. 2011, Goff et al. 2012). The Mediterranean Sea has also been subject of intensive geo-scientific research mainly focusing on coastal environmental changes and sea level evolution (e.g. Jahns 1993, 2005, Perrisoratis & Conispoliatis 2003, Kraft et al. 2005, Vött 2007, Brückner et al. 2010, Avramidis et al. 2013) or palaeogeographies (e.g. Raphael 1973, Kraft et al. 1975, 1977, 1980, 1985, Zangger et al. 1997, Vött et al. 2006a, 2006b, 2006c, 2007b, 2007c, Engel et al. 2009) but also palaeo-tsunami research (e.g. Tinti 1991, Guidoboni & Comastri 1997, Hindson & Andrade 1999, Altinok et al. 2001, Kortekaas 2002, Koretkaas & Dawson 2007, Shaw et al. 2008, Barbano et al. 2010).

In Greece, the eastern Ionian Sea, coastal Akarnania and the western- and southern Peloponnese were under detailed investigation by Vött et al. (2006a, 2006b, 2006c, 2006d, 2007a, 2007b, 2007c, 2008, 2009a, 2009b, 2010, 2011a, 2011b, 2013). All these studies show that the coastal geomorphology underwent widespread palaeogeographical changes during the Holocene. The long term gradual coastal evolution revealed several anomalies in the stratigraphical records which were related to the influence of extreme wave events from the

sea side. According to Vött et al. (2006d, 2007a, 2008, 2009a, 2009b, 2010, 2011a,2011b, 2013), May et al. (2007, 2012) and Scheffers et al. (2007), a great number of these short time interferences in the coastal evolution are related to strong tsunamigenic impact. Within the course of these studies, investigations have been carried out along the coasts of the eastern Ionian Sea to add valuable geo-scientific information on palaeo coastal research.

The need of geo-scientific research on palaeo-tsunami events is not negligible (e.g. Bryant 2008, Keating et al. 2008). A widespread understanding about the past tsunami hazards is necessary to provide a reliable risk assessment and protection on a local and regional scales (e.g. Satake & Atwater 2007, Mamo et al. 2009). Information of magnitude and frequency of tsunamis are necessary for an effective hazard assessment (e.g. Tappin 2007, Ebeling et al. 2012). Combining palaeo-tsunami research and the analysis of historical accounts, near-coast geological archives deliver an excellent potential to reconstruct a geo-chronological view of tsunami impact. Coastal lowlands, river deltas and coastal swamps represent sediment archives providing excellent resolution in time and space (e.g. Vött 2007, 2009b). Palaeo-event research is fundamental to understand the event related palaeo-shoreline evolution, the coastal responses of tsunami or storm impact and the influence on coastal morphodynamics (e.g. Goff et al. 2001, 2009, Morton et al. 2007, 2008, Shiki et al. 2008).

1.2 Study area

The study areas considered within the present work comprise the Ionian Island Cefalonia, the coastal lowlands along the Gulf of Kyparissia near Aghios Ioannis and Kato Samiko and the Gialova Lagoon at the southwestern Peloponnese (Fig.1-1). The primary aims of this geo-scientific study were to gain valuable information on Holocene coastal changes and palaeogeographical evolution along the shores of the eastern Ionian Sea and to geo-scientifically fill in gaps of the geochronological record established by palaeo-event research in the Mediterranean so far. In the following, the respective areas are presented in respect of their geographical and tectonic situation which is mainly responsible for triggering extreme wave events and the preservation of stratigraphical information on extreme events in the geological record.

1.2.1 Tectonic setting of the study areas

The eastern Ionian Sea is one of the seismotectonically most active regions in the Mediterranean (e.g. Pirazzoli et al. 1996, Shaw & Jackson 2010). The coasts of the study areas (Fig. 1-1) are directly exposed to the Hellenic Arc, the main collision zone between the African plate and the Aegean microplate. The highly active tectonic zone is characterized by complex crustal motion, deformation and high seismicity (e.g. Koukouvelas et al. 1996, Clement et al. 2000, Lagios et al. 2007, Hollenstein et al. 2008). Cefalonia Island is directly exposed to the Cefalonia Transform Fault (CTF) to the west and the extension of the North Anatolian Fault (NAF) system to the north (Fig. 1-1). The right-lateral strike slip CTF links the zone of prevailing subduction in the south to a continental collision in the north (e.g. Louvari et al. 1999, Sachpazi et al. 2000, Kokinou et al. 2006). The rates of crustal motion at the CTF (~ 5 mm/a) are comparatively low in comparison to those found offshore the Peloponnese and Crete (up to ~ 40 mm/a, e.g. Kahle et al. 2000, Hollenstein et al. 2006).

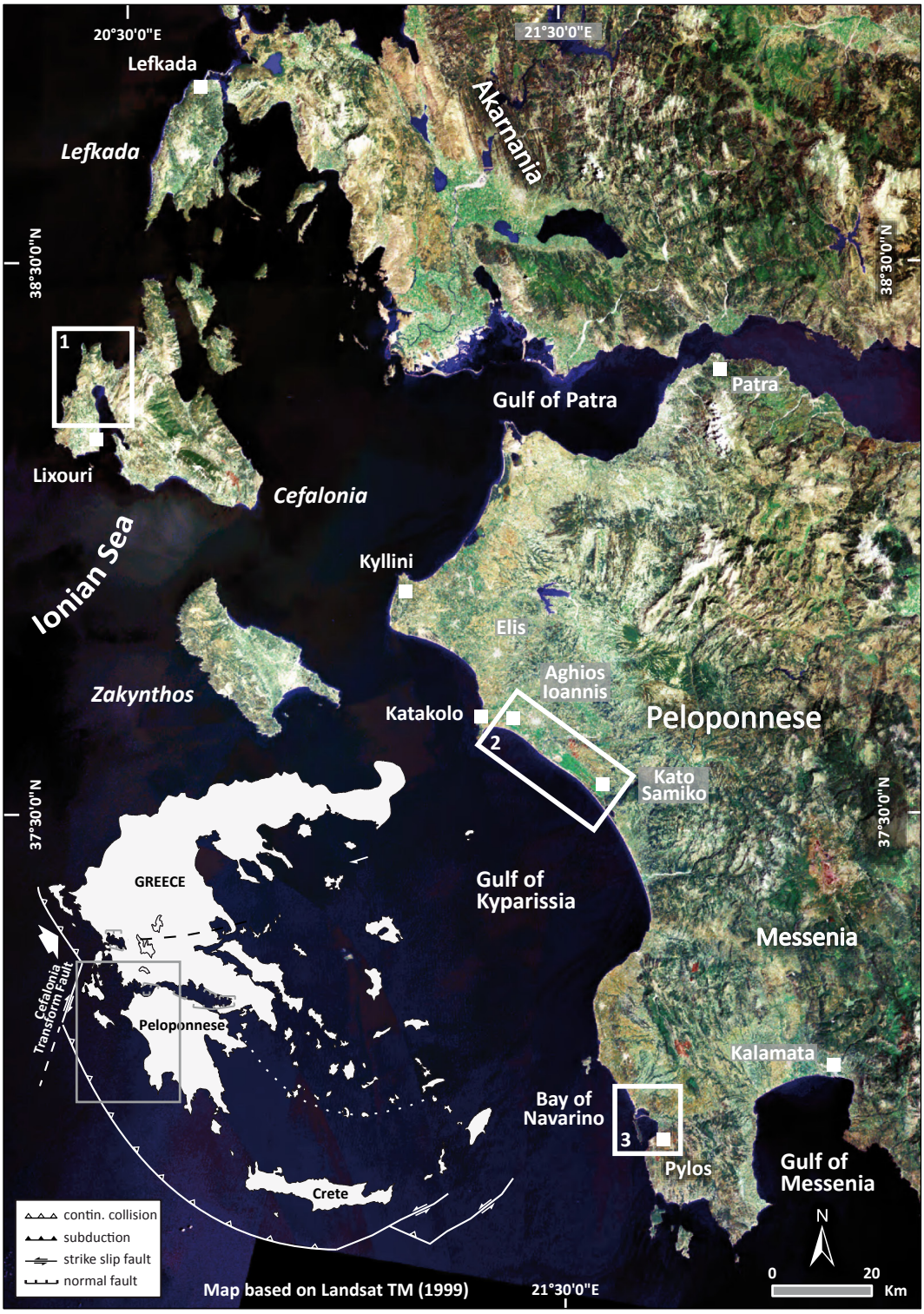

Fig. 1-1: Topographic and geo-tectonic overview of the Eastern Ionian Sea with study sites at the Peloponnese and Cefalonia Island. Study area are marked by a white box - 1. Cefalonia Island, 2 - Gulf of Kyparissia, 3 Gialova Lagoon. Simplified tectonic inlay map is modified after: Clews et al. (1989), Sachpazi et al. (2000) and van Hindsbergen et al. (2006), topographic overview based on Landsat TM 5 true composite satellite image (1999).

The fact that the study areas are subject to a high tsunami risk has been known for many decades (e.g. Cocard et al. 1999). Earthquakes (e.g. Stiros et al. 1994, 2010) and partly even volcanism and submarine mass movements (Tinti et al. 2005) along the subduction zone of the Hellenic Trench are the main factors for triggering tsunamis along the coasts of the Peloponnese and the eastern Ionian Islands (e.g. Papazachos & Dimitriu 1991, Koukouvelas et al. 1996, Benetatos et al. 2004)

1.2.2 Geographical context

From a topographical point of view the areas under investigation comprise the Lixouri coastal lowlands and the northern Golf of Argostoli on Cefalonia Island, the former Mouria Lagoon along the coastal lowlands at the shores of the Gulf of Kyparissia as well as the alluvial plain of Kato Samiko and the Gialova Lagoon near the Bay of Navarino at the southwestern Peloponnese (Fig. 1-1).

The Livadi coastal plain and the Lixouri coastal lowlands on Cefalonia Island are located in the northernmost part of the adjacent Gulf of Argostoli (Figs. 2-2). The recent environment of the Livadi coastal plain is characterized by a back beach swamp separated from the Argostoli Gulf by a beach barrier. On the contrary, the Lixouri coastal lowlands consist of alluvial fan deposits and beach ridges. The energetic environment along in the inner Argostoli Gulf is significantly weak and the sediment transport is low compared to the coastal sections in the south and in the west of the island which are directly exposed to the open Ionian Sea.

The study areas along the Gulf of Kyparissia comprise the former Mouria Lagoon near Aghios Ioannis and the coastal plain of modern Samiko at the southern fringe of the former Agoulenitsa Lagoon (Fig. 1-1). The present day geomorphological setting of the Mouria Lagoon can be described as a low-lying coastal plain, intensely used for agricultural purposes, while the recent coastline is dominated by the occurrence of barrier accretions, barrier accretion plains, coastal dune fields and swamps. The study sites near Aghios Ioannis are located behind the recent coastal barrier accretions, on recent dune fields and the lower elevated plain of the former Lagoon (Fig. 3-1, 3-2). Kato Samiko, lies adjacent to the southwestern fringe of the former Agoulenitsa Lagoon, which spans the coastal area between ancient Samiko to the south and the mouth of the Alpheios River to the north. Like the Mouria Lagoon, it has been drained in the 1960s. The study site at Kato Samiko is located in a small valley opening towards the southeastern fringe of the former Agoulenitsa lagoonal environment (Fig. 3-9). Towards the south, the Lapithas mountain range, a cretaceous outcrop of massive limestone on top of which the ancient city of Samikon is located, dominates the local topography (Koukouvelas et al. 1996).

The Gialova Lagoon, located at the southwestern Peloponnese near the modern Pylos, is part of the northern fringe of the Navarino Bay, a tectonic depression (IGME 1980a). The shallow lagoon is separated from the Bay of Navarino by a beach barrier system to the south and the semi-circular Bay of Voidokilia to the west. Three bedrock outcrops (Fig. 4-2) out of Eocene-Paleocene limestone build a sharp boundary to the Ionian Sea. The semi-circular Bay of Voidokillia is encircled to the south and the north by the limestone ridges. The Gialova Lagoon embayment is the youngest geological unit in the study area, mainly out of Holocene

alluvial sediments and lagoonal and limnic muds (e.g. IGME 1980a, Kraft et al. 1980, Zangger et al. 1997).

The presented study sites have in common that (i) the geo-archives of shallow lagoonal systems and alluvial fans seem to be excellent sediment traps for the reconstruction of coastal palaeogeographies and the influence of extreme wave events on the coastal evolution. (ii) All study sites are exposed to seismically highly active zones and therefore hold a high potential in terms of tsunami risk. (iii) The influence of extreme storm influence is negligible because of the sheltered geomorphological situations. (iv) All investigated sedimentary environments are characterized by quiescent conditions and provide termporally consistent sediment archives for the Holocene.

The selected geo-archives can be seen as representative sediment traps for the reconstruction of palaeo-event research, palaeo-sea level reconstructions and palaeogeographical evolution at the shores of the eastern Ionian Sea.

1.3 Aims of the study

For the coasts of the eastern Ionian Sea an extraordinary high seismicity is evident (see 1.2.1). For the study areas along the western Peloponnese and Cefalonia, sedimentary imprints of tsunamigenic impact in near-coast geo-archives must be assumed and have been already documented by investigations in the eastern Mediterranean (Fig. 1-2). Tsunami impact thus must be recorded in the sedimentary record. This dissertation therefore focuses on the sedimentary imprint of tsunamis in the geological record.

The main objectives for this dissertation are:

(i) the reconstruction of Holocene coastal palaeogeographies along the coasts of the western Peloponnese and Cefalonia Island,

(ii) the detection of event related sedimentary units in the stratigraphical record,

(iii) to decipher the hydromorphic processes which induced the event deposits, namely, distinguishing between tsunami and storm deposits,

(iv) to establish a geochronology of tsunami generations in local and supra-regional scales for the eastern Ionian Sea,

(v) to find out potential relationships between the selected study areas and looking forward for their sedimentary similarities and differences in terms of palaeogeographies and tsunami deposits,

(vi) deciphering of the influence of high-energy impact at the local- and regional coastal evolution in general and in specific cases,

(vii) to detect relative sea level fluctuations and potential tectonic movement against the palaeogeographical context.

In summary, this study focuses on Holocene coastal changes and the influence of extreme wave events on the coastal evolution. Moreover, this study delivers new insights into geo-

scientific findings along the coast of the eastern Ionian Sea and may enhance the data pool of palaeo-tsunami deposits as well as potential risk assessment for specific regions. Bringing together the results of Cefalonia Island, the Gulf of Kyparissia and the Gialova Lagoon is a first step for the understanding of supra-regional palaeogeographies and event related coastal changes as well as the detection of similarities and differences in Holocene coastal evolution.

1.4 The Eastern Ionian Sea Tsunami project - Study outline and hypothesis

The key topic of this dissertation is dealing with the analysis of Holocene sedimentary archives along the coasts of Cefalonia Island and the western Peloponnese (Fig. 1-3). Numerous of historical accounts (e.g. Smid 1970, Guidoboni & Comastri 1997, Stefanakis 2006, Pasaric et al. 2012), catalogue entries (e.g. Antonopoulos 1979, Soloviev 1990, Soloviev et al. 2000, Tini et al. 2004, Guidoboni & Ebel 2009, Ambraseys & Synolakis 2010, Hadler et al. 2012) and field evidences (see references on Fig.1-2) show that tsunami sediments have to be expected in near coast geo-archives. A detailed introduction into sedimentary characteristics of high energy events is given in the introduction of each case study with respect to require

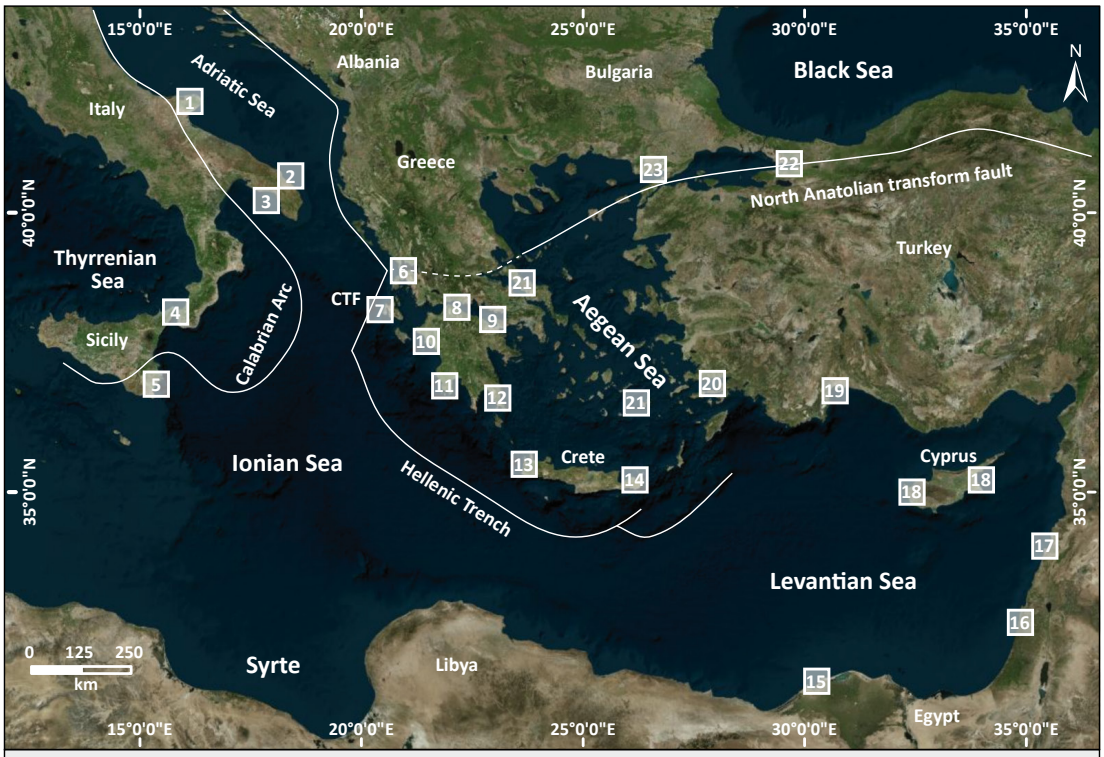

1 - Gianfreda et al. (2001); De Martini et al. (2003)
2 - Mastronuzzi & Sanso (2004)
3 - Mastronuzzi & Sanso (2000)
4 - Pantosti et al. (2008)
5 - Scicchitano et al. (2007), Smedile et al. (2011)
6 - Vött et al. (2006, 2007, 2008, 2009a,b, 2011a); May et al. (2007, 2012)
7 - Vött et al. (2010, 2013); Willershäuser et al. (2013)
8 - Kontopolus & Avramidis (2003); Alvarez-Zarikian et al. (2008)
10 - Vött et al. (2010, 2011b)
11 - Scheffers et al. (2008)
12 - Scheffers et al. (2008)
13 - Scheffers & Scheffers (2007)
14 - Bruins et al. (2008)
15 - Bernasconi et al. (2006); Stanley & Bernasconi et al. (2006)
16 - Reinhardt et al. (2006); Goodman-Tschernov et al. 2009
17 - Morhange et al. (2006)
18 - Kelletat & Schellmann (2002)
19 - Kelletat (2005)
20 - Minoura et al. (2000)
21 - Dominey-Howes et al. (2000)
22 - Altinok et al. (2001)
23 - Erginal et al. (2009)

Fig. 1-2: Topographic overview of the eastern Mediterranean with geo-scientific tsunami findings. (Map based on Bing Aerial maps 2013 - ARC GIS 10.1 2013-11-19, tectonics are modified after Clews et al. (1989) and Sachpazi et al. (2000).

the local geographical characteristics. The idea that historical and pre-historical tsunami events must be found in sedimentary archives along the coasts of the eastern Ionian Sea was realized in the Eastern Ionian Sea Tsunami project. Studies of further investigations at coastal Akarnania (e.g. Vött et al. 2006d, 2009a, 2009b, 2010, 2011a, 2011b, Floth et al. 2009, May et al. 2012) already showed that tsunamigenic impact is significant along widespread areas and is characterized by many similarities in time and space.

According to these findings this study will hypothesize that:

(i) The near-coast geo-archives along the western Peloponnese and Cefalonia deliver adequate sediment traps for the detection of Holocene tsunamigenic impact in the eastern Mediterranean.

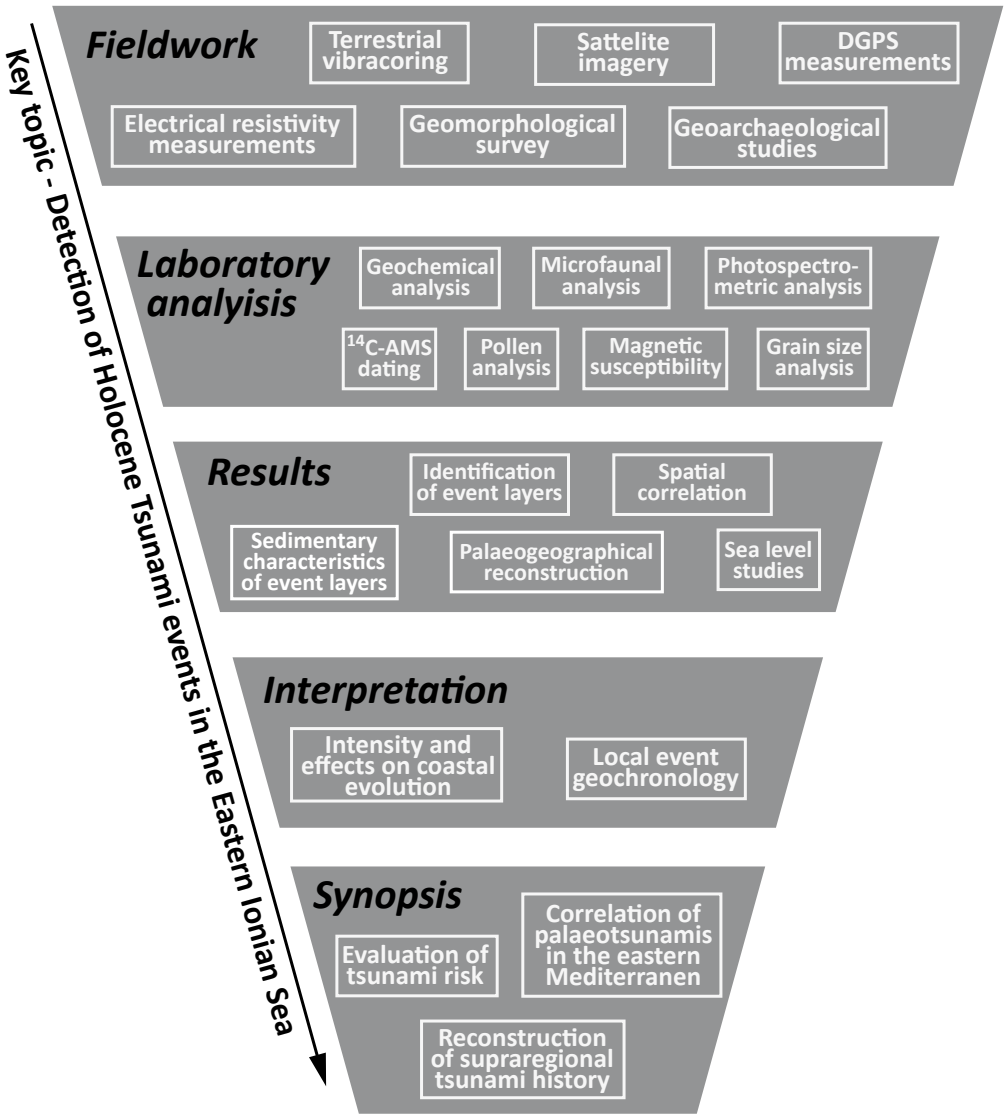

Fig. 1-3: Research design and workflow.

(ii) Geochronological investigations show similarities to historical accounts and sedimentary findings along the coasts of the eastern Mediterranean Sea.

(iii) Tsunami deposits and tsunami dating allows to reconstruct the origin and intensity of the deciphered palaeo-events.

To realize these **goals**, the study sites were selected by their potential to serve as representative sediment traps for the Holocene, and to cover an adequate geographical area for the correlation on supra-regional scales. Based on this focus the following cases studies were carried out.

Chapter 2 presents detailed sedimentary evidences for Holocene tsunamigenic impact on Cefalonia Island at the northern Gulf of Argostoli and the Bay of Livadi. The Holocene coastal evolution is based on detailed sedimentological, geomorphological, geochemical, microfaunal and geophysical analysis of sedimentary units in the stratigraphical record. The interpretation of the sedimentary findings is described in detail against the background of the local geographical and geomorphological inventory. Furthermore detailed geotectonic, geographical and methodological introductions are given for the interpretation of the results.

Chapter 3 is dealing with the coastal evolution and evidences of high-energy impact in the Gulf of Kyparissia along the shores of the western Peloponnese. The related geomorphodynamic processes, controlling mechanisms and the interaction to the coastal evolution is discussed in detail. The coastal evolution and the effects of extreme events were realized applying an extensive inventory of geo-scientific methods.

In chapter 4, the environs of the Gialova Lagoon were subject of investigations. Detailed sedimentary findings of coarse grained allochthonous deposits intersecting quiescent muddy deposits were deciphered and joined together in a geochronological framework. The influence of extreme events and long-term gradual geomorphodynamics on the local palaeogeography was realized by geo-scientific methods and the results were interpreted and discussed in detail.

Finally, chapter 5 synthesizes the results of tsunamigenic sedimentary signatures in the stratigraphical records and chrono-stratigraphies. A detailed synopsis of all study sites and a geochronological correlation focuses on the regional and supra-regional similarities and differences of the study sites.

2 Holocene tsunami landfalls along the shores of the inner Gulf of Argostoli (Cefalonia Island, Greece)*

Abstract. Cefalonia Island, directly exposed to the Hellenic Trench, is one of the tectonically most active regions in the Eastern Ionian Sea showing both aseismic and coseismic movements. Geo-scientific studies were carried out in the Livadi coastal plain and along the western coast of the inner Gulf of Argostoli. Terrestrial vibracorings and geophysical investigations brought insight into the local stratigraphical record. Geochronostratigraphical data were based on radiocarbon dating and the archaeological age estimation of diagnostic ceramic fragments. Geomorphological, sedimentological and geochemical methods were used to reconstruct the local palaeogeographical evolution and relative sea level changes since the mid-Holocene. Allochthonous sand sheets intersecting paralic swamp deposits and a mixture of badly sorted marine and terrestrial sediments document, among others, repeated tsunami landfall in the Livadi coastal plain. Our results showed that tsunami impact has been of major significance for the overall Holocene coastal evolution of the Livadi coastal area. Sedimentary evidence of tsunami impact was found for the mid-Holocene (before around 5700 cal BC and before around 4250 cal BC, respectively) as well as for the younger Holocene (post 780 cal AD). The local event-geochronostratigraphy found for the inner Gulf of Argostoli is in good agreement with results from studies in nearby coastal Akarnania and the western Peloponnese. Our results further show that the local relative sea level has never been higher than at present.

2.1 Introduction and objectives

Cefalonia Island is directly exposed to the subduction zone of the Hellenic Arc, a tectonically and seismically highly active region in the Mediterranean (Hollenstein et al. 2008). In the eastern Mediterranean, tectonic mechanisms of transform faulting, co-seismic crustal dynamics, submarine mass movements and volcanic eruptions (Ferentinos 1992, Cocard et al. 1999) are mainly responsible for triggering tsunamis (Papazachos & Dimitriu 1991). Numerous historical accounts as well as modern tsunami and earthquake catalogues document that the Mediterranean is a global hot spot in tsunami occurrence (e.g. Antonopoulos 1979, Soloviev 1990, Minoura et al. 2000, Soloviev et al. 2000, Tinti et al. 2004, Guidoboni & Ebel 2009, Ambraseys & Synolakis 2010, Hadler et al. 2012). Today's tsunami-risk therefore is significantly high and, in case of risk assessment, distinctly underestimated while early warning is problematic due to short coast to coast distances (cf. Tselentis et al. 2010).

Historical descriptions of tsunami landfall, for example by Thucydides in 5th cent. BC (Crawley 2009), Strabo in the 1st century AD (Strabo Geography VIII 3.20-21 after H. L. Jones 1923) and Ammianus Marcellinus in the 4th century AD (Seyfarth 1971), show that tsunamis caused severe destruction throughout the centuries. Inspired by the giant tsunami

* This chapter is based on: Willershaeuser, T., Vött, A., Brückner, H., Bareth, G., Nelle, O., Nadeau, M.J., Hadler, H. & Ntageretzis, K. (2013): Holocene tsunami landfalls along the shores of the inner Gulf of Argostoli (Cefalonia Island, Greece). – Zeitschrift für Geomorphologie (DOI: 10.1127/0372-8854/2013/S-00149).

events of the past decade, geo-scientific studies in palaeo-tsunami research has strongly increased (e.g. Goto et al. 2007, Okal et al. 2011, for the Indian Ocean Tsunami (IOT) 2004; e.g. Bahlburg & Spiske et al. 2012 for the Chile tsunami 2010; e.g. Sugawara et al. 2012 for the Japan tsunami 2011) with the intention to improve risk assessment with regard to future tsunami events.

Most of the geo-scientific studies focus on different types of tsunami sediment signatures mainly differentiating between allochthonous fine-grained sediments and coarse clasts of high-energy origin. The first group of tsunami deposits consists of dislocated boulders. Examples from the eastern Mediterranean are given by Mastronuzzi & Sanso 2000 and Mastronuzzi et al. 2007 (for Italy), Scheffers et al. 2008 and Vött et al. 2006d, 2008, 2009a & 2010, May et al. 2012 (for mainland Greece) and Scheffers & Scheffers 2007 (for Crete) and recent events e.g. in the IOT 2004 (e.g. Goto et al. 2007, 2010a). In these cases, boulders are interpreted as ex situ deposits transported by tsunami waves. The second group is represented by comparatively fine-grained allochthonous event deposits consisting out of sand, gravel and as well shell debris. Further characteristics are mixing of sublittoral and littoral sediments, erosional unconformities, fining upward sequences and thinning landward appearances, rip up clasts of eroded underlying sediments. (e.g. Dominey-Howes et al. 2000, 2006, Gianfreda et al. 2001, Kortekaas 2002, Vött et al. 2006d, 2008, 2009a, 2009b, 2010 & 2011a, 2011b, Pantosti et al. 2008, Hadler et al. 2011a, 2011b, Smedile et al. 2011, Willershäuser et al. 2011a, 2011b & 2012, Sugawara et al. 2012). Vött et al. (2010) describe the third group of tsunamites, namely beachrock-type, lithified calcaranitic event deposits which were calcified by post event pedogenetic processes. The fourth group is focusing on tsunami sediments mixed with cultural remains in geoarchaeological contexts (Vött et al. 2011a, 2011b, Hadler et al. 2011a, 2011b, 2012, 2013). Finally, submarine deposits are getting more and more in the focus of palaeotsunami research (Reinhardt et al. 2006, Nomikou et al. 2011, Sakkellariou et al. 2011, Smedile et al. 2011, Feldens et al. 2012, Sakuna et al. 2012).

Being part of the seismo-tectonically highly active northern part of the Hellenic Arc, Cefalonia Island has not yet been subject to systematical palaeotsunami studies. In fact, Cefalonia has experienced some of the most severe earthquakes in the eastern Mediterranean during the recent past (Papazachos & Papazachou 1997). This paper is an important step towards a better understanding of the palaeotsunami history of this island. For the reconstruction of the palaeogeographical evolution, tsunami influence on the coastal geomorphology and relative sea level studies at Cefalonia, we explored near-coast geological archive such as paralic swamps, flood plains and beach ridges. The aims of our studies in the inner Argostoli Gulf were (i) to detect potential event layers in the coastal sedimentary record, (ii) to decipher the influence of tsunami events on the local coastal evolution, (iii) to set up an event-geochronostratigraphy and compare it with the (supra-)regional imprint, and (iv) to evaluate high-energy events against the background of relative sea level changes and the palaeogeographical evolution of the study area.

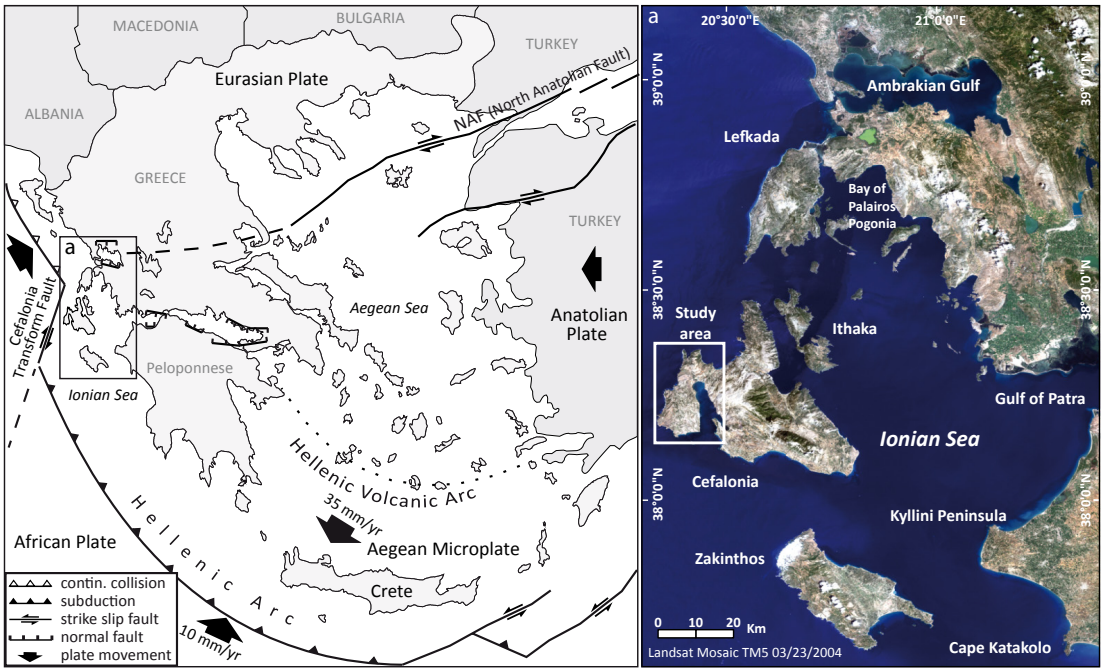

Fig. 2-1: Topographic and tectonic overview of the Eastern Ionian Sea including the coasts of the Peloponnese and the Ionian Islands. The study area on Cefalonia Island is encircled by a white box. Tectonic setting modified after Clews et al. (1989), Sachpazi et al. (2000) and Van Hindsbergen et al. (2006), topographic overview based on Landsat TM 5 true composite satellite image.

2.2 Geotectonic and natural setting of the study area

The Ionian Islands are directly exposed to the seismically highly active Hellenic Trench to the south-west, the Cefalonia transform fault (CTF) to the west and the extension of the North Anatolian Fault system to the north (Fig. 2-1). The right-lateral strike slip CTF links the zone of prevailing subduction to the south to a continental collision in the north (Louvari et al. 1999, Sachpazi et al. 2000). The rates of crustal motion at the CTF (~ 5 mm/a) are comparatively low in comparison to those found offshore the Peloponnese and Crete (up to ~ 40 mm/a, Kahle et al. 2000, Hollenstein et al. 2006). Also, the collision zone between the African plate and the Agean microplate to the north of the study area is characterized by complex crustal motion, deformation and high seismicity (Koukouvelas et al. 1996, Clement et al. 2000, Lagios et al. 2007, Hollenstein et al. 2008).

Since the early Pliocene, complex crustal movements result in phases of strong uplift of western Cefalonia. During the Pleistocene the Paliki Peninsula was affected by another phase of uplift (Van Hinsbergen et al. 2006). Furthermore halo-kinetic movements take control on local tectonics (Lagios et al. 2007, Hollenstein et al. 2008). The tectonic situation of the Ionian Islands is highly complex because collision, subduction, transform faulting and spreading mechanisms are concentrated in a small region (Sachpazi et al. 2000). Concerning tsunamigenic focal mechanisms, the risk of seismically induced tsunamis is very high (Papazachos & Dimitriu 1991). Since the Miocene, complex tectonic movements in the area of the Ionian Islands resulted in a fragmentation of lithospheric blocks and created uplifted land masses and subsiding deep-water basins. The Kerkyra-Cefalonia submarine

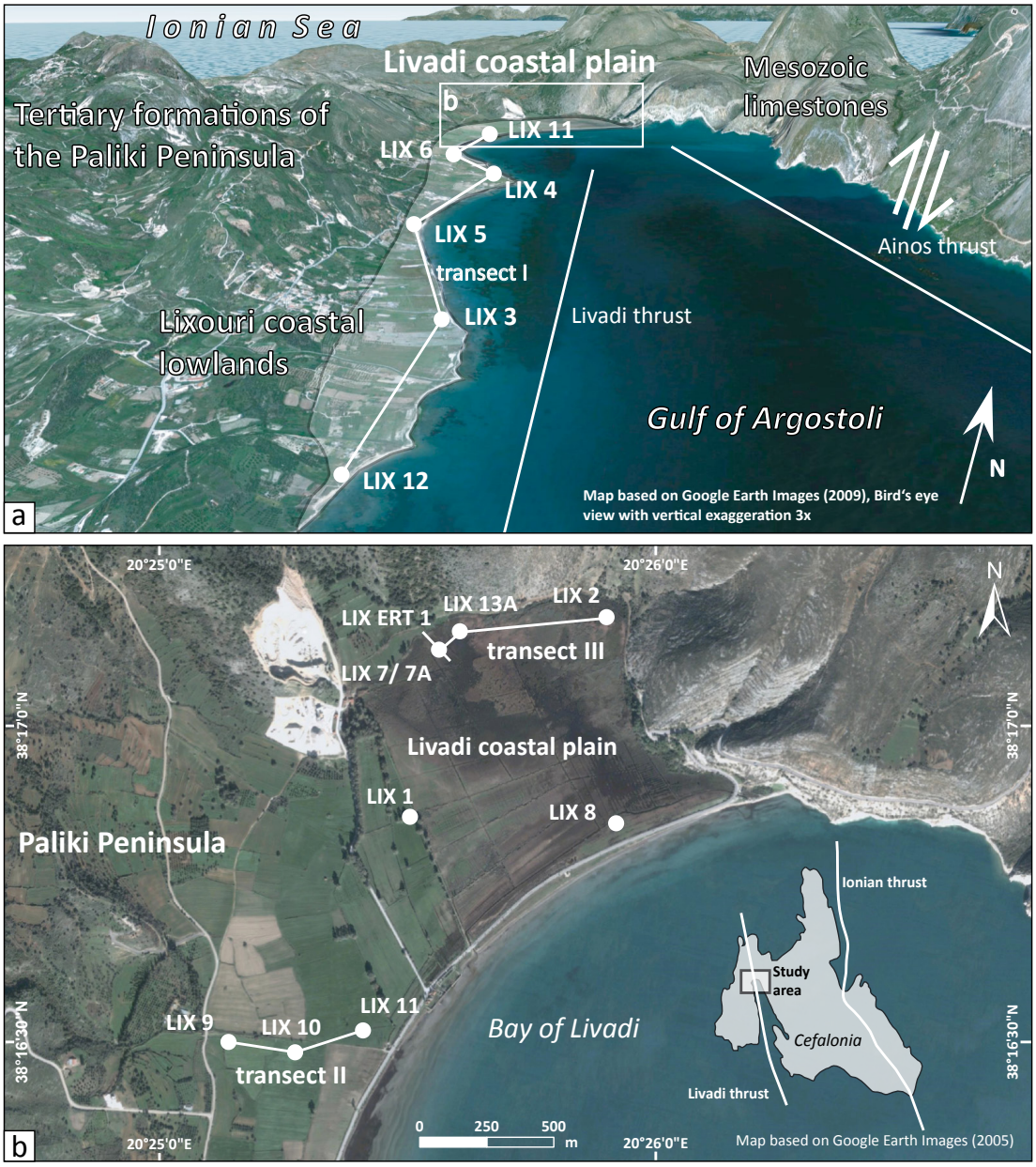

Fig. 2-2: Topographic overview of the study area, the Lixouri coastal lowlands and the Livadi coastal plain. (a) Bird's eye view of the inner Gulf of Argostoli with vibracoring sites (white dots) along transect I, the tectonic situation of the study area and the main geological formations. (b) Detail of the Livadi coastal plain with vibracoring sites (white dots) along transect II and III as well as geoelectrical transect LIX ERT 1. Inset map shows the location of study sites on Cefalonia Island and a simplified geotectonic overview. Maps based on (a) Google Earth digital elevation model with a vertical exaggeration factor of 3x and view direction NNW (2009) and (b) Google Earth areal images (2005).

trough shows extensive mass movements that have a very high potential in triggering tsunamis (Ferentinos 1992, Poulos et al. 1999). During the strong earthquake in 1953, the western part of Cefalonia experienced sudden co-seismic uplift up to 70 cm (Stiros et al. 1994), documenting that there is a direct relation between coastal evolution and earthquake activity.

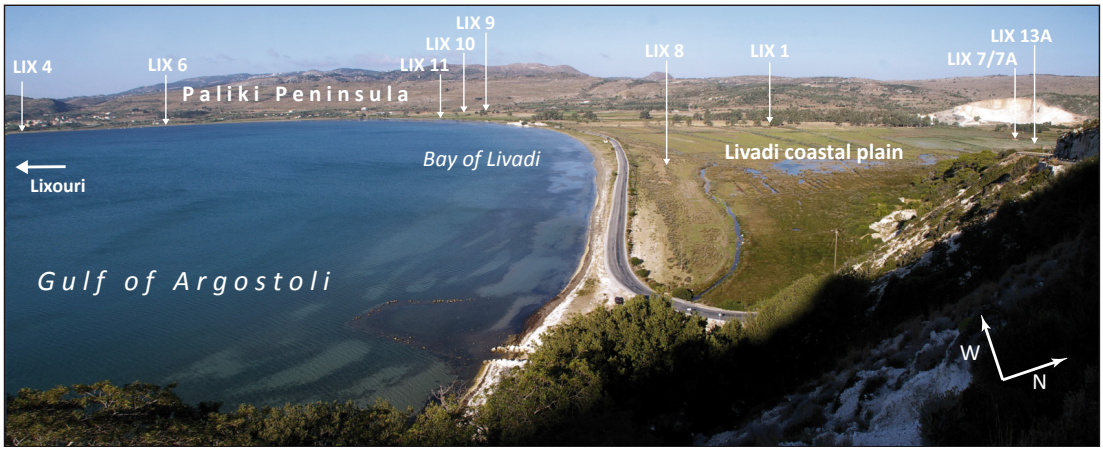

Fig. 2-3: View of the inner Gulf of Argostoli and the Livadi coastal plain. The swash zone and the range of maximum tide and storm activity does not extend more than 10 m inland. The beach barrier works as a protective system for the backswamp area. The left background shows the northern part of the Lixouri coastal lowlands with the tertiary ridges of the Paliki peninsula. Photo taken by S.M. May (2007).

The Paliki Peninsula (Fig. 2-1) is separated from the main body of Cefalonia Island by the N-S trending fault system of Livadi thrust (Stiros et al. 1994). Our study areas, the Livadi coastal plain and the Lixouri coastal lowlands are located in the northernmost part of the adjacent Gulf of Argostoli (Figs. 2-2 and 2-3). Their catchment area is made out of Mesozoic limestone and Tertiary marl (IGME 1982a, Underhill 1989). The recent environment of the Livadi coastal plain is characterized by a back beach swamp separated from the Argostoli Gulf by a beach barrier. On the contrary, the Lixouri coastal lowlands consist of alluvial fan deposits and beach ridges. The energetic environment along in the inner Argostoli Gulf is significantly weak and the sediment transport is low compared to the coastal sections in the south and in the west of the island which are directly exposed to the open Ionian Sea. As storm activity is mostly bound to predominant winds from westerly directions (Soukissian et al. 2008) it is short fetch. The bathymetrical conditions in the inner Gulf are characterized by shallow water depths down to 5-25 m below present sea level (m b.s.l.) and by low slope gradients. Only 30 km to the southeast of the island, however, water depths are more than 3000 m with steep slope gradients (UKHO 1992, Elias 2010). The Argostoli Gulf shows a funnel-type coastline configuration. Palaeotsunami evidence was already described for the Koutavos Bay at its easternmost edge in an archaeological context close to the harbour of ancient Krane. Here, Vött et al. (2013) found that palaeotsunami dynamics were strongly influenced by wave amplification, diffraction and refraction mechanisms.

2.3 Methods

In this paper a multidisciplinary approach was used to decipher the sedimentary record of the study area. We drilled 13 vibracores in the Livadi coastal plain and the Lixouri coastal lowlands (Fig. 1-3) using an Atlas Copco mk1 vibracorer and core diameters between 6 cm and 3.6 cm. Sedimentary characteristics of the vibracores, such as sediment colour, grain size distribution, pedogenic features, macrofossil and carbonate content, were documented based on Ad hoc Arbeitsgruppe Boden (2005).

Selected cores were retrieved using plastic inliners of 5 cm diameter for the analysis of the foraminiferal and pollen content. Foraminiferal studies were carried out using ca. 15 ml of sediment extracted from relevant stratigraphical units. Samples were sieved in fractions of >0.4 mm, 0.4-0.2 mm, 0.2-0.125 mm and <0.125 mm and subsequently analyzed using a stereo microscope (type Nikon SMZ 745T). Digital photos were taken from selected specimens using a light-polarizing microscope (type Nikon Eclipse 50i POL with Digital Sight DS-FI2 digital camera back 5 MP).Geoelectrical investigations were accomplished by means of a Syscal R1+ Switch 48 electrical resistivity tomography (ERT) unit to detect the near-surface underground down to 10 m below surface (m b.s.) and to check the spatial variabilities of the local geostratigraphies found in the vibracores. We used a Wenner-Schlumberger array with 48 electrodes and an electrode spacing of 2 m. The pseudosection model was calculated by means of the RES2Dinv software.

Laboratory studies comprised the analysis of the organic content (loss of ignition by heating to 550°C), the calcium carbonate content (Scheibler-method), the pH-value and the electrical conductivity of selected sediment samples (Barsch et al. 2000). All samples were analyzed for total contents of Ca, Mn, Fe and more than 20 further elements using a portable XRF-analyzer (type Thermo Niton XL3t 900S GOLDD, calibration mode SOIL).

A Topcon HiperPro FC-200 DGPS instrument was used to measure position and elevation data of vibracoring sites and ERT transects with an accuracy of +/- 2 cm.

A geochronological framework was established based on ^{14}C-AMS dating of organic material and marine shells as well as on archaeological age determination of diagnostic ceramic fragments. For radiocarbon dating, we preferred samples out of autochthonous deposits like peat or articulated marine molluscs in living position. Samples out of reworked material only yield a maximum age for the event. Calibration was accomplished using the software Calib 6.0 after Reimer et al. (2009).

Samples for palynological analyses were taken from relevant stratigraphic positions and consisting of peat guaranteeing a satisfactory pollen preservation. Peat sediment samples of 1 cm^3 were treated according to standard methods (Faegri et al. 1989) including the use of hot KOH, Nitric acid, HF and acetolysis. Pollen, spores were counted on microscope slides with a light microscope. The nomenclature for pollen types follows Beug (2004), diagrams were realized with TILIA and TGView software solutions.

2.4 High-energy impact at the coastal lowlands of the Paliki Peninsula

2.4.1 Vibracore transects I-III

Vibracoring sites were arranged along and across the present coastline in order to document characteristics of differences in sedimentary dynamics.

Transect I (Fig. 2-2a) is trending in south-north direction comprising vibracores LIX 12 (N 38°13‘12.4“, E 20°26‘17.6“), LIX 3 (N 38°13‘51.8“, E 20°26‘09.6“), LIX 5 (N 38°14‘36.6“, E 20°25‘45.2“), LIX 4 (N 38°15‘21.2“, E 20°25‘48.5“), LIX 6 (N 38°15‘47.7“, E 20°25‘24.1“) and LIX 11 (N 38°16‘30.4“, E 20°25‘25.3“). Detailed vibracore stratigraphies are summarized in Fig. 2-5, Fig. 2-7 & Fig. 2-9. The bases of cores LIX 12, 3, 4 and 11 show

thick homogenous silty to fine sandy deposits representing a comparatively long-enduring shallow marine environment. At sites LIX 12, 3 and 4, these littoral deposits are abruptly affected by the input of gravel and shell debris mixed with unsorted sand, partly following on top of an erosional unconformity. Cores LIX 12 (7.91-7.57 m b.s.l.) and LIX 3 (10.35-10.03 m b.s.l.) are furthermore characterized by beachrock-type cemented sand within this layer. At site LIX 6, unsorted coarse-grained deposits directly overlie bedrock marls (Fig. 2-5).

Typical features of sea-borne high-energy impact (Reineck & Singh 1980, Einsele 2000, Schäfer 2005) such as erosional unconformities (e.g. LIX 3 at 0.35 m b.s.l. and LIX 6 at 0.23 m b.s.l., see Fig. 2-5) fining upward sequences (e.g. LIX 11 at 0.62 m b.s.l.-0.41 m

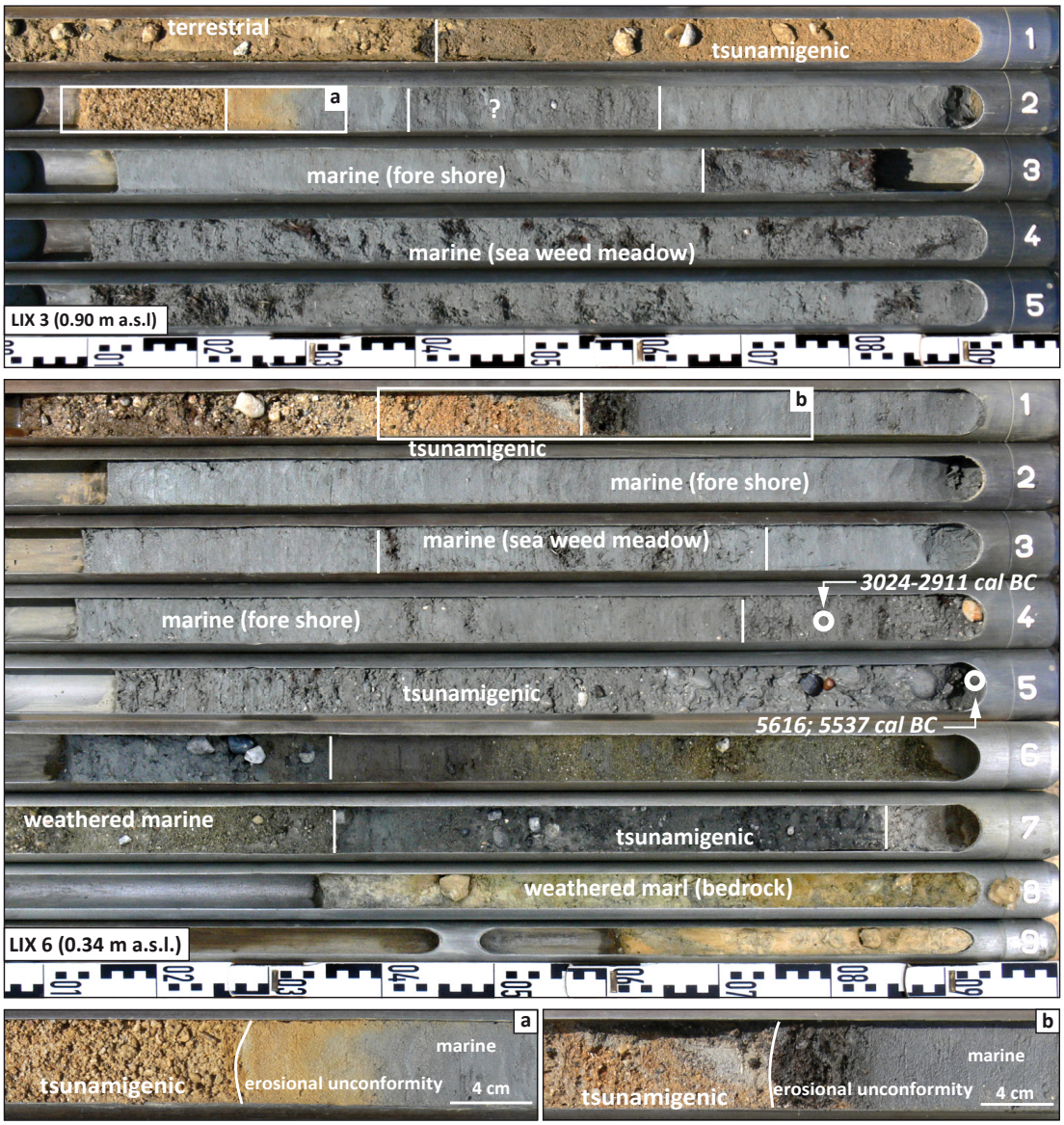

Fig. 2-4: Simplified facies profile of vibracores LIX 3 and LIX 6. Selected areas (a+b) show significant interferences in the stratigraphical record characterized by allochthonous coarse-grained material on top of well sorted autochthonous marine sediments with sharp erosional contacts.

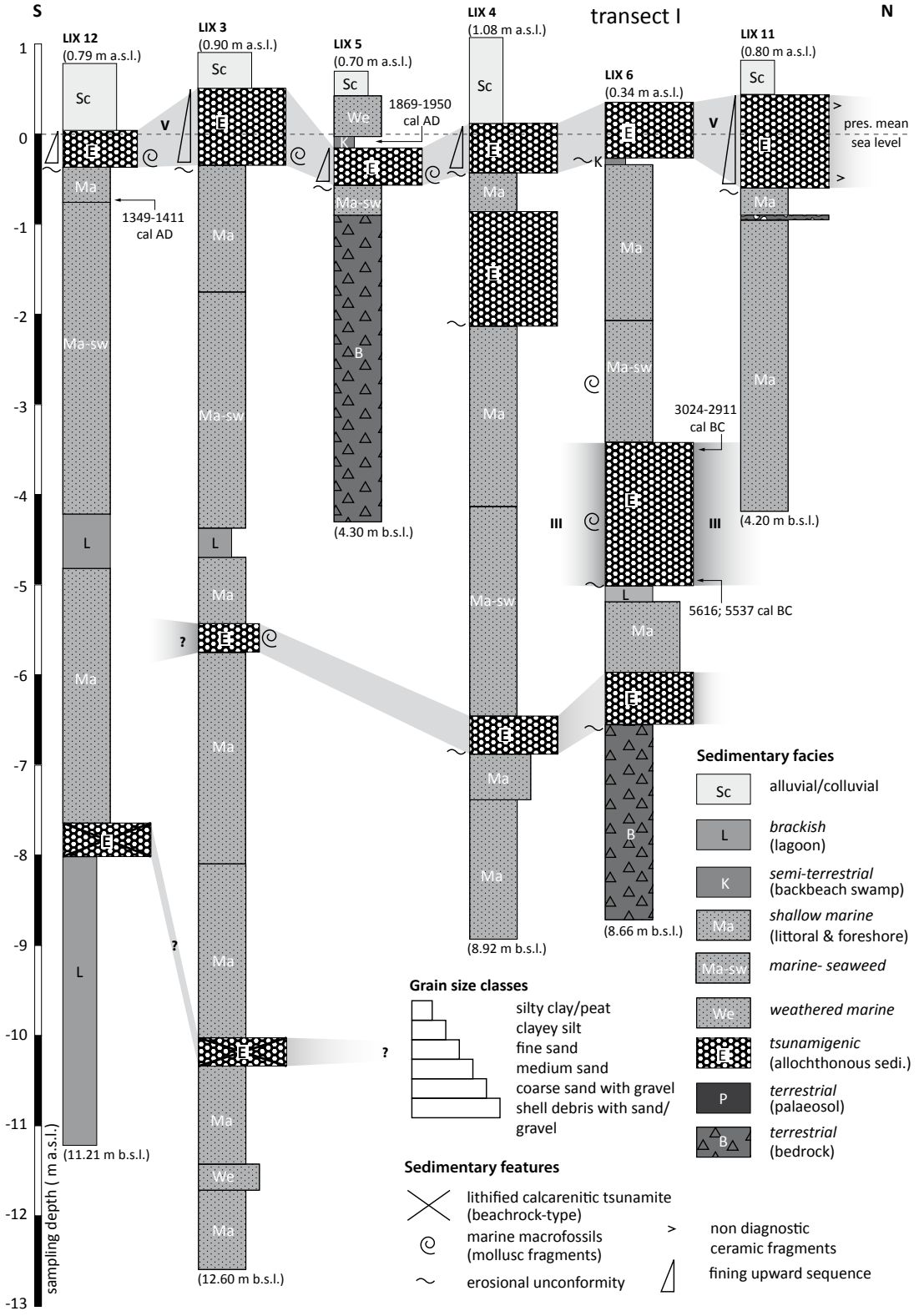

Fig. 2-5: Stratigraphical record and facies distribution of vibracores drilled along transect I in the coastal lowlands of the eastern Paliki peninsula (Fig. 2-2a+b) along a total distance of 6.2 km.

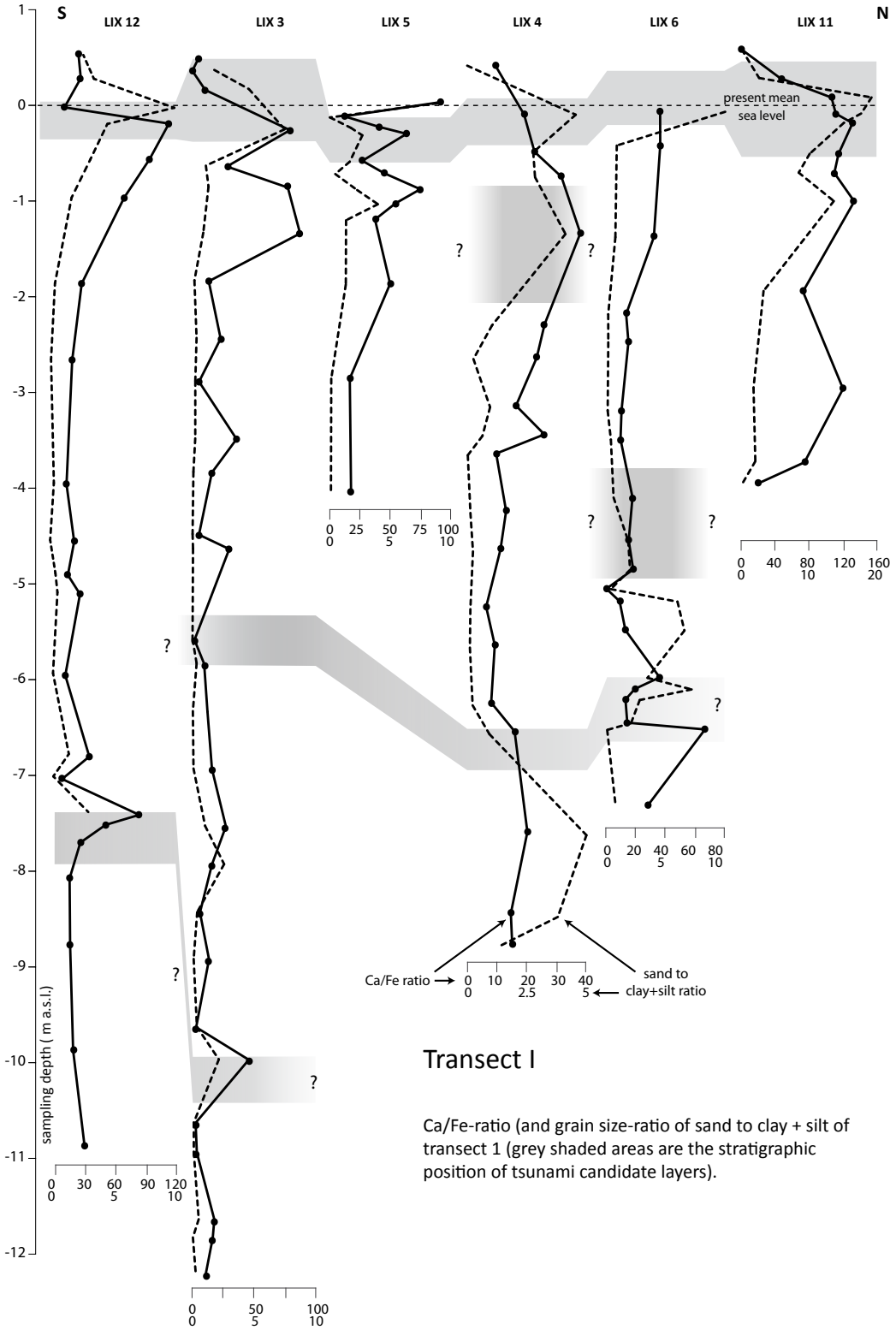

Fig. 2-6: Ca/Fe ratios based on XRF-measurements and results of grain size analyses for vibracore transect I. Grain size ratio represents a ratio of sand to clay + silt. Stratigraphic positions of high-energy layers in the sedimentary record are shaded in grey. Ca/Fe ratio is shown by continuous line, grain size ratio is shown by dashed line.

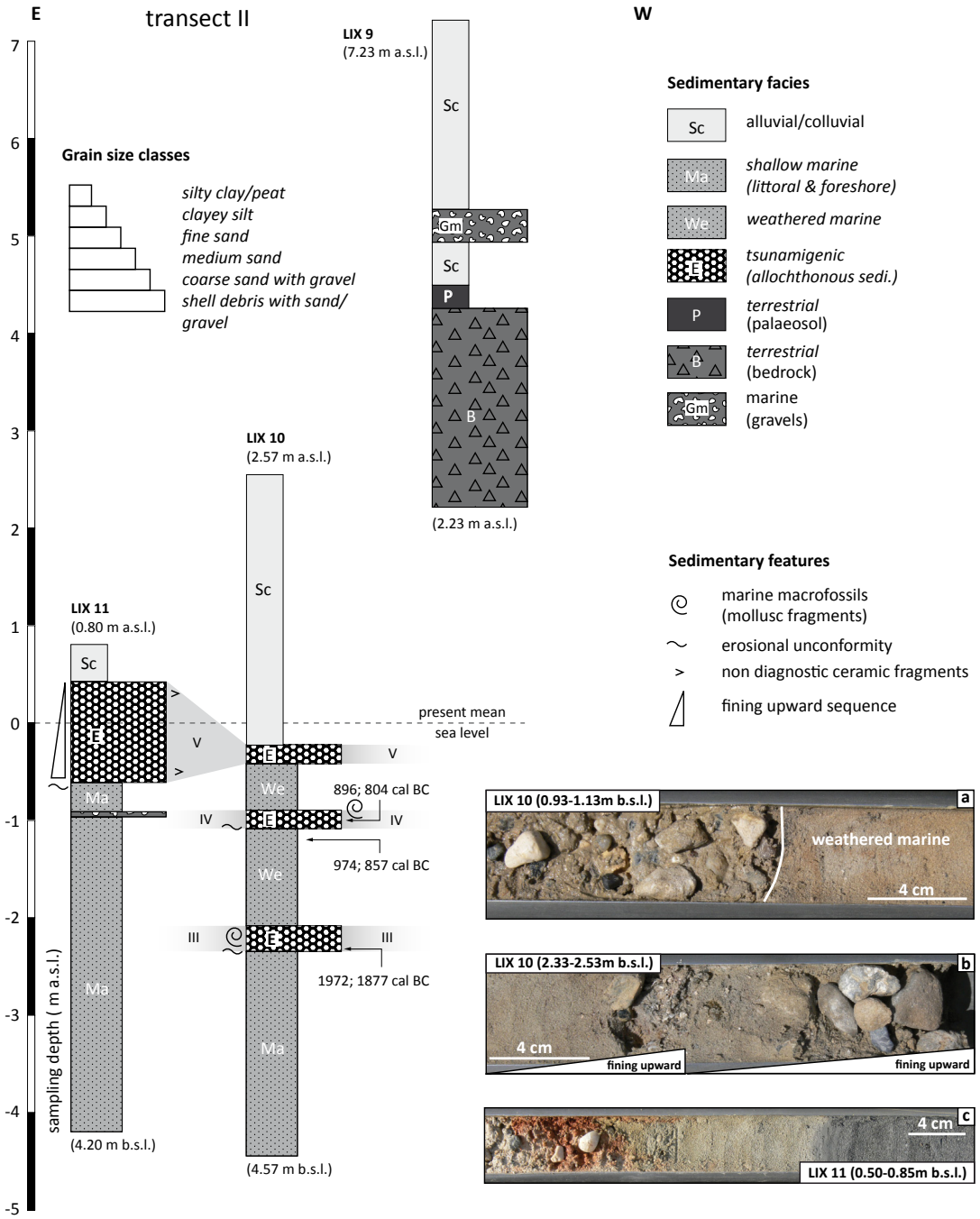

Fig. 2-7: Stratigraphical record and facies distribution of vibracores drilled along transect II in the inner Argostoli Gulf (Fig 2-2 b). Inset photos show details of high-energy layers encountered in vibracores LIX 10 and LIX 11. Location of inset photos – see marked areas in Fig. 2-8.

a.s.l, LIX 12 at 0.37 m b.s.l.-0.04 m a.s.l) and mixing of littoral, sublittoral and terrigenous sediments (e.g. LIX 11 at 0.62 m b.s.l.-0.41 m a.s.l) are existing in consistent stratigraphical positions along the transect in a distance of 25-80 m from the sea (see Fig. 2-5 section V). Autochthonous sedimentary conditions are mainly represented by shallow marine silty fine sand (e.g. LIX 4 at 6.45-2.15 m b.s.l., LIX 12 7.57-0.74 m b.s.l.) and loam deposited by

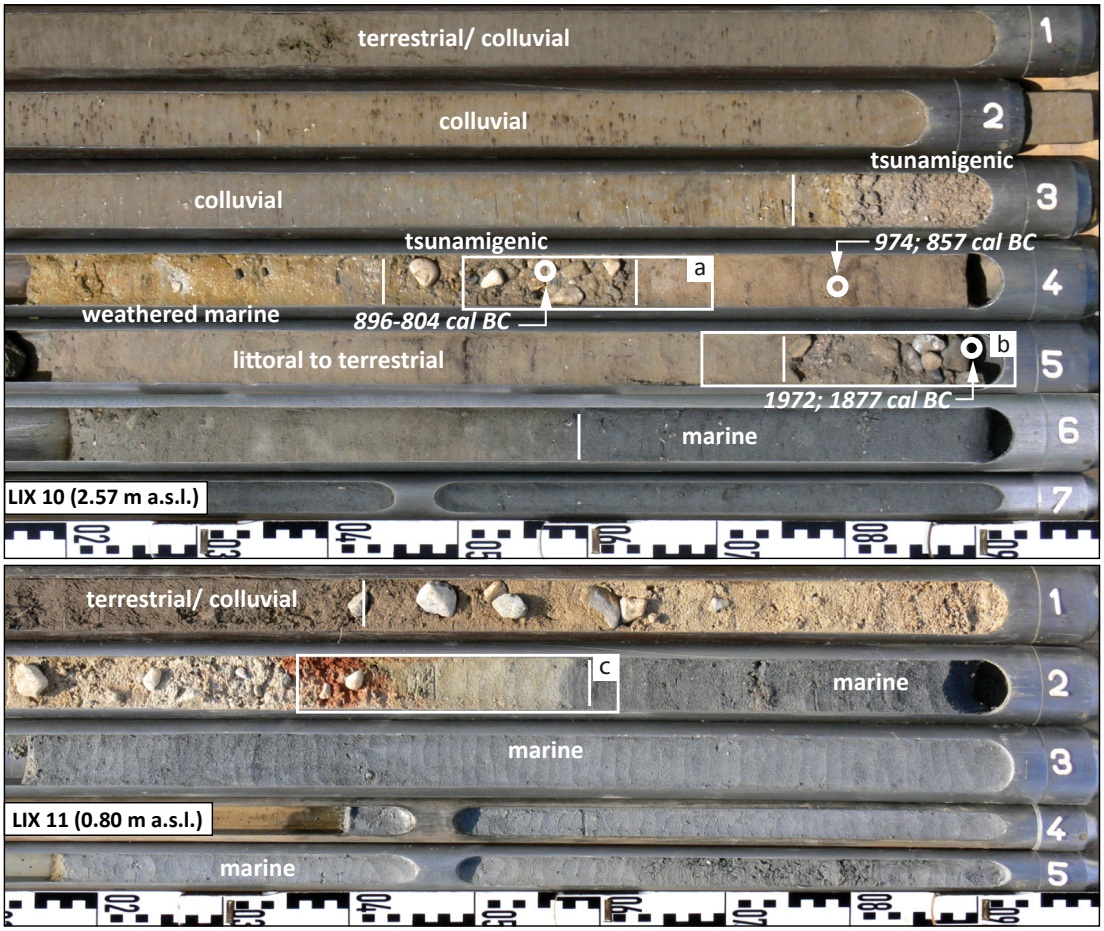

Fig. 2-8: Vibracore photos of transect II with simplified facies distribution and calibrated radiocarbon dating results. The marked areas (a-c) are shown in detail in Fig. 2-7.

colluvial and/or alluvial processes (e.g. LIX 5 at 0.42-0.70 m a.s.l.). High energy interferences of the local environments show a clearly marine fingerprint; there are no alluvial fan systems existing in the vicinity of the coring sites.

Transect II, comprising vibracores LIX 9 (N 38°16‘30.9“, E 20°25‘07.8“), LIX 10 (N 38°16‘29.5‘, E 20°25‘18.6“) and LIX 11 is situated at the northern margin of the Livadi coastal plain and trends in a west-east direction (Fig. 2-2b+ Fig. 2-3). It is arranged across the gently inclined slope of the eastern Paliki Peninsula hills covering elevation differences of around 7 m. Detailed vibracore stratigraphies are summarized in Fig 2-7. Vibracores LIX 10 and 11 are characterized by intersecting units of coarse-grained and mainly unsorted sediments of high-energy origin including marine macro-faunal debris and, in case of LIX 11, non-diagnostic ceramic fragments (see Fig. 2-7 inset Photos and Fig. 2-8). In every core, a sharp erosional unconformity at the base of the event layer marks a clear change in the depositional energy (LIX 10 at 2.33 m b.s.l., 1.07 m b.s.l., 0.41 m b.s.l. and LIX 11 at 0.62 m b.s.l.). The internal structure of the allochthonous layers found in core LIX 10 is characterized by multiple fining upward sequences starting with coarse gravel at the base (at 2.33-2.19 m b.s.l., 1.07-0.89 m b.s.l.) followed by a coarse sand and silty fine sand (Fig. 2-8).

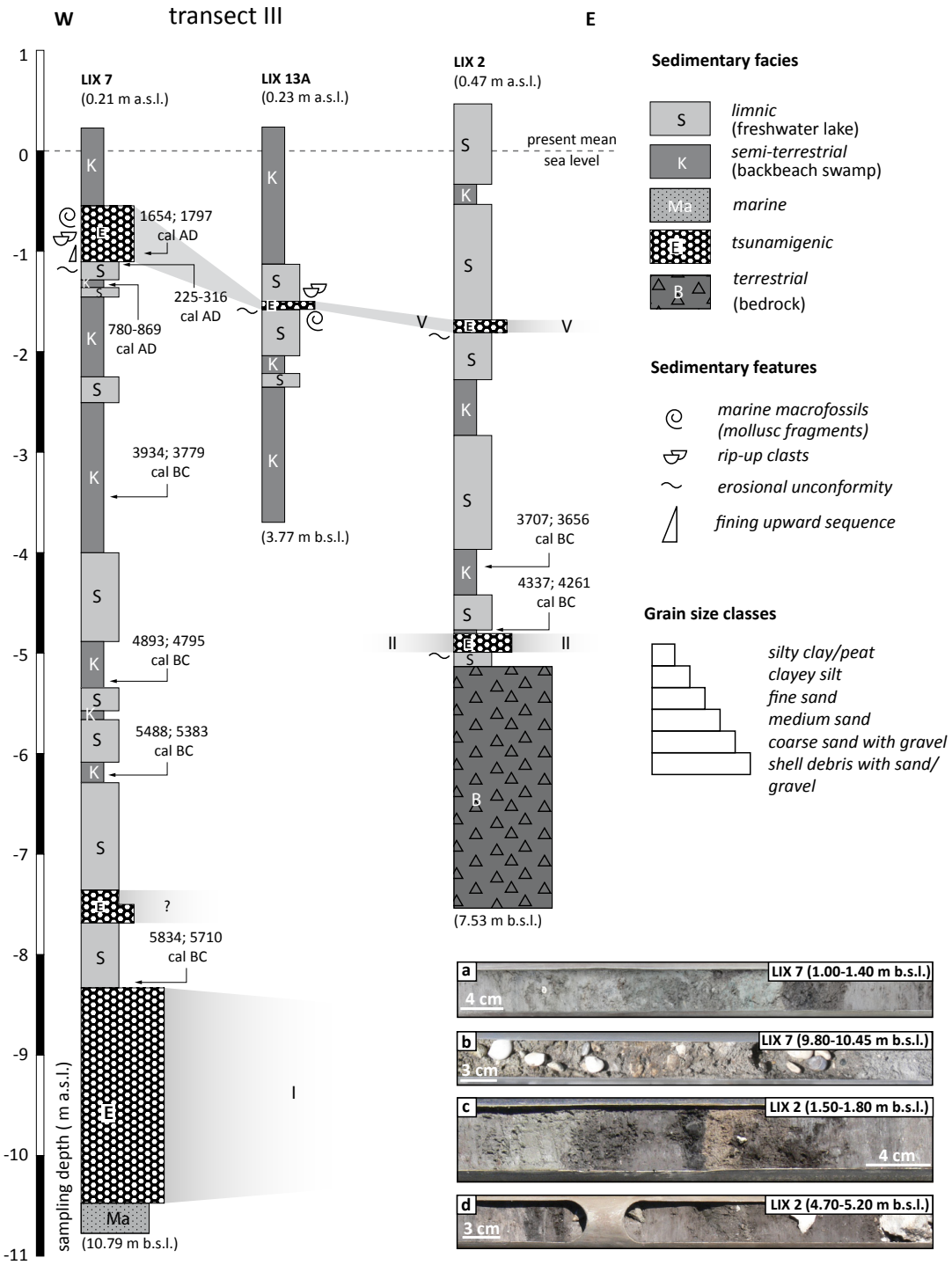

Fig. 2-9: Stratigraphical record and facies distribution along vibracore transect III in the northern Livadi coastal plain. The transect runs from west to east parallel to the present coast approximately 800 m inland (Fig. 2-2). Photos show details of high-energy layers. Location of inset photos – see marked areas in Fig. 2-10.

Fig. 2-10: Vibracore photos of transect III cores LIX 2 and LIX 7 with simplified facies distribution and calibrated radiocarbon dating results. The marked areas (a-d) are shown in Fig. 9.

In case of vibracore LIX 10 and LIX 11, high-energy event layers mark the transition between marine and terrigenous strata; thus, shoreline shifting and shoreline destruction seem to be associated to high-energetic impact. Usually predominating littoral dynamics seem to be merely responsible for the re-arrangement of sediments after major impacts.

Sample	Depth (m b.s.)	Depth (m b.s.l.)	Description	Lab No.	δ 13 C (ppm)	^{14}C Age BP	1σ max; min cal Bp	1σ max; min cal BC	2σ max; min cal BC
LIX 2/16+ PR	5.24-5.28	4.75-4.81	Peat	KIA 39720	-28.00 ± 0.16	4920 ± 30	5605; 5656	3707; 3656	3764; 3647
LIX 2/19 PR	5.48-5.50	5.01-5.03	Peat	KIA 39719	-31.03 ± 0.13	5435 +35/-30	6210; 6286	4337; 4261	4345-4240
LIX 5/2 PR	0.83-0.85	0.13-0.15	Plant remain (sea weed)	KIA 39721	-15.60 ± 0.15	445 ± 20	500-514	1436-1450 cal AD	1426-1466 cal AD
LIX 5/2 PR	0.83-0.85	0.13-0.15	Plant remain (sea weed)	KIA 39721	-15.60 ± 0.15	445 ± 20	0-81*	1869-1950*cal AD	1820-1950*
LIX 6/7 PR	3.80	3.46	Plant remain (sea weed)	KIA 39723	-12.97 ± 0.12	4695 ± 35	5326; 5567	3618; 3377	3630; 3371
LIX 6/7 PR	3.80	3.46	Plant remain (sea weed)	KIA 39723	-12.97 ± 0.12	4695 ± 35	4860-4973*	3024-2911*	3088-2885*
LIX 6/10+ PR	5.28	4.94	Plant remain	KIA 39722	-28.89 ± 0.11	6630 ± 35	7486; 7565	5616; 5537	5625-5509
LIX 7/4 PER	1.25	1.04	Plant remain	KIA 39730	-29.63 ± 0.23	220 ± 20	153; 296	1654;1797 cal AD	1645-1954 cal AD
LIX 7/5 PR2	1.33	1.12	Plant remain (sea weed)	KIA 39729	-16.35 ± 0.13	2090 ± 20	2006-2110	161; 57	172-48
LIX 7/5 PR2	1.33	1.12	Plant remain (sea weed)	KIA 39729	-16.35 ± 0.13	2090 ± 20	1634-1725*	225-316 cal AD*	172-349 cal AD*
LIX 7/7+ PR	1.52-1.54	1.31-1.33	Peat	KIA 39728	-28.25 ± 0.09 [2] -29.18 ± 0.17 [1]	1200 ± 20 [2] 1740 ± 25 [1]	1081; 1170 [2] 1615; 1697 [1]	780-869 cal AD [2] 253; 335 cal AD [1]	774-887 cal AD [2] 240-381 cal AD [1]
LIX 7/12+ PR	3.83-3.85	3.62-3.64	Peat	KIA 39727	-29.00 ± 0.14	5030 ± 25	5728; 5756	3934; 3779	3944; 3715
LIX 7/16+ PR	5.54-5.56	5.33-5.35	Peat	KIA 39726	-29.20 ± 0.13	5960 ± 25	6744; 6842	4893; 4795	4934-4773
LIX 7/18+ PR	6.44-6.46	6.23-6.25	Peat	KIA 39725	-24.75 ± 0.17	6495 ± 30	7332; 7437	5488; 5383	5518-5375
LIX 7/22 PR	8.60	8.39	Peat	KIA 39724	-29.92 ± 0.17	6870 ± 50	7659; 7783	5834; 5710	5877-5661
LIX 10/6 M	3.55	0.98	Mollusc	KIA 39733	-2.10 ± 0.27	3040 ± 40	2753-2845	896-804	962-778
LIX 10/7+ HR	3.81	1.24	Wood fragment	KIA 39731	-27.81 ± 0.12	2775 ± 25	2806; 2923	974; 857	997-844
LIX 10/10 M	4.90	2.33	Articulated Mollusc	KIA 39732	1.19 ± 0.15	3900 ± 30	3826; 3921	1972; 1877	2025-1818
LIX 12/5+ PR	1.53-1.55	0.74-0.76	Plant remain (sea weed)	KIA 39735	-15.01 ± 0.14	965 ± 20	803; 926	1024; 1147 cal AD	1020;1153 cal AD
LIX 12/5+ PR	1.53-1.55	0.74-0.76	Plant remain (sea weed)	KIA 39735	-15.01 ± 0.14	965 ± 20	539-601*	1349-1411 cal AD*	1326-1430 cal AD*
LIX 12/19+ PR	9.32-9.40	8.53-8.61	Plant remain	KIA 39734	-19.21 ± 0.32	43650 +960/-860	45717-47825	45876-43768	47218-43239

Tab. 2-1: ^{14}C-AMS dating results used for establishing a local geochronological framework. Notes: b.s. = below surface; b.s.l. = below sea level; Lab. No. - laboratory number, University of Kiel (KIA); 1 σ max; min cal BP/BC (AD)- calibrated ages according to the radiocarbon calibration program Calib 6.0 (Reimer et al. 2009); 1σ & 2 σ range ";" – several possible age intervals because of multiple intersections with the calibration curve (oldest and youngest ages given); asterisk (*) marks calendar age yielded interval by means of marine calibration dataset; [1]humic acid fraction dated; [2]alkali fraction dated.

Grain size and sedimentary characteristics suggest that following high-energy impacts, lower energetic conditions were soon re-established and thus cover high-energy deposits. In some cases, post depositional weathering may be triggered by coseismic uplift effects (Section 2).

Transect III is situated at the northern edge of the Livadi coastal plain and comprises vibracoring sites LIX 2 (N 38°17‘10.5“, E 20°25‘55.0“), LIX 7 (N 38°17’07.8”, E 20°25’32.8”) and LIX 13A (N 38°17‘09.6“, E 20°25‘35.9“). The transect runs in a west-east direction (Fig. 2-2b). Detailed vibracore stratigraphies are summarized in Fig 2-9.

The sedimentary records of vibracores LIX 2, 7 and 13A show significant discrepancies between silt-dominated autochthonous sediments and repeatedly intersecting high-energy sand, the latter clearly pointing to episodic high-energy influence. The gradual long term coastal evolution as reflected by autochthonous deposits does not show storm laminae or other regular intereferences of the palaeogeographical evolution. High-energy sedimentary imprint on the coring sites is documented by erosional contacts (LIX 7/7A at 1.14 m b.s.l., LIX 13A at 1.58 m b.s.l. and LIX 12 at 1.80 m b.s.l.), multimodal grain size distributions (e.g. LIX 7/7A at 10.79-8.35 m b.s.l.), fining upward sequences (e.g. LIX 7/7A at 1.14-0.78 m b.s.l.) and mixtures of marine and terrestrial sediments (e.g. LIX 2 at 4.99-4.81 m b.s.l.; Fig. 10). All investigated cores have in common that the uppermost high-energy layer was found in consistent stratigraphical position over a distance of more than 550 m.

2.4.2 Radiocarbon dating results

The event-geochronostratigraphy in this paper is based on 17 ^{14}C-AMS ages retrieved from peat and plant remains as well as from biogenetically produced calcium carbonate (Table 2-1). Because of the still unsolved problem of the spatio-temporal variabilities of the marine (palaeo-)reservoir effect for marine samples we used an average of ~408 years of reservoir age for the eastern Mediterranean (Reimer & McCormac 2002, Reimer et al. 2004), during the calibration by using the Software Calib 6.0 (Reimer et al. 2009). With regard to samples LIX 5/2 PR, LIX 6/7 PR, LIX 7/5 PR2 and LIX 12/5+ PR out of sea weed, δ^{13} C values < 15 ± 3 ppm suggest marine calibration (Walker 2005).

Our sampling strategy was to use only autochthonous organic matter or articulated mollusc shells right above or below the event layer (sandwich dating approach, Vött et al. 2009b, 2011b). If possible, we used plant remains instead of marine shells to avoid marine reservoir effects. Donato et al. (2008) used articulated molluscs that were transported and deposited alive, in order to obtain the most reliable ages for event-related sediment deposition. Dating samples taken from allochthonous high-energy deposits yields maximum ages only (*termini ad* or *post quos*) for the event. Dated samples from post-event sedimentary units represent *termini ante quos* for the event. Screening of the quality of each sample on the basis of δ^{13}C values is important, especially with regard to differences of isotope fractions of C4 and C3 plants (Wagner 1998). In case of plants from marine environments (e.g. sea weed) the age has also to be corrected for the marine reservoir effect. Radiocarbon ages of autochthonous C3 land plants yield the most reliable results.

Radiocarbon dates used for establishing the geochronostratigraphy for the study area are listed in Table 2-1. Sample LIX 12/19+PR (45879-43768 cal BC) was not considered as reliable, because the Pleistocene age indicates reworking of older material. In case of differing ages obtained for one and the same event layer, the younger age is considered as more reliable maximum age.

The age inversion produced by sample LIX 7/5 PR2 (atmospheric calibration: 161; 57 cal BC; marine calibration: 225-316 cal AD) may be explained by bioturbation, reworking and/ or hard water as well as marine reservoir effects (Wagner 1998, Walker 2005); the obtained age was thus excluded from further interpretation. Sample LIX 7/7+PR was taken from a peat layer, yielding an age of 253; 335 cal AD based on the humic acid fraction and of 780-869 cal AD based on the alkali fraction. The influence of older and mobile humic acids of groundwater fluxes is great, thus, the radiocarbon age of the humic acid fraction is less reliable. On the contrary, the alkali fraction is less vulnerable to these fluxes and therefore preferred for interpretation (Wagner 1998).

2.4.3 Electrical resistivity measurements

We carried out electrical resistivity measurements along a transect at the northern margin of the Livadi coastal plain right across coring site LIX 7 and LIX 7A as a base for the selection of best fit coring sites. The ERT transect trends from northwest to southeast. Fig. 2-11 depicts the simplified results based on the 3rd iteration with an absolute error of 2.3%.

The transect runs from slightly elevated hillslope position right into the Livadi swamp lowlands. The inverse model resistivity results are divided into three main subsurface categories. The first category with resistivity values between 0.5-2 Ωm is restricted to the upper parts down to a depth of 4 m b.s. in the northwest and 8 m b.s. in the southeast. As shown by core LIX 7, it represents alternating limnic and swampy fine-grained deposits. The second category covers resistivity values between 2-4.5 Ωm representing fine-grained limnic silty clay. The third category is characterized by values ranging from 4.5-10.5 Ωm and represents the coarse-grained base of core LIX 7 made out of marine sand. Towards the northwest of the transect, comparatively high resistivity values reach the recent surface. This zone is interpreted as the transition fault zone between the Livadi swamp and the adjacent bedrock area. Together with the Livadi or Ainos fault system (Fig. 2-2), the fault system encountered near site LIX 7 may also be active during aseismic periods and coseismic events.

A more detailed comparison between the ERT results and the stratigraphy of core LIX 7/7A is problematic because more transects with closer electrode spacings would be needed. However, our results clearly depict the sharp contact between the basal marine sand and gravel unit and the overlying limnic silt deposits.

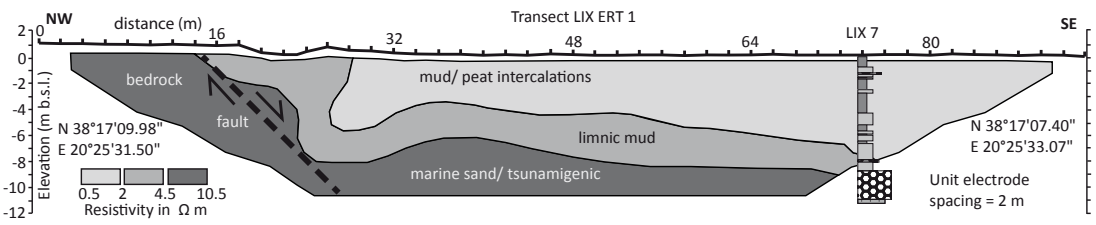

Fig. 2-11: Model resistivity section (simplified) based on electrical resistivity measurements along transect LIX ERT 1. Detailed map of the Livadi coastal plain with position of vibracorings and the ERT-transect are shown in Fig 2-2. Vibracoring site LIX 7 is located at meter 74 of the ERT transect. Maps based on Google Earth images (2005).

2.4.4 Pollen analysis

In this paper, we present, for the first time, palynological data retrieved from a sediment core drilled in the Livadi coastal plain. Pollen analysis was carried out in order to check the pollen record in layers of high energy impact against the background of the overall vegetation development. We selected 35 sediment samples from specific stratigraphic positions of vibracore LIX 7A which were prepared; subsequently, the pollen taxa were determined and the pollen grains were counted. Prepared samples that turned out to include no pollen grains were recorded with a total sum of nil.

The pollen record in the Livadi coastal area can be grouped in four main pollen zones (Fig. 2-12a+b). The base of the stratigraphy (Pollen Zone A) shows a moderate abundance but high diversity of grove taxa (e.g. *Pinus* sp., *Quercus* sp., *Ulmus* sp. and many others), as well as comparatively high numbers of typical swamp and marsh taxa (e.g. Cyperaceae p.p., *Sparganium* sp.). Moreover, Poaceae are high in most samples, and a moderate number of herbaceous pollen grain types (e.g. *Apiaceae* sp. and Compositae). Wetland plants increase in the second half of the zone.

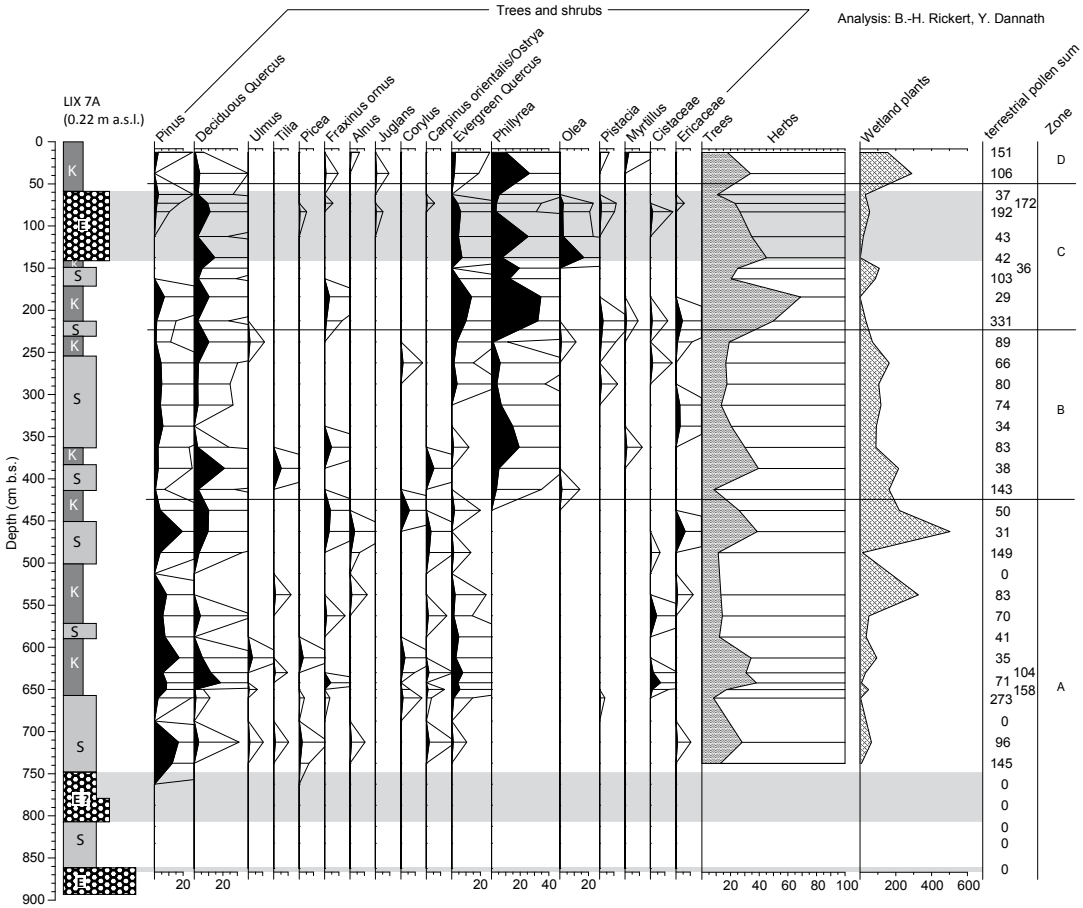

Fig. 2-12a: Pollen diagram of selected pollen types for vibracore LIX 7A drilled in the northern Livadi coastal plain with focus on trees and shrubs. Percentages based on the terrestrial pollen sum, lines with depth bars give x10 exaggeration.

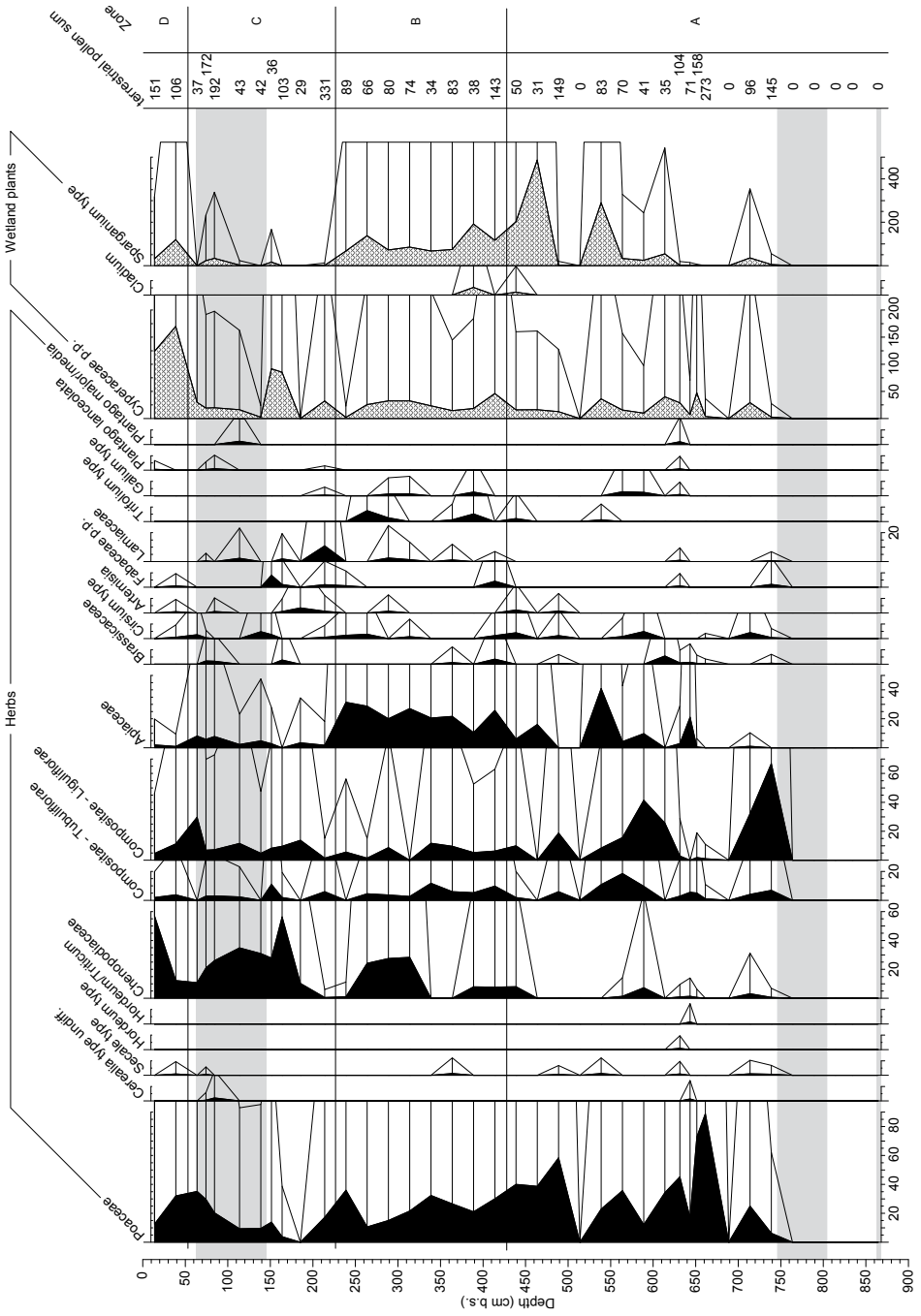

Fig. 2-12b: Pollen diagram for vibracore LIX 7A drilled in the northern Livadi coastal plain with focus on herbs. For detailed explanations see text. Stratigraphic position of high-energy tsunami deposits are shaded in grey. Further occurences (depth in cm/grain no.): *Abies* (83/1); *Betula* (287.5/1); Campanulaceae (212.5/1, 387.5/1); Cannabinaceae (630/1, 642/1); Caryophyllaceae (73); *Castanea* (642/2); *Celtis* (630/1); *Centaurea jacea* (73/3); *Cerastium* type (412.5/1, 562.5/1); *Echium* (62.5/1); *Ephedra disticha* (642/2); *Ephedra fragilis* (73/3); *Gratiola officinalis* (630/1); *Fraxinus excelsior* (630/1), *Juniperus* (12.5/1); *Knautia* (37.5/1); *Nymphaea* (83/1); *Ophioglossum* (73/1, 83/1); *Pediastrum* (562.5/1); *Polygonum aviculare* (83/1, 642/1); *Potentilla* type (73/2, 237.5/1); Ranunculaceae (73/1, 412.5/1, 630/1); Rosaceae (37.5/1, 237.5/1, *Rumex acetosa* type (83/1, 262.5/1, 630/1); *Salix* (83/1); *Sarcopterium* type (12.5/1, 212.5/1); *Vitis* (642/2); Fern spores (12.5/1, 630/2, 642/1, 650/1, 737.5/1).

Pollen Zone B is characterized by a reduced diversity of grove taxa. *Pinus* decreases. On the contrary, taxa of macchia and garrigue-type vegetation appear (*Phillyrea*, evergreen *Quercus*). Swamp and marsh plants are on a uniformly high level similar to Zone A, whereas the number of *Poaceae* sp. is slightly reduced. However, an increasing number of herbaceous-type pollen (*Apiaceae* and *Chenopodiaceae*) become prominent.

In Pollen Zone C *Olea* sp. is strikingly more abundant. The zone is characterized by high amounts of Chenopodiaceae, paralleled by a decrease of Poaceae. *Sparganium*, which was present throughout Zones A and B with considerable percentags, has almost completely disappeared from the LIX 7 pollen record. Pollen Zone D is characterized by abundant pollen of *Cyperaceae*, typical of the present swamp environment, and again by a rising amount of *Sparganium* pollen grains. The total amount of *Chenopodiaceae* found in Zone D is the highest of the entire profile. Pollen from maccia and garrigue-type vegetation is only represented by *Phillyrea* sp., whereas the amount of grove pollen is negligible.

It is striking that the uppermost stratigraphic unit consisting of allochthonous high-energy marine sediments is characterized by a clearly decreased terrestrial pollen sum. The marine sediments at the base of LIX 7A are even totally void of pollen grains.

2.4.5 Microfossil analyses

Microfossil analyses are an established scientific approach in palaeogeographical and palaeotsunami studies (e.g. Gupta 2002, Donato et al. 2008, Vött et al. 2009b, 2011a). Shell remains of foraminifera, ostracods and molluscs provide valuable information to be used for the reconstruction of long-term palaeoenvironmental conditions and short-term impacts.

Specific environmental needs of the organisms as well as major environmental changes are reflected in the composition of the microfaunal assemblage (Mamo et al. 2009). Especially ostracods and foraminifera tolerate a wide spectrum of environmental conditions, so that gradual shifts in the foraminiferal assemblage are represented by the abundance of individual species. Sudden changes in the environmental settings may be reflected in a non-gradual progression or sudden and temporary appearance of specific species as well as by a strongly mixed and unsorted microfossil record (Murray 2006).

We used 18 samples from vibracore LIX 7A, equivalent to core LIX 7 (closed core in 5 cm pipe), for detailed microfossil analyses focusing on the overall palaeogeographical evolution of the Livadi Bay as well as on the record of high-energy events. Fig. 2-13 depicts the results of microfossil studies compared to sampling depth and associated stratigraphic position of every investigated sample.

The base of LIX 7A is characterized by sandy deposits of marine origin with a fining upward trend regarding the grain size distribution. In sample LIX 7A/29, we found, on the one hand, an assemblage of foraminifer species typical of autochthonous shallow marine environments consisting of, for example, *Ammonia beccarii*, *Cibicides advenum*, *Elphidium* sp. and others). On the other hand, this sample also contains specimens from open water environments such as *Globigerina* sp. and *Globigerinella* sp. which document allochthonous influence from the outer, more open Ionian Sea to the Livadi foraminiferal record. Moreover, the encountered

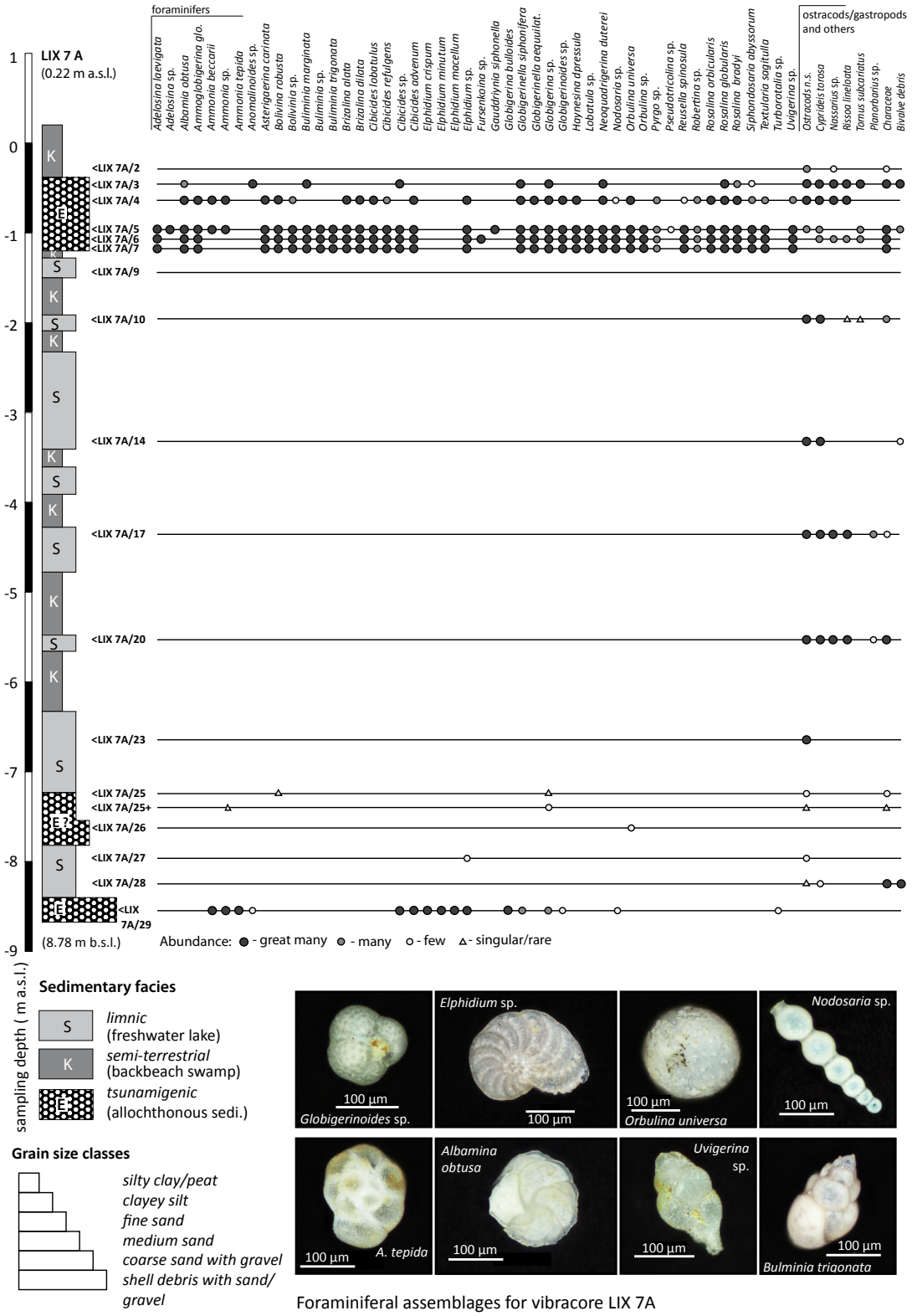

Fig. 2-13: Results of micro- and macrofossil analyses of selected samples from vibracore LIX 7A. Photos of selected specimens were taken by a polarized light microscope and a digital camera. Specimens were determined after Loeblich & Tappan 1988, Cimerman & Langer 1991, Poppe & Goto 1991, 2000, Murray 2006, Gupta 2002, Rönnfeld 2008.

foraminifera are not well preserved which indicates that they have undergone temporary subaerial weathering before the stratigraphical unit was covered by limnic deposits. The subsequent fine-grained, silt-dominated layers (samples LIX 7A/28, LIX 7A/27) only show a very thin microfossil record documenting quiescent water conditions of slightly brackish to predominating limnic conditions as shown by the occurrence of Characeae. Samples LIX 7A/26, LIX 7A/25+ and LIX 7/25 revealed few specimens of *Orbulina* sp. and *Ammonia* sp. in a fine sandy to muddy sediment which may indicate temporary marine influence. However, the marine signal is very weak. Starting with sample LIX 7A/23 up to sample LIX 7A/10, the subsequent sequence of mud and peat is completely void of any foraminiferal remains which documents a freshwater environment of purely (swampy to) limnic character. Limnic conditions seem to be directly linked to the strong discharge of karstwater springs which we found near coring site LIX 7A, obviously bound to the tectonic fault system detected nearby (Fig. 2). In sample LIX 7A/9 no microfossils were found at all. The subsequent samples LIX 7A/7, LIX 7A/6 and LIX 7A/5 were taken from a unit of marine fine sand. Both grain size and microfossil content reflect an abrupt change of the environmental conditions; altogether, more than ~35 different species were found. The microfossil assemblage is widely spread and highly diverse; the spectrum of species comprises fully marine, both benthic and planktonic (e.g. *Rosalina* sp., *Globigerina* sp.) to shallow marine (e.g. *Ammonia* sp., *Elphidium* sp.) and brackish specimens (e.g. *Cyprideis torosa*) (Murray 2006). The microfossil content of samples LIX 7A/4 and LIX 7A/3 shows a significant reduction in the total number of foraminferal specimens and a distinct increase of limnic and brackish gastropods and ostracods. LIX 7A/2 is characterized by the abundance limnic and semi terrestrial fossils. The distribution pattern of the microfossil record depicted in the upper part of Fig. 2-13 clearly documents the strictly temporary nature of strong saltwater inflow at site LIX 7A at some point of time during the recent past associated to the highly dynamic input of local to regional beach and marine sediments into the Livadi swamp.

2.4.6 XRF measurements and grain size analysis

Geochemical parameters as well as grain size data are useful indicators for the detection of significant facies changes in the stratigraphical record (Vött et al. 2002, Zhu & Weindorf 2009). (Vött et al. 2011a, 2013, Sakuna et al. 2012) detected abrupt environmental changes associated to high-energy impacts using Ca/Fe-ratios or Ca/Ti-ratios. Such a ratio is a helpful dimensionless tool for evaluating different processes in the sedimentary environment. In near coast-geological settings, a high Ca/Fe-ratio documents the input of biogenically produced, mostly marine calcium carbonate. Low Ca/Fe values caused by comparatively high iron concentrations may reflect dominating subaerial weathering and oxidation. Additionally, we use grain size data for interpreting the depositional setting and the geomorphodynamic potential. In this study, we used a grain size ratio of sand in relation to the sum of clay and silt. A high ratio indicates high-energy dynamics that produce strong input of sand, whereas a low ratio stands for predominating quiescent conditions associated to the deposition of silt and clay.

Geochemical parameters and grain size data show significant discrepancies between autochthonous quiescent and allochthonous high-energy deposits (Fig. 2-6). High-energy

sediments differ significantly in sorting and grain size distribution from sediments accumulated under predominantly quiescent conditions.

The general trend of transect I in Ca/Fe ratio and grain size distribution is summarized as follows. Fig. 2-6 shows that stratigraphic high-energy interferences are reflected by a significant peak in the Ca/Fe ratios. This is best visible for the upper high-energy unit found close to the present ground surface. Similar to Vött et al. (2011a, 2011b, 2013) we found that the massive input of biogenically produced marine carbonate in high-energy sediment layers produces a strong peak in the Ca/Fe curve. Moreover, curves depicted for the Ca/Fe ratio and the grain size index show a quasi-parallel structure.

2.5 Discussion

2.5.1 Identification of tsunami layers

The study area in the inner Gulf of Argostoli is sheltered from the influence of strong storm wave activities. This is due to the circumstance that storms winds come from western to northwestern directions (Medatlas 2004), so that the encircling mountain ranges of the Paliki Peninsula form an efficient protection system. The bathymetrical setting of the Gulf of Argostoli is characterized by shallow water depths between 25 m at the entrance and mostly around 5 m in the innermost gulf (UKHO 1992). We therefore conclude that the overall geomorphodynamic potential of storm-wave driven littoral processes in the inner gulf is low. On the contrary, in the open Ionian Sea, storms generate maximum wave heights of 6-7 m (Scicchitano et al. 2007, Soukissian et al. 2008).

The Holocene stratigraphical record along the Lixouri and Livadi coast presented in this paper documents repeated high-energy sediment influence. From a sedimentological point of view, most sedimentary characteristics associated with the encountered high-energy deposits are well known and described in detail from (sub-) recent (e.g. Kortekaas & Dawson 2007, Jankaew et al. 2008, Shaw et al. 2008, Goto et al. 2007, 2010a, 2010b, Chagué-Goff et al. 2011, Okal et al. 2011, Richmond et al. 2011, Bahlburg & Spiske 2012, Mitsoudis et al. 2012, Sakuna et al. 2012, Szczucinski et al. 2012) as well as from well-known historic and pre-historic tsunami events (e.g. Bondevik et al. 2005, Cisternas et al. 2005, Billi et al. 2008). Moreover, palaeotsunami studies along selected coasts of the eastern Ionian Sea has also revealed comparable geomorphological and sedimentary palaeotsunami traces (Vött et al. 2006d, 2007a, 2008, 2009a, 2009b, 2010, 2011a, 2011b, 2013). It is well known from historic accounts and numerous tsunami and earthquake catalogues that tsunami events in the Mediterranean Sea are very frequent with relatively short recurrence intervals lying between decades and centuries depending on the period under observation (e.g. Antonopoulos 1979, Guidoboni & Ebel 2009, Hadler et al. 2012). Sedimentological, geochemical and microfaunal palaeotsunami features encountered in vibracores along transects I to III comprise the following: (i) sandy to gravelly intersections of autochthonous silt-dominated deposits bound to erosional unconformities; (ii) fining upward of grain size with high-energy sedimentary units; (iii) thinning landward of overall consistent high-energy deposits; (iv) rip-up clasts of underlying units incorporated in high-energy deposits; (v) strong input of biogenically produced calcium carbonate during high-energy events through faunal shell

debris; (vi) temporary input of clearly allochthonous fauna during high-energy events. High-energy event layers were found in stratigraphically consistent positions all over the study area.

Especially strong and abrupt marine signals are documented by the high diversity and abundance of marine microfossils encountered in down- and up-core positions at site LIX 7A (Fig. 13, samples LIX 7A/29, LIX 7A/3 to LIX 7A/7). These signals are associated to sedimentary features typical of high-energy dynamics which leads us to the conclusion that corresponding layers reflect strong tsunami impact on the Livadi coastal plain. The fact that samples LIX 7A/25, LIX 7A/25+, LIX 7A/26 show a slight marine influence may rather be due to the short distance to the palaeo-coastline (wind drifted material?) than to the influence of an extreme event.

Moreover, several vibracore profiles along transects I and II (Figs. 2-4 and 2-8; cores LIX 3, 4 and 10) show that allochthonous event layers underwent subaerial weathering after sediment deposition. This implies a deposition above the local sea level at that time - a phenomenon which is well known to have happened during (palaeo)-tsunami landfall (Vött et al. 2010, 2011a, 2011b, 2013). Finally, in certain stratigraphic positions, we encountered beachrock-type cemented allochthonous sand (Fig. 2-4; cores LIX 3 and 12). After Vött et al. (2010) ex situ-high-energy deposits accumulated by tsunami processes potentially undergo decalcification and carbonate cementation of upper and lower parts of the tsunamite, respectively, triggered by percolation of rain water and subaerial weathering.

Along the Lixouri and Livadi shores, high-energy deposits were encountered in consistent stratigraphic positions over distances more than 5 km parallel to the coast (transect I, Fig. 2-4) and more than 850 m inland (transect III, Fig. 2-9). The Livadi geological archive turned out to be highly valuable in terms of palaeotsunami research as it documents the repeated interference of a predominantly quiescent swamp environment by the input of allochthonous marine sand. Along all vibracore transects in the study area, we found that pre-event conditions were re-established after the high-energy tsunami impact.

The combination of event-stratigraphical characteristics, geochemical fingerprints and microfaunal evidence let us conclude that the high-energy deposits encountered in the study area were caused by tsunami impact. Storm influence as well as superordinate alluvial (torrential) or mass denudation processes were not found within the littoral deposits or were beyond the analytical resolution of the methods applied in this study.

Based on palynological data from core LIX 7A, it is striking that pollen samples taken from the youngest tsunami candidate layer which was detected between 1.20-0.39 m b.s.l. (pollen sampling depths 1.52 m b.s.l., 1.39 m b.s.l., and 1.13 m b.s.l., see Figs. 2-11a, 2-11b) are characterized by a significantly reduced terrestrial pollen sum. This can be interpreted as the result of strong dilution of the pollen concentration due to strong inundation by marine waters and the abrupt and temporary increase of the sedimentation rate. A similar phenomenon was already observed for tsunami sediments retrieved from the Lake Voulkaria in northern Akarnania, northwestern mainland Greece (Vött et al. 2009b). Our data thus indicate that strong inundation of coastal wetlands by major tsunami impact considerably affects the pollen record. This has to be taken into account when pollen from coastal geoarchives is regarded as

base for reconstructing the local vegetation history.

This is supported by the high amount of Chenopodiaceae, indicating marine influence, and the paralleling low amount of Sparganium, which is an indicator of more limnic conditions.

Our study shows that the Livadi coastal plain offers an excellent sediment trap for palaeotsunami deposits. The funnel shape coastline configuration of the Gulf of Argostoli which opens to the south and is directly exposed to the Ionian Sea and the Hellenic Arc is expected to play a major role in tsunami wave propagation inside the gulf. A tsunami triggered in the Ionian Sea and travelling northwards will be accelerated in the funnel shaped coast and is expected to produce highest run up values along the inner Gulf of Argostoli.

Palaeotsunami findings in the inner Argostoli Gulf are in very good accordance with palaeotsunami traces described from the cul de sac-type southeastern annex of the Gulf, the Bay of Argostoli (Vött et al. 2013). This bay is known as one of the best natural storm-protected harbor settings in the eastern Mediterranean.

2.5.2 Local event geochronostratigraphy

The local tsunami event geochronostratigraphy for the inner Gulf of Argostoli is based on ^{14}C-AMS dating's and archaeological age estimations of diagnostic ceramic fragments. Altogether, traces of five different tsunami generations were found in the Lixouri and Livadi coastal plains which bear a clear regional to even supra-regional signature.

Tsunami generation I

The oldest tsunami generation dated in the study area was found in transect III at the base of LIX 7. Sample LIX 7/22 PR yielded an age of 5834; 5710 cal BC which has to be considered as *terminus ante quem* for the corresponding tsunami event. In a supraregional context, this age corresponds well with an event of which was dated to around 5900-6000 cal BC in the Palairos coastal plain (Vött et al. 2011a), the Bay of Aghios Nikolaos and the Sound of Lefkada (Vött et al. 2009a), as well as the ancient harbour site Pheia in the western Peloponnese (Vött et al. 2011b). We assume that these traces document the same tsunami event that affected coastal Akarnania, the Ionian Islands and the western Peloponnese.

Tsunami generation II

At site LIX 2, sample LIX 2/19 PR provided a *terminus ante quem* of 4337; 4261 cal BC for an older tsunami event. This age is regarded as highly reliable as it marks the onset of sediment deposition right after the event. On a supra-regional scale, this fits with a palaeotsunami record from Pheia, the ancient harbour of Olympia (western Peloponnese), which was dated to 4300 ± 200 cal BC (Vött et al. 2011b). Another correlating deposit is described from the Palairos-Pogonia coastal plain in Akarnania dated to around 4400 cal BC (Vött et al. 2011a). On a local scale, correlating traces were found near ancient Krane which is located only some 15 km to the south-southeast of the Livadi coastal plain at the eastern end of the inner Bay of Argostoli, a cul de sac-type annex of the southern Argostoli Gulf. Here, this tsunami event was dated to 4150 ± 60 cal BC (Vött et al. 2013). Taking into account the various uncertainties with respect to radiocarbon dating of tsunami deposits (Section II, Fig. 2-9), it is assumed

that these traces document the same tsunami event that took place in the first half of the 5th millennium BC and affected parts of coastal Akarnania in the north, Cefalonia on the Ionian Islands as well as the western Peloponnese.

Tsunami generation III

We also found singular records of tsunami imprint which were difficult to correlate. With regard to the palaeotsunami record, coring site LIX 6 provides two maximum ages for an older event. The corresponding samples were taken directly out of the event layer including lots of reworked material. Sample LIX 6/10+ PR yielded an age of 5616; 5537 cal BC and sample LIX 6/7 PR an age of 3024-2911 cal BC. Provided that both maximum ages are reliable, the event took place at or after 3024-2911 cal BC. From a stratigraphical point of view, this tsunami deposit may correlate with the basal tsunami trace encountered at site LIX 10 at transect III. Here, sample LIX 10/10 M was taken from the base of the tsunami layer. The resulting age of 1972; 1877 cal BC must thus be regarded as maximum age (*terminus ad* or *post quem*). This tsunami generation may therefore be dated to the time between the beginning of the 2nd millennium BC and is possibly consistent with an event that hit the Bay of Palairos-Pogonia during the same time period (Vött et al. 2011a).

Tsunami generation IV

The mid-position tsunami layer encountered in core LIX 10 is well dated by sample LIX 10/7+ HR yielding an age of 974; 857 cal BC as *terminus post quem* and by sample LIX 10/6 M yielding an age of 896; 804 cal BC as *terminus ad* or *post quem* for the event. Note that the second age is regarded as less reliable because it is derived from a marine mollusc and the (palaeo-) reservoir effect was only estimated (Section IV, Fig. 7). Vött et al. (2013) describe a tsunami deposit in the Koutavos Bay near ancient Krane that was dated to around 650 ± 110 cal BC. Of course, it may be possible that the Lixouri deposit correlates with this event. Alternatively, a potential correlation candidate is a major event that is recorded in the Lake Voulkaria sediment trap in nearby coastal Akarnania (Vött et al. 2006d, 2009b) which was dated to around 1000 cal BC.

Tsunami generation V

At coring site LIX 12, sample LIX 12/5+PR yields a maximum age of 1349-1411 cal AD for the overlying tsunami deposit. At coring site LIX 5, a plant remain out of an autochthonous peat layer overlying the stratigraphically consistent tsunami deposit dates to 1869-1950 cal AD (Fig. 2-4). The youngest tsunami imprint encountered at site LIX 7 is dated to 780-869 cal AD (sample LIX 7/7+ PR) and 225-316 cal AD (sample LIX 7/5 PR2), respectively, as *termini post quos* for the event. Sample LIX 7/4 PR (1654-1797 cal AD) is considered to have been affected by reworking effects or contamination by younger root material.

Due to the fact that the tsunami deposits at sites LIX 7 and LIX 12 were found in consistent stratigraphical positions, we conclude that the best-fit age for this event is between 780 cal AD and recent times. Unfortunately, the time interval for the tsunami generation V event cannot be reliably narrowed to a closer time span because there are obvious calibration problems with dating marine plant material (Section 4.2, Table 2-1).

However, in a supra-regional context, it may be speculated that this event also hit the southern Peloponnese where Scheffers et al. (2008) describe tsunami traces dated to around 1300 cal AD. On a local scale, potentially correlating deposits are described from the Koutavos Bay near ancient Krane (Argostoli Bay) where tsunami impact was dated to around 930 cal AD or later (Vött et al. 2013). From Lefkada Island, Vött et al. (2006d) report on tsunami traces dating to 1000-1400 cal AD. In the wider area of the eastern Mediterranean, palaeotsunami impact was dated to the time between 930-1170 cal AD for Sicily (Smedile et al. 2011). We therefore hypothesize that the tsunami traces at Livadi may belong to a major impact which hit the shores of the Ionian Sea between Lefkada, Cefalonia, the Peloponnese and possibly also Sicily around 1300 cal AD.

2.5.3 Relative sea level evolution at the Livadi coastal plain

For the eastern Mediterranean there are many studies dealing with the reconstruction of relative sea level (RSL) fluctuations based on sedimentological and geoarchaeological indicators (e.g. Pirazzoli et al. 1994, Kraft et al. 2005, Vött 2007, Engel et al. 2009). There are considerable differences in the local relative sea level evolution in the Mediterranean due to differences in regional tectonics, sediment compaction, sediment supply, and coastal dynamics (Vött 2007, Brückner et al. 2010). On Cefalonia Island, co-seismic movements during the 1953 earthquake resulted in a 0.3-0.7m "quasi-rigid-body uplift and westward tilting" of the central part of Cefalonia island (Stiros et al. 1994). At the same time, along the coastline of Lixouri almost no co-seismic movement was detected. Lagios et al. (2007) and Hollenstein et al. (2006, 2008) studied the results of high resolution DGPS measurements, which show that distinct tendencies in different vertical and horizontal motion of Cefalonia Island are given. The general trend is that the western part of the Paliki Peninsula is being continually downwarped by the ongoing subduction whereas episodic relaxation goes hand in hand with coastal uplift effects during major earthquakes. Both types of tectonic dynamics are expected to leave their traces in the RSL history of the study area. Tsunami events can be considered as temporary and short term RSL highstands with an enormous potential to influence the coastal configuration and the overall coastal evolution.

The reconstruction of the local RSL evolution for the study area was accomplished by dating peat samples from paralic swamps and one articulated mollusc. Paralic swamps are typical of coastal environments and their surface adjusted to the average sea level. After Vött (2007) the negative effect of peat compaction has to be considered and differs in its spatial extent depending on the grain size, organic content, water saturation and thickness of the overlying sediments. The RSL band reconstructed for the Livadi coastal plain is based on eight sedimentological sea level markers and calibrated radiocarbon dates (Reimer et al. 2009, Fig. 2-14, Table 2-1).

In general, the presented RSL band correlates well with RSL curves from Elis (Vött 2007), Messenia (Engel et al. 2009) and Elis (Kraft et al. 2005) with quasi linear and logarithmical progressions. During the Holocene, the palaeogeographical evolution of the Livadi coastal area shows, that the local RSL has never been higher than at present.

However, it may be speculated that the unexpected peak in the RSL band around 3950-3750

cal BC (sample LIX 7/12+ PR, Table 2-1) - if not due to local differences in the tectonics history of different sites - is the result of a co-seismic uplift in the order of 1 m comparable to the one described for the 1953 earthquake (Stiros et al. 1994), followed by a co-seismic subsidence of secondary order dated to around 3700-3650 cal BC (sample LIX 2/16+ PR, Table 1). For coastal Akarnania and the western Peloponnese, Vött (2007) identified periods of intense tectonic activities around 4000, 2500, 500 and 250 cal BC as well as 250 and 1250 cal AD. Against this background, the peak in the RSL band at around 3950-3750 cal BC found for the Livadi coastal plain may reflect supra-regional mid Holocene seismo-tectonic activities. However, our local RSL band has only a low resolution so that further up- and down-movements may exist but are not depicted in Fig. 2-14.

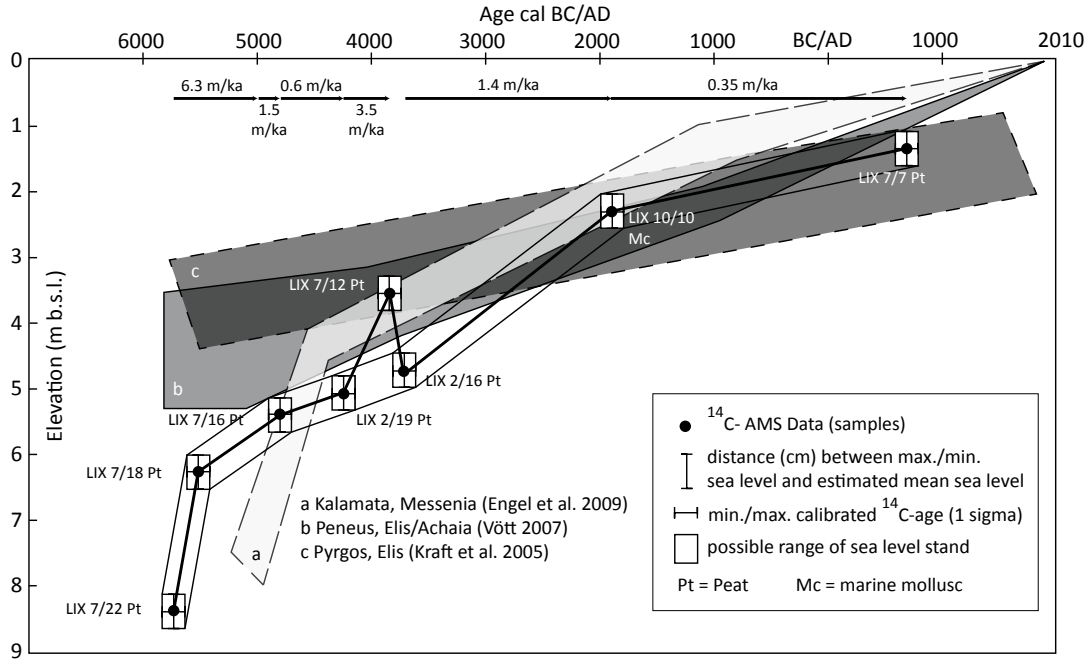

Fig. 2-14: Relative local sea level evolution of the Livadi coastal plain since the mid-Holocene and comparative sea level bands for the Peloponnese (Kraft et al. 2005, Vött 2007 and Engel et al. 2009).

2.6 Conclusions

The Lixouri and Livadi coastal plains in the inner Gulf of Argostoli (Cefalonia Island, Greece) were investigated by sedimentological, geomorphological, geophysical, geochemical, palynological and microfossil analyses. Our main objectives were to check the Holocene stratigraphical record for major high-energy impacts and to reconstruct the palaeogeographies of the study area. Our stratigraphical data is based on vibracores and electrical resistivity measurements together with geochemical analyses. Radiocarbon AMS dating allowed to establish a detailed event-geochronostratigraphy as well as to obtain insight in the relative local sea level evolution. Based on our results the following conclusions can be made.

(i) Sedimentary sequences show that the autochthonous sedimentation in the inner Argostoli Gulf is repeatedly interrupted by allochthonous sandy to gravelly deposits associated to abrupt and temporary high-energy impact.

(ii) Against the background of prevailing storm winds and waves from the western quadrant, the narrow north-south trending Gulf of Argostoli is well protected from storms. It is thus excluded that high-energy interferences of the coastal stratigraphies is due to storm wave activity. Sediment composition and local geomorphological settings also exclude alluvial or denudation processes as potential causes.

(iii) Allochthonous high-energy layers can be stratigraphically correlated over more than five kilometers parallel to the coast and more than 800 m inland (Fig. 2-2). High-energy deposits show characteristic sedimentary features typical of tsunami influence such as basal erosional unconformities, fining upward and thinning landward sequences and rip up clasts. It is thus concluded that high-energy influence is due to repeated tsunami landfall.

(iv) Detailed microfaunal studies prove that the Livadi swamp was completely inundated by tsunami waters, up to 800 m distant from the present shoreline, which left behind allochthonous assemblage of foraminifera shells.

(v) Due to its direct exposure to the Hellenic Trench and a well-known tsunami and earthquake history, a possible tsunami inundation scenario starts with northward prograding tsunami waves entering the Gulf of Argostoli. By the tube-like coastline configuration as well as by refraction, diffraction and reflection effects, tsunami waters are accelerated and led into the innermost parts of the gulf.

(vi) Our event-geochronological data document five different palaeotsunami generations since the mid-Holocene. Tsunami generation I took place in the early 6th millennium BC, tsunami generation II before around 4250 cal BC, tsunami generation III probably at the beginning of the 2nd millennium BC, tsunami generation IV in the beginning of the 1st millennium BC and tsunami generation V after 780 cal AD.

(vii) Comparing the palaeotsunami record of the inner Argostoli Gulf with other coastal areas in the Ionian Sea region shows outstanding correlations which underline possible mega-tsunami events of supra-regional nature at the beginning of the 6th millennium BC and before around 4250 cal BC. Especially the Livadi coastal plain turned out to be an excellent sediment trap for tsunami signatures of supra-regional nature.

(viii) Our results show that considerable coastal changes are often initiated and controlled by tsunami landfall. The palaeogeographical evolution, namely the shifting or destruction of the coastline, must be considered in the light of tsunamigenic dynamics. The role of gradual coastal processes and changes seems to be restricted to the re-arrangement of sediments after major impacts.

(ix) Palaeo-sea-level studies at the Livadi coastal plain show that the relative local sea level has never been higher than at present. A mid Holocene sea level highstand may be associated to seismic crustal movements at that time, going hand in hand with tsunami impact.

3 Geo-scientific evidence of tsunami impact in the Gulf of Kyparissia (western Peloponnese, Greece)*

Abstract. In this study, we present geo-scientific evidence of repeated tsunami impact on the coastal lowlands of the Gulf of Kyparissia between Cape Katakolo and Lake Kaiafa. As known from literature and previous geo-scientific studies along the coasts of the eastern Ionian Sea, tsunami influence in the area is a strong and dominant factor in the overall coastal evolution. We combined sedimentological, geomorphological and geophysical studies with geochemical and microfaunal analyses to reconstruct the palaeoenvironmental evolution of the former Mouria Lagoon near Aghios Ioannis and adjacent areas, namely around Kato Samiko and the former Agoulenitsa Lagoon. Our main objective was to look for traces of palaeotsunami impact with the sedimentary records of different coastal geo-archives. In the area of the former Mouria Lagoon we found four distinct allochthonous sediment layers of tsunamigenic origin that are at least traceable up to 2 km inland from the present day coastline. Three of the high-energy events caused major environmental changes and obviously lead to massive modifications of the palaeo-coastline. Moreover, our results show that the local relative sea level rise has its maximum at present and has never been higher during the Holocene. High-energy deposits encountered near Kato Samiko are characterized by strongly unsorted sediments including marine shell debris mixed with abundant archaeological remains deposited on top of an erosional unconformity. Here, high-energy sediments occur as channel deposits out of allochthonous coarse-grained sediments that are clearly detectable by the combination of electrical resistivity measurements and terrestrial vibracoring. The local event-geochronostratigraphy was realized by radiocarbon dating and shows that a first tsunami event hit the Mouria Lagoon and probably also the coastal plain of Kato Samiko in the 5th millennium BC (tsunami generation I). A second tsunami event was dated to the mid to late second millennium BC (tsunami generation II) while tsunami generation III took place between the 1st cent. BC and the early 4th cent. AD. Tsunami generation IV is most probably related to one of the well-known tsunami events that affected wide areas of the eastern Mediterranean in 365, 521 or 551 AD.

3.1 Introduction and regional setting

The eastern Ionian Sea is one of the seismotectonically most active regions in the Mediterranean (Hollenstein et al. 2008). The fact that the study area is subject to a high tsunami risk has been known for many decades (e.g. Cocard et al. 1999, Hollenstein et al. 2008). Earthquakes, volcanism and submarine mass movements along the subduction zone of the Hellenic Trench are the main factors in triggering tsunamis along the coasts of the Peloponnese (e.g. Papazachos & Dimitriu 1991, Koukouvelas et al. 1996, Benetatos et al. 2004). Historical accounts (e.g. Antonopoulos 1979, Soloviev 1990, Soloviev et al. 2000, Ambraseys & Synolakis 2010) as well as geoarchaeological studies show that extreme events may considerably affect the overall coastal evolution (e.g. Soloviev et al. 1990, Vött et al. 2009a, Hadler et al. 2013). In some cases, tsunamis must also be held responsible

* This chapter will be submitted to Zeitschrift für Geomorphologie N.F. Suppl. Vol. as: Willershäuser, T., Vött, A., Hadler, H., Fischer, P., Röbke, B., Ntageretzis, K. & Brückner, H.: Geo-scientific evidence of tsunami impact in the Gulf of Kyparissia (western Peloponnese, Greece).

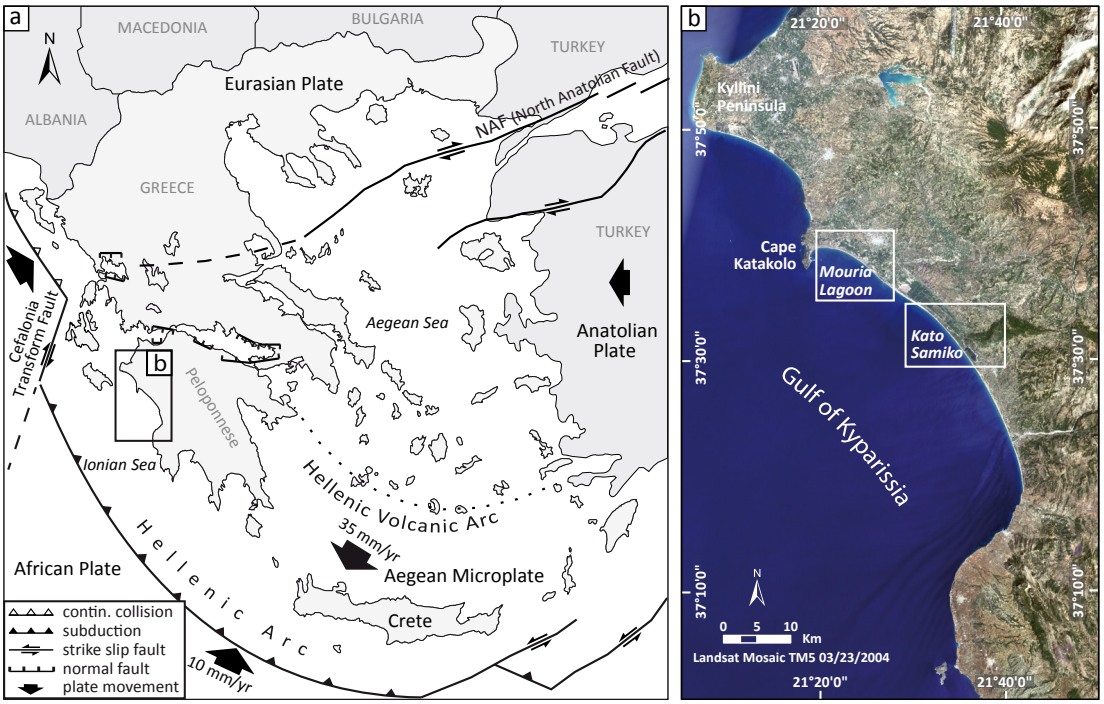

Fig. 3-1: Tectonic and topographic overview. (a) Tectonic situation of the eastern Mediterranean with special focus on the study area at the western Peloponnese and the eastern Ionian Sea (map modified after Celws et al. 1989, Sachpazi et al. 2000, Van Hindsbergen 2006) (b) Both study areas are situated on the western Peloponnese at the Gulf of Kyparissia (map modified after Landsat TM 5, 2005).

for the destruction of ancient coastal settlements and infrastructure (Hadler et al. 2011a, 2011b, 2013, Vött et al. 2011a, 2011b, 2013). As known from recent events (e.g. Japan 2011), coastal areas that have once been affected by tsunami impact are highly prone to future tsunami landfall (Vött et al. 2013, ZfG ed.). In order to estimate the tsunami hazard and to enable a realistic tsunami risk management, it is necessary to reveal the palaeotsunami record for different coastal areas. Although many historical tsunami events are recorded in tsunami catalogues for the eastern Mediterranean and Greece, there is still a wide gap in the palaeotsunami record (Hadler et al. 2012).

To fill in these gaps and to assess the extent and consequences of known historical extreme events, geoscientific studies aim at the detection and identification of sedimentary traces left by palaeotsunami events in near-coast geological archives. Sedimentary characteristics of recent and subrecent tsunami deposits for example comprise (a) shell debris layers, (b) mixed littoral and sublittoral material, (c) a multi-modal grain size distribution, (d) rip up-clasts out of pre-existing material, (e) basal erosional unconformities, (f) fining upward and thinning landward tendencies, (g) lithified beachrock-type calcarenites, (h) washover deposits and (i) backwash channels (e.g. Dawson & Stewart 2007, Dominey-Howes et al. 2006, Vött et al. 2009a, 2009b, 2010, 2011a, 2011b, Bahlburg & Spiske 2012, Willershäuser et al. 2011a, 2011b, 2013). However, to evaluate whether sedimentary traces of high-energy events were left by tsunami or storm impacts, field and laboratory data have always to be considered against the local geomorphological background.

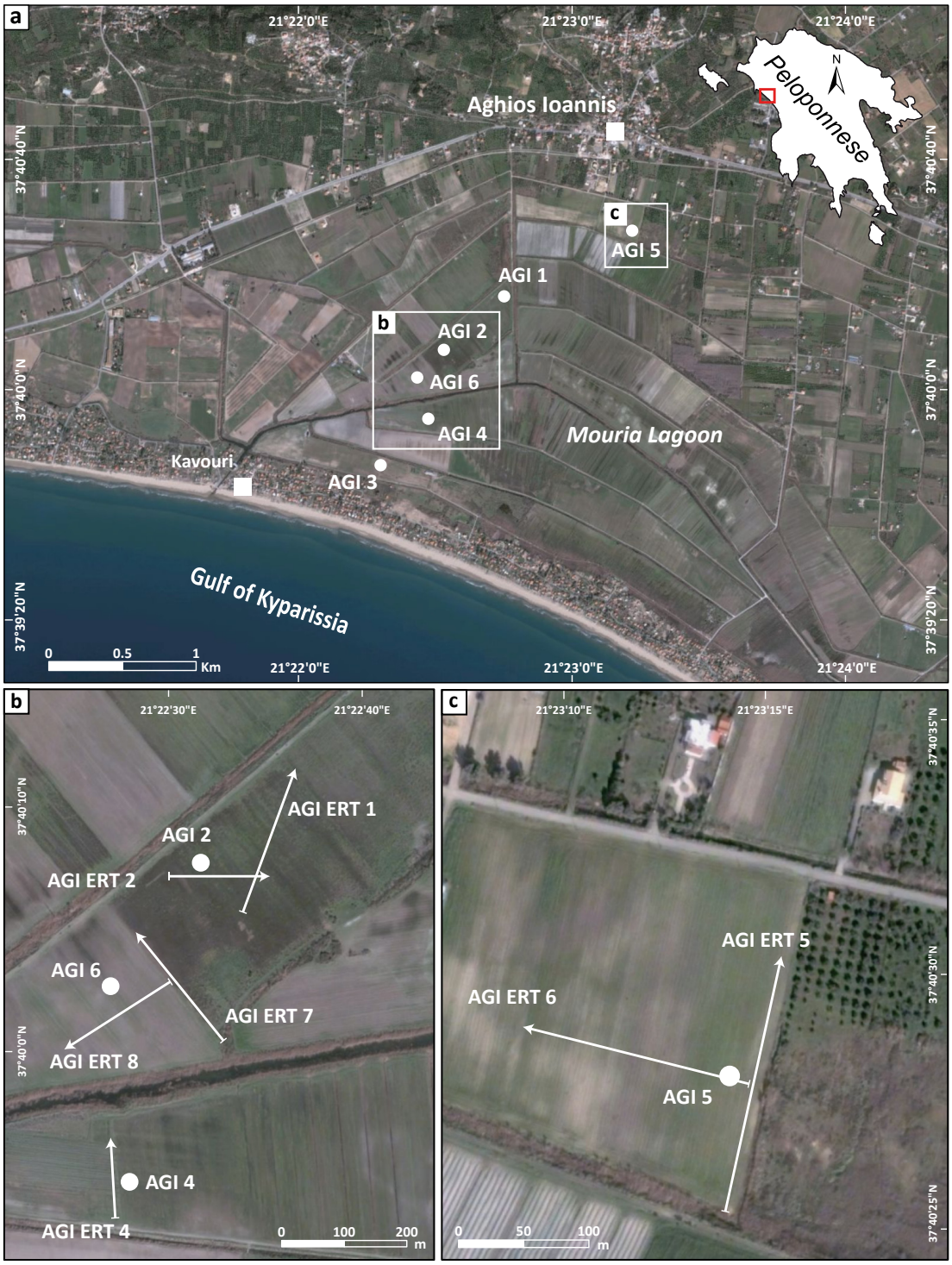

Fig. 3-2: Overview of the Mouria Lagoon (a), and detailed view study sites (b, c). Vibracore locations are marked by white dots and electrical resistivity transects are shown as white lines with measuring-direction (maps modified after Bing Aerial Maps, 2013).

The study areas considered in this study are located along the Gulf of Kyparissia and comprise the former Mouria Lagoon near Aghios Ioannis and the coastal plain of Kato Samiko at the southern fringe of the former Agoulenitsa Lagoon (Fig. 3-1).

Along the Gulf of Kyparissia between Cape Katakolo and the southern end of the Agoulenitsa lagoon near Kato Samiko, palaeogeographical studies by Kraft et al. (2005) document permanent changes of the coastal configuration. A NNW-SSE trending barrier system is about 30 km long, reaching from the Neogene marls of Cape Katakolo to the limestone outcrops of Kato Samiko (IGME 1980b, 1982b). This system is described by Kraft et al. (2005) as consisting of different generations of Holocene beach ridges, namely the early Helladic Mouria barrier and the modern Agoulenitsa barrier. According to Kraft et al. (2005) the Alpheios river delta is mainly responsible for the sediment supply and the subsequent littoral processes along the shores of the Gulf of Kyparissia.

Drained since the 1960's, the former lake bottom of the Mouria Lagoon presents the modern terrain surface with most parts of it lying below the present sea level (Pillay 1966). The area is being continuously drained by large electric pumps and used for agricultural purposes. Our study sites near Aghios Ioannis are located behind the recent coastal barrier accretions, on recent dune fields, on the former bottom and the former shore of the Mouria Lagoon (Fig. 3-2).

Kato Samiko, the second study area, lies adjacent to the southwestern fringe of the former Agoulenitsa Lagoon, which spans the coastal area between ancient Samiko to the south and the mouth of the Alpheios River to the north. Like the Mouria Lagoon, it has been drained in the 1960s (Pillay 1966, Fig. 3-9). The ancient settlement of Samiko (Bisbee 1937) is located at around 150 m above present sea level (m a.s.l.) on top of a ridge of the Lapithas mountains out of Cretaceous limestone some 900 m to the south of the Kato Samiko coastal plain (IGME 1982b). Our study area is located to the north of ancient Samiko in a small W-E trending valley opening towards the southeastern fringe of the former Agoulenitsa lagoonal environment (Fig. 3-9). Strabo (63 BC - 23 AD) described the palaeogeographical situation of the ancient settlements as follows: […] "*near the sea, and above it is situated a lofty hill which is in front of the Samicum of to-day, on the site of which Samus once stood, and therefore Samus was not visible from the sea. Here too, is a plain called Samicum; and from this one might get more conclusive proof that there was once a city called Samus*" (Strabo Geography VIII 3.20-21 after Jones 1923).

Kraft et al. (2005) describe swales and ridges of a former sand barrier system and suggest approximate shoreline reconstructions for the time since the mid-Holocene. In accordance with Strabo and Holocene sea level curves for the Peloponnese (Vött 2007, Engel et al. 2009), these shoreline reconstructions indicate a continuous seaward shifting of the coastline. Some rocky outcrops located below ancient Samiko bear archaeological remains from Bronze Age or even earlier times (Kraft et al. 2005) and are suggested to have been islands (Rohn & Heiden 2009) at the time when they were occupied.

In order to reconstruct the (palaeo-)tsunami history of the Gulf of Kyparrisia, the main aims of our studies are (i) to check the local stratigraphical record for allochthonous high-energy

deposits and to discriminate between tsunami and storm signals, (ii) to establish a detailed geo-chronological framework along a transect crossing the former Mouria Lagoon inland from the recent coastline and (iii) to reconstruct the Holocene palaeogeographical setting and relative sea level changes in the Kato Samiko coastal area.

3.2 Methods

For vibracore AGI 5A, also detailed photospectrometric and magnetic susceptibility measurements and microfossil analyses were carried out. The color was identified by a Minolta CM-600d Spectrophotometer with a fixed aperture setting of 8 mm. The colorimeter uses a silicon photodiode array (dual 36-element) detector and a light source of pulsed xenon lamp with UV cut filter. The illumination/viewing system is arranged with 8-degree viewing angle (diffused illumination) for the detection of specular component included (SCI) and specular component excluded (SCE) (Konica-Minolta 2013). The head of the device was protected by a glass window and calibrated with a white and black standard plate. The output of measured color data was the CIE-L*a*b* standard.

Magnetic susceptibility measurements were realized using a Bartington MS3 Magnetic Susceptibility Meter and a MS2K Surface Sensor with a response area 25.4 mm^2 in diameter and maximum depth of response of 8 mm (Dearing 1999). The measuring periods were defined by 1 sec and a calibration after 10 measurements as well as a control sample for post processing and shift corrections.

Foraminiferal studies were carried out using ~15 ml of sediment extracted from relevant stratigraphical units. These samples were sieved in fractions of > 0.4 mm, 0.4-0.2 mm, 0.2-0.125 mm and < 0.125 mm and subsequently analysed using a stereo microscope (type Nikon SMZ 745T). Digital photos were taken from selected specimens using a light-polarizing microscope (type Nikon Eclipse 50i POL with Digital Sight DS-FI2 digital camera back 5 MP and NIS Elements Basic Research 4 Software (Nikon 2012)).

To detect subsurface structures, a total number of 12 electrical resistivity measurements (ERT) was realized using a Syscal R1 Plus Switch 48 multi-electrode unit. A Wenner-Schlumberger array was applied for all ERT transects. In comparison with sedimentary evidence retrieved from vibracoring, the resistivity transects allow to interpret the subsurface stratigraphical conditions. Electrical resistivity data were processed using the software RES2DINV applying the least-squares inversion by a quasi-Newton method (Loke & Barker 1996). Position and elevation data of each coring site and the ERT transects were obtained by means of a Topcon Hiper Pro differential GPS System (FC-250 Handheld) with a total resolution accuracy of +/- 2 cm.

In this study, the overall geochronological framework is based on 13 ^{14}C-AMS ages from organic samples and marine shells as well as on archaeological age determination of diagnostic ceramic fragments. For radiocarbon dating, we preferred samples out of autochthonous deposits like peat or articulated marine molluscs in living position to avoid age inversions due to reworking. Samples out of reworked material only yield a maximum age for the event. Calibration was accomplished using the software Calib 6.0 after Reimer et al. (2009).

3.3 Traces of high-energy impact from the former Mouria Lagoon

Six vibracores (AGI 1-6) were arranged in a transect across the coastal plain of Aghios Ioannis in order to reconstruct the palaeogeographical evolution of the former Mouria Lagoon and to identify traces of high energy impact. With a total length of 2.2 km, the SSW to NNE trending vibracore transect reaches from the present day coastline in landward direction and covers a wide area of the former Mouria Lagoon (Fig. 3-2).

3.3.1 The AGI vibracore transect and event stratigraphical correlations

The vibracore transect starts with AGI 3, located some 350 m distant from the recent beach in a distal landward position to the present beach ridge. Vibracore AGI 5/5A was drilled in a maximum distance of nearly 2.2 km at the former shore of the former Mouria Lagoon. It is significant that the present surface lies about up to 2.5 m below present sea level and is coupled to the drainage systems.

The base of AGI 3 (ground surface at 0.66 m b.s.l., N 37°39‘46.8“, E 21°22‘16.9“) is characterized by homogenous silty fine sand of greyish beige colour and organic remains (10.66-10.47 m b.s.l). Subsequently, a sequence of well sorted medium to fine grained sand documents on-going shallow marine conditions with sporadic occurrence of mollusc fragments (10.47-6.85 m b.s.l.). From 6.85-6.40 m b.s.l., the sediment shows an increasing amount of organic matter that finally forms a peat layer, indicating the establishment of semi-terrestrial conditions (6.40-6.11 m b.s.l.). A transition layer including reworked peat clasts is obviously associated to a sudden environmental change (6.11-5.97 m b.s.l.). Locally enriched with freshwater macrofossils, the following unit marks an environmental change towards limnic conditions. Abruptly appearing lagoonal conditions (5.14-2.54 m b.s.l.) prevail the upper part of the core as documented by homogeneous mud with fairly well preserved molluscs. Occasionally, macrofossils also occur as shell debris layers and thus indicate the reworking of autochthonous deposits. A sharp erosional contact marks the boundary to a stratum of fine to medium grained sand that covers the lagoonal deposits (2.54-2.16 m b.s.l.). The grey sand unit is characterized by several fining upward sequences alternating from medium sand to silty fine sand. Further up-core (2.16-1.30 m b.s.l.), the layered sand is weathered and mixed up with numerous mollusc fragments. Finally, the upper sandy layer of core AGI 3 (1.30-0.66 m b.s.l.) incorporates many plant remains and correlates to recent dune formation.

The lower part of AGI 4 (ground surface at 2.05 m b.s.l., N 37°39‘54.3“, E 21°22‘27.9“) consists of well sorted marine silt and fine sand (9.05-4.97 m b.s.l.) with brownish root channels and signs of initial weathering such as oxidic spots. From 4.97-4.67 m b.s.l., we found brownish sand with an increased content of organic substance as well as mollusc fragments. Water-saturated silty fine sand of whitish to grey colour dominates the subsequent sedimentary unit (4.67-3.65 m b.s.l.). On top of it, we encountered muddy lagoonal deposits that document a change towards quiescent environmental conditions (3.65-3.00 m b.s.l.). A thin layer of fine sand intersects the lagoonal sequence (3.43-3.41 m b.s.l.). Shell debris embedded in a matrix of clayey silt occurs from 3.31-3.27 m b.s.l. As a consequence of anthropogenic drainage, the lagoonal mud has then been turned into compact weathered clayey silts (3.30-2.05 m b.s.l.), still incorporating molluscs and shell debris. From 2.77-2.73 m b.s.l., a layer of fine sand intersects the clayey deposits.

Vibracore AGI 6 (ground surface at 0.25 m a.s.l., N 37°40‘01.7“, E 21°22‘27.2“) is characterized at its base by well sorted marine sand (6.75-5.10 m b.s.l.). Overlying silty deposits document the short-term establishment of quiescent sedimentation conditions (5.10-5.02 m b.s.l.) that change into peat-dominated semi-terrestrial conditions (5.02-4.70 m b.s.l.). Subsequently, fine-grained limnic deposits prevail (4.70-3.15 m b.s.l.). Shell-enriched deposits (3.15-2.75 m b.s.l.) on top of an erosional unconformity mark the abrupt change towards lagoonal conditions that dominate the stratigraphical record from 2.75-1.15 m b.s.l.. In the upper part of the profile (1.15 m b.s.l.-0.25 m a.s.l.) brownish homogenous mud is repeatedly intersected by shell debris layers, up to 1 cm thick, between 0.32-0.65 m b.s.l. The uppermost part is again strongly influenced by modern anthropogenic drainage activity.

At the base of AGI 2 (ground surface at 2.29 m b.s.l., N 37°40‘05.8“, E 21°22‘29.9“) well sorted greyish (medium to) fine sand with blackish coloured root channels (13.29-7.49 m b.s.l.) documents a shallow marine environment, comparable to the stratigraphies of cores AGI 3 and AGI 6. Between 11.06 m b.s.l. and 10.46 m b.s.l., the colour of the sand is light brown indicating palaeosol formation at the top of the former beach ridge. A following layer of organic-rich, clayey to sandy silt indicates a significant environmental change towards quiescent sedimentary conditions reflecting limited saltwater influence. Subsequently, a distinct layer of peat and organic mud indicates semi-terrestrial conditions (6.77-6.58 m b.s.l.) showing well-preserved organic components and a high amount macrofossil fragments. A sharp contact then separates the semi-terrestrial unit from the following limnic deposits (6.58-3.95 m b.s.l.). Reworked peat fragments also indicate an erosive event prior to the establishment of limnic conditions. Following another sharp erosional contact, the limnic facies is subsequently covered by fine sandy clayey silt (3.95-3.47 m b.s.l.). At 3.86 m b.s.l, rip up-clasts from the limnic unit are a significant feature of strongly increased energetic conditions. From 3.47 m b.s.l. towards the top, lagoonal conditions were re-establish but show strong influences of anthropogenic drainage. A shell debris layer (2.97-3.07 m b.s.l.) marks temporary high-energy influence which caused strong reworking of autochthonous deposits.

At the base of vibracore AGI 1 (ground surface at 2.32 m b.s.l., N 37°40‘16.3“, E 21°22‘46.4“) homogenous sand (14.32-13.10 m b.s.l.) documents marine conditions. The sand is covered by peat and/or organic-rich mud (13.10-12.89 m b.s.l.) with a distinct shell debris layer on top (12.89-12.79 m b.s.l.). The overlying muddy facies (12.79-7.47 m b.s.l.) then documents lagoonal conditions, locally incorporating abundant molluscs, mollusc fragments, gastropods and plant remains. Following a limnic phase (7.47-7-13 m b.s.l.), another peat layer indicates again semi-terrestrial conditions (7.13-6.92 m b.s.l.). A sharp erosional contact then marks the transition to greyish clayey silt that document quiescent limnic conditions (6.92-6.32 m b.s.l.). Locally embedded are gastropods, molluscs, charcoal fragments and plant remains while hydromorphic features indicate increasingly ephemeral conditions (6.32-3.77 m b.s.l.). From 3.73-3.03 m b.s.l., clayey silt and fine to medium sand including shells and shell debris indicate an abrupt change towards high-energy conditions. However, lagoonal conditions were re-established from 3.03-2.87 m b.s.l. and again covered by fine sand in a matrix of clayey silt and shell debris (2.87-2.72 m b.s.l.). Towards the top, lagoonal sediments show

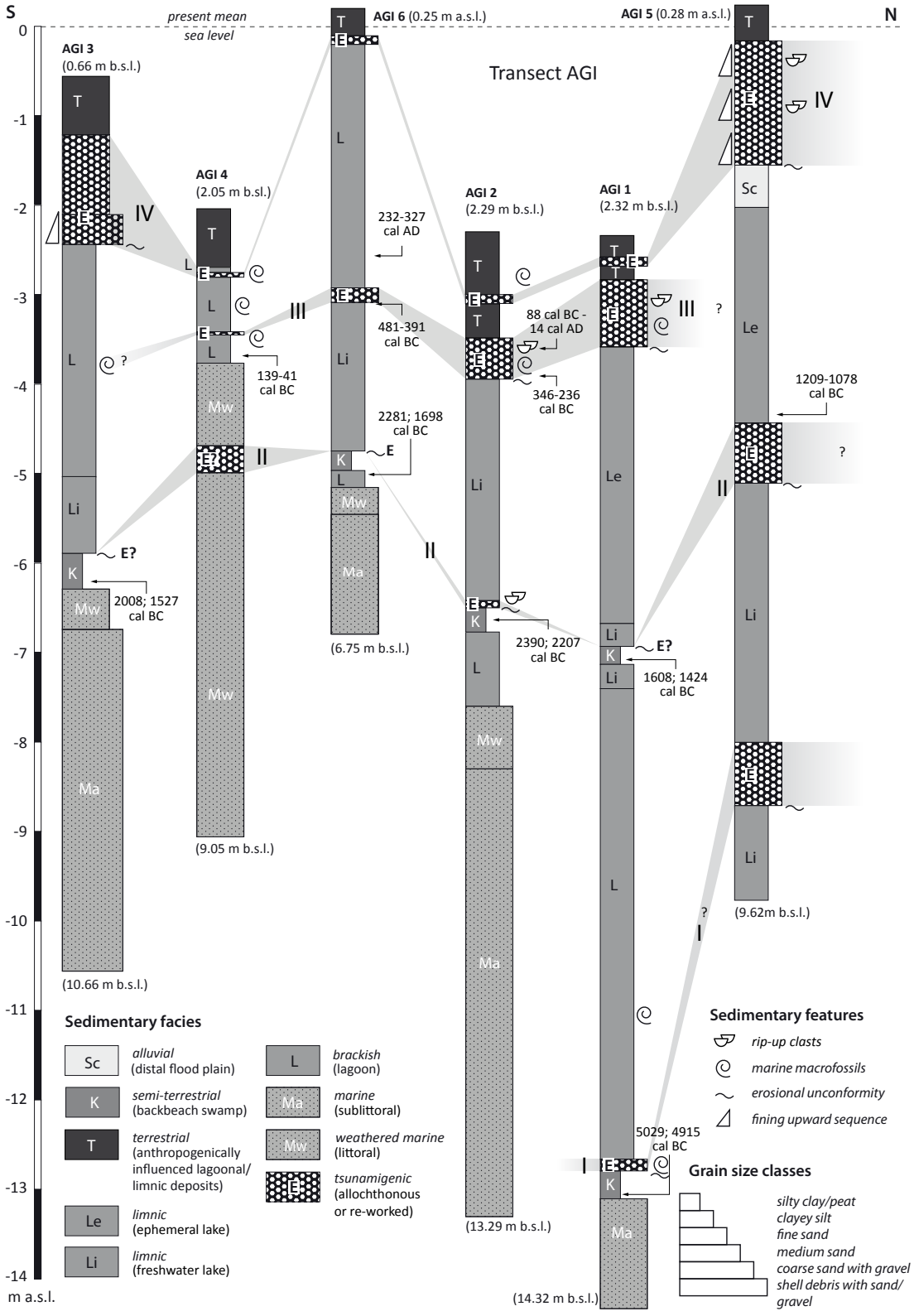

Fig. 3-3: Stratigraphical record and facies distribution of vibracores drilled along transect AGI in the coastal lowlands former Mouria lagoon (Fig. 3-2) along a total distance of 1.9 km.

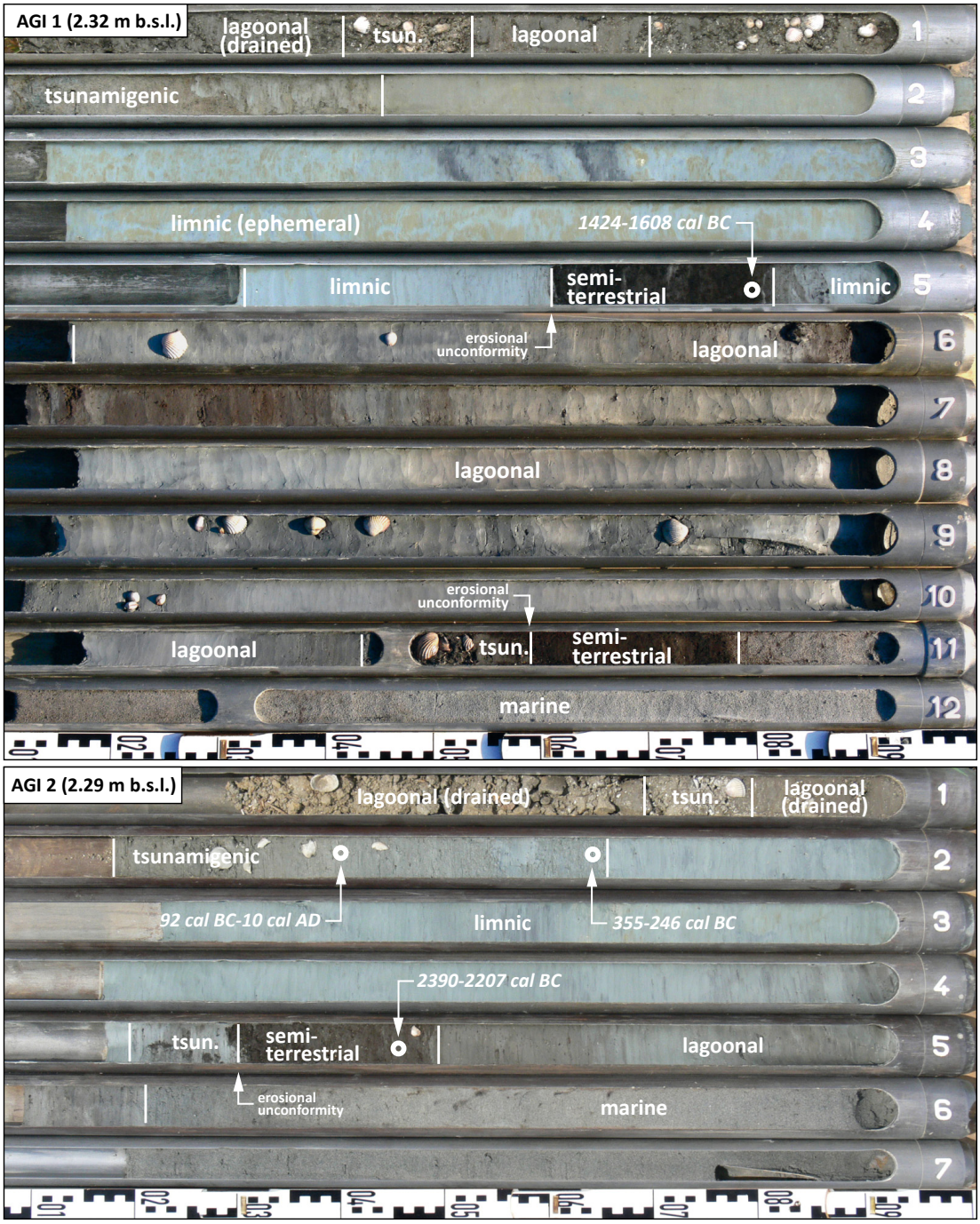

Fig. 3-4: Simplified facies profile of vibracores AGI 1 and AGI 2. Note that core meters 8-11 of vibracore AGI 2 are not depicted. Photos by T. Willershäuser, 2009, 2010. For location see Fig. 3-2.

traces of increased weathering due to modern drainage activities (2.72-2.32 m b.s.l.).

The stratigraphical record of AGI 5 (ground surface at 0.28 m a.s.l., N 37°40‘28.1“, E 21°23‘14.0“) indicates a limnic environment at the base of the profile (9.72-8.67 m b.s.l.). As a major difference to the stratigraphies described so far, no autochthonous marine deposits were found. Following a sharp erosional contact, however, fine sand and clayey silt

(8.67-7.95 m b.s.l.) cover the limnic deposits. The sedimentary sequence is characterized by several distinct fining upward sequences reaching from sand to clayey silt. Subsequently, muddy deposits document the re-establishment of limnic conditions (7.95-2.00 m b.s.l.). From 4.72-4.43 m b.s.l., the homogenous limnic sequence is again interrupted by sand topped with a mud cap, but quiescent conditions were immediately re-established afterwards. Increasing hydromorphic features suggest a shallow lake under ephemeral conditions. The limnic sequence is then covered by silty to sandy deposits that may indicate fluvial influence (2.00-1.84 m b.s.l.). From 1.84-0.11 m b.s.l., a massive sequence of allochthonous sands

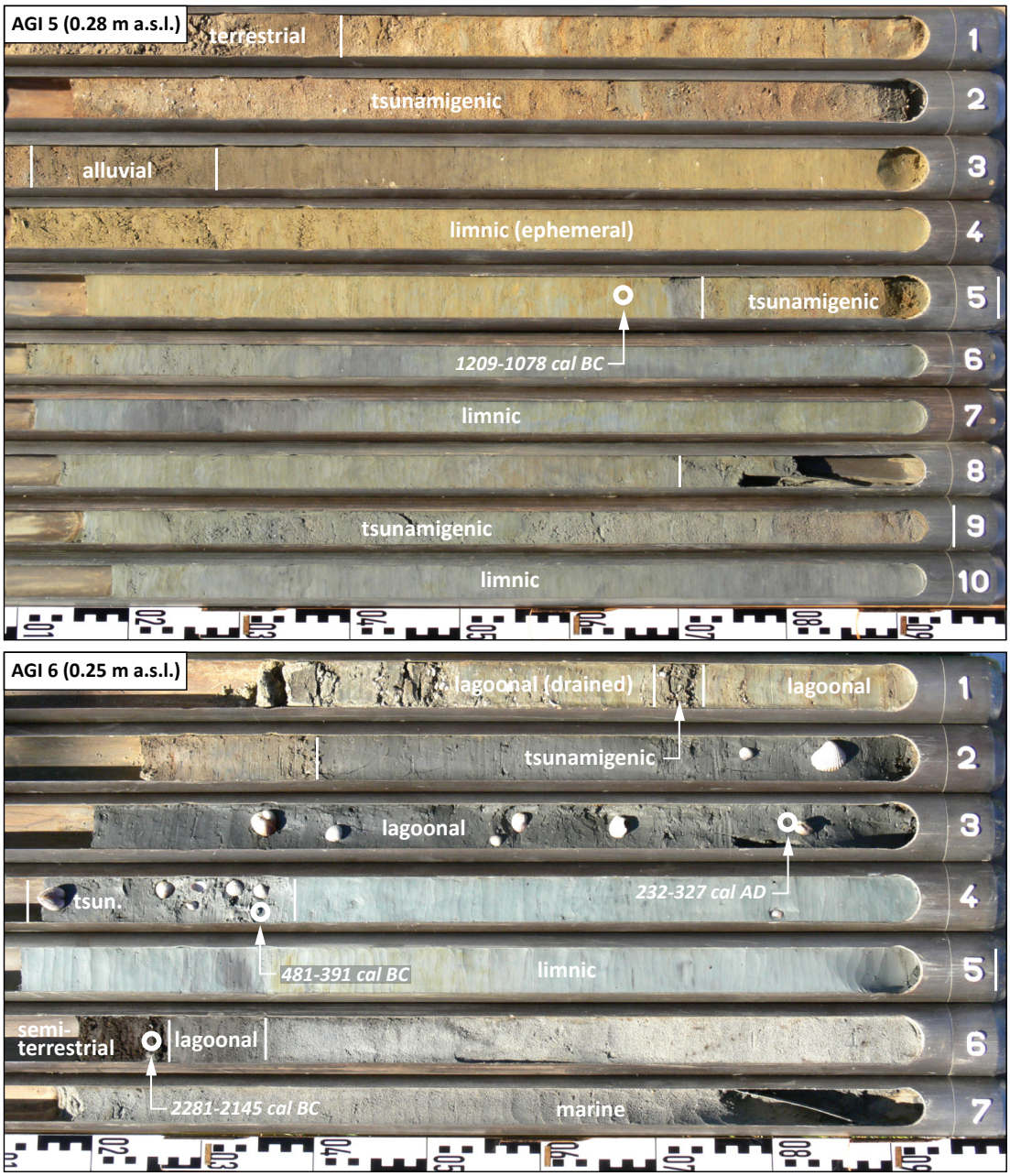

Fig. 3-5: Simplified facies profile of vibracores AGI 5 and AGI 6. Note that core meters 8-11 of vibracore AGI 6 are not depicted. Photos by T. Willershäuser, 2010. For location see Fig. 3-2.

and silts covers the underlying deposits marked by an erosional unconformity. Several fining upward sequences including fine gravel, sand, silt and mud caps document repeated high-energy impulses followed by constantly decreasing transport energy. A high content of marine macrofossils proves a seaward origin of the sediments. The top of profile AGI 5 consists of silty to sandy deposits which have been subject to subaerial weathering and anthropogenic influence (0.11 m b.s.l-0.28 m a.s.l.).

The synoptic view of all vibracore stratigraphies reveals distinct disturbances of the autochthonous quiescent lagoonal and limnic environs of the former Mouria Lagoon. Intersecting layers of sand and shell debris document the repeated input of allochthonous sediments up to more than 2 km inland related to high-energy impacts. Event deposits are characterized by sharp basal erosional contacts, fining upward cycles of the grain size and/or reworking of the underlying sedimentary unit due to strong inundation dynamics. The rapid re-establishment of pre-existing quiescent low-energetic environs or abrupt environmental changes initiated by high-energy impulses underline the temporary, short-term character of high-energy interferences.

3.3.2 Geophysical subsurface investigations

Geophysical methods such as electrical resistivity tomography (ERT) are well established within the framework of geomorphological and geoarchaeological studies (e.g. Griffith & Barker 1994, Kneisel 2003, Hecht & Fassbinder 2006, Vött et al. 2011a). Based on the different resistivity behaviour of different sediment types, it is possible to detect subsurface structures with a high vertical resolution depending on electrode spacings. In combination with vibracoring, ERT measurements provide a powerful tool to correlate subsurface stratigraphies from different locations and to trace significant stratigraphical changes (e.g. Martorana et al. 2009). Concerning the interpretation and comparison of ERT measurements, it has to be taken into account that different local factors influence the electrical conductivity of the subsurface material, e.g. the mineral composition, soil temperature, pore water content, structure of pore volume and salt water influence (e.g Reynolds 1997, Kearey et al. 2006, Schrott & Sass 2008). Thus, measured values must not be correlated with specific sediments but have to be evaluated against the stratigraphical record and the local environmental conditions at the time of the measurement.

In the area of the former Mouria Lagoon, eight electrical resistivity measurements were carried out at four different sites (for locations see Fig. 3-2). For each ERT transect the obtained simplified model resistivity sections (3rd iteration) as well as a simplified stratigraphy of the adjacent vibracore are illustrated in Fig. 3-6.

Transect AGI ERT 1 can be divided in two sections. While relatively low resistivity values dominate the near surface underground down to ~8 m b.s.l. (2-12 Ωm) , higher values (> 12 Ωm) occur at the bottom of the profile (8-20 m b.s.l.). The lower section slightly declines in NNE direction. Low resistivity values also characterize AGI ERT 2 down to ~7 m b.s.l. (< 7 Ωm) while increased values occur at the base (> 7 Ωm, up to 16 m b.s.l.). Comparing both ERT transects with the stratigraphical record of core AGI 2, major changes detected by geophysical measurements clearly correlate to changes in the vibracore stratigraphy. Well

conductive limnic and lagoonal deposits occur up to ~7.5 m b.s.l. and reflect the lower resistivity values. On the contrary, higher resistivity values characterize the coarse-grained marine sands at the bottom of the vibracore profile.

For transect AGI ERT 4, high resistivity values (19 to > 90 Ωm) only occur in the uppermost southern part of the transect and are related to the compacted and dry sediments of a nearby dirt road. The undifferentiated lower part of the transect shows low values corresponding to

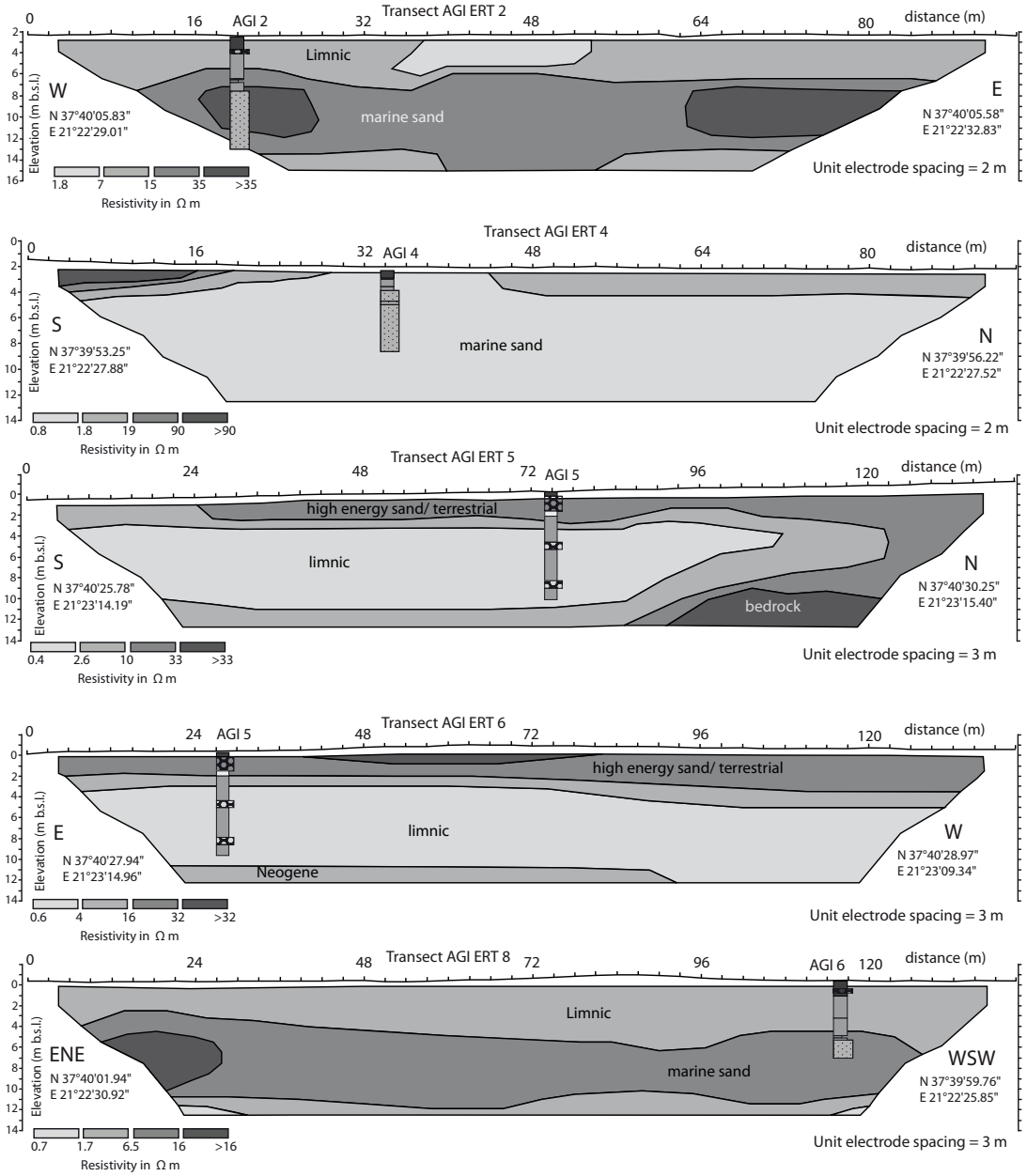

Fig. 3-6: Simplified pseudosections for electrical resistivity transects AGI ERT 2, 4, 5, 6 & 8 on the coastal lowlands of the former Mouria lagoon. Electrical resistivity sections were measured using the Wenner-Schlumberger electrode array and electrode spacings between 4 and 2m. Vibracores lying on the transects are shown with simplified facies distribution. For location of geoelectrical transects see Fig. 3-2.

the homogeneously sandy stratigraphical record of vibracore AGI 4. Due to a methodical loss of near-surface data, the upper lagoonal sequence is not depicted in Fig. 3-6.

The near-surface underground (~3 m b.s.l.) of AGI ERT 7 is characterized by quite low resistivity values (< 9 Ωm). From 3 m b.s.l. downwards, higher resistivity values (> 9 Ωm) document a thick horizontal unit. Transect AGI ERT 8 is characterized by a section of comparably low resistivity values (< 6.5 Ωm) in the upper part of the transect (~4 m b.s.l.) and increasing values below (> 6.5 Ωm). The modelled resistivity sections of AGI ERT 7 and 8 directly correspond to the stratigraphy of AGI 6 (Fig. 3-6).

Transects AGI ERT 5 and AGI ERT 6 depict high resistivity values (10-33 Ωm) in the upper part of the profiles (down to 2 m b.s.l.) while a significant shift in resistivity values (< 5 Ωm) marks the contact to the underlying unit (2-12 m b.s.l.). As shown by vibracore AGI 5, the fine-grained sediments from the base up to 2 m b.s.l. are represented by comparatively low resistivity values. The overlying sand sheets are characterized by high resistivity values. As for transect AGI ERT 6, the simplified model resistivity section is also in good accordance with the stratigraphy of vibracore AGI 5.

Within the study, ERT measurements represent a valuable method to detect major subsurface stratigraphical correlations. However, the vertical resolution of the measurements does not allow to detect most of the event deposits. Only at site AGI 5, where thick high-energy deposits occur close to the surface and on top of limnic sediments, the spatial extent of these event deposit is clearly depicted by the ERT transect (Fig. 3-6).

3.3.3 Grain size analyses and XRF measurements

Depending on the environmental conditions, each geo-archive holds specific sedimentary and geochemical characteristics. Gradual or abrupt environmental changes therefore imply significant changes in the facies sequence (e.g. Einsele 2000). In order to assign specific facies to different sedimentary sequences and to reconstruct the palaeogeographical conditions at the time of deposition, geochemical as well as sedimentological studies are valuable tools (Vött et al. 2002). Due to constant weathering, sediments of terrestrial origin often show an increased amount of iron (Fe) or titanium (Ti), while more or less unweathered marine deposits may for instance comprise a comparably high amount of biogenically produced calcium carbonate. By defining the geochemical fingerprint of different facies encountered in the stratigraphical record, it is possible to discriminate between gradual environmental changes and high-energy events (e.g. Vött et al. 2011a, 2011b).

Also the grain size composition and sorting are significant indicators for palaeogeographical conditions and the energetic potential of different facies at the time of deposition (e.g. Reineck & Singh 1980, Einsele 2000, Schäfer 2005). While gradual changes in the grain size distribution document gradual changes in the environment, abrupt changes in the sedimentation pattern are often associated with significant changes of the energetic sedimentary environment. Grain size ratios of gravel and sand in relation to clay and silt can be used as a valuable tracer to determine the energetic conditions of transport and deposition (Willershäuser et al. 2013). Due to their increased energetic potential but also depending on the availability of sediments, high-energy events like storm surges or tsunamis are often

marked by the sudden input of coarse-grained deposits in otherwise quiescent sedimentary environments (e.g. Dominey-Howes et al. 2006). For vibracore AGI 5A, detailed results of grain size analyses as well as XRF measurements are illustrated in Fig. 3-7.

By XRF-measurements, the stratigraphical record was analysed for the Ca/Fe ratio as a base to distinguish between the terrestrial or marine origin of sediments. After Vött et al. (2011a, 2011b), the marine production of biogenic calcium carbonate is documented by comparably high ratios of Ca/Fe whereas low values are predominantly associated with increased weathering under terrestrial conditions. Lowest Ca/Fe ratios commonly occur, where intense subaerial weathering lead to the decalcification of sediments while oxidation leads to a relative increase of the iron content. For the stratigraphical record of vibracore AGI 5A, results obtained from XRF measurements show significant facies-related variations in the Ca/Fe ratio (Fig. 3-7). Throughout the stratigraphical record, autochthonous deposits that are associated to the limnic facies are characterized by overall low ratios. As already indicated by hydromorphic features in the upper part of the limnic facies ephemeral conditions led to the subsequent weathering of the deposits. Additionally, the overall content of carbonate producing fossils is low. A significant Ca/Fe peak at 5.43-5.65 m b.s.l. marks the accumulation of macrofossils, embedded in a layer of mud with high organic content. Concerning the allochthonous sediment input, results have to be differentiated according to the time of deposition. Due to a long-term decalcification under more or less subaerial conditions, the lower two event deposits are not detectible by XRF measurements. According to their stratigraphical position, both event layers are rather old and were in the near-shore of the former Mouria Lagoon. Thus, we assume that constant weathering has "deleted" the original geochemical fingerprint. The youngest event deposit in the upper part of the stratigraphical record is, however, characterized by a distinct increase of the Ca/Fe ratio. Subsequently to the event, the decreasing Ca/Fe ratio reflects the re-establishment of autochthonous sedimentary conditions. In our study, the application of XRF measurements for the detection of high-energy allochthonous deposits is case-dependent. With regard to the age of an event-related deposit and the preservation potential of the respective geo-archive, the geochemical fingerprint can either be well preserved or lost.

With regard to the stratigraphical distribution of different facies types, selected sediment samples of AGI 5A were analysed for their grain size distribution. As documented by lowest energetic values, the autochthonous sediment deposition at vibracoring site AGI 5A is dominated by quiescent conditions. However, increased energetic conditions mark the designated event deposits. Concerning the lower event deposits encountered at site AGI 5A, slightly increased peaks document the input of fine-grained sandy sediments while the upper event layer, due to several fining upward cycles, is characterized by strongly increased but variable energetic ratios. Highest ratios may indicate the initial wave impacts. The abrupt interruption of low-energetic conditions and the immediate re-establishment of quiescent environs emphasize the short-term character of the high-energy impact. As shown by our results, grain size analyses and the calculation of energetic ratios provide a valuable approach to detect high-energy traces in the sedimentary sequence of a quiescent geo-archive.

3.3.4 Magnetic susceptibility and photospectrometric measurements

The magnetic susceptibility is defined as the 'magnetisability' of sediments and describes the response of sediments to an external magnetic field. The grade of magnetization is divided by the strength of the magnetic field and given in a dimensionless unit, the susceptibility index (SI). Ferromagnetic minerals like goethite, hematite or magnetite generate high positive

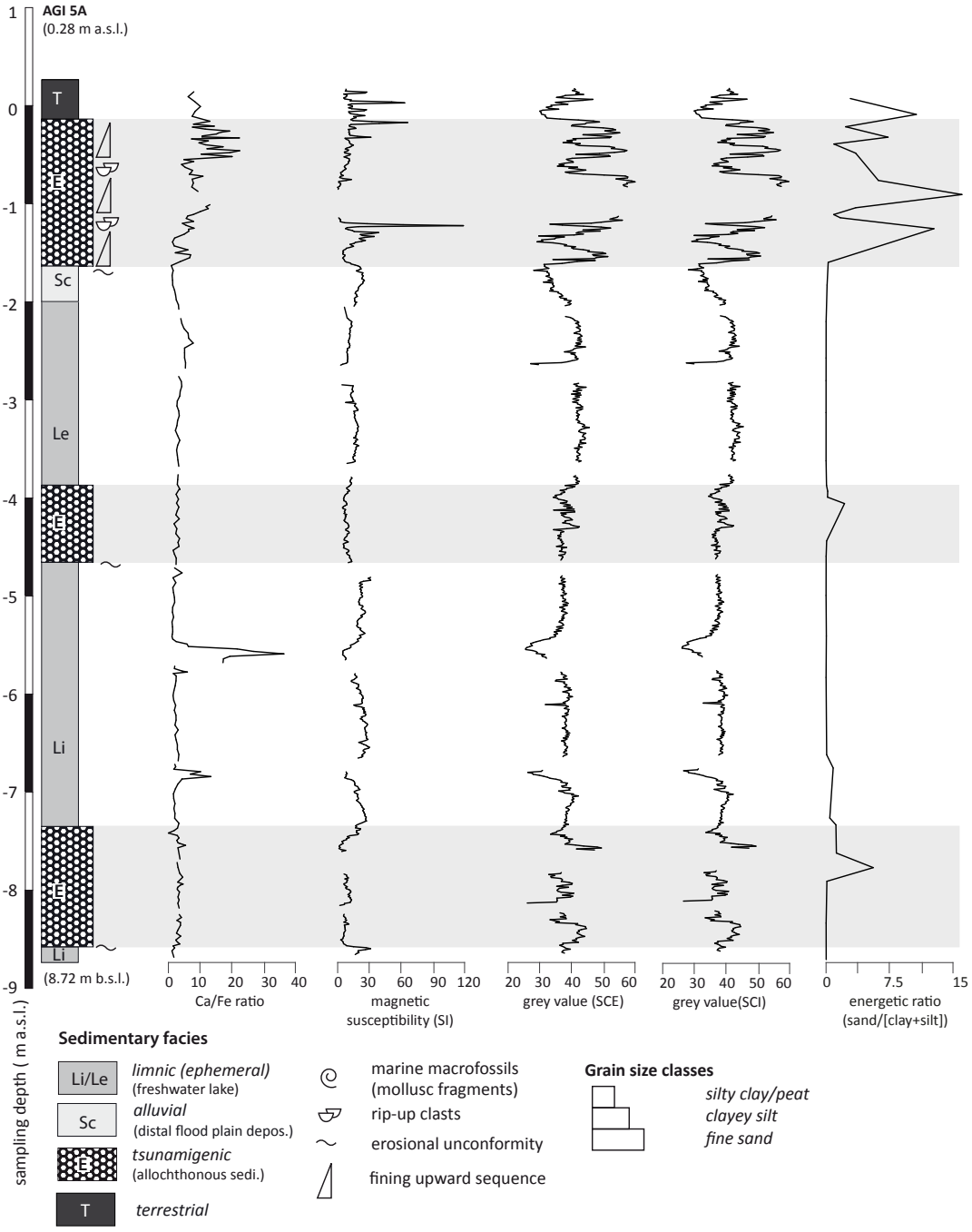

Fig. 3-7: Stratigraphical record, facies distribution and detailed geochemical analyses of vibracore AGI 5A at the most northwestern end of the former Mouria lagoon. For location of the coring site see Fig. 3-2.

values of the susceptibility, whereas diamagnetic minerals like quartz or calcium carbonate show minor to slightly negative values (Dearing 1999). Dominated by weathering and pedogenic processes, a high SI index is generally expected for terrestrial materials; however, magnetic heavy minerals are often enriched in marine deposits and may thus also produce high magnetosusceptibility signals (e.g. Mullins 1977). In our study, susceptibility values range between 0 and 120 x 10^{-5} SI with maximum values obtained for the uppermost high-energy event layer (Fig. 3-7).

With regard to photospectrometric measurements (Fig. 3-7), the homogeneous limnic section encountered at site AGI 5A shows consistent values ~40 L*a*b SCE/SCI; decreasing values of ≤ 30 L*a*b SCE/SCI merely occur where the content of organic matter is increased. On the contrary, allochthonous sand units are characterized by variable and generally high values (maximum 40-60 L*a*b SCE/SCI) mostly due to weathering (oxidation) effects (e.g. Scheinost & Schwertmann 1999) and the input of relocated soil material, for instance originating from beach ridges overflowed during inundation events.

In case of core AGI 5A, a distinct magnetic susceptibility and photospectrometric fingerprint was identified for the autochthonous limnic facies that clearly differs from the allochthonous high-energy deposits.

3.3.5 Microfossil analysis of AGI 5A

In order to reconstruct the overall palaeogeographical and palaeoenvironmental evolution of the former Mouria Lagoon and to identify high-energy imprints from the coastal geo-archive, 25 sediment samples from vibracore AGI 5A were prepared for detailed microfossil analyses (closed core in 5 cm inliner). Results are depicted in Fig. 3-8. Skeletal remains of foraminifera, molluscs and/or ostracods provide detailed information on the long-term palaeogeographical evolution as well as short-term variability of coastal environments. Shifts in the microfaunal assemblage are represented by varying abundances of individual species and species-communities. Abrupt environmental changes are often depicted by a sudden and temporary occurrence or disappearance of specific species. Concerning a high-energy interference of the environment, microfossil assemblages may additionally be strongly disturbed where allochthonous species are transported to atypical environs (Murray 2006).

The silty base of core AGI 5A (8.72-8.55 m b.s.l.) is nearly void of microfossils. Merely single specimens of *Grambastichara* sp. (Characeae) were found (sample AGI 5A/38). Subsequently (8.55-7.43 m b.s.l.), few *Orbulina universa* and single specimens of *Ammonia tepida* and *Ammonia parkinsoniana* appear (samples AGI 5A/36, AGI 5A/34). From 7.43-4.65 m b.s.l, foraminifera are scarce. In the homogenous muddy deposits the microfossil assemblage comprises few ostracods (e.g. *Cyprideis torosa*), gastropods (e.g *Nassarius* sp.) and Characeae (e.g. *Grambastichara* sp., samples AGI 5A/30, 5A/29, 5A/27 and 5A/25). They document predominantly autochthonous limnic freshwater conditions.

However, a relatively high amount of marine foraminifera (samples AGI 5A/22 and 5A/19) with high species diversity (e.g. *Ammonia beccarii*, *Bulminia marginata*, *Cibicides* sp., *Globigerina callida*, *Elphidium crispum, Peneroplis pertusus, Orbulina universa,* etc.) suddenly occurs in the overlying stratigraphical unit (4.65-3.87 m b.s.l.).

The subsequent silty unit from 3.87-2.05 m b.s.l. incorporates nearly no microfaunal species at all (samples AGI 5A/17, AGI 5A/15, AGI 5A/14 and AGI 5A/12). Only single Ostracods and few specimens of *Ammonia beccarii* and *Ammonia tepida* as well as a single specimen of

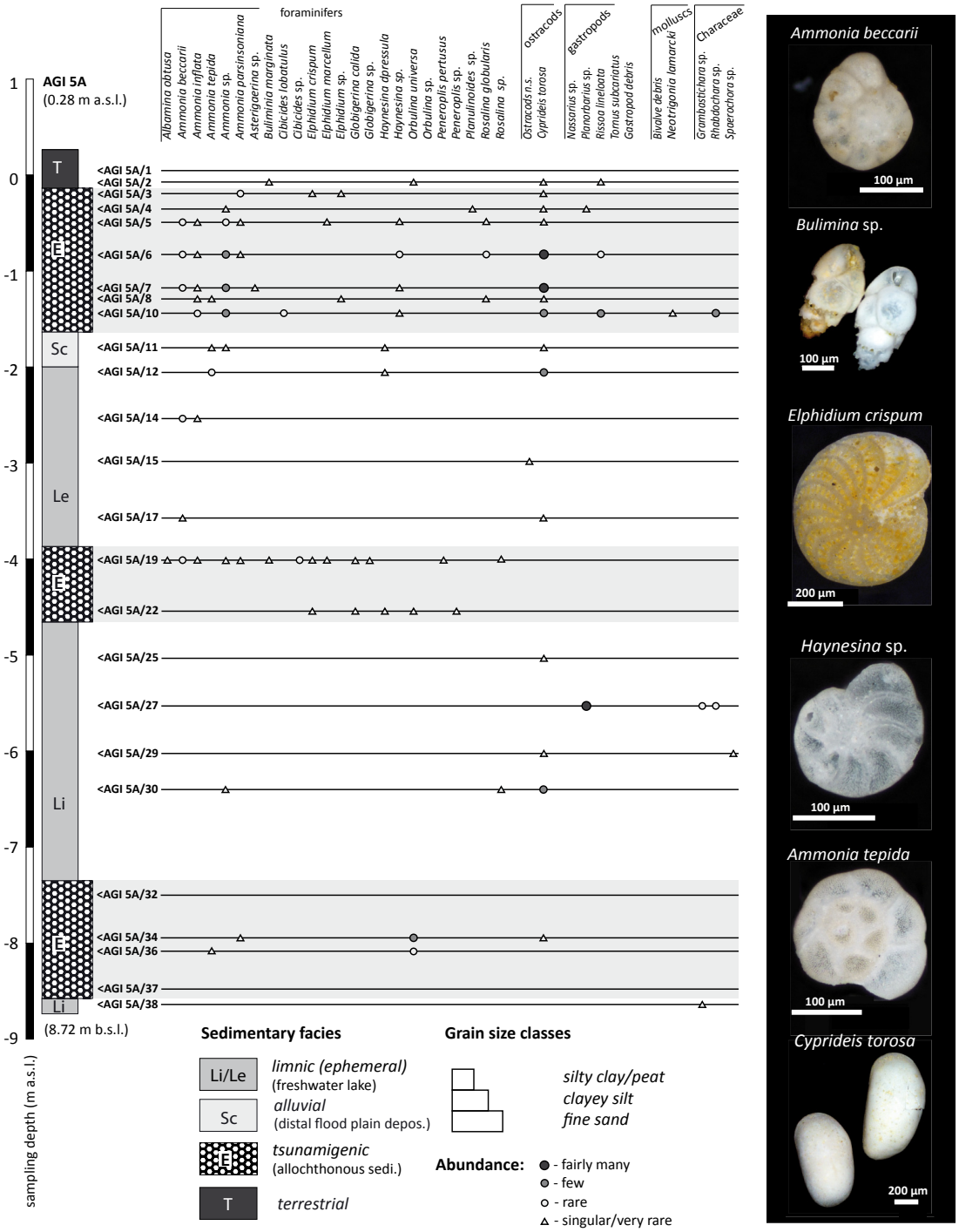

Fig. 3-8: Results of micro- and macrofossil analyses of selected samples from vibracore AGI 5A. Photos of selected specimens were taken by a polarized light microscope and a digital camera. Specimens were determined after Loeblich & Tappan 1988, Cimerman & Langer 1991, Poppe & Goto 1991, 2000, Murray 2006, Gupta 2002, Rönnfeld 2008.

Ammonia inflata occur. The microfossil content thus reflects the re-establishment of the former freshwater-dominated environment. Concerning the following fine-grained distal flood plain deposits (2.05-1.62 m b.s.l.), the microfossil content is limited to singular specimens of *Ammonia* sp., *Ammonia tepida* and *Haynesina depressulla* as well as *Cyprideis torosa* (sample AGI 5A/11).

In a strong contrast to the lower facies, a highly diverse microfossil assemblage suddenly occurs in the sandy and silty high-energy facies from 1.62-0.15 m b.s.l (samples AGI 5A/10, AGI 5A/8, AGI 5A/7, AGI 5A/6, AGI 5A/5, AGI 5A/4 and AGI 5A/3). Within this unit, we found highly diverse species associated with fully marine (e.g. *Rosalina globularis*, *Orbulina universa*), shallow marine (e.g. *Ammonia inflata*, *Ammonia parkinsoniana, Ammonia* sp.*, Asterigerina* sp.*, Haynesina* sp.etc.), brackish (*Cyprideis torosa*), and even limnic and freshwater conditions (*Rissoa lineolata*, *Planorbius* sp., *Rhabdochara* sp.).

The uppermost part of vibracore AGI 5A (0.15 m b.s.l. - 0.28 m a.s.l.) is characterized by a clearly reduced microfossil spectrum. Only sample AGI 5A/2 includes single specimens of *Bulimina marginata* and *Orbulina universa* as well as *Cyprideis torosa* and *Rissoa lineolata* while sample AGI 5A/1 is void of microfossils.

3.4 The coastal area of Kato Samiko

3.4.1 Stratigraphcal record of vibracore SAM 1

Vibracore SAM 1 (ground surface at 11.18 m a.s.l., N 37°32‘31.5“, E 21°35‘56.3) was drilled to the southeast of the former Agoulenitsa Lagoon at the mouth of a small valley near the village of Kato Samiko. The coring site lies about 2.5 km distant from the recent coast (see Figs. 3-1 and 3-9). Towards the north, a ridge of Pliocene sediments flanks the valley while a ridge of Cretaceous limestone raises to the south (IGME 1982b) on top of which the ancient city of Samiko is located.

The base of SAM 1 (0.18-0.68 m a.s.l.) is made out of fine-grained sand including marine macrofossils that is subsequently covered by limnic grey clayey silt (0.68-1.04 m a.s.l.). From 1.04-1.23 m a.s.l., a layer of mean to coarse sand covers the limnic unit, thus indicating a change from low- to high-energetic conditions. The following fluvio-limnic silty to sandy grey deposits (1.23-1.90 m a.s.l.) are dominated by numerous mollusc fragments of marine origin. An overlying brownish-grey layer consists of coarse-grained sand and again contains marine mollusc fragments (1.90-2.00 m a.s.l.). Increased grain size again documents increased energetic conditions. The deposit is covered by a unit of brownish to beige silty fine sand (2.00-2.72 m a.s.l.), followed by weathered clayey silts which prove the establishment of a quiescent ephemeral lake (2.72-3.58 m a.s.l.).

The limnic deposits are successively covered by alluvial sediments (3.58-8.39 m a.s.l.) that vary from clayey silt to fine sand, bear hydromorphic features and occasionally incorporate ceramic fragments and pieces of charcoal. From 6.43-6.50 m a.s.l., a distinct layer of fine sandy silt occurs. In the upper part of vibracore SAM 1 (8.39-10.33 m a.s.l.), a massive layer of coarse clasts, that are embedded in an unsorted loamy matrix follows on top of the alluvial facies. An associated sharp erosional contact proves an abrupt and rapid high-energy event.

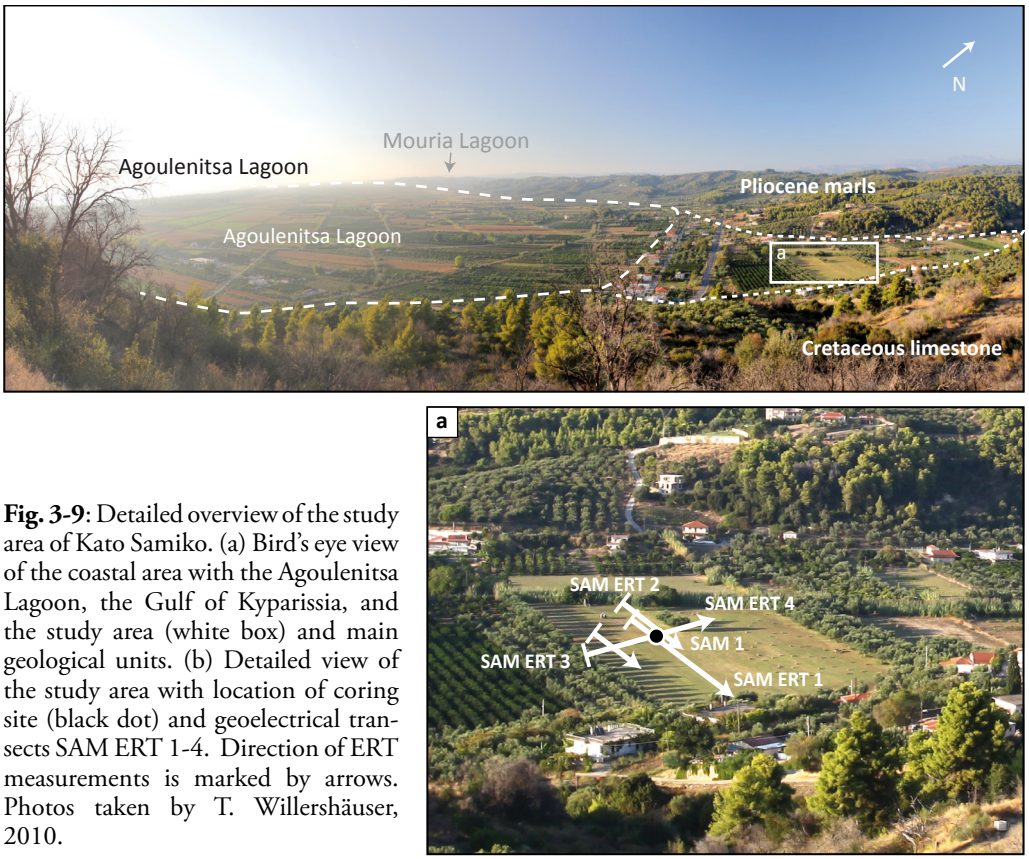

Fig. 3-9: Detailed overview of the study area of Kato Samiko. (a) Bird's eye view of the coastal area with the Agoulenitsa Lagoon, the Gulf of Kyparissia, and the study area (white box) and main geological units. (b) Detailed view of the study area with location of coring site (black dot) and geoelectrical transects SAM ERT 1-4. Direction of ERT measurements is marked by arrows. Photos taken by T. Willershäuser, 2010.

The event-associated unit incorporates numerous ceramic and tile fragments, marine shell debris and pieces of charcoal. The intermediate subsequent fine sandy silt (9.65-9.85 m a.s.l.) is well sorted and almost void of coarse components. The uppermost part of the deposit (9.85-10.33 m a.s.l.) is, however, characterized by a matrix of silt including coarse sand and grus as well as ceramic remains and mollusc fragments. The top of the core (10.33-11.06 m a.s.l.) finally consists of homogenously dark brown silty to sandy sediments that are associated with the distal part of an alluvial fan system.

3.4.2 Geochemical analysis and grain size distribution of vibracore SAM 1

The stratigraphical record of vibracore SAM 1 is predominantly characterized by fine-grained alluvial sediments that were deposited under rather low-energy conditions. The sandy units in the lower part of the core indicate increased energetic conditions. Also, in the upper part of the core, the increased energetic ratio marks the abrupt high-energy input of allochthonous coarse-grained sediments into the predominating quiescent environment. Although rust coloured sediments and numerous ceramic fragments attest a terrestrial origin of the deposit, the occurrence of marine macrofossils as well as geochemical characteristics prove an additional marine influence (Figs. 3-10, 3-11).

Sediment samples of vibracore SAM 1 were analysed, among others, by XRF measurements

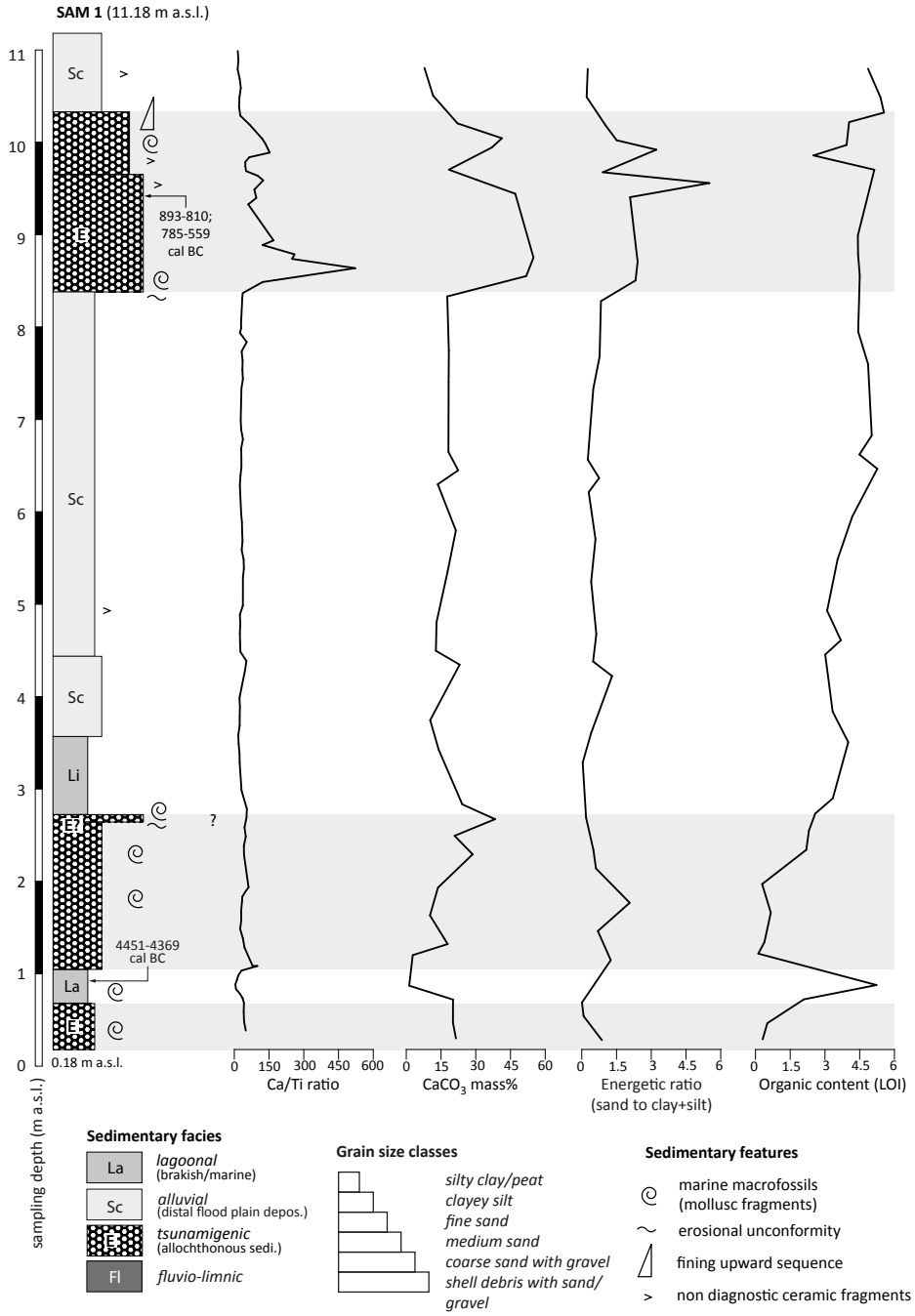

Fig. 3-10: Stratigraphical record, facies distribution and geochemical analyses of vibracore SAM 1 drilled in the Kato Samiko alluvial plain. For location of vibracoring site, see Fig. 3-9.

in order to distinguish between terrestrial and marine facies and to geochemically determine major environmental changes. As a result, limnic, fluvial and alluvial deposits found at site SAM 1 all bear a constantly low Ca/Ti ratio. Compared to terrestrial conditions, marine environments generally hold a higher amount of Ca due to the high production of biogenic calcium carbonate by marine organisms. Regarding the uppermost high-energy event layer, the total content of calcium carbonate is about twice as high as for the terrestrial facies above

and below. The increased Ca/Ti ratio as well as the occurrence of marine shell debris further documents the input of marine sediments.

Considering the geochemical fingerprint as well as the high-energy character of the associated sediments, site SAM 1 experienced sea-borne high-energy impacts that caused a massive reworking of terrestrial deposits. According to the high amount of ceramic fragments (Fig. 3-11), the event obviously affected an ancient settlement.

3.4.3 Microfossil analyses of cores SAM 1 and SAM 1A

For vibracore SAM 1A (equivalent to core SAM 1, closed core in 5 cm inliner, core length 10.68-8.18 m a.s.l.), 8 sediment samples were analysed. Another 4 samples from the base of core SAM 1 were studied for their microfossil content. The results of microfossil analyses are depicted in Figs. 3-10 and 3-11.

At the base of SAM 1 (Fig. 3-11), microfossil samples were taken at 0.43-0.53 m a.sl. (SAM 1/33), 0.71-0.76 m a.sl. (SAM 1/32), 0.83-0.93 m a.s.l. (SAM 1/31) and 1.33-1.38 m a.s.l. (SAM 1/29). The base of SAM 1 contains foraminifers like *Ammonia tepida*, *Ammonia beccarii* and *Ammonia* sp. indicating mostly quiescent brackish to shallow marine conditions. Furthermore *Cibicides* sp., *Elphidium* sp., *Heynesina* sp. and *Nonion* sp. occur. Some foraminifers are weathered and appear orange to yellow in colour (Fig 3-10, sample 4) but most of them are well preserved. The foraminiferal content of samples SAM 1/32, SAM 1/31 and SAM 1/29 is dominated by *Ammonia* sp. and contains only few specimens of *Nonion* sp.

The lowermost part of core SAM 1A (8.18-8.30 m a.s.l.) corresponds to the alluvial facies encountered in vibracore SAM 1(Fig. 3-11), that is characterized by distal flood plain deposits (sample SAM 1A/8). The microfossil content is characterized by a low quantity of orange-coloured to yellowish specimens that show clear signs of weathering, especially oxidation. Few specimens of *Ammonia sp.*, *A. beccarii, Nonion* sp. and *Rosalina* sp. as well as unspecified remains of ostracods, molluscs and gastropods were encountered. As sediments are supposed to include reworked Plio- to Pleistocene bedrock material from the hinterland that was partly deposited under marine conditions, it is difficult to discriminate between bedrock-borne and potential Holocene microfossils.

The overall microfossil abundance of the lower part of the subsequent high-energy event deposit (samples SAM 1A/7 and SAM 1A/6) remains low and still characterized by *A. beccarii* and *Ammonia* sp. Additionnally, few specimens of *Elphidium* sp. and a strongly increased amount of marine shell debris was found.

While the foraminiferal assemblage in the upper part of the high-energy event layer (SAM 1A/5, SAM 1A/4 and SAM 1A/3) is still dominated by *Ammonia* types, diversity and abundance of encountered microfossils are significantly increased. New species associated with brackish and marine conditions like *Fursenkonia acuta*, *Haynesina* sp., *Nonion* sp. or the planktonic *Orbulina universa* were found. Although many foraminiferal tests appear weathered and in orange to yellow colours, the majority of specimens look fresh, unweathered, and resemble modern-day specimens; they thus appear to be Holocene age. In the uppermost layer of SAM 1A (samples SAM 1A/2 and SAM 1A/1) the microfossil assemblage is similar to the one found for the underlying sandy event layer.

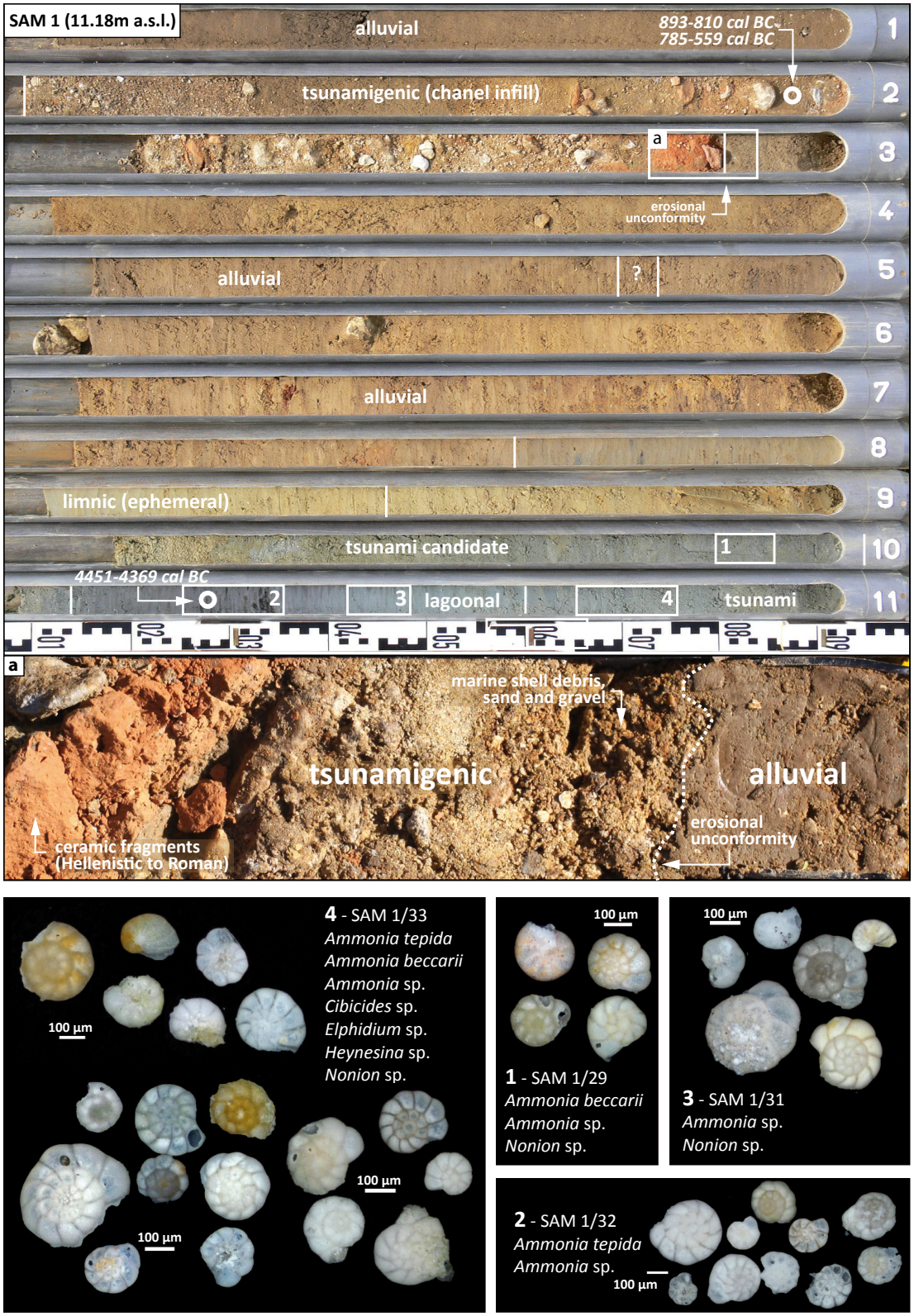

Fig. 3-11: Vibracore SAM 1 with simplified facies interpretation. Results of micro- and macrofossil analyses of selected samples are marked (1-4). Photos of selected specimens were taken by a polarized light microscope and a digital camera. Specimens were determined after Loeblich & Tappan 1988, Cimerman & Langer 1991, Poppe & Goto 1991, 2000, Murray 2006, Gupta 2002, Rönnfeld 2008.

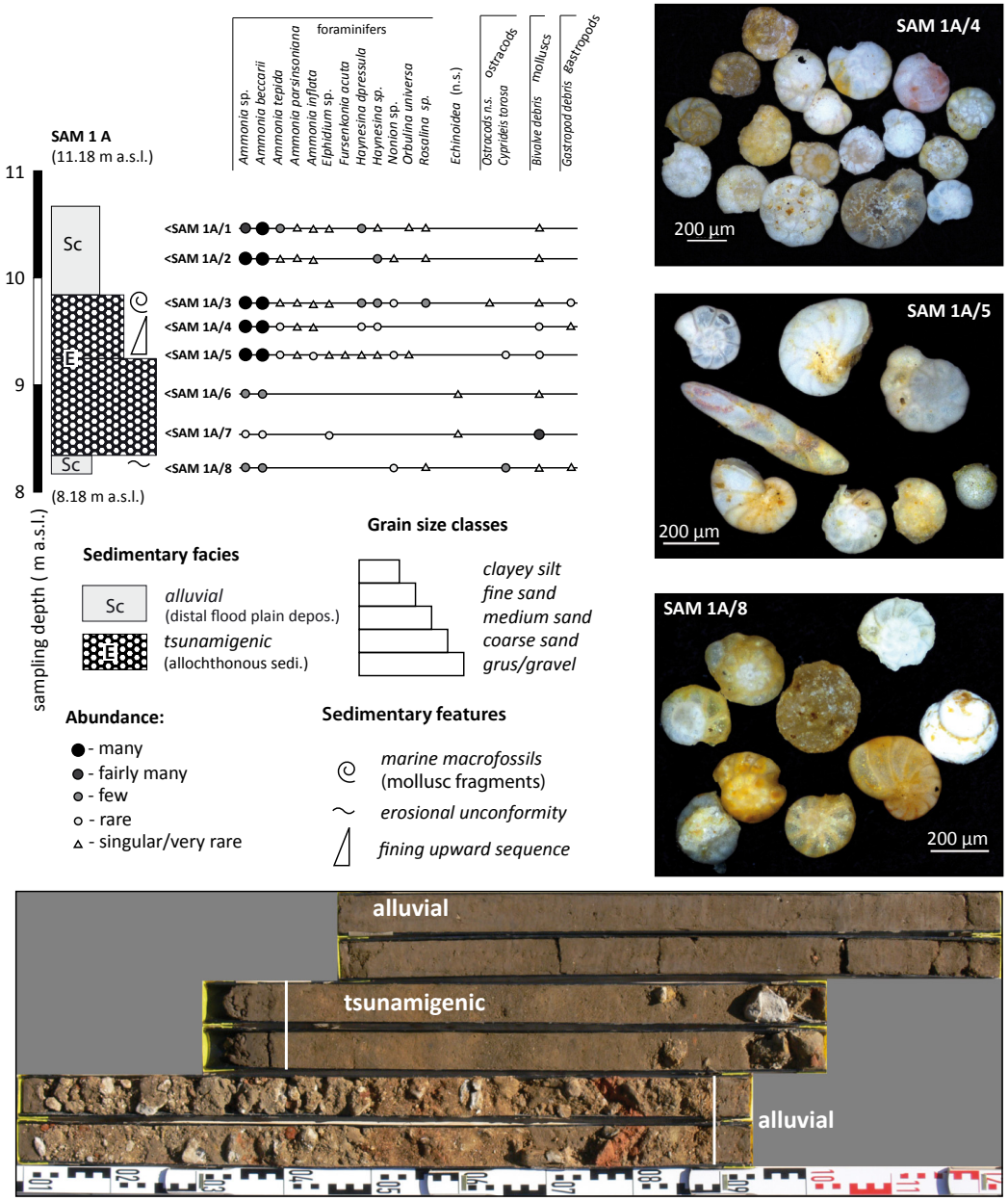

Fig. 3-12: Results of micro- and macrofossil analyses of selected samples from vibracore SAM 1A. Photos of selected specimens were taken by a polarized light microscope and a digital camera. Specimens were determined after Loeblich & Tappan 1988, Cimerman & Langer 1991, Poppe & Goto 1991, 2000, Murray 2006, Gupta 2002, Rönnfeld 2008.

Findings of numerous foraminifers in the uppermost alluvial deposits either indicate a direct relation with the event layer (for instance decelerated final backflow dynamics) or is due to alluvial reworking of event deposits.

The microfossil content of vibracore SAM 1 thus supports the idea of a marine-borne high-energy impact to the study area of Kato Samiko. Unweathered Holocene foraminifera, atypical for the local bedrock, allow a differentiation between allochthonous marine sediments and reworked bedrock material and autochthonous deposits.

3.4.4 Subsurface investigations by electrical resistivity measurements

Electrical resistivity measurements were carried out along four transects across the valley bottom near Kato Samiko (Fig. 3-9). Results of resistivity measurements are depicted in Fig. 3-13.

As visible from transect SAM ERT 1, resistivity values between 15-25 Ωm represent silty to sandy deposits found in the lowermost part of vibracore SAM 1. Lowest resistivity values of 6-15 Ωm mark alluvial deposits found on top of them. The upper part of the transect is characterized by resistivity values between 30-50 Ωm that correspond to alluvial/colluvial sediments. Highest resistivity values of >50 Ωm were found associated to two near-surface channel fills that correlate with the high-energy event deposit encountered in the upper part of core SAM 1.

Transects SAM ERT 2, 3 and 4 generally show similar subsurface structures. Our ERT transects attest the existence of a channel structure, that widens in westward direction and is filled with high-energy event deposits.

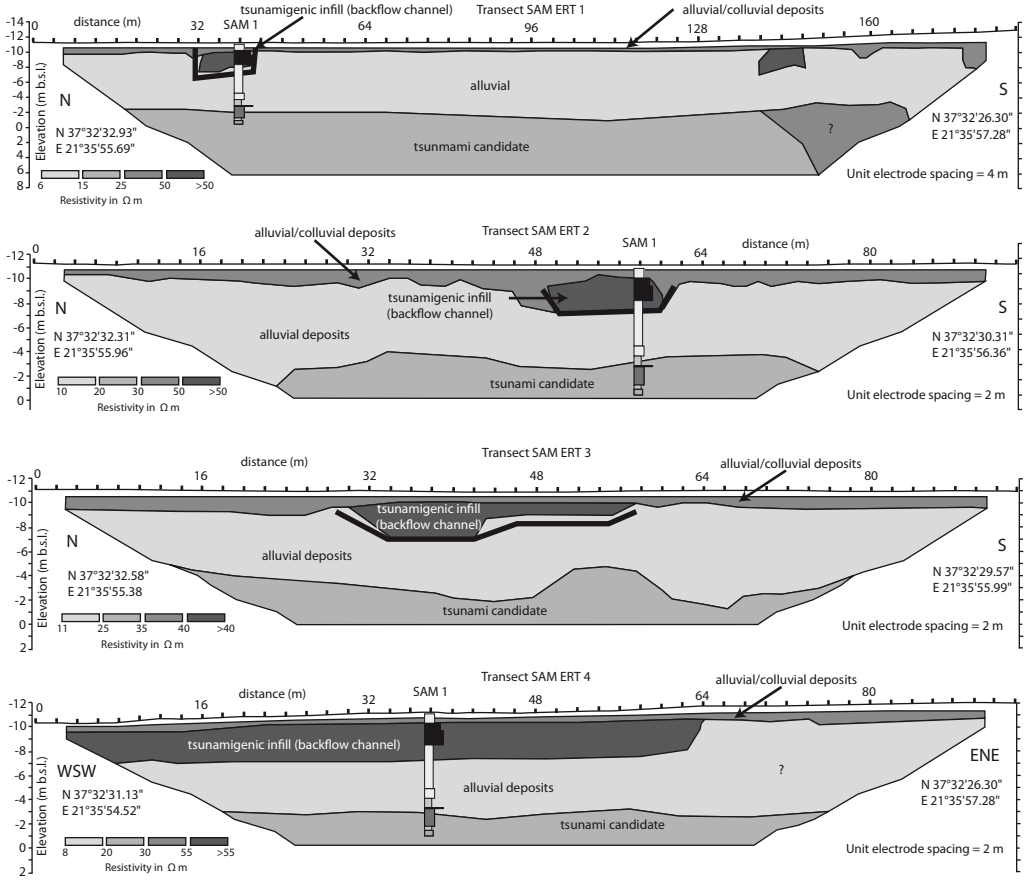

Fig. 3-13: Simplified earth resistivity pseudosections for transects SAM ERT 1, SAM ERT 2, SAM ERT 3 and SAM ERT 4 in the alluvial plain south of Kato Samiko. Earth resistivity sections were measured using the Wenner-Schlumberger electrode array and electrode spacings between 4 and 2 m. Vibracore SAM 1 is shown with simplified facies distribution. For location of geoeletrical transects see Fig. 3-9.

3.5 Dating approach

The local geochronostratigraphy for the Mouria Lagoon as well as for Kato Samiko is based on 12 ^{14}C-AMS ages obtained from peat, plant remains and charcoal as well as marine molluscs (Table 3-1). As the problem of the spatio-temporal variability of the (palaeo-)reservoir effect for marine samples remains still unsolved, an average of 408 years for the eastern Mediterranean was used for calculating calendar ages for marine samples (Reimer & McCormac 2002, Reimer et al. 2004). All dating results were calibration using the Software Calib 6.0 (Reimer et al. 2009).

In order to avoid dating of reworked material, we aimed at time-bracketing an event layer by sampling autochthonous organic matter or articulated bivalves close to it (sandwich dating approach, Vött et al. 2009b, 2012). Where possible, plant remains instead of marine shells were preferred to avoid marine reservoir corrections. Where marine molluscs had to be used for dating, only articulated specimens were sampled in order to obtain the most reliable age for the event-related sediment deposition. According to Donato et al. (2008), articulated bivalves were transported and deposited alive or died shortly after the event. Samples taken from allochthonous high-energy deposits only yield maximum ages for the event (*termini ad* or *post quos*). On the contrary, samples from post-event sedimentary units represent *termini ante quos* for the event.

Sample AGI 1/13+PR2, taken from a peat layer, yielded an age of 1608-1523 cal BC based on the humic acid fraction and of 1492-1424 cal BC based on the alkali fraction. Sample AGI 3/20+PR yielded an age of 1608-1527 cal BC for the humic fraction and 2008-1899 cal BC for the alkali fraction, and the peat sample AGI 6/17+PR yielded 1874-1698 cal BC for humic acid and 2281-2145 for the alkali fraction. Due to the potential mobility of humic acids the radiocarbon age of the humic acid fraction is supposed to be less reliable than the age given by the alkali fraction (Wagner 1998). This would usually result in younger humic acid ages compared to alkali fraction ages. However, results for sample AGI 1/13+PR2 show the contrary so that, in this case, neither the humic acid age nor the alkali fraction age can be favoured and both ages have to be taken into consideration.

Marine calibration was carried out for plant remains showing δ^{13} C (ppm) values <-15 ± 3% (Walker 2005). Sample SAM 1/8+ HK was dated twice yielding two slightly differing conventional age intervals.

3.6 Discussion

3.6.1 The Holocene sea level evolution of the Mouria Lagoon

Geo-scientific studies that focus on the reconstruction of palaeogeographical scenarios for coastal regions have to consider relative local sea level changes (RSL). The relative sea level around the former Mouria lagoon was already reconstructed by Kraft et al. (2005). Adjacent areas towards the south (Messenia) and north (Elis) were already investigated by Engel et al. (2009) and Vött (2007), respectively. Based on 5 radiocarbon dates (see Tab. 3-1) obtained from peat which is one of the most reliable relative sea level markers, we reconstructed a local relative sea level band for the former Mouria Lagoon near Aghios Ioannis (Fig. 3-14).

Sample	Depth (m b.s.)	Depth (m b.s.l.)	Description	Lab No.	δ 13 C (ppm)	^{14}C Age BP	1 σ max; min cal BP	1 σ max; min cal BC	2 σ max; min cal BC
AGI 1/13+ PR2	4.70-4.74	7.02-7.06	Peat	KIA 39718	-28.99 ± 0.33 [2] -27.76 ± 0.14 [1]	3175 ± 25 [2] 3285 ± 25 [1]	3373; 3441 [2] 3472; 3557 [1]	1492; 1424 [2] 1608; 1523 [1]	1497-1413 [2] 1619-1506 [1]
AGI 1/28+ PR	10.75-10.77	13.07-13.09	Peat	KIA 39717	-28.06 ± 0.12	6065 +35/-30	6864; 6978	5029; 4915	1620-1501
AGI 2/3+ M	1.39	3.68	Mollusc	KIA 45967	-3.15 ± 0.57	2365 ± 30	1940; 2041	88 cal BC-14 cal AD	146 cal BC-52 cal AD
AGI 2/5 M	1.64	3.93	Mollusc	KIA 45968	-10.19 ± 0.30	2560 ± 35	2195-2304	346-236	378-192
AGI 2/15+ PR	4.45-4.48	6.74-6.78	Plant remain	KIA 45969	-23.15 ± 0.05	3840 ± 30	4156;4339	2390; 2207	2458;2202
AGI 3/20+ PR	5.68-5.71	5.02-5.05	Peat	KIA 45970	-27.78 ± 0.07 [2] -25.06 ± 0.16 [1]	3590 ± 30 [2] 3290 ± 25 [1]	3848; 3957 [2] 3557; 3476 [1]	2008; 1899 [2] 1608; 1527 [1]	2028;1883 [2] 1622;1507 [1]
AGI 4/8 M	1.62	3.67	Mollusc	KIA 45971	-8.37 ± 0.36	2405 ± 30	1998-2096	139-41	189-1cal BC
AGI 5/20+ HK	4.65-4.70	4.37-4.42	Charcoal	KIA 45972	-11.70 ± 0.21	3260 ± 35	3051-3181	1209-1078	1280-1031
AGI 6/11+ M	2.82	2.57	Mollusc	KIA 45973	-8.83 ± 0.26	2100 ± 25	1632-1733	232-327 cal AD	161-351 cal AD
AGI 6/12 PR	3.35	3.10	Plant remain	KIA 45974	-15.53 ± 0.49	2705 ± 25	2350-2449	481-391	576-378
AGI 6/17+ PR	5.25-5.26	5.00-5.01	Peat	KIA 45975	-24.14 ± 0.44 [2] -25.75 ± 0.49 [1]	3785 ± 33 [2] 3460 ± 30 [1]	3094; 4230 [2] 3647; 3823 [1]	2281; 2145 [2] 1874; 1698 [1]	2337; 2057 [2] 1879; 1691 [1]
SAM1/8+ HK	1.87	9.31 (m a.s.l.)	Charcoal	KIA 46016 (1)	-23.58± 0.14	2695± 25	2759;2842	893; 810	898-807
SAM1/8+ HK	1.87	9.31 (m a.s.l.)	Charcoal	KIA 46016 (2)	-24.77± 0.13	2525± 35	2508; 2734	785; 559	795; 539
SAM 1/31 HR/PR	10.26-10.28	0.90-0.88 (m a.s.l.)	Plant remain	KIA 46017	-24.24 ± 0.27	5585 ± 30	6318; 6400	4451; 4369	4484; 4352

Tab. 3-1: ^{14}C-AMS dating results used for establishing a local geochronological framework. Notes: b.s. = below surface; b.s.l. = below sea level; Lab. No. - laboratory number, University of Kiel (KIA); 1σ max; min cal BP/BC (AD)- calibrated ages according to the radiocarbon calibration program Calib 6.0 (Reimer et al. 2009); 1σ & 2 σ range ";" – several possible age intervals because of multiple intersections with the calibration curve (oldest and youngest age given); [1]humic acid fraction dated; [2]alkali fraction dated.

According to Vött (2007) and Brückner et al. (2010) near-shore paralic swamps are most suitable for sea level reconstructions as their evolution is directly linked to the marine water level. With respect to the known problem of sediment compaction, peat samples provide an optimal approximation to the palaeo sea level. Vött (2007) emphasizes that the local relative sea level signal of an area is a mixed signal resulting from climatic, regional tectonic, local sediment supply and coastal geomorphodynamic effects.

For the Mouria Lagoon, dating inaccuracies are marked according to a 1σ range while compaction is estimated with a vertical range of +/- 0.5 m (Vött 2007).

In accordance to the worldwide post-glacial Holocene sea level evolution, the relative sea level band for the former Mouria Lagoon reflects a constant rise during the last seven millennia.

Compared to the relative sea level evolution of Messenia and Elis, data from Aghios Ioannis show that the relative sea level evolution is characterized by considerably higher rates of sea level rise since the mid-Holocene. Around 5000 cal BC, for example, the difference in relative sea level stands between Messenia and Elis on the one hand and Aghios Ioannis on the other hand is about 9 m. Around 500 cal BC, the relative sea level at Aghios Ioannis is still ca. 1 m lower than in Messenia and Elis. This difference in relative sea level evolution is due to

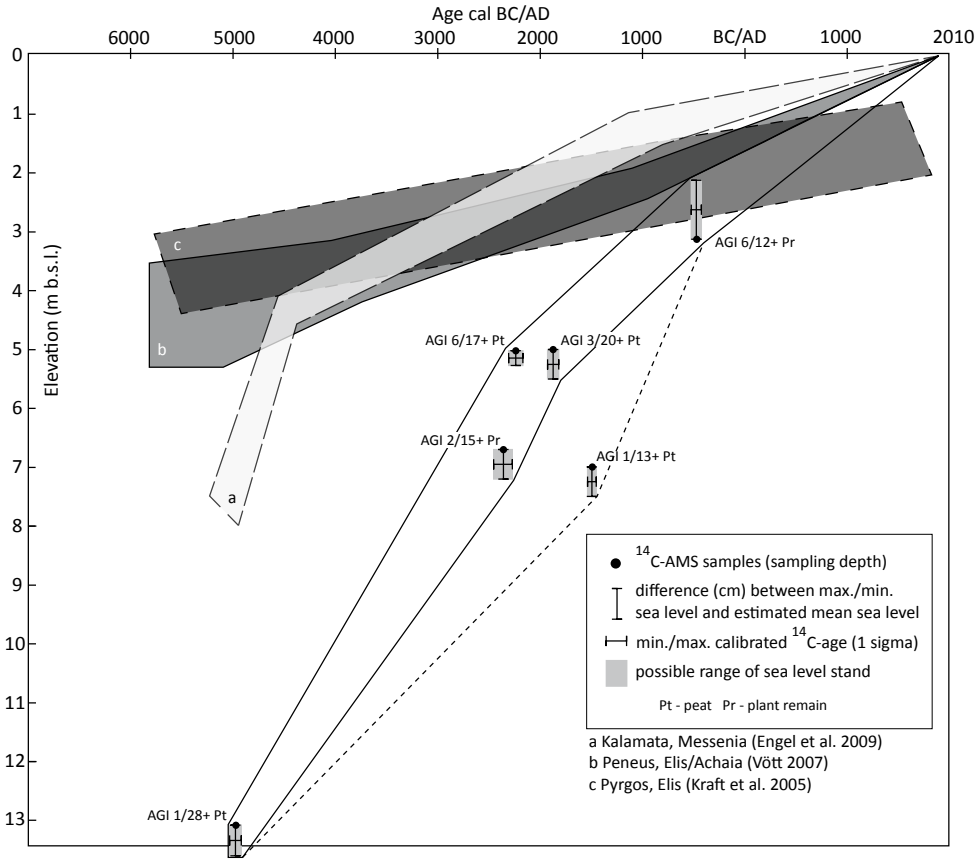

Fig. 3-14: Relative local sea level evolution of the former Mouria lagoon since the mid-Holocene and comparative sea level bands for the Peloponnese (Kraft et al. 2005, Vött 2007 and Engel et al. 2009).

tectonic reasons (Vött 2007); obviously the subsidence rate around Aghios Ioannis is much higher than this is the case towards the north and the south along the coast of the Peloponnese (Papanikolaou et al. 2007). Compared to sea level reconstructions of Kraft et al. (2005) for Elis, who collected data from a large area between the Kyllini Peninsula and Lake Kaiafa, where tectonic influences are heterogenous (Papanikolaou et al. 2007), the reconstruction of the relative sea level for the immediate environs of the Aghios Ioannis coastal area is based on consistent and homogenous conditions. Moreover, Kraft et al. (2005) used molluscs as sea level indicator which are known to only yield a wide range of rough sea level estimates. The specimen of Cerastoderma edule and peat dated by Kraft et al. (2005) originating from the area between Cape Katakolo and Aghios Ioannis most probably originate from reworked material associated with massive tsunami impacts on ancient Pheia (Pheia tsunami generations I and II, Vött et al. 2011b) and thus do not represent reliable sea level indicators. Compared to relative sea level data of Vött (2007), the mid-Holocene was in general characterized by high rates of sea level rise, which is also the case for Aghios Ioannis in this study.

3.6.2 The influence of high-energy events to the palaeogeographical evolution of the former Mouria Lagoon

Palaeoenvironmental changes around the Mouria Lagoon are partly related to the Holocene sea level evolution presented above but are also significantly influenced by high-energy impacts.

Kraft et al. (2005) postulated that the palaeo-shoreline in the environs of the Mouria Lagoon during the mid-Holocene was located further inland. From our results, the most landward marine sediments of mid-Holocene age (around 5000 cal BC) where found ~1.8 km distant to the recent shoreline and some 13 m below present-day sea level at coring site AGI 1. It remains unclear whether the marine environment extended even further inland because marine sediments may exist beyond the final coring depth at site AGI 5/5A (Fig. 3-3 & 3-5).

At vibracoring sites AGI 1 and AGI 2, two different stratigraphical units were encountered in the lowermost parts of the cores. While marine conditions continue to exist at site AGI 2, site AGI 1 is characterized by semi-terrestrial back beach swamp conditions (Fig. 3-4). Later, a sharp erosional contact followed by a shell debris layer at site AGI 1 then marks a first high-energy impact to the study area. Most likely triggered by the extreme event and subsequently affected by Holocene sea level rise, lagoonal conditions established. As marine conditions still continue to exist at site AGI 2, a palaeo-coastline must be located between both coring sites.

Marine conditions also dominate the lower sedimentary sequence of AGI 3, 4, 6 and 2. Subsequently, brackish conditions extend in seaward direction from site AGI 1 to AGI 2 and 6 that form a widespread lagoonal system, in some extent the predecessor of the Mouria Lagoon. Our data show that in a seaward direction a beach ridge (AGI 4) separated the lagoon from the open Ionian Sea.

As best visible at site AGI 2, a semi-terrestrial environment was hit by a high-energy erosive contact that marks the abrupt transition from lagoonal to limnic conditions. Erosive contacts in similar stratigraphical positions can be observed all along the vibracore transect.

After this event, an extensive coastal lake developed at sites AGI 6, 2 and 1. It is probably even connected to the formerly separated limnic environs at site AGI 5.

On-going Holocene sea level rise leads to a constantly increased marine influence at the seaward part of the transect. The beach-ridge associated marine sands at site AGI 4 are covered by lagoonal deposits. Yet, extensive limnic environs still prevail in landward direction east of the coastal barrier, so that an eastward relocation of the barrier system must be assumed.

Both the established lagoonal and limnic system are then affected by a rapid and massive environmental change. At sites AGI 3 and 4, shell debris layers indicate intensely reworked lagoonal deposits. At site AGI 6, an erosional unconformity is followed by a distinct shell debris layer that marks the abrupt environmental transition from limnic to lagoonal conditions. Similar evidence is given for sites AGI 2 and AGI 1. With regard to the sedimentary characteristics and spatial distribution of the intersecting layers, this strong environmental change is related to high-energy impact. As indicated by the abrupt establishment of a lagoonal system, the event obviously caused a breach of the coastal barrier, so that the limnic system was re-connected to the adjacent lagoonal system. However, limnic conditions at sites AGI 2 and AGI 1 were not re-established after the event. Consistent lagoonal deposits encountered along the transect yet indicate the existence of a beach ridge further south that separated the Mouria Lagoon from the Gulf of Kyparissia.

Lagoonal deposits at site AGI 3 were abruptly covered by marine sand, almost 1.5 m thick (Fig. 3-3) which, towards the top, show signs of weathering (partly decalcification and oxidation). This shows that the event deposits were partly accumulated above the relative sea level at that time, namely under subaerial conditions.

Stratigraphical correlations along vibracore transect AGI 1 allow to identify several high-energy impacts to the Mouria Lagoon. The establishment and development of the Mouria Lagoon during several phases of the Holocene coastal evolution seems to have been strongly controlled by high-energy impacts rather than by gradual coastal changes. At site AGI 1, early high-energy impact led to a strong modification of the former coastline. Event deposits encountered in the upper parts of cores AGI 6, 3, 2 and 1 are closely associated to the subsequent establishment of lagoonal conditions.

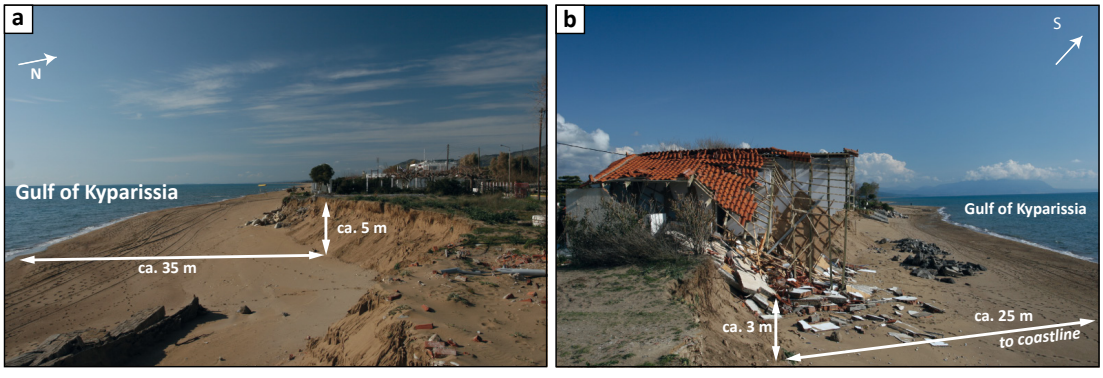

Fig. 3-15: Storm activities along the coast of the Gulf of Kyparissia. Winterstorm erosion is limited to a maximum inundaton of about 35 m (a) and mainly takes control on the recent cliff morphology. Near coastal buildings (b) are directly affacted to storm wave action. It is significant that the waves cannot overflow the dune belt, stormaction is restricted on the small coastline. Photos by T. Willershäuser 2009.

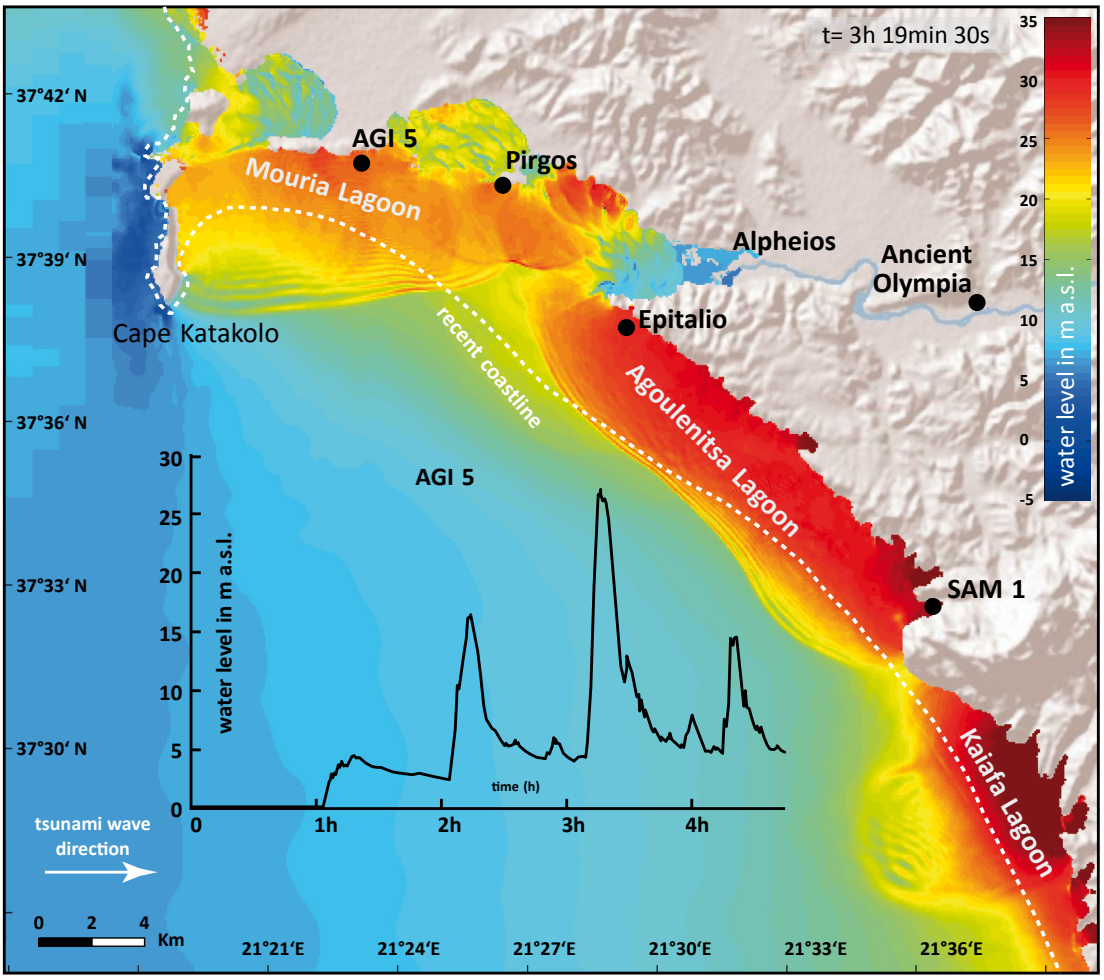

Fig. 3-16: Extreme tsunami inundation scenario and water levels at the northern coast of the Gulf of Kyparissia at the arrival of the third tsunami wave after tripartite wave trains of 2.5 m, 5 m and 10 m. Modified after Röbke et al (2013).

3.6.3 Evidence of high energy impact – storm versus tsunami

Sedimentary structures preserved in vibracores from the study area document the repeated input of allochthonous coarse-grained sediments of marine origin into predominantly autochthonous quiescent limnic or lagoonal environments.

In the open Ionian Sea, the potential for storm generated waves is limited to maximum wave heights of 6-7 m (Medatlas 2004, Soukissian et al. 2008). Close to the coastline, the maximum wave height decreases to less than 4 m in the swash zone (Cavaleri et al. 2005). Coastal dynamics along the Gulf of Kyparissia may be affected by intense winter storms, in the way that moderate to strong coastal erosion causes cliff formation along the dune belt. However, storm wave action does not exceed the present beach zone (Fig. 3-15).

Vibracore locations along the AGI transect and near Kato Samiko are located more between 1-2.5 km distant from the present coastline. Neither storms nor so called Medicanes (tropical storm equivalents for the Mediterranean Sea) (e.g. Ernst & Matson 1983, Phytaroulis et al. 2000) are capable to overflow the existing beach barrier systems, some of them being 200-

600 m wide. Thus, both study areas are protected from storm wave influence. Shallow water conditions of former lagoonal environments also exclude the development of large storm waves far inland. It must therefore be concluded that the observed traces of widespread high-energy impact cannot be explained by and associated with storm wave activity.

Computer simulations of wave inundation scenarios for the Gulf of Kyparissia demonstrate that tsunami events with a maximum wave height higher than 2 m are capable to overflow the protective dune belt along the coastline and inundate far inland (Röbke et al. 2013). Minor events simulated as single wave trains of about 0.5 m and 1 m height, however, do not have the ability to overflow the coastal dune belt. For vibracore location AGI 5, the moderate scenario predicts a maximum run up of 6 m a.s.l. in case of landfall of a tripartite tsunami wave train (0.5 m, 1 m and 2 m, Röbke et al. 2013). The calculated maximum of tsunami run-up however depends on the direction of the approaching wave. Highest run up was calculated for wave train simulations that approach the coastline from a southwestern direction. Extreme tripartite wave train scenarios (wave heights of 2.5 m, 5 m and 10 m) are able to flood areas as far as 15 km inland. Within the Alpheios river valley, for instance, the maximum inundation depth may reach about 25 m. Röbke et al. (2013) show that such an extreme tripartite tsunami scenario would flood the coastal area of Kato Samiko and vibracore location SAM 1, situated about 11 m a.s.l. (Fig. 3-16) whereas scenarios simulated with lower wave heights (e.g. a tripartite tsunami wave train of 0.5 m, 1m and 2 m) would not flood the study site.

Moreover, previous geo-scientific studies identified traces of palaeotsunami impact along the shores of the Gulf of Kyparissia (e.g. Vött et al. 2011b, Willershäuser et al. 2012, Röbke et al. 2013). Results presented in this paper also provide clear evidence of high-energy impact that affected both, the former Mouria lagoon as well as the vibracore location of SAM 1. Against the respective geomorphological setting, the identified sedimentary structures, geochemical fingerprints and microfossil content of each event-associated layer as well as results from geophysical studies emphasize the tsunamigenic origin of the event deposits.

Sedimentary characteristics and geochemical signatures of the high-energy event deposits encountered in the stratigraphical record comprise features like (i) erosional unconformities at the base of allochthonous sediments, (ii) shell debris layers, (iii) fining upward sequences, (iv) rip-up-clasts of eroded underlying sediments, (v) mud caps, (vi) allochthonous microfaunal assemblages, (vii) significant geochemical changes and interferences in the Ca/Fe and Ca/Ti ratios as well as (viii) high variabilities in the magnetic susceptibility of the units and (ix) a wide range and high variabilities in the colour light spectrum. Most sedimentary characteristics have been observed in deposits that are associated with recent and sub-recent tsunami events (e.g. Chile 2010 - Bahlburg & Spiske 2012; Samoa 2009 - Okal et al. 2011, Richmond et al. 2011; Indian Ocean Tsunami 2004 - Srinavaslu et al. 2007, Srisutam & Wagner 2010). As various studies show, similar sedimentary and geochemical structures may also occur in storm deposits (e.g. Kortekaas & Dawson 2007, Morton et al. 2007, 2008). Against the background of the local (palaeo-)geographical setting discussed above, major storm events have to be considered incapable of overflowing the coastal barriers. Palaeotsunami studies concerning the Ionian Sea (e.g. Smedile et al. 2011, Vött et al. 2009a, 2009b, 2010, 2011a,

2011b, 2013), are however, in very good accordance with the sedimentary finding along the presented vibracore transect.

Microfaunal analysis carried out for selected key sites in both study areas (AGI 5A, SAM 1/1A) show that the overall microfaunal assemblage significantly varies between autochthonous facies and high-energy allochthonous sediments. The encountered microfossil content reflects an abrupt change of the environmental conditions and documents a distinct marine-borne influence. The marine character of the allochthonous deposits is strengthened by the complete absence of brackish or limnic micro- and macrofossils as seen in the stratigraphic units below. The rapidly increased abundance of marine species indicates a short-term and abrupt shift of the predominating environmental conditions. At the same time, the heterogeneous assemblage documents the synchronous input of fossils from a broad variety of sedimentary environments, which cannot be explained by gradual processes but rather documents a widespread and catastrophic disturbance of different adjacent sites. Here, marine species clearly prove a high-energy event originated from the sea-side.

In the Mouria Lagoon, autochthonous limnic units comprise a very low microfossil content where only brackish ostracods, freshwater gastropods as well as *Characeae* occur in significant numbers. In contrast, the microfaunal content of the allochthonous layers is significantly higher and provides a clear marine signal as the assemblage is characterized by the occurrence of foraminifera from Holocene marine and/or shallow marine environments. Allochthonous marine foraminifera were encountered up to 1.9 km inland at site AGI 5A. In the study area

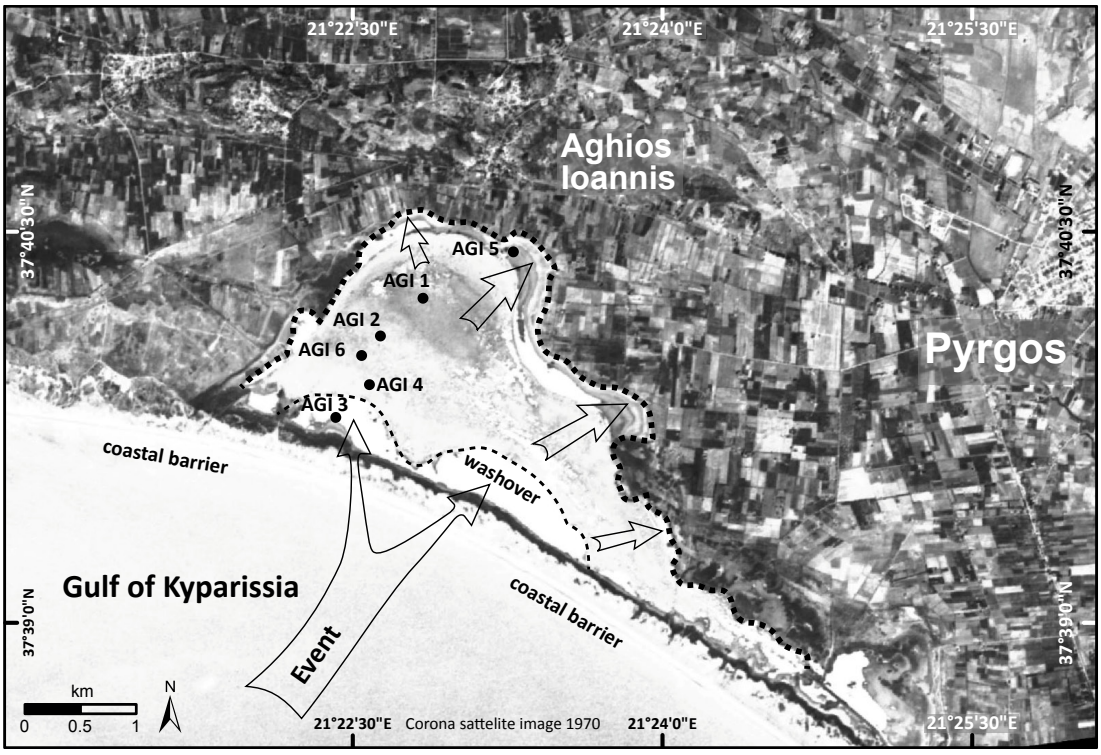

Fig. 3-17: Wash-over structure at the study site of Aghios Ioannnis clearly show parallels to massive ingressional chararcter and overflow dynamics of tsunmigenic impact. Maps based on Corona Sattelite image of 1970.

of Kato Samiko, an increased content of recent marine foraminifera was encountered in event-related allochthonous coarse-grained deposits mixed with anthropogenic remains. Located about 2.4 km distant from the present coast and 10 m a.s.l., even extraordinarily high storm activity must be excluded as triggering factor for this event deposit. Studies on relative sea level changes moreover exclude that the local relative sea level in the Holocene has ever been higher than today (Kraft et al. 2005, Vött 2007, Engel et al. 2010). Considering a lower relative sea level for the past millenia, the occurence of Holocene marine deposits (> a.s.l.) at the base of SAM 1 thus must be related to high-energy impact.

In accordance with the sedimentary features of the high-energy layers, already characterized as high-energy signatures, microfossil analyses for both study areas emphasize the tsunamigenic character of the deposits in the study area. Similar observations of foraminiferal dislocation were made by Sugawara et al. (2012) and Pilarczyk et al. (2012) for the 2004 Indian Ocean and the 2011 Japan tsunamis.

For both study areas, results from ERT measurements are in good accordance with the stratigraphic record and give the possibility to extrapolate the subsurface palaeo-landscape. The detection and spatial tracing of tsunami signatures by electrical resistivity measurements however appeared to be quite difficult where the sedimentary structure of the event layer strongly resembles autochthonous deposits in terms of grain size, pore volume and water saturation.

ERT transects in the study area of Kato Samiko prove the existence of a channel-like structure, filled with allochthonous coarse-grained and mostly unsorted high-energy deposits that significantly vary from autochthonous fine-grained sediments underneath. Considering the present environmental conditions, neither a river nor a creek with episodic torrential runoff dynamics exists in the area of Kato Samiko. Obviously, there is a discrepancy between the present geomorphodynamic potential and the high-energy character of detected channel structure. Regarding the local geomorphological setting with a funnel-like valley entrance, the marine-borne high-energy event most probably flooded the study area at Kato Samiko. The widening of the detected channel structure in seaward direction and the massive incorporation of terrestrial components both indicate strong erosion and subsequent sediment deposition during backflow processes.

As documented by Bahlburg & Spiske (2012) for the 2010 Chile tsunami, tsunamigenic flooding of an area may produce channelized backflow dynamics along local depressions. Increased flow velocities may then cause the incision of channels that are subsequently filled with tsunami backflow deposits. With regard to the local climate conditions, the funnel-like shape of the valley, the marine character of the channel infill and the elevation above sea level, the channel structure at Kato Samiko cannot be explained by fluvial processes but seems to be related to tsunamigenic backflow dynamics.

With regard to the local geomorphological setting and compared to signatures of high-energy impacts from study areas in the eastern Mediterranean and worldwide, we finally conclude that coarse-grained allochthonous event layers encountered in both study areas, the Mouria Lagoon as well as Kato Samiko, were caused by repeated major tsunami events that also led to considerable impulses on the overall coastal evolution.

3.6.4 The event-geochronology of the Mouria lagoon and Kato Samiko

The event-geochronology for the former Mouria Lagoon as well as Kato Samiko is based on 13 ^{14}C-AMS datings as well as age estimations of archaeological remains and diagnostic ceramic fragments. Altogether, sedimentary traces of four different tsunami generations were found.

Tsunami generation I

Sample AGI 1/28+ PR provides an age of 5029-4915 cal BC which has to be considered as *terminus post quem* for the oldest tsunami event encountered in the study area. As the sample dates the lowermost part of the underlying peat deposit and also the degree of event-related peat erosion remains unclear, the obtained age is a mere maximum age the event may have occurred some centuries later. Tsunami impact that affected the nearby harbour site of ancient Pheia at Cape Katakolo was dated to around 4300 ± 200 cal BC (Vött et al. 2011b). The lowermost tsunami deposit found in core AGI 5 (8.67-7.95 m b.s.l.) is in stratigraphical correlation with the AGI 1 mid-Holocene event layer (12.89-12.79 m b.s.l.) may thus have been caused by the same tsunami event. Plant remains from the limnic facies below the oldest event deposit found at site SAM 1 near Kato Samiko were dated to 4451-4369 cal BC (SAM 1/31 HR/PR) and provide a *terminus post quem*. This age is in perfect accordance with the tsunami dates from Pheia (Vött et al. 2011b) and with the oldest tsunami event detected at sites AGI 1 and 5. The tsunami that hit the Gulf of Kyparissia around 4300 +- 200 cal BC probably was of (supra-)regional extent and seems to havehad widespread effects along the coasts of the eastern Ionian Sea. Strong tsunami impact at around 4400 cal BC was found for the Bay of Palairos-Pogonia (northern Akarnania, Vött et al. 2011a), the Bay of Koutavos (Cefalonia Island, Vött et al. 2013) and the Bay of Lixouri (Cefalonia Island, Willershäuser et al. 2013).

Tsunami generation II

Stratigraphically correlating tsunami traces were found at sites in mid-core positions of all vibracores along the AGI vibracore transect. Sample AGI 1/13+ PR2 yielding an age of 1608-1424 cal BC provides a termini post quem and sample AGI 5/20+ HK yielding an age of 1209-1070 cal BC provides a termini ante quem for the event. The latter can therefore be time-bracketed between the 17th and 11th centuries BC.

The radiocarbon dates do not allow to exclude that tsunamite generation II found in the Gulf of Kyparissia is associated to the Santorini/Thera tsunami which is dated to the 17th century BC (~1600-1627 cal BC after Friedrich et al. 2006 and 1613 cal BC after Friedrich 2013). However, it is more probable that Aghios Ioannis tsunami generation II is associated with a tsunami event around 1000-1200 cal BC described by Vött et al. 2011a for the Bay of Palairos-Pogonia, by Vött et al. 2009b for the Lake Voulkaria and by Willershäuser et al. for the Gialova Lagoon (see Section 4).

Tsunami generation III

Five radiocarbon ages provide minimum and maximum ages for the third tsunami layer which can be followed in stratigraphically consistent position along the vibracore transect (sample AGI 2/3+ M: 88 cal BC-14 cal AD). The resulting *terminus post quem* for the event is 88

cal BC – 14 cal AD (AGI 2/3+ M), the resulting *terminus ante quem* for the event is 232-327 cal AD (AGI 6/11+ M). Tsunami generation III deposits can thus be time-bracketed to around 88 cal BC to 327 cal AD; the event thus occurred during Roman times. This result is pretty well consistent with geochronological data from nearby Kato Samiko: Dating of the channelled backflow tsunami deposit detected at site SAM 1 yielded the ages of 893-810 cal BC and 785-559 cal BC as *termini ad* or *post quos* for the event. Diagnostic sherds (Fig. 3-11) which were also incorporated into the event layer were dated to Hellenistic to Roman times. In addition to radiocarbon results, the archaeological remains provide another maximum age of the event. As younger artifacts were not found, for example from the Byzantine period, it is, however, assumed that the event actually took place between the 4th cent. BC and the 3rd cent. AD.

To be considered: most ages calibrated regarding marine reservoir effect of 408 years. Time interval for tsunami generation will shift in case if the real marine reservoir age considerably differs from that!

Tsunami generation IV

The youngest tsunami layer encountered in the study area is dated by the terminus post quem of 232-327 cal AD provided by sample AGI 6/11+ M. Possible historical candidates for this tsunami within a (supra-)regional context are the 365 AD event (Shaw et al. 2008) or the 521 and 551 AD events (Soloviev et al. 1990, Fokaefs et al. 2007).

Morover, two more sand and shell debris layers in top-core positions at vibracoring sites AGI 2, AGI 4, AGI 6 (circa 0.75 m b.s.), AGI 1 (circa 0.45 m b.s.) and AGI 6 (circa 0.48 m b.s.) were detected and mark two younger generations of tsunami deposits which could not yet be dated in the framework of this study.

Additionally, vibracores, geophysical and multi-proxy palaeoenvironmental data as well as geomorphological evidence resulting from field surveys and remote sensing data (Fig. 3-17) lead to the conclusion that the shape of the Mouria Lagoon – drained since the 1960s – is due to high-energy impact: massive washover fans along the coastal barrier at the former coastline and tsunami surge deposits at the former inland shores of the lagoon document the high-energy character of the lagoonal indentations to be seen in Fig. 3-17.

3.7 Conclusions

Detailed geo-scientific investigations were carried out in the former Mouria Lagoon and the area of Kato Samiko, western Peloponnese (Greece) in order to reconstruct the palaeogeographical evolution and to decipher evidence of palaeo-tsunami impacts. Based on vibracores, geophysical measurements and multi-proxy palaeoenvironmental data, the following conclusions can be made:

(i) Autochthonous limnic and lagoonal deposits are repeatedly intersected by allochthonous layers of marine sands and shell debris which document the short-term impact of high-energy events on the coastal area.

(ii) Intersecting allochthonous coarse-grained deposits show a high amount of marine microfauna (foraminifera, molluscs) and shell debris. In contrast to autochthonous facies, these assemblages emphasize the marine character of the event layer.

(iii) Since the local geographical setting excludes the influence of storm surges, high-energy traces have to be interpreted as tsunami deposits. Tsunami traces in the former Mouria Lagoon are stratigraphically consistent over a distance of several kilometres and up to 1.9 km inland. Depending on the palaeogeomorphology, palaeotsunami deposits vary in thickness, composition and in sedimentary characteristics. In some cases, palaeotsunami traces are merely preserved as erosional contact.

(iv) The relative sea level in the study area has never been higher than at present. Compared to neighbouring areas, the study site is obviously characterized by extraordinarily high subsidence rates since the mid-Holocene. Consequently Holocene marine sediments at Kato Samiko, deposited well above the present-day sea level, do not represent natural marine conditions, but are directly related to tsunami impact.

(v) Although the coastal evolution of the study area is linked to Holocene sea level changes, palaeogeographical scenarios for the former Mouria lagoon underline that tsunamigenic high-energy impacts do temporarily control the overall coastal evolution.

(vi) Event-stratigraphical correlations allowed the identification of four different tsunami events since the mid-Holocene. 4300 ± 200 cal BC, the mid to late 2nd mill. BC, Roman times (1st cent. BC to early 4th cent. AD) and most possible one of the well-known 365/521/551 AD historic tsunamis. Additionally two more younger events can not be excluded.

4 Holocene palaeotsunami imprint in the stratigraphical record and the coastal geomorphology of the Gialova Lagoon near Pylos (southwestern Peloponnese, Greece)*

Abstract The coastal area around the Gialova Lagoon (southwestern Peloponnese, Greece) is directly exposed to the tectonically highly active Hellenic Trench. As known from historical sources, it was repeatedly affected by tsunamigenic impacts. Detailed geo-scientific studies were carried out in the environs of the Gialova Lagoon in search of high-energy event deposits. Geomorphological, sedimentological and geochemical methods were applied to reconstruct the fingerprints of Holocene tsunami events and the palaeogeographical evolution based on 8 terrestrial vibracorings. Microfossil studies were applied along a transect of three vibracores to decipher detailed changes in the palaeoenvironmental setting. Our results show that the palaeogeographical evolution of the Gialova Lagoon was strongly affected by high-energy impacts. Coarse-grained allochthonous sediments of marine origin were found intersecting low-energy lagoonal and limnic muds. Based on sedimentary characteristics, the local (palaeo-)geomorphological setting and the geomorphodynamic potential of modern-day storms, we conclude that high-energy events were associated to tsunami impacts. Radiocarbon datings allowed to give age estimations of six tsunami generations that took place between the 4th millennium BC and medieval times resulting in a rough recurrence interval of 1.2 ka. Geomorphological characteristics of the study area such as the Voidokilia washover fans and beachrock structures along the coastline also give evidence of repeated tsunamigenic landfalls.

4.1 Introduction and aims

The eastern Mediterranean, especially the Ionian Sea, is a tectonically active region with a high tsunami risk (Papazachos & Dimitriou 1991). The plate boundary of the Hellenic Arc, where the African Plate is being subducted underneath the Aegean microplate (Clement et al. 2000), is a hot spot for earthquakes (Koukouvelas et al. 1996, Benetatos et al. 2004,) and therefore highly capable of triggering tsunamis (Tselentis et al. 2010). Numerous historical accounts show that the shores of the Ionian Sea were strongly influenced by tsunami impacts (e.g. Antonopoulos 1979, Soloviev 1990, Minoura et al. 2000, Soloviev et al. 2000, Tinti et al. 2004, Guidoboni & Ebel 2009, Ambraseys & Synolakis 2010, Hadler et al. 2012). One example is the description of *Ammianus Marcellinus* regarding damages and fatalities caused by the 21 July 365 AD tsunami. He also mentions the ancient settlement of Methoni, unfar Pylos, where this tsunami caused inland inundation of at least 2 km (Seyfarth 1971).

Apart from historical reports listed in tsunami catalogues, the last decades have given rise to an increasing number of geo-scientific studies all around the Mediterranean is in search of palaeotsunami traces. Sedimentological and geomorphological tsunami impacts were, for instance, detected in southern Italy (e.g. Mastronuzzi & Sansò 2000, Gianfreda et al. 2001,

* This chapter will be submitted to Zeitschrift für Geomorphologie N.F. Suppl. Vol. as: Willershäuser, T., Vött, A., Hadler, H., Ntageretzis, K. & Brückner, H.: Holocene palaeotsunami imprint in the stratigraphical record and the coastal geomorphology of the Gialova Lagoon near Pylos (southwestern Peloponnese, Greece).

Fig. 4-1: Topographic and geo-tectonic overview of the Eastern Ionian Sea with study sites at the Peloponnese and Cefalonia Island. The study area of the Gialova lagoon is encircled by a white box. Simplified tectonic inlay map is modified after Clews et al. (1989), Sachpazi et al. (2000) and van Hindsbergen et al. (2006), topographic overview based on Landsat TM 5 true composite satellite image (1999).

De Martini et al. 2003, Scicchitano et al. 2007, Mastronuzzi et al. 2007, Pantosti et al. 2008, Smedile et al. 2011), the Ionian Islands and Akarnania (e.g. Kortekaas 2002, Vött et al. 2006d, 2007a, 2008, 2009a, 2009b, 2010, 2011a, 2011b, 2013, Willershäuser et al. 2013), the western and southern Peloponnese (e.g. Scheffers et al. 2008, Vött et al. 2010, 2011a), the Aegean (e.g Pirazzoli et al. 1999, Dominey-Howes et al. 2000, Mitsoudis et al. 2012), Crete and Cyprus (e.g. Kelletat & Schellmann 2002, Scheffers & Scheffers 2007, Bruins et al. 2008, Shaw et al. 2008) and northern Africa (e.g. Morhange et al. 2006, Reinhardt et al. 2006, Stanley & Bernasconi 2006).

Throughout the last 20 years, tsunami research has been intensified and resulted in the detection of a bundle of sedimentary and geomorphological characteristics found associated with tsunami deposits. Among others, recent and subrecent tsunamis are characterized by (a) allochthonous sand and shell debris layers, (b) mixture of littoral and sublittoral material, (c) multi-modal grain size distribution, (d) rip up-clasts, (e) basal erosional unconformities, (f) fining upward and thinning landward tendencies with regard to high-energy layers, (g) lithified beachrock-type calcarenites, (h) dislocated boulders and (i) washover deposits (e.g. Dominey-Howes et al. 2006; Dawson & Stewart 2007, May et al. 2012; Vött et al. 2009a, 2009b, 2010, 2011b).

The main objectives of this study are to detect allochthonous high-energy deposits in the local stratigraphical record by sedimentary evidence, geochemical and microfossil analyses, to reconstruct palaeotsunami events against the background of the palaeogeographical evolution and relative sea level changes of the Gialova Lagoon during the Holocene.

4.2 Regional setting of the study area

The study area, located at the southwestern Peloponnese near the modern town of Pylos, comprises the shallow waters of the Gialova Lagoon and two extended beach barrier systems which separate the lagoon from the Ionian Sea and the Bay of Navarino, the latter being a tectonic depression (IGME 1980a) (Fig. 4-1). The region is directly exposed to the subduction zone of the Hellenic Trench and therefore holds a high tsunami risk (e.g. Papazachos & Dimitriou 1991, Ferentinos 1992, Sachpazi et al. 2000, van Hinsbergen et al. 2006, Hollenstein et al. 2008). To the west, the semi-circular Bay of Voidokilia is characterized by a wide dune belt. Bound to local fault systems, three bedrock outcrops (Fig. 2-2) out of Eocene-Paleocene limestone form a sharp boundary towards the Ionian Sea and protect the Bay of Navarino from the Ionian Sea making this bay to one of the most prominent natural harbour of the Mediterranean. The limestone ridges of Palaeokastro and Sphacteria are separated by the inlet of the Sykia channel. The hinterland towards the east consists of Pliocene marls and conglomerates, which mainly provide the sediments that built up the central Typhlomytis alluvial plain at the northern fringe of the Gialova Lagoon (e.g. IGME 1980a, Kraft et al. 1980, Zangger et al. 1997).

The Bay of Navarino is a almost 60 m deep, measuring 10 km in north-south and 4 km in east-west direction. The Gialova Lagoon is about 3 km wide (from east to west) and 2 km long (from north to south). The average water depth does not exceed ~10 m. Offshore, the region is characterized by a 2 km-wide shelf zone. Towards the west, however, bathymetric

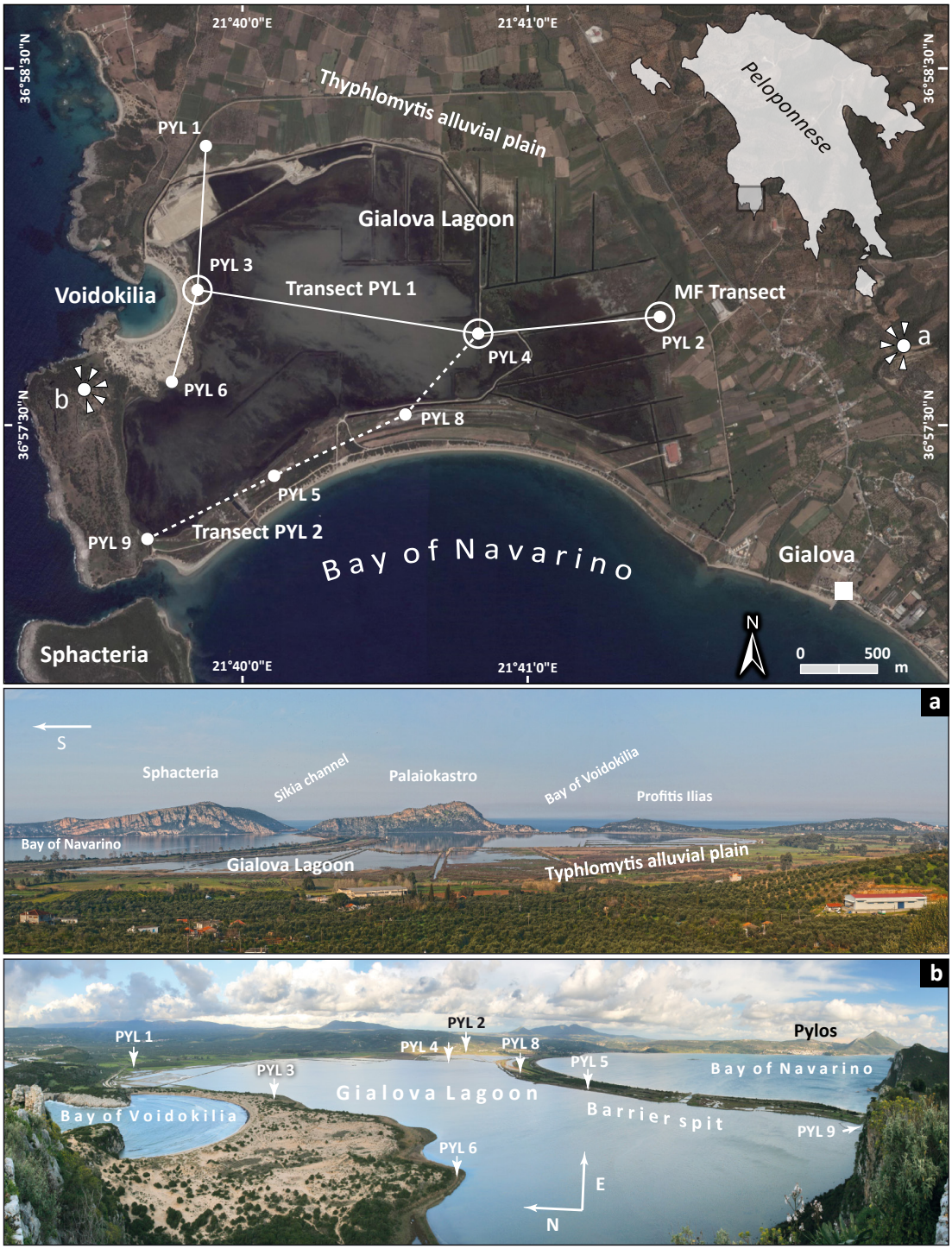

Fig. 4-2: Topographic overview of the Gialova Lagoon and the northern part of the Navarino Bay with vibracoring sites PYL 1-9. Vibracore transect PYL 1 is signed by a solid line, Vibracore transect PYL 2 by dashed line. Vibracores of the microfossil transect are encircled. (a) Bird's eye view of the Gialova Lagoon from north eastern direction (viewing angle and position is marked with "a") towards the Ionian Sea. (b) Birds eye view on top of the Palaiokastro ridge with view direction to the east (position of the Photo and viewing angle is marked with "b"). Aerial image is modified after Google Earth images (2009).

conditions strongly steepen. Water depth reaches about 3000 m at a distance of 20 km from the recent coast (Elias 2010) and more than 5000 m at a distance of 70 km (Zangger et al. 1997, Davis 2008). The extreme slope gradient is mainly controlled by the subduction zone of the Hellenic Arc (e.g. Cocard et al. 1999, Hollenstein et al. 2008). Intense Neogene tectonics resulted in the fragmentation of the Eocene-Paleocene limestone into ridges along sharp fault and scarp systems with a quasi-vertical drop into the Navarino Bay (Kraft et al. 1980). Strong Neogene uplift and subsidence combined with local fault tectonics are mainly responsible for the present day geomorphological setting in the wider area of the Navarino Bay (Zangger et al. 1997).

4.3 Methods

For deciphering the palaeogeographical and geomorphological changes in the study area and to identify traces of palaeotsunami impact, a multidisciplinary approach was applied.

This paper is based on 8 vibracorings, carried out in the vicinity of the Gialova Lagoon. Vibracorings were accomplished using an Atlas Copco mk1 coring device with core diameters of 6 cm and 5 cm. The maximum coring depth was 12 m below ground surface (= m b.s.). Position and elevation data of the coring sites were obtained by means of a Leica differential GPS System (Leica SR 530) with a total resolution accuracy of +/- 2 cm.

Moreover, X-ray fluorescence (XRF) measurements were carried out for sediment samples using a handheld XRF spectrometer (Niton Xl3t 900S GOLDD). Around 30 elements were measured for each sediment sample (Thermo Fischer Scientific 2010).

Additionally, laboratory studies comprised the determination of the pH-value, content of calcium carbonate, electrical conductivity and organic content (loss on ignition) for selected sediment samples (Barsch et al. 2000).

Foraminiferal studies were carried out using ca. 15 ml of sediment extracted from relevant stratigraphical units. These samples were sieved in fractions of > 0.4 mm, 0.4-0.2 mm, 0.2-0.125 mm and < 0.125 mm and subsequently analysed using a stereo microscope (type Nikon SMZ 745T). Digital photos were taken from selected specimens using a light-polarizing microscope (type Nikon Eclipse 50i POL with Digital Sight DS-FI2 digital camera back 5 MP and NIS Elements Basic Research 4 Software from Nikon ver. 2012) and determined after Loeblich & Tappan 1988, Cimerman & Langer 1991, Poppe & Goto 1991, 2000, Hottinger et al. 1993, Murray 2006, Gupta 2002 & Rönnfeld 2008.

The geochronological framework was established on the basis of 14 ^{14}C-AMS ages of organic samples and marine shells. For radiocarbon dating, we preferred samples taken from autochthonous deposits such as peat, or articulated marine molluscs. To time-bracket allochthonous high-energy deposits, the sandwich dating technique was applied. Samples taken from reworked material only yield maximum ages. Calibration was accomplished using the software Calib 6.0 after Reimer et al. (2009).

4.4 Sedimentary record of the quiescent near-shore environments of the Gialova Lagoon

4.4.1 Vibracore transect I & II

Vibracoring sites at the Gialova embayment were arranged across the lagoon in order to detect the spatial variability and differences in the sedimentary characteristics. Transect I comprises vibracores PYL 6 (ground surface at 0.13 m a.s.l., N 36°57‘33.7“, E 21°39’41.8“), PYL 3 (ground surface at 0.22 m a.s.l., N 36°57‘51.6“, E 21°39’51.3“) PYL 4 (ground surface at 0.99 m a.s.l., N 36°57‘43.8“, E 21°40’49.6“), PYL 2 (ground surface at 0.47 m a.s.l., N 36°57‘46.9“, E 21°41’29.3“) and PYL 1 (ground surface at 1.73 m a.s.l. N 36°58‘19.3“, E 21°39‘52.0“) and is trending in west-eastern direction (see Fig 4-2. for location). Detailed vibracore stratigraphies are depicted in Fig. 4-3.

Vibracore PYL 6 was drilled on the south-western fringe of the Voidokilia dune complex in the back beach marsh area. The profile shows silty fine sand (10.87-8.71 m b.s.l.) at its base with an intersecting layer of clayey silt indicating temporary quiescent conditions (10.44-10.11 m b.s.l.) Following a clear erosional unconformity, the subsequent sedimentary unit (8.71-7.50 m b.s.l.) consists of grey sand and gravel with two fining upward cycles. This coarse-grained stratum appears to be poorly sorted in contrast to the underlying and overlying units and documents temporary high-energy influence to the sedimentary environment. It is covered by homogenous clayey silt deposited in a quiescent lagoonal environment with high macrofossil content (7.50-6.67 m b.s.l.). Fine sandy silt once again intersect the lagoonal facies between 6.67-6.40 m b.s.l. Between 6.40-2.08 m b.s.l., the lagoonal deposits show higher contents of organic material. Another high-energy marine sand layer was found intersecting the lagoonal mud between 2.08-1.49 m b.s.l.. The lagoonal deposits are covered by sand rich in faunal remains of marine origin (1.17-0.18 m b.s.l.). Characterized by a sharp contact at its base, this unit indicates another high-energetic sediment input into the lagoonal system. On top, we found silty back beach swamp deposits (0.18 m b.s.l.-0.13 m a.s.l.).

The base of PYL 3 is made out of well sorted fine sandy silt which, due to its macrofaunal content, is of quiescent shallow marine origin (9.78-8.36 m b.s.l.). This facies is separated by a sharp erosional unconformity from following coarse-grained and unsorted sand and gravel with distinct fining upward sequences and sublayers including well-rounded gravel (8.36-7.34 m b.s.l.). Subsequently (7.34-6.49 m b.s.l.), silt-dominated limnic deposits were accumulated. A second sharp erosional unconformity (6.49 m b.s.l.) indicates another abrupt environmental change and the input of marine sand. The fairly unsorted sediments consist of a mixture of gravel, grus, sand and loam. This part of the profile is again characterized by fining upward cycles and rip up-clasts of eroded underlying muddy sediments (6.49-5.77 m b.s.l.). Following the high-energy inerference, quiescent depositional conditions were quickly re-established (5.77-3.44 m b.s.l.). Towards the top of vibracore PYL 3, the lagoonal environment was influenced by another distinct input of marine sand (3.44-3.22 m b.s.l.). This intersecting layer is characterized by rip up-clasts and several fining upward sequences. However, pre-existing quiescent lagoonal conditions were rapidly re-established after the event (3.22-2.36 m b.s.l.). Subsequently, we found another layer of sand rich in marine macrofaunal remains

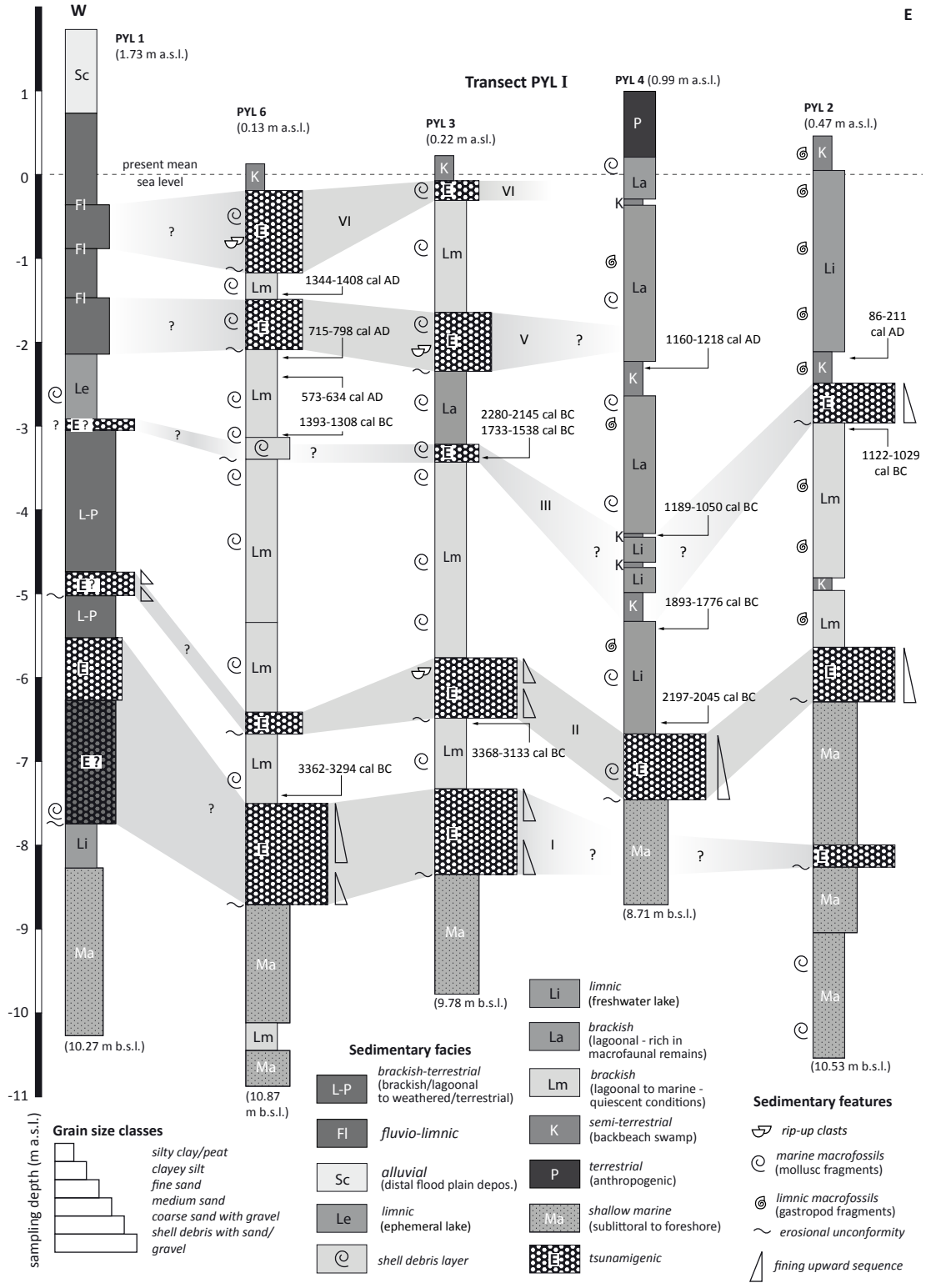

Fig. 4-3: Stratigraphical record and facies distribution of vibracores drilled along transect I crossing the Gialova Lagoon (for location see Fig. 4-2). Details of selected radiocarbondatings are listed in Table 4-1.

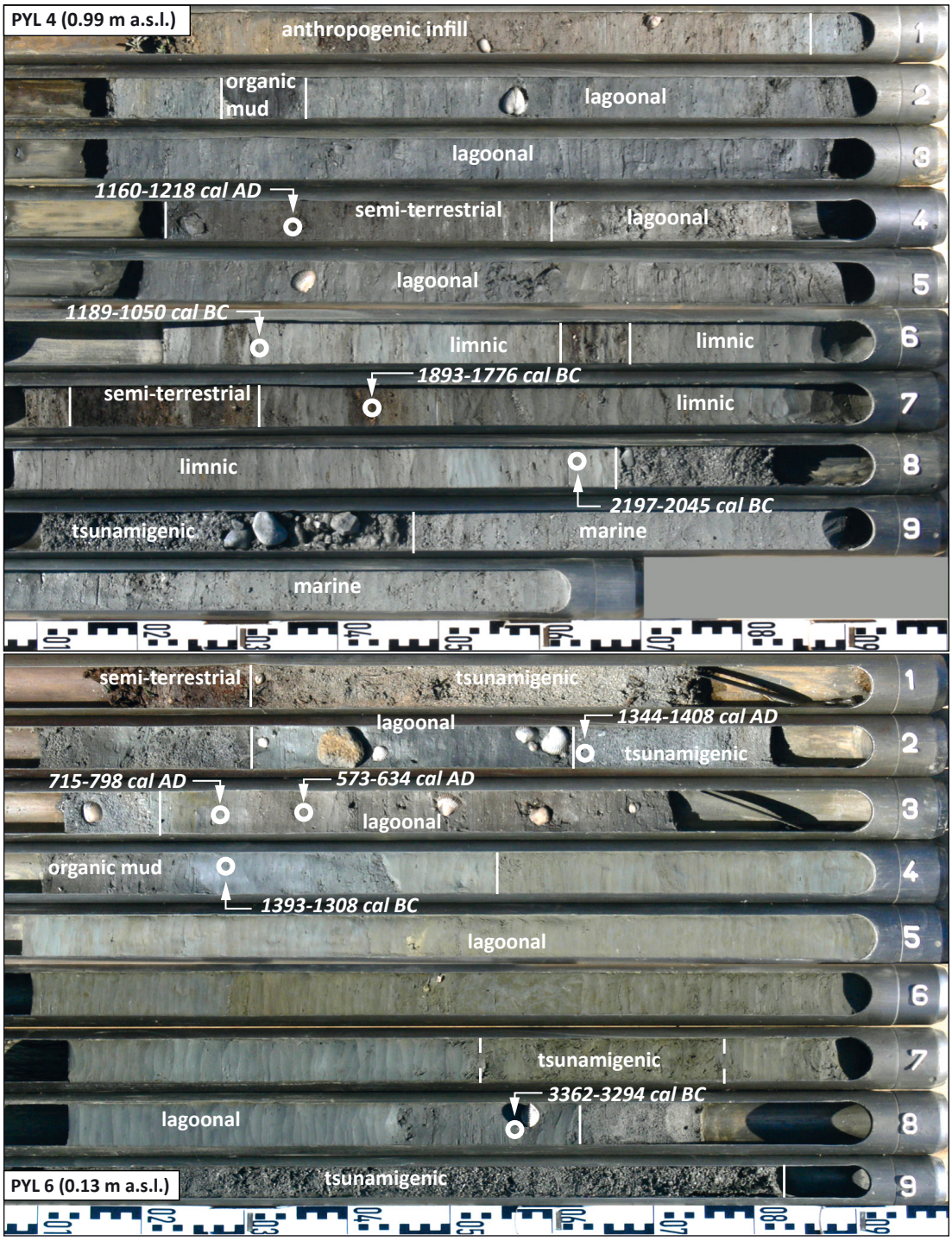

Fig. 4-4: Simplified facies profile and tagged radiocarbondatings of vibracores PYL 4 and PYL 6 drilled in central part and eastern end of the Voidokilia Dunes (for location see Fig. 4-2, details of radiocarbondatings are shown in table 4-1. At photo PYL 6, meter 9-10 is missing because of core loss.

(2.36-1.66 m b.s.l.), again covered by quiescent deposits (1.66-0.53 m b.s.l.). Between 0.53-0.08 m b.s.l. marine sand was encountered, finally covered by silt-dominated marsh deposits (0.08 m b.s.l.-0.22 m a.s.l.).

The base of PYL 4 begins with grey silty fine sand, locally enriched with gravel and sand (8.71-7.47 m b.s.l.). This basal unit is abruptly covered by an unsorted matrix of massive sand and gravel showing fining upward sequences (7.47-6.68 m b.s.l.). Subsequently follows a unit of homogenous mud (6.68-5.33 m b.s.l.). which becomes, further upcore, enriched in organic substance and finally includes layers of peat (5.33-4.29 m b.s.l.). The overlying thick layer of lagoonal deposits (4.29-0.36 m b.s.l.) is locally intersected by layers of peat (4.70-4.62 m b.s.l., 4.32-4.20 m b.s.l., 0.36-0.30 m b.s.l.). The uppermost part of the profile consists of manmade infill for the construction of the dirt road on top of which core PYL 4 was drilled (0.30 m b.s.l.-0.99 m a.s.l.).

At the base of PYL 2, mainly fine sandy silt was found (10.52-8.25 m b.s.l.). On top of a sharp erosional contact, a layer of coarse-grained sand and gravel (8.25-8.00 m b.s.l.) follows. Homogenous and well sorted medium to fine sands of marine origin were found on top (8.00-6.28 m b.s.l.). A gravelly layer between 6.28-5.63 m b.s.l. with distinct fining upward cycles and a sharp boundary towards the underlying stratum reflects temporary high-energy sediment input. The high-energy event goes hand in hand with major environmental changes, as lagoonal conditions establish between 5.63-2.94 m b.s.l. Following another sharp contact, quiescent water deposits are covered by unsorted grus, gravel and massive limestone concretions (2.94-2.52 m b.s.l.). Subsequently, semi-terrestrial conditions develop as indicated by a peat layer (2.53-2.24 m b.s.l.). On top, organic mud (2.24-1.78 m b.s.l.) is overlain by limnic deposits (1.78 m b.s.l. and 0.08 m a.s.l.). Finally recent marsh sediments were found (0.08-0.39 m a.s.l.).The present-day surface is characterized by several karst springs which are assumed to have influenced the environmental conditions in the lagoon since the mid-Holocene.

The sedimentary results for vibracore PYL 1 can be summarized as follows. At the base of the profile (10.27-8.27 m b.s.l.), clayey silt, partly enriched with fine sand, document brackish to shallow marine conditions. This unit is covered by homogenous clayey silt which was accumulated in a quiescent environment (8.27-7.74 m b.s.l.). Subsequently, loamy sediments including partly weathered sections reflect a brackish to terrestrial facies (7.47-4.99 m b.s.l.) which is partly intersected by fine sand (6.27-5.52 m b.s.l.). On top, a sharp erosional contact (4.99 m b.s.l.) is followed by the sand and gravel documenting high-energy influence. Subsequently, silt-dominated homogenous sediments (4.71-2.89 m b.s.l.) indicate a re-establishment of low-energy conditions. In between 2.89-2.15 m b.s.l., a unit of brownish grey clayey silt was encountered. The overlying stratum (2.15-0.36 m b.s.l.) mainly consists of clayey silt with laminae of fine sand. The top of the profile (0.36 m b.s.l. -1.73 m a.s.l.) is made out of homogenous clayey silt of recent alluvial deposits.

The sedimentary results for transect PYL I can be summarized as follows.

(i) At all coring sites, the basal unit out of silt and fine sand, marked by an erosional unconformity, is abruptly covered by unsorted gravel and coarse sands. The erosional contacts are typical of high-energy events (e.g. Reineck & Singh 1980, Einsele 2000, Schäfer 2005).

(ii) After the basal high-energy event, the palaeoenvironmental conditions at sites PYL 3 and 6 underwent significant changes towards predominantly quiescent conditions. Site PYL 1 first

was under quiescent conditions before they gradually experienced more and more terrestrial influence.

(iii) At sites PYL 2, PYL 3 and PYL 6 a second erosional unconformity implies another high-energy event. Vibracoring site PYL 1 and PYL 4 was also affected by this impact. Later, lagoonal conditions were re-established at sites PYL 3 and PYL 6 and sites PYL 2 and PYL 4 also came under quiescent conditions.

(iv) Quiescent sedimentary conditions along transect I persist up to the recent surface. However, intercalations of allochthonous sand and gravel are evident (e.g. PYL 3 at 3.44-3.22 m b.s.l., 2.36-1.66 m b.s.l. and 0.53-0.08 m b.s.l.; PYL 6 at 2.08-1.49 m b.s.l. and 1.17-0.19 m b.s.l.; PYL 2 at 2.94-2.52 m b.s.l.).

(v) Erosional unconformities and associated event layers were found in consistent stratigraphic positions all across vibracore transect I (e.g. PYL 6 at 8.81 m b.s.l., 6.67 m b.s.l., 2.08 m b.s.l., 1.17 m b.s.l.; PYL 3 at 8.36 m b.s.l., 6.49 m b.s.l., 3.44 m b.s.l., 2.36 m b.s.l. and 0.53 m b.s.l.; PYL 1 at 4.99 m b.s.l., PYL 4 at 7.47 m b.s.l.; PYL 2 at 8.25 m b.s.l., 6.28 m b.s.l., 2.94 m b.s.l.) and document the widespread influence of high-energy impacts to the Gialova Lagoon.

Vibracore transect II (detailed vibracore stratigraphies are depicted in Fig. 4-5) comprises vibracores PYL 9 (ground surface at 0.73 m a.s.l., N 36°57‘10.1“, E 21°39’38.4“), PYL 5 (ground surface at 0.23 m a.s.l., N 36°57‘22.4“, E 21°40’07.6“), PYL 8 (ground surface at 0.38 m a.s.l., N 36°57‘30.9“, E 21°40’30.7“) and PYL 4 and runs parallel to the beach barrier system which separates the Gialova Lagoon from the Bay of Navarino (Fig. 4-2).

The stratigraphy of vibracore PYL 9 is dominated by fine sand of shallow marine origin, containing plant remains and marine mollusc fragments (7.27-2.07 m b.s.l.), with several intersections of unsorted coarse sand and gravels associated to sharp erosional contacts (at 7.18-7.06 m b.s.l., 4.68-4.51 m b.s.l., 3.97-3.87 m b.s.l. and 2.66-2.56 m b.s.l.). From 2.07-0.14 m b.s.l., we encountered weathered sand incorporating sherds and stone fragments. Subsequently, we found a layer of unsorted grey fine sand (0.14 m.b.sl.-0.28 m a.s.l.) with sherds, gravels and stones. On top, anthropogenic influence is documented by a distinct accumulation of sherds and stones embedded in a brown soil rich in organic material (0.28-0.73 m a.s.l.).

The sedimentary sequence of PYL 5 starts with homogenous clayey silt, followed by fine sand and silt (8.77-5.39 m b.s.l.). The following unit (5.39-5.21 m b.s.l.) is characterized by a sharp erosional contact at its base and consists of unsorted gravel in a coarse sandy matrix. Subsequently, (5.21-2.50 m b.s.l.), a well sorted fine sand was found showing some coarse sand layers. This unit is abruptly covered by coarse sand (2.50-2.12 m b.s.l.) including fining upward tendencies. This unit is overlain by homogenous coarse- and medium sand (2.12-0.97 m b.s.l.) and well sorted fine- and medium sand containing plant remains and marine molluscs, (0.97-0.05 m b.s.l.). Finally, light brown, fine and medium sand were deposited (0.05 m b.s.l.-0.23 m a.s.l.).

Vibracore PYL 8 is characterized by grey fine sandy silt at its base and fine sand in its middle part (8.62-5.03 m b.s.l.). The sediments are well sorted and homogenous, and subsequently

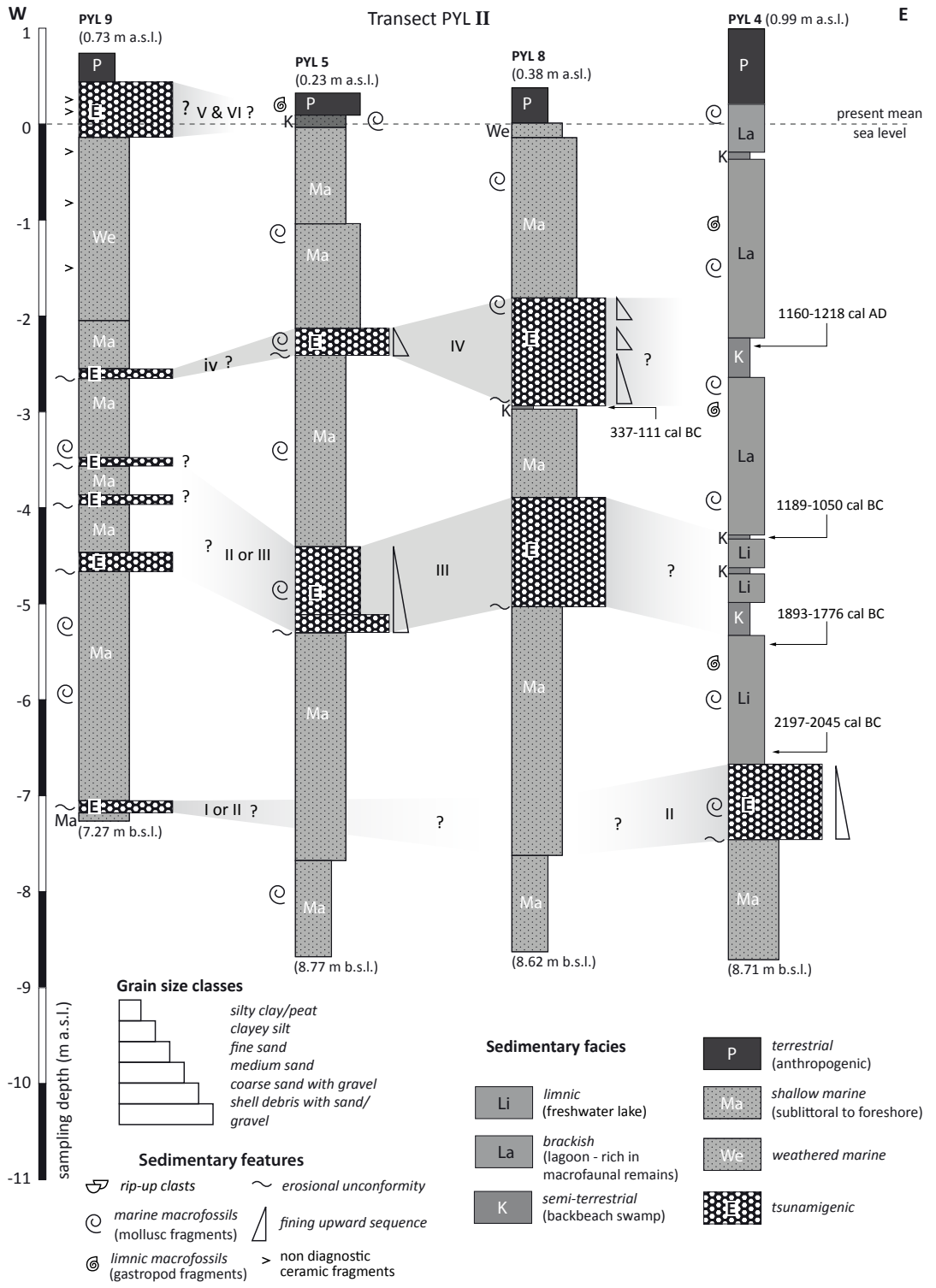

Fig. 4-5: Stratigraphical record and facies distribution of vibracores drilled along transect II on the barrier spit which is separating the Gialova Lagoon to the north and the Bay of Navarino to the south (for location see Fig. 4-2).

covered by a stratum (5.03-3.89 m b.s.l) with a sharp basal contact. The following unit is made out of unsorted sand and gravel and is characterized by multiple fining upward clycles. In the upper part, the unit shows signs of weathering under subaerial conditions which took place after sediment deposition. Towards the top, well sorted fine sand (3.89-2.97 m b.s.l.), locally intersected by homogenous layers of coarse sand and fine gravel, were found. A subsequent peat layer (2.97-2.96 m b.s.l.) is abruptly covered by unsorted sand and gravel (2.96-1.81 m b.s.l.) showing several fining upward sequences from gravel to fine sand. Subsequently, well sorted sand was deposited (1.81-0.13 m b.s.l.). The uppermost part is made out of grey fine sand (0.13 m b.s.l.-0.01 m a.s.l.) and anthropogenically influenced beige clayey silt (0.01 m a.s.l.-0.38 m a.s.l.).

Fig. 4-6: Simplified facies profile and tagged radiocarbondatings of vibracores PYL 8 and PYL 9 drilled on the barrier spit (see Fig. 4-2 for locations).

The sedimentary results for vibracore transect PYL II can be summarized as follows.

(i) All along transect II, the basal units were affected by the input gravel and coarse sand associated to erosional unconformities (PYL 9 at 4.68 m b.s.l.; PYL 4 at 5.39 m b.s.l.; PYL 8 at 5.03 m b.s.l.) in nearly constant stratigraphical position. The unsorted sediments show multiple fining upward sequences which are typical of high-energy impulses.

(ii) After the deposition of the high-energy borne sediments, pre-existing palaeoenvironmental conditions were re-established.

(iii) Another interference, which affected all coring sites in consistent stratigraphical positions, provides evidence of a second high-energy impact to the study area (PYL 9 at 2.66-2.56 m b.s.l.; PYL 5 at 2.50-2.12 m b.s.l. and PYL 8 at 2.96-1.81 m b.s.l.). At site PYL 9 two more high-energy interferences were found (3.97-3.87 m b.s.l. and 3.57-3.48 m b.s.l.).

4.4.2 Grain size analyses and XRF measurements

For the detection and evaluation of facies distributions, geochemical as well as micro-morphological studies are highly diagnostic scientific tools (e.g. Vött et al. 2002, Zhu & Weindorf 2009). XRF values were measured for sediment samples taken from the main stratigraphical units of all investigated vibracores. Environmental changes are not only recorded in the core stratigraphies but are also mirrored by changing geochemical parameters. High-energy impacts are associated with abrupt changes of energetic conditions and therefore induce significant changes in grain sizes and the geochemical fingerprint. For instance, the ratio out of calcium carbonate, partly brought into the system by marine fossils, and iron, produced by weathering processes, is an appropriate tool to differentiate between allochthonous low-energy and sea-borne autochthonous high-energy sedimentation in coastal environments (Vött et al. 2011a, 2011b, 2013, Sakuna et al. 2012). Grain size composition and sorting are further significant indicators of the energetic potential, transport mechanism and environmental conditions (e.g. Schäfer 2005).

Results from XRF measurements and grain size analyses are depicted in Fig. 4-7 and Fig. 4-8.

Detailed grain size analysis of samples from core PYL 3 (Fig. 4-8) show that (i) the basal stratum is dominated by fine to medium sand, (ii) quiescent lagoonal environments are represented by clay and silt, (iii) whereas high-energy event layers are consistently characterized by gravel and coarse sand. Grain size data for core PYL 3 allows a differentiation between autochthonous sediments accumulated under quiescent environmental conditions and allochthonous coarse-grained sedimentats associated to high-energy impacts. Altogether, five different high-energy events are illustrated by the grain size data in Fig. 4-8.

Ca/Fe ratios found for cores PYL 6 and PYL 3 clearly document that high-energy event layers are characterized by strongly increased values compared to the lower equilibrium level of the Ca/Fe ratio found for autochthonous conditions (Fig. 4-7).

In a summary view, both grain size data and geochemical parameters such as the Ca/Fe ratio are helpful tools to distinguish between autochthonous sedimentary conditions and temporary high-energy influence in the stratigraphic record.

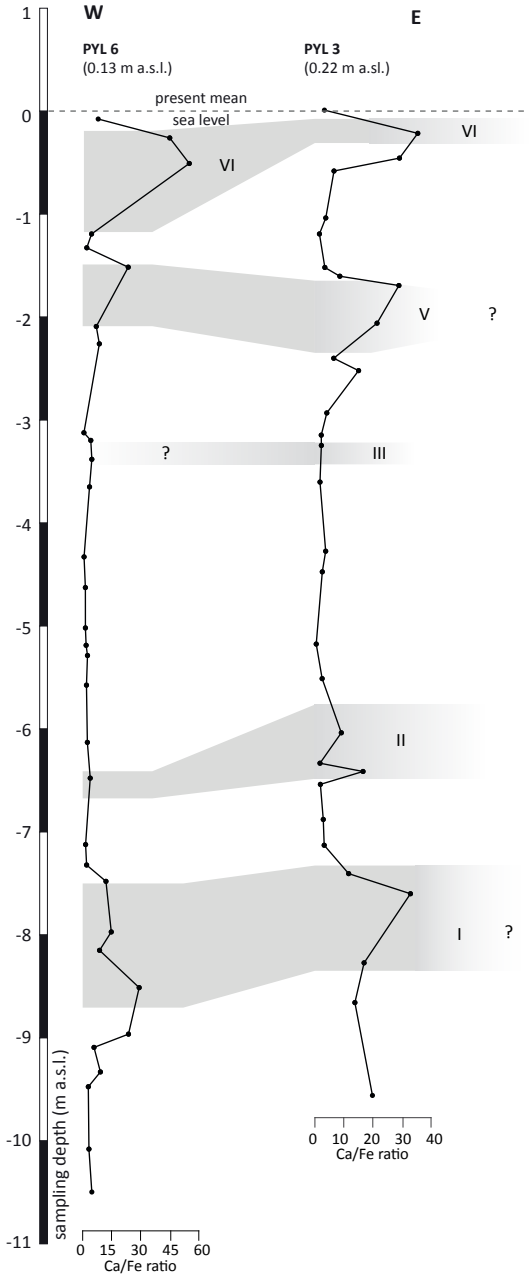

Fig. 4-7: Ca/Fe ratios based on XRF-measurements of vibracores PYL 3 and PYL 6. Stratigraphic positions of high-energy layers in the sedimentary record are shaded in grey.

4.4.3 Microfossil studies

Microfaunal analyses deliver most helpful palaeoenvironmental proxies used for the detection of both gradual paleoenvironmental changes and temporary high-energy borne influences, for instance caused by tsunami events (e.g. Williams & Hutchinson 2000, Gupta 2002, Alvarez-Zarikian 2008, Donato et al. 2008, Vött et al. 2009b, 2011a, Di Bella et al. 2011, Hadler et al. 2013, Willershaeuser et al. 2013). The microfaunal record of sediment samples documents the specific environmental needs of the foraminifera, ostracods and molluscs as well as major impacts to the environment (e.g. Rohling et al. 1993, Mamo et

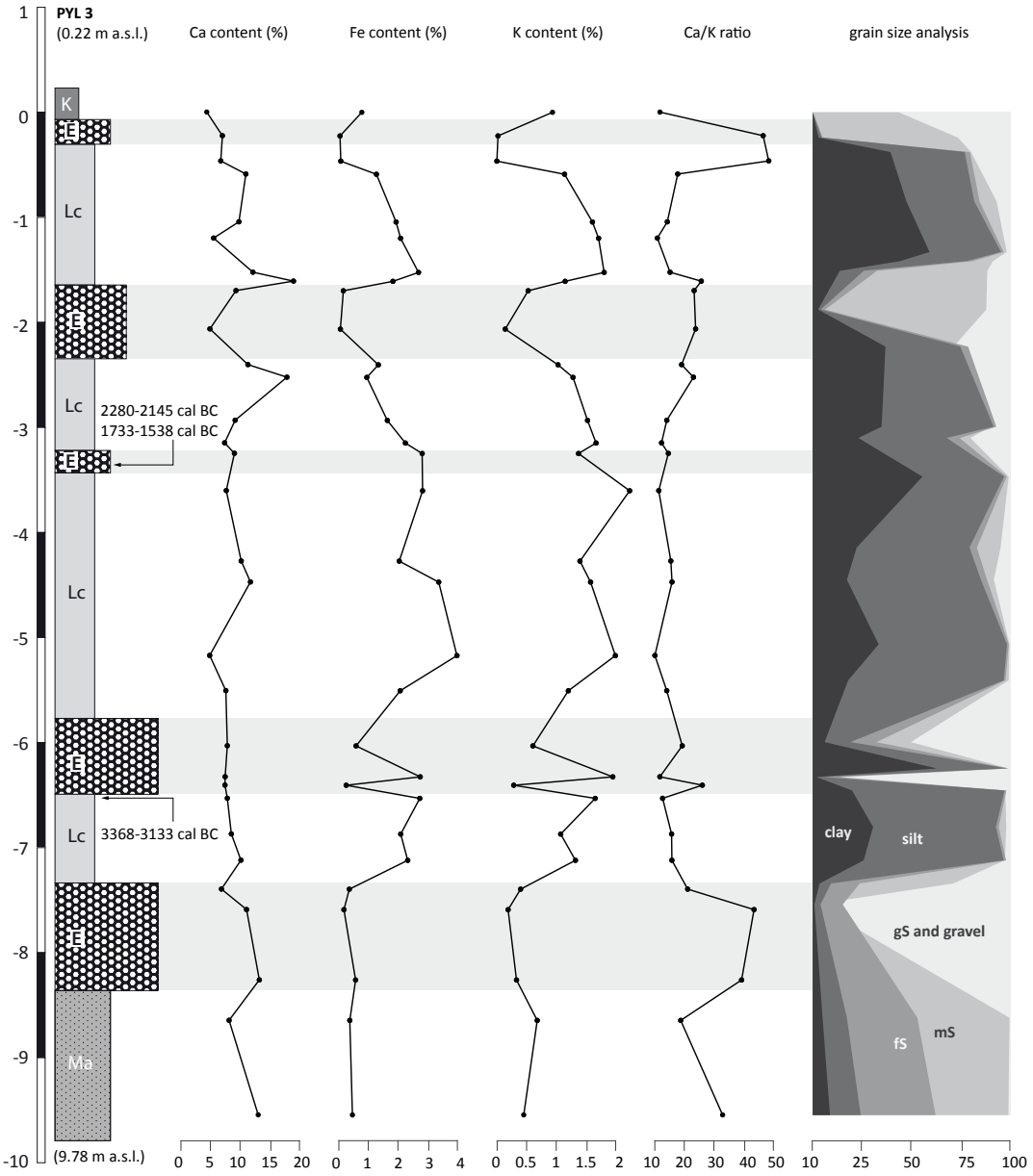

Fig. 4-8: Detailed XRF and grain size analysis of Vibracore PYL 3. Stratigraphic positions of high-energy layers in the sedimentary record are shaded in grey. Grain sizes are drawn as cumulative diagrams.

al. 2009). Ostracods as well as foraminifera tolerate a wide spread spectrum of environmental conditions, so that gradual shifts in the microfaunal assemblage are represented by the abundance of individual species. Abrupt changes in the environmental settings are reflected in a non-gradual progression or sudden and temporary appearance of specific species as well as by a strongly mixed and unsorted microfossil record (e.g. Arvanitides et al. 1999, Murray 2006, Williams 2009).

Samples from three vibracoring sites were analysed for their specific microfossil contents aiming to correlate the palaeoenvironmental evolution across the Gialova Lagoon. Semi-quantitative microfossil studies were conducted for 21 sediment samples from vibracore PYL 2, comprises,

23 sediment samples from vibracore PYL 3 and 17 sediment samples from vibracore PYL 4. Our investigations focused on the foraminiferal content of the local stratigraphy with special focus on the encountered high-energy layers.

The following results of the vibracore-microfossil transect can be made.

The sedimentary bases of cores PYL 2 (Fig. 4-10), PYL 3 (Fig. 4-9) and PYL 4 (Fig. 4-11) are characterized by a great abundance and quite high diversity of predominantly fully marine and inner shelf species like *Asterigerinata mamilla*, *Bolivina* sp., *Bulimia* types, *Cibicides* sp., *Cibicides refulgens, Elphidium sp., Gyrodinia soldanii, Gyrodinia* sp.*, Globigerina* sp., *Haynesina* sp. etc (see. Fig. 4-9, 4-10 and 4-11 for details).

The foraminiferal assemblage, characteristic for the mid-core quiescent sedimentation conditions (PYL 2 at 5.63-2.94 m b.s.l., PYL 3 at 5.77-3.44 m b.s.l.), is characterized by a significant influence of the marine surroundings and the distance to the littoral environment representing autochthonous sedimentary conditions. Cores PYL 2 and PYL 3 show significant differences concerning the recurrence of marine species, mixed with limnic gastropods and ostracods. At site PYL 4 no significant marine influence is given (6.68 m b.s.l.-0.99 m a.s.l.) at a comparable stratigraphic position.

Further up-core, sites PYL 3 (at 3.22-2.36 m b.s.l and 1.66-0.53 m b.s.l.) and PYL 4 (at 6.68 m b.s.l.-0.30 m a.s.l.) are characterized by an environmental sequence which is dominated by freshwater-indicating ostracod and gastropod species as well as by abundant *Characeae* remains. Our data show that *Ammonia* sp. and *Ammonia tepida* do have a very wide ecological spectrum (Almogi-Labin et al. 1995) and, here in coexistence with *Cyprideis* sp. and limnic gastropods, are able to survive and proliferate under hyposaline conditions. However, site PYL 2 (2.53 m b.s.l.-0.39 m a.s.l.), where the salinity is supposed to be reduced to a minimum due to strong freshwater discharge from several nearby karst springs, is characterized by the total absence of *Ammonia* sp. documenting more limnic conditions and significantly lower salinities (Murray 1991, Petihiakis 1999, Debenay et al. 1998, Koutsoubas et al. 2000, Fiorini et al. 2004). The limnic influence is additionally represented by the occurrence of Characeae remains.

High-energy event-associated sediment layers are characterized by the occurrence of *Uvigerina* sp. and *Uvigerina mediterranea* (PYL 3 & PYL 4, Figs. 4-10 and 4-11). *Uvigerina* generally occur in benthic and bathyal environments (e.g. Murray 1973, Gupta 1999, Bernasconi et al. 2006). At site PYL 2, mid-core high-energy deposits (6.28-5.63 m b.s.l.) are characterized by an extraordinarily high amount and diversity of marine microfossils and a lower amount of brackish to limnic fossils. In case of up-core high-energy event layers found at site PYL 3 (at 3.44-3.22 m b.s.l. and 2.36-1.66 m b.s.l.), a mixture of typically brackish (*Cyprideis* types and *Ammonia* types) and marine species (e.g. *Elphidium* sp., *Gyrodinia* sp., *Orbulina universa*, etc.) was found, thus documenting the marine interference of autochthonous lagoonal environs.

Generally, the preservation potential of the foraminiferal assemblages found in high-energy deposits is restricted. Most microfossils underwent significant recrystallization processes during post-depositional weathering. Especially samples from sites PYL 3 (at 8.36-7.34 m b.s.l.)

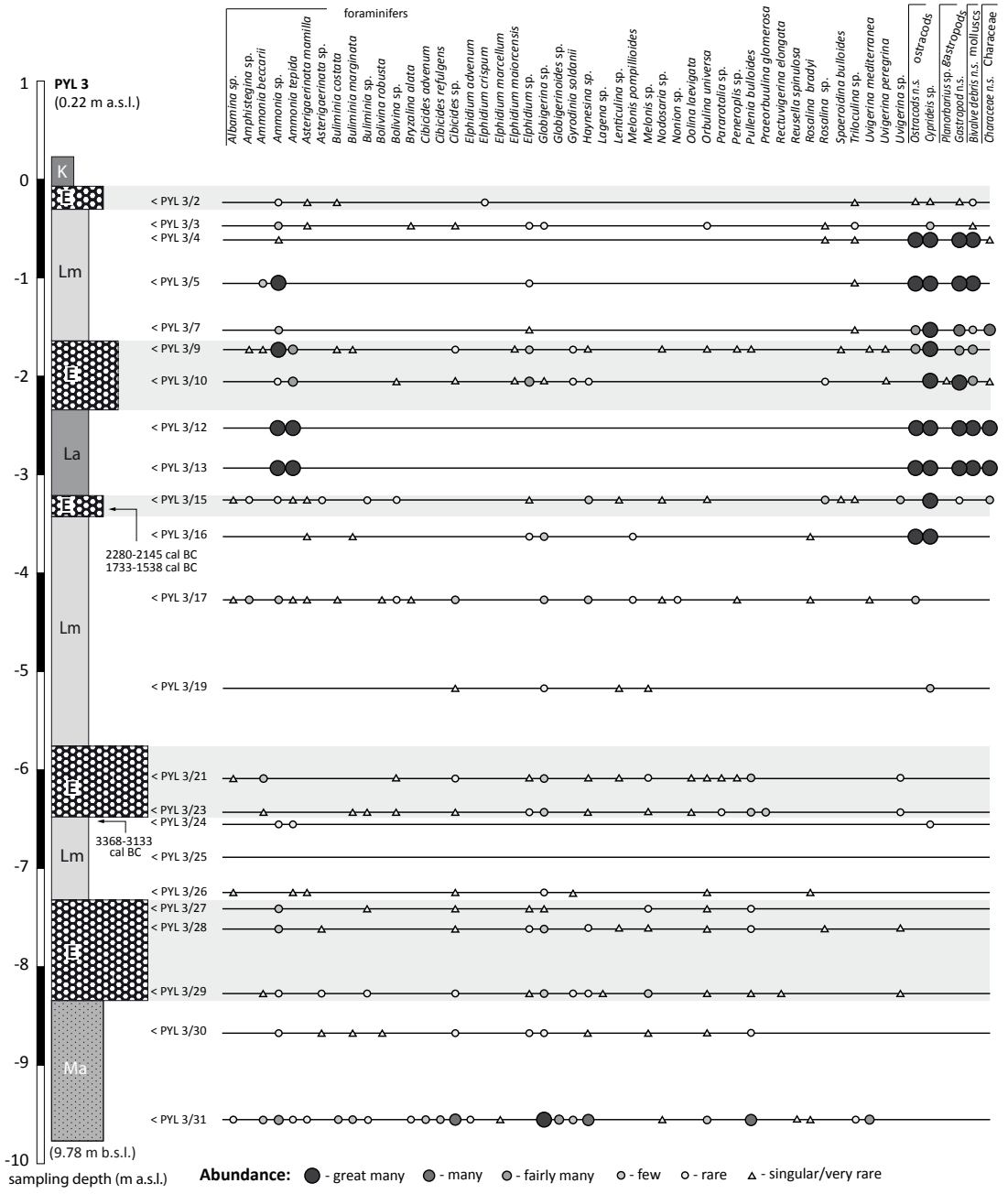

Fig. 4-9: Results of micro- and macrofossil analyses of selected samples from vibracore PYL 3. Specimens were determined after Loeblich & Tappan 1988, Cimerman & Langer 1991, Poppe & Goto 1991, 2000, Murray 2006, Gupta 2002, Rönnfeld 2008.

and PYL 2 (at 8.25-8.00 m b.s.l. and 6.28-5.63 m b.s.l) show a high number of weathered specimens in the high-energy sedimentary units. The preservation of the autochthonous sediments is mostly good, no significant recrystallization was observed.

In a summary view, microfossil analyses document that the high-energy deposits encountered in the stratigraphical record of the Gialova Lagoon represent an allochtonous facies out of dislocates marine sediments transported inland from the foreshore, shelf, bathyal and benthic

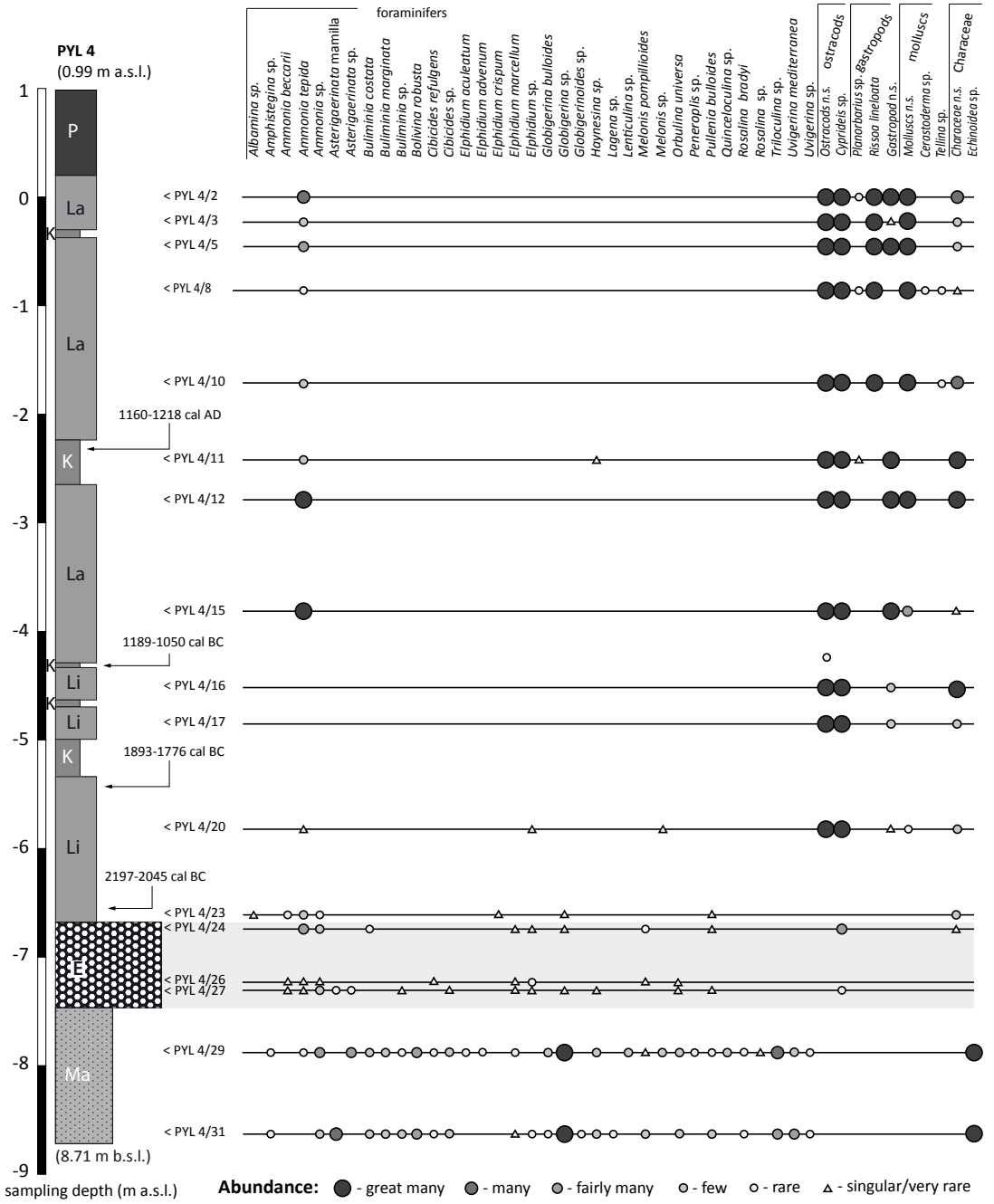

Fig. 4-10: Results of micro- and macrofossil analyses of selected samples from vibracore PYL 4. Specimens were determined after Loeblich & Tappan 1988, Cimerman & Langer 1991, Poppe & Goto 1991, 2000, Murray 2006, Gupta 2002, Rönnfeld 2008.

zones of the Ionian Sea. At the same time, event deposits include a mixture of terrigenous and limnic microfossils as well as fossils from the pre-lagoonal basal marine sediments. Microfossil analyses therefore provide convincing evidence, that the palaeoenvironmental setting of the Gialova Lagoon experienced repeated high-energy influence from the sea side which strongly affected existing environments and also led to the reworking of older deposits. Our data clearly

show that the overall decrease in abundance of marine species along the transect PYL 3, PYL 4 and PYL 2 is in correlation with the increasing distance to the sea (Fig. 4-9, 4-10 and 4-11).

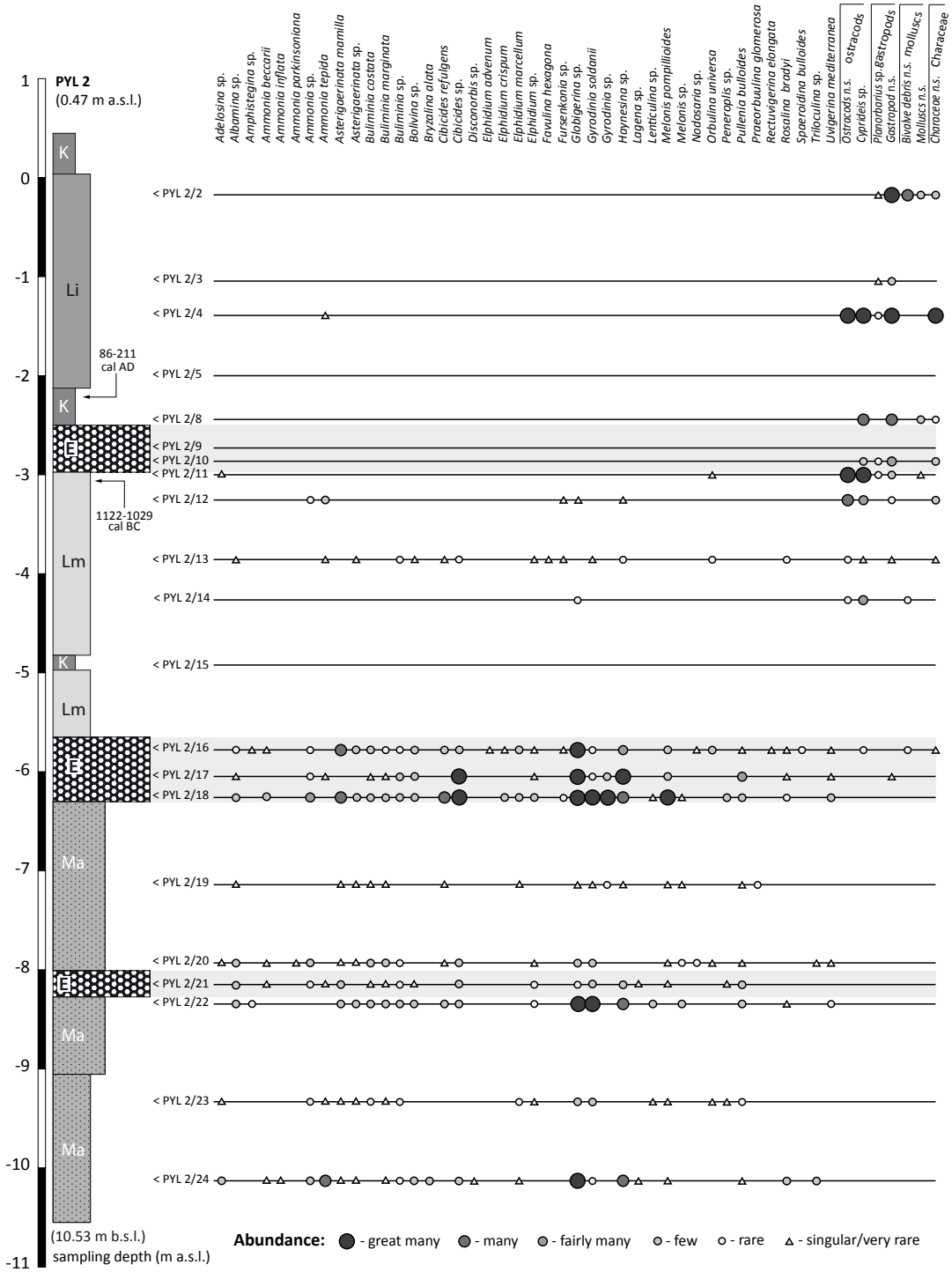

Fig. 4-11: Results of micro- and macrofossil analyses of selected samples from vibracore PYL 2. Specimens were determined after Loeblich & Tappan 1988, Cimerman & Langer 1991, Poppe & Goto 1991, 2000, Murray 2006, Gupta 2002, Rönnfeld 2008.

4.4.4 Geomorphological findings – beachrock-type deposits and washover structures

First studies on the occurrence of beachrock along the coastline of Pylos were made by Kraft et al. (1980), who mentioned that the beachrock-type deposits include sherds of probably Roman age. No further information was given on the internal structure of the beachrock or the geomorphological and sedimentary contexts. However, recent studies that focus on beachrock-type calcarenitic deposits in adjacent coastal areas revealed a post-depositional pedogenetic decalcification and cementation of (palaeo-) tsunami deposits as trigger for beachrock formation (Vött et al. 2010, Hadler 2013).

Fig. 4-12 and Fig. 4-13 provide an overview of onshore and offshore findings from eroded and fragmented beachrock. At Vromoneri (10 km to the north of the Gialova Lagoon, Fig. 4-12, (a) box I), we found beachrock-type deposits injected in between bedrock units characterized by basal erosional discontinuities. The beachrock partly shows a well-laminated structure, embedded intra-clasts and features of a distinct landward flow direction. Additionally, large dislocated and imbricated boulders are visible on top of the strongly karstified elevated marine terraces along the recent coastline (Fig. 4-12 (a), box II). At Romanou (Fig. 4-12 (a), box III), the basal section of the beachrock-type deposit is dominated by gravel, followed by coarse, medium and fine sand and thus exhibits a distinct fining upward sequence.

Sedimentary features such as basal erosional unconformities, injection structures or fining upward sequences within the beachrock-type calcarenitic sediments clearly document high-energy impact to the coastline around Pylos. Sherds found incorporated into the beachrock-type calcarenites prove that these events took place while man was present, most probably even in historic times.

The geomorphology of the Bay of Voidokilia is characterized by a semi-circular shape which is explained by wave refraction processes (Kraft et al. 1980, Zangger et al. 1997, Zangger 2008). The recent beach of the Voidokilia Bay is less than 10 m wide while the massive dune complex towards the east extends for more than 350 m into the direction of the lagoonal embayment. Both beach ridge and dune complex separating the Gialova Lagoon from the Bay of Navarinio work as an efficient protection of the Gialova Lagoon against wind-generated wave action and storm influence (see Fig. 4-2). This circumstance makes the shallow lagoonal Gialova embayment a sheltered and excellent sedimentary archive for high-energy events.

Intense geomorphological surveys as well as local stratigraphies recorded at sites PYL 3 and PYL 6 show that the recent dune complex has developed on top of fan-like structures that reach far into the Gialova embayment. In Fig. 4-13 (c) the outer contour lines of these structures were drawn into a satellite image from 1970 clearly documenting that several lobes even extend beyond the lagoonal shore and continue under water. Comparing the present day aerial images with the one from 1970, it can be seen that the water level of the lagoon strongly varies due to natural and human influences (Loy & Wright 1972, Petihakis et al. 1999). However, the lobe-structures are better visible in the older image.

From a geomorphological point of view, the mentioned structures together with their sedimentary characteristics correspond to washover fans associated with high-energy wave impacts intruding into the lagoonal embayment from the Ionian Sea. Another piece of

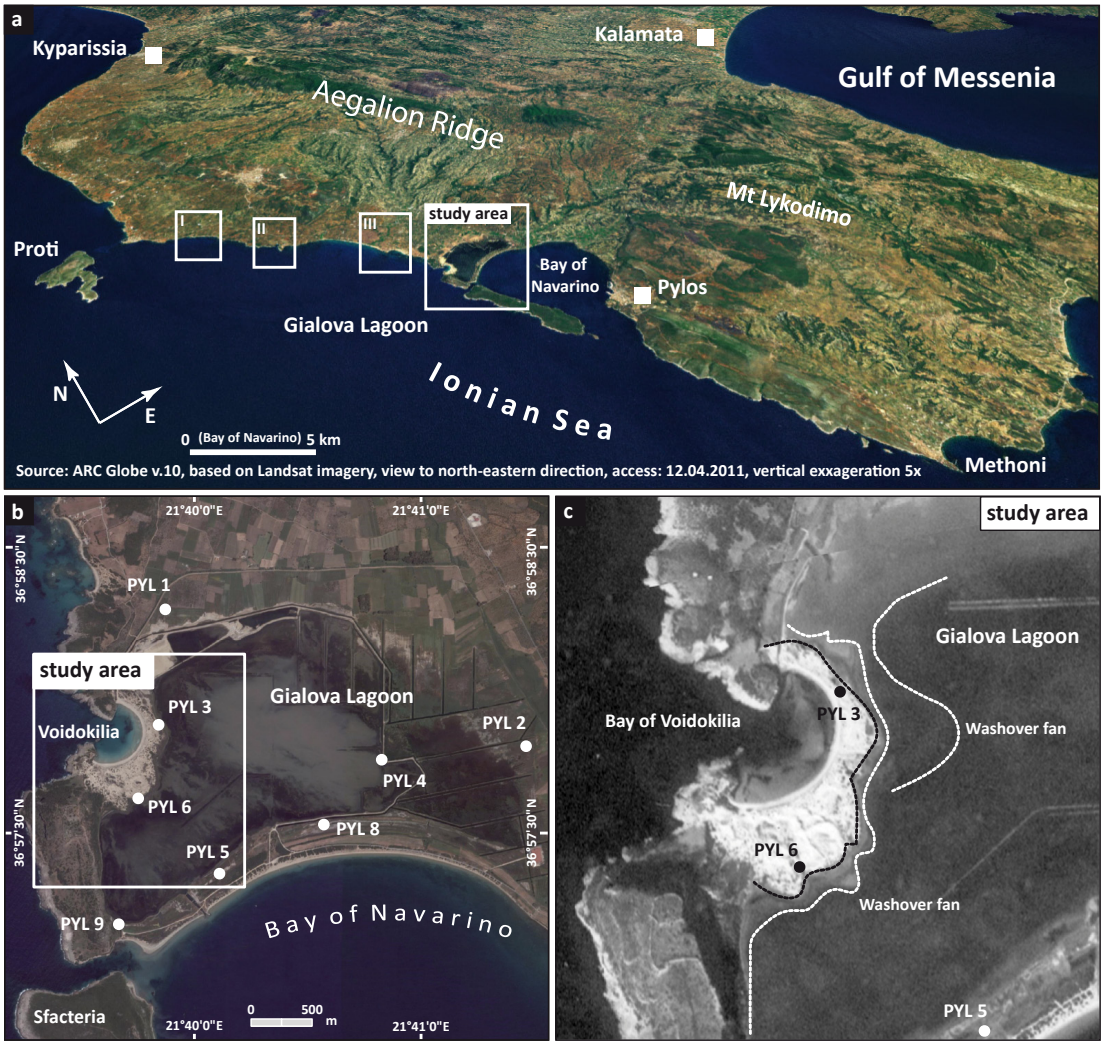

Fig. 4-12: Overview of geomorphological surface findings of Beachrock along the northern coast of the study area (boxes I-III, see Fig. 4-13 for details). (a) Birds eye view of the southern Messenian Peninsula with focus on the Bay of Navarino. (b) Overview of the Gialova Lagoon at 2009 (Aerial images modified after Google Earth images 2009) and (c) the situation at 1970 (Aerial image modified after Corona satellite Image 1970). The extension of the washover structure is marked by dashed line.

evidence for high-energy impact is the fact that the longitudinal axes of the lobes vary from NW-SE to W-E which documents diverging water masses after they have passed the narrow entrance of the bay between the hills of Palaiokastro and Profitis Ilias. The extension of the washover is, however, far beyond winter storm activities and must hence be generated by extraordinary wave events.

In addition to high-energy event markers encountered in local stratigraphies (Sections 4.4.1 and 4.4.2), geomorphological findings of beachrock-type lithified deposits and large washover fans along the coastline of the study area cannot be explained by all-day geomorphodynamic processes and thus provide distinct evidence of high-energy wave impact.

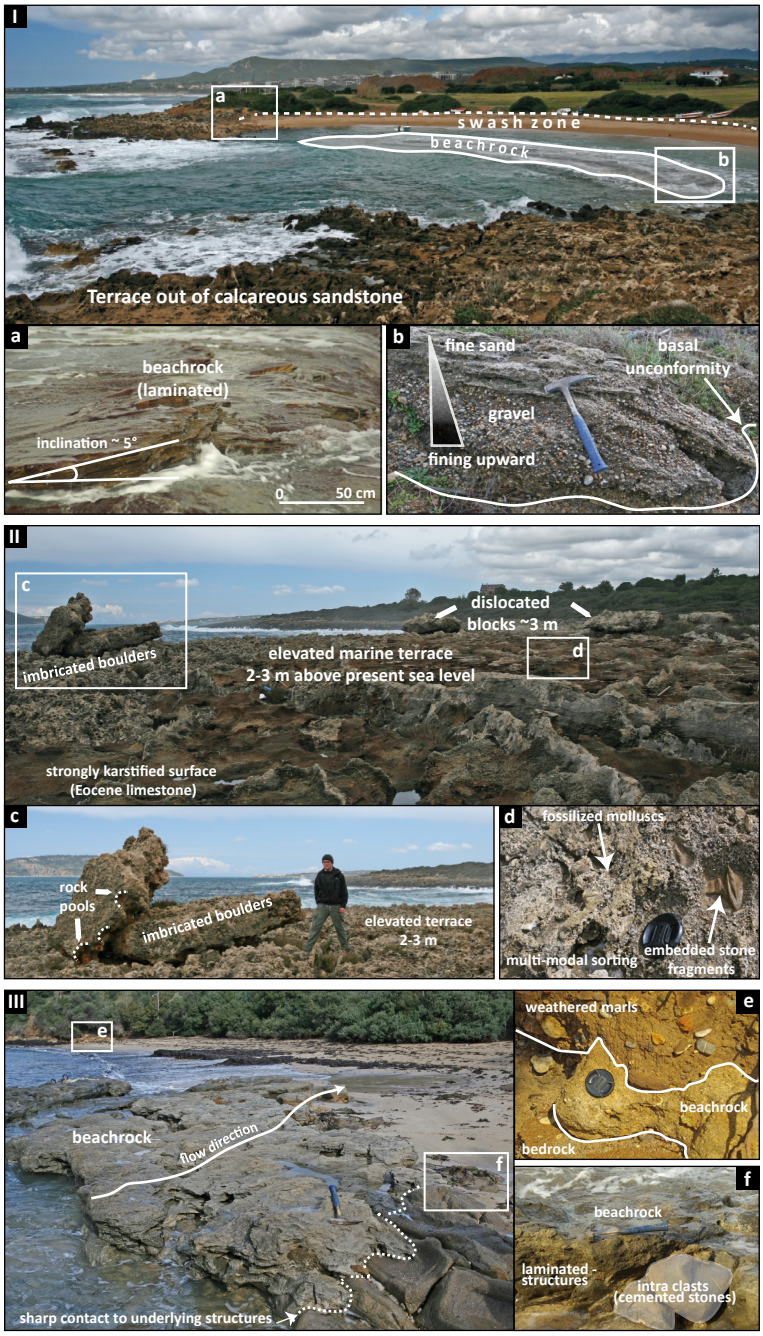

Fig. 4-13: Beachrock-type tsunami deposits along the north-western shores of the Bay of Navarinio (see Fig. 4-12 for locations I-III and further explanations in the text).

4.4.5 Radiocarbon datings

The geochronostratigraphical framework for palaeoenvironmental changes in the environs of the Gialova Lagoon presented in this paper is based on 14 ^{14}C-AMS ages retrieved from peat, plant remains and charcoal as well as from marine molluscs (Table 4-1). Due to the still unsolved problem of the spatio-temporal variability of the marine (palaeo-)reservoir effect for marine samples an average of ~408 reservoir age for the eastern Mediterranean was used

(Reimer & McCormac 2002, Reimer et al. 2009). Radiocarbon ages were calibrated using the Software Calib 6.0 (Reimer et al. 2009).

Our sampling strategy was to focus on autochthonous organic matter or articulated mollusc shells right above or below event layers (sandwich dating approach, Vött et al. 2009b). If possible, we used plant remains instead of marine shells to avoid marine reservoir effects. Donato et al. (2008) used articulated molluscs that are supposed to have been transported and deposited alive and died within a short time after the event in order to obtain the most reliable ages for event-related sediment deposition. Dating samples taken from allochthonous high-energy deposits only yield maximum ages (*termini ad* or *post quos*) for the event. Dating samples taken from post-event sedimentary units represent *termini ante quos* for the event. We evaluated the quality of dating of each sample on the basis of the $\delta^{13}C$ value with special regard to differences of isotope fractions of C4 and C3 plants. Radiocarbon ages of autochthonous C3 land plants yield the most reliable results. (Wagner 1998). In case of plants from marine environments (e.g. sea weed) calibrated ages were corrected for the marine reservoir effect.

Radiocarbon dates used to establish the geochronostratigraphy of transects PYL I and II are listed in Table 1. Samples PYL 6/7 PR and PYL 6/7+ PR2 were calibrated by marine correction as the δ^{13} C (ppm) values around <-15 ± 3% indicate marine influence (Walker 2005). Sample PYL 3/15+PR, taken from a peat layer, yielded an age of 1733-1538 cal AD based on the humic acid fraction and of 2280-2145 cal AD based on the alkali fraction. Due to the potential mobility of older and mobile humic acids the radiocarbon age of the humic acid fraction is supposed to be less reliable than the age given by the alkali fraction (Wagner 1998). However, final evaluation of these ages has to be based on geochronological and stratigraphical correlations.

4.5 Discussion

4.5.1 Tsunami events in the environs of the Gialova Lagoon

The studies revealed distinct geo-scientific evidence of multiple marine-borne high-energy impacts in the environs of the Gialova Lagoon. Geomorphological, sedimentological and microfaunal findings show that marine sediments were transported inland and were subsequently trapped in the quiescent and shallow sedimentary environment of the Gialova Lagoon.

The following main geomorphological and sedimentological features were observed.

(i) Coarse-grained high-energy deposits of marine origin were in between autochthonous littoral sediments, limnic and semi-terrestrial environments. Allochthonous deposits are, in some cases, characterized by sharp basal erosional unconformities which document the high energetic impulse of the events.

(ii) In most cases, allochthonous coarse-grained materials are characterized by distinct fining upward sequences. Fining upward sequences are atypical for transgressional gradual coastal evolution where coarsening upward structures would be expected (e.g. Schäfer 2005) Stratigraphical and sedimentary findings presented in this study require high-energy wave

Sample	Depth (m b.s.)	Depth (m b.s.l.)	Description	Lab No.	δ 13 C (ppm)	^{14}C Age BP	1 σ max; min cal BP	1 σ max; min cal BC	2 σ max; min cal BC
PYL 2/7+ PR	2.83-2.89	2.36-2.42	Peat	KIA 39702	-26.83 ± 0.25	1865± 25	1739; 1864	86; 211 cal AD	79-223 cal AD
PYL 2/10+ PR	3.41-3.43	2.94-2.96	Plant remain	KIA 39703	-26.45 ± 0.23	2895 ± 0.12	2978; 3071	112; 102	1193-1003
PYL 3/15+ PR	3.63	3.41	Plant remain	KIA 39704	-25.50 ± 0.23 -27.69 ± 0.20	3785 ± 25 3355 ± 50	4094; 4229 [2] 3487;3682 [1]	2280; 2145 [2] 1733; 1538 [1]	2288-2140 [2] 2453; 2036 [1]
PYL 3/24 PR	6.75-6.77	6.53-6.55	Plant remain	KIA 39705	-27.60 ± 0.17	4565± 30	5082; 5317	3368;3133	3490-3107
PYL 4/10+ PR2	3.30-3.34	2.31-2.35	Peat	KIA 39706	-26.19 ± 0.25	860 ± 30	732-790	1160-1218 cal AD	1049; 1257
PYL 4/15+ PR	5.28-5.31	4.29-4.32	Peat	KIA 39707	-27.71 ± 0.10	2915 ± 25	2999; 3138	1189; 1050	1211-1015
PYL 4/19+ PR	6.42-6.44	5.43-5.45	Peat	KIA 39708	-26.06 ± 0.45	3520 ± 25	3725;3842	1893; 1776	1921; 1758
PYL 4/23+ PR	7.62-6.44	6.63-6.67	Peat	KIA 39708	-28.24 ± 0.13	3730 ± 30	3994; 4146	2197, 2045	2264; 2032
PYL 6/5+ M	1.62	1.49	Mollusc	KIA 39709	-6.34 ± 0.22	985 ± 25	542-606	1344-1404 cal AD	1317-1426
PYL 6/7+ PR	2.27	2.14	Plant remain	KIA 39711	-14.66 ± 0.25	1620 ± 30	1152-1235	715-798 cal AD	678-830 cal AD
PYL 6/7+ PR2	2.32-2.36	2.19-2.23	Plant remain	KIA 39712	-15.34 ± 0.12	1815 ± 20	1316-1377	573-634 cal AD	511-655 cal AD
PYL 6/9 M	3.28	3.15	Mollusc	KIA 39714	-6.46± 0.29	3420± 30	3257-3342	1393-1308	1432-1264
PYL 6/22 M2	7.59	7.46	Mollusc	KIA 39715	-6.88± 0.16	4935± 30	5243-5311	3362-3294	3476; 3249
PYL 8/8+ PR	3.34-3.35	2.96-2.97	Peat	KIA 39716	-25.80 ± 0.13	2135 ± 30	2060;2286	337; 111	351; 54

Tab. 4-1: ^{14}C-AMS dating results used for establishing a local geochronological framework. Notes: b.s. = below surface; b.s.l. = below sea level; Lab. No. - laboratory number, University of Kiel (KIA); 1σ max; min cal BP/BC (AD)- calibrated ages according to the radiocarbon calibration program Calib 6.0 (Reimer et al. 2009); 1σ & 2 σ range ";" – several possible age intervals because of multiple intersections with the calibration curve (oldest and youngest age given); [1]humic acid fraction dated; [2]alkali fraction dated.

events with a characteristically decreasing transport energy during landfall dynamics associated to sediment transport and deposition.

(iii) Rip up-clasts, out of eroded underlying sediments were frequently found within the high-energy deposits documenting massive erosion and reworking of the autochthonous deposits during sea-borne inundation.

(iv) Macro- and microfaunal analyses document abrupt and temporary changes of local sedimentary environments by the input of different allochthonous species and sediments, These findings implicate long distance transport from (sub-)littoral and shelf zones in landward direction. Microfossil contents therefore allow a clear differentiation between phases with the temporarily strong and heterogeneous input of marine species and phases with gradually changing environmental conditions resulting in gradually changing species assemblages.

(v) The spatial distribution of allochthonous high-energy traces, namely the fact that high-energy interferences in local stratigraphies exist in consistent positions over long distances, is far beyond the reach of normal littoral processes e.g. winter storms or gradual longshore drift by constant wave action. This is also true for large washover fans documenting inflow of marine waters into quiescent lagoonal to limnic environments over a distance of at least 350 m which is the length of the fans as such. Geomorphological forms as well as related stratigraphies require extraordinary geomorphodynamics which – regarding energetic potential and amount of intruding waters – are beyond the reach of storm activities.

(vi) Ceramic fragments were found embedded into a multimodal mixture of marine and terrigenous gravel, sand and loam deposits reflecting that high-energy events affected human settlements and infrastructure.

The western Peloponnese is directly exposed to the open Ionian Sea so that the region is facing predominant west to north-west winds. Wind-generated waves may reach maximum wave heights of ~6-7 m in the open Ionian Sea (e.g. Scicchitano et al. 2008, Soukissian et al. 2007). Annual winter storms produce average wave heights of less than 4 m (Medatlas Group 2004, Cavaleri 2005). Tide gauges, as short time sea level fluctuations, are only a few decimetres resulting in sediment accretion and erosion rates by general wave activity and longshore transport to be nearly nil (Tsimplis & Shaw 2010). Although the study area is directly exposed to the open Ionian Sea, the Bay of Navarino is protected from storms by the Tertiary limestone outcrops of the islands of Sphacteria and Palaiokastro and the peninsula Profitis Ilias (Fig. 4-2). Since antiquity, the Bay of Navarino has been used as natural harbour because it is outstandingly well protected against storm influence (Loy 1967, Zangger 1997, Davis 2008, Papatheodorou et al. 2005); it therefore belongs to one of the best storm-protected natural harbours in the eastern Mediterranean. The overall wind-generated wave regime of the Bay of Navarino and the adjacent Gialova lagoon is thus weak and provides a limited energetic potential with regard to coastal geomorphology processes.

The beach barriers that separate the Gialova Lagoon from the Bay of Navarino and the Bay of Voidokolia are between 200-300 m wide and therefore provide a massive natural protection that neither storms nor so called Medicanes (tropical storm equivalents for the Mediterranean

Sea) (e.g. Ernst & Matson 1983, Pytharoulis et al. 2000) have been capable to overflow. It has to be concluded that the Bay of Navarino and the Gialova Lagoon are not endangered to be severely struck by storm dynamics.

Considering the geographical, climatological and geomorphological settings at the Gialova Lagoon, the possibility that storms are responsible for the formation of the allochthonous marine deposits encountered in the study area – in case of sites PYL 3, 5, 6 and 8 being up to more than 1 m thick – is nil. The fact that washover fans reach more than 350 m into the Gialova Lagoon can also not be explained by storm influence (cf. May et al. 2012). Our findings from around the Gialova Lagoon show that the disturbance and destruction of palaeo-environments by extraordinary strong wave action occurred episodically and with short-term character, and left a stratigraphically widespread sediment signature. Storm action is known for high frequency and a significantly smaller magnitude represented as interfering layers in the sedimentary record of local geo-archives. Storm-borne intercalations have neither been described for the western Peloponnese as a significant feature in the sedimentary record nor are there catalogues listing extraordinarily strong storm events. The influence of storm-driven coastal changes therefore seems to be restricted to the littoral zone and has a strongly limited energetic potential only.

With regard to the sedimentary traces of high-energy impacts encountered in the study area, comparable sedimentary characteristics are well known associated to recent (e.g. Goto et al. 2007, 2010a, 2010b, Srinivasalu et al. 2007, Jankaew et al. 2008, Srisutam et al. 2010, Chagué-Goff et al. 2011, Richmond et al. 2011, Okal et al. 2011, Bahlburg & Spiske 2012, Feldens et al. 2012, Sakuna et al. 2012) as well as historic and prehistoric tsunami events (e.g. Hindson & Andrade 1999, Bondevik et al. 2005, Donato et al. 2008). We therefore conclude, that high-energy deposits encountered in the environs of the Gialova Lagoon were deposited by tsunamis and not by storms. Furthermore, detailed sedimentological, geomorphological and microfaunal arguments against the interpretation of these sediments as storm-borne are discussed by Vött et al. (2006d, 2007a, 2008, 2009a, 2009b, 2010, 2011a, 2011b & 2013) and Hadler et al. (2011a, 2011b, 2013). The fact that an exceptional number of documents and catalogues reporting on tsunami impacts and strong earthquakes exists (Hadler et al. 2012 and literature therein) but there are no catalogued historical reports on storm events does also underline the overestimation of storm-borne influence on the littoral zone and the Holocene coastal evolution. Our results document that the Gialova Lagoon was repeatedly affected by tsunami impacts and that the local coastal evolution was considerably influenced, partly even controlled by tsunami events.

Along the coast near the Gialova Lagoon, we found several sites where beachrock-type deposits appear in the immediate environs of the present coastline (see Section 4.4.4). Sedimentary features, such as (i) erosional unconformities, (ii) multiple fining upward sequences, (iii) rip up intraclasts, (iv) multimodal sorting, (v) laminated structures indicating laminar flow, and (vi) associated dislocated boulders along the study sites let us assume that the encountered beachrock-type deposits represent high-energy deposits rather than simple beach deposits. Similar cases of post-depositionally calcified beachrock-type calcarenites where first interpreted as tsunamites by Vött et al. (2010) for several coastal areas in western Greece. Also around

Gialova Lagoon, we found many sedimentary features atypical of a littoral processes, features which are rather described for recent tsunami deposits (e.g. Dominey Howes et al. 2006, Kortekaas & Dawson 2007, Morton et al. 2007, Bahlburg & Spiske 2012).

4.5.2 Establishing of an event-geochronology for the Gialova Lagoon

High-energy interferences of local stratigraphies in the environs of the Gialova Lagoon were correlated based on stratigraphical comparison and radiocarbon dating (see table 4-1).

Tsunami generation I

Samples PYL 3/24 PR and PYL 6/22 M2 yielded 3368-3133 cal BC and 3362-3294 cal BC, respectively, as *termini ante quos* for the oldest tsunami generation recorded in the Gialova stratigraphies (Fig. 4-3).

With respect to dating accuracies, a correlate candidate for this event was found in coastal Akarnanina and dated by Vött et al. 2011a to the 4th millennium BC. Provided that the tsunami deposits lay uncovered for a long time after sediment deposition, generation I tsunamites from the Gialova region may even correspond to a tsunami of supraregional extent dated to around 4300 +- 200 cal BC which affected ancient Pheia and the adjacent Gulf of Kyparissia (Vött et al. 2011a, Chapter 3), the Bay of Koutavos (Cefalonia Island, Vött et al. 2013) and the Bay of Lixouri (Cefalonia Island, Willershäuser et al. 2013). However, we did not find clear signs of subaerial weathering of the tsunamite so that it has to be suggested that the event deposit was covered by subsequent lagoonal muds soon after its deposition. Thus, generation I tsunamite was accumulated most probably not before the 4th millennium BC.

Tsunami generation II

Samples PYL 3/24 PR and PYL 6/22 M2 yielded 3368-3133 cal BC and 3362-3294 cal BC, respectively, as *termini post quos* for the tsunamite generation II. Sample PYL 4/23+PR resulted in an age of 2197-2045 cal BC which is a *terminus ante quem* for the event.

In a (supra-)regional context, a potentially correlating event is known from Cefalonia Island and for coastal Akarnania where Vött et al. (2009a, 2009b, 2011a, 2013) dated tsunami impact to around 3000-2800 cal BC.

Tsunami generation III

Tsunamite generation III in the environs of the Gialova Lagoon can be dated on the base of samples PYL 2/10+ PR, sample PYL 6/9 M and sample PYL 3/15+ PR yielding 1122-1029 cal BC, 1393-1308 cal BC and 1733-1538 cal BC, respectively, as *termini post quos* for the event. Samples PYL 8/8+ PR and PYL 2/7+ PR yielded 337-111 cal BC and 86-211 cal AD, respectively, as *termini ante quos*. However, the tsunami event generation II is suggested to be considerable older that these minimum ages as indicated by traces of subaerial weathering that affected the corresponding tsunamite for a longer time after deposition. We therefore assume that Gialova tsunami generation III took place in a comparable time range as it is known from the Sound of Lefkada, the Lake Voulkaria and the Bay of Palairos-Pogonia where strong tsunami impact at around 1000-1200 cal BC (Vött et al. 2006d, 2009a, 2009b, 2011) caused enormous destruction to the coast and ancient settlements.

Tsunami generation IV

Sample PYL 8/8+ PR yielded 337-111 cal BC as *terminus post quem* for Gialova tsunami generation IV. However, it cannot definitely be excluded that tsunamite generation IV is identical with the younger generations V or VI because there are no *termini ante quos* which could be used for time bracketing the event. Provided that tsunami generation VI took place shortly after 337-111 cal BC, there are potential correlations with a tsunami event near Lefkada dated by Vött et al. (2006d, 2008) between Classical to Hellenistic times and/or with traces from the Koutavos coastal plain (Cefalonia) where Vött et al. (2013) found tsunami traces with a maximum age dated to around 650 cal BC.

Tsunami generation V

Sample PYL 6/7 PR yielded 715-798 cal AD as *terminus post quem* and sample PYL 6/5+ M yielded 1344-1408 cal AD as *terminus ante quem* for Gialova tsunami generation V so that the event can be sandwich dated to the time between the 8th and the 14th/15th centuries AD.

There is historical evidence of a well-known tsunami that hit the eastern Mediterranean in 1303 AD (e.g. Soloviev et al. 2000, Guidoboni & Ebel 2009) which is a probable correlation candidate with tsunami generation V traces found in the environs of the Gialova Lagoon. Tsunamites that probably belong to this supraregional event are described by Vött et al. (2006d) and Scheffers et al. (2008) for the Sound of Lefkada and the southern Peloponnese, respectively. However, there is also a potential correlation to palaeotsunami impact that was dated to the time between 930-1170 cal AD for Sicily (Smedile et al. 2011).

Tsunami generation VI

Sample PYL 6/5+ M yielded 1344-1408 cal AD as *terminus post quem* for Gialova tsunami generation VI. According to Hadler et al. (2012) there are several potential tsunami events which were reported for the eastern Ionian Sea and the western Peloponnese after the 14th century. However, it remains a matter of speculation to correlate Gialova tsunami generation VI traces with one of these events unless more precise tsunami age estimations will be realized.

4.5.3 Palaeogeographical evolution of the Gialova Lagoon

First geo-scientific studies in the environs of the of the Gialova that aimed at reconstructing the palaeogeographipcal evolution were already carried out by Wright (1972), Loy & Wright (1972) and Kraft et al. (1980). Within the Pylos Regional Archaeological Project Zangger et al. (1997) intended to reconstruct the landscape evolution in the wider Gialova area with regard to archaeological evidence of human settlements. Recent studies, carried out by Yazvenko et al. (2008), investigated the palynological record of the Gialova Lagoon.

Although all publications present (detailed) palaeogeographical reconstructions for the study area, neither of these scenarios considers the occurrence of major extreme events as a crucial factor for palaeoenvironmental changes. Following, we thus present new geo-scientific results on the palaeogeographical evolution of the Gialova Lagoon. Within the light of our findings, previous studies will be reviewed, compared and discussed.

As shown by our stratigraphic and geochronological data, palaeoenvironmental changes in the environs of the Gialova Lagoon are partly related to the Holocene sea-level evolution and gradual coastal changes, but also document significant influence of high-energy tsunami impacts on the overall coastal evolution. Bringing together the stratigraphical sequences recovered along the PYL I and PYL II vibracore transects, the main aspects of the palaeogeographical evolution in the environs of the Gialova lagoon can be summarized as follows.

Our vibracore data shows that the palaeo-shoreline of the mid-Holocene marine embayment of the Gialova Lagoon was located 2.2 kilometers further inland (PYL 1). Kraft et al. (1980) reconstructed the coastline about 2.5 km to the north of the present position of the Gialova lagoonal shore for the time around 9500 cal BP. Sites PYL 1, PYL 3, PYL 6 and PYL 2 were subject to marine conditions until ~3300 cal BC and ~2100 cal BC, respectively. By stratigraphical correlations, marine influence at coring site PYL 1 is documented, before ~3300 cal BC.

Microfossil data from the Gialova Lagoon (Fig. 4-9, 4-10 & 4-11) emphasize a significant progradation of the shoreline from north-eastern in south-western direction since the mid-Holocene. The distribution of autochthonous foraminiferal species along the microfossil transect furthermore reflects the increasing distance to the shore by a significant reduction of the diversity and abundance of fully marine species.

After around 3300 cal BC, quiescent lagoonal conditions were established at vibracoring sites PYL 3 and PYL 6 right after Gialova tsunami generation I hit the coast while at sites PYL 4 and PYL 2 marine conditions still prevailed. Thus, the initial establishment of lagoonal conditions seems to be directly related to tsunamigenic influence. At coring site PYL 4, the stratigraphy documents a phase of limnic conditions between around 2100-1100 cal BC as the results of the microfaunal analysis show (Fig. 4-10). In the northern part of the Gialova lagoon, at coring site PYL 1, the palaeogeographical situation around 3300 BC is initially under brackish and subsequently terrestrial influence. Loy & Wright (1972) postulated that the development of the lagoonal system started around 2000 BC. Furthermore, Kraft et al. (1980) described the influence of alluvial sedimentation by the river systems from northern direction. At coring site PYL 1, the influence of distal alluvial deposition is documented in the stratigraphical record; we assume that alluvial deposits come from northern direction (Fig. 4-3).

At the beach barrier which separates the Gialova Lagoon from the Bay of Navarino, shallow marine conditions were re-established soon after the first tsunamigenic impact. As described above, the formation of the present barrier accretion spit was associated to a second tsunami event after around 300 cal BC (Fig. 4-5). This is around 400 years after the time period for which Kraft et al. (1980) reconstructed the formation of the present beach ridge (2745 BP) whereas Loy & Wright (1972) hypothesize that the sandbar was already in its present-day position at a time around 2000 BC.

Reconstructions of palaeo sea levels by Kraft et al. (1977, 1980) and Zangger et al. (1997) and our palaeogeographical reconstructions are in good accordance with the results presented in this study. Loy & Wright (1972) postulated that no significant tectonic instability affected

the relative sea level evolution in the area. They conclude that the palaeogeographical evolution of the Gialova Lagoon was predominantly controlled by the eustatic Holocene sea level rise and sediment accumulation of the hinterland. Our results, however, emphasize that the influence of tsunami events is a major control mechanism for the coastal evolution and present-day coastal constellation within the study area. Corresponding tsunami deposits at sites PYL 8 and PYL 9 were found strongly weathered; this means that tsunami sediment deposition took place under subaerial conditions. The deposition of tsunamigenic sediments above sea level and subsequent pedogenetical processes are a well-known phenomenon affecting recent (e.g. Morton et al. 2008) and sub-recent tsunamites (e.g. Vött et al. 2009a, 2009b).

According to our results, palaeotsunami impacts turned out to have had a major influence on the palaeogeographical settings and the present coastal configuration. The tsunami theorie is supported by results from pollen analysis and radiocarbon datings of Wright (1972) , for example, that clearly depict the high-energy sediments of tsunami generation III (Fig. 4-14) that hit the Gialova Lagoon around 1100 BC. Significant changes in the pollen spectrum of Wright (1972) show similarities to findings of Vött et al. (2009b) for the Lake Voulkaria and of Willershäuser et al. (2013) for the Gulf of Argostoli who documented that changes in the pollen spectra, such as dilution effects and post-event exploding abundances of specific pollen, are due to tsunami influence and do not reflect changes in the vegetation history.

Investigations of Zanger et al. (1997) and Yazvenko (2008) at the Gialova Lagoon also show several anomalies in the pollen record. They detect coarse sand sheets which were "unsuitable for pollen analysis" in between 4.5-4 m b.s. (dated by the authors to the time between 5420 BC and 2000 BC) and around 2.5 m b.s. (1350 BC and 1010 BC). Compared to our study, both sedimentary record and ages fit well to our reconstruction of the local tsunami event chronology (Fig. 4-14). Findings of Kraft et al. (1980) also documents the input of gravels intersecting muddy deposits, but no geochronological classification was given at that time.

As the interpretation of stratigraphical and palaeoenvironmental data by Loy & Wright (1972), Wright (1972), Kraft et al. (1980), Zangger et al. (1997) and Yazvenko (2008) do not consider the extraordinary high tsunami risk, along the coasts of the southwestern Peloponnese, a tsunami-borne origin of allochthonous high-energy sand and gravel was not discussed at the time of publication. Tsunami influence was hence not taken into consideration as responsible for the massive changes in the environment of the Gialova embayment since the mid-Holocene (Fig. 4-14).

In a summary view, the six high-energy tsunami impacts which were identified for the Gialova Lagoon seem to have had a major influence on the palaeogeographical evolution of the area. Vibracore transect I documents significant environmental changes by the first and second tsunami impacts. The coincidence of tsunami influence and shift from an open marine to a quiescent lagoonal to limnic environment is evident and causalities are obvious. Closing of the Bay of Voidokilia was most probably triggered by tsunami generations I and II. The event-associated deposition of sediments from western direction formed a massive barrier which cut the area off the Ionian Sea.

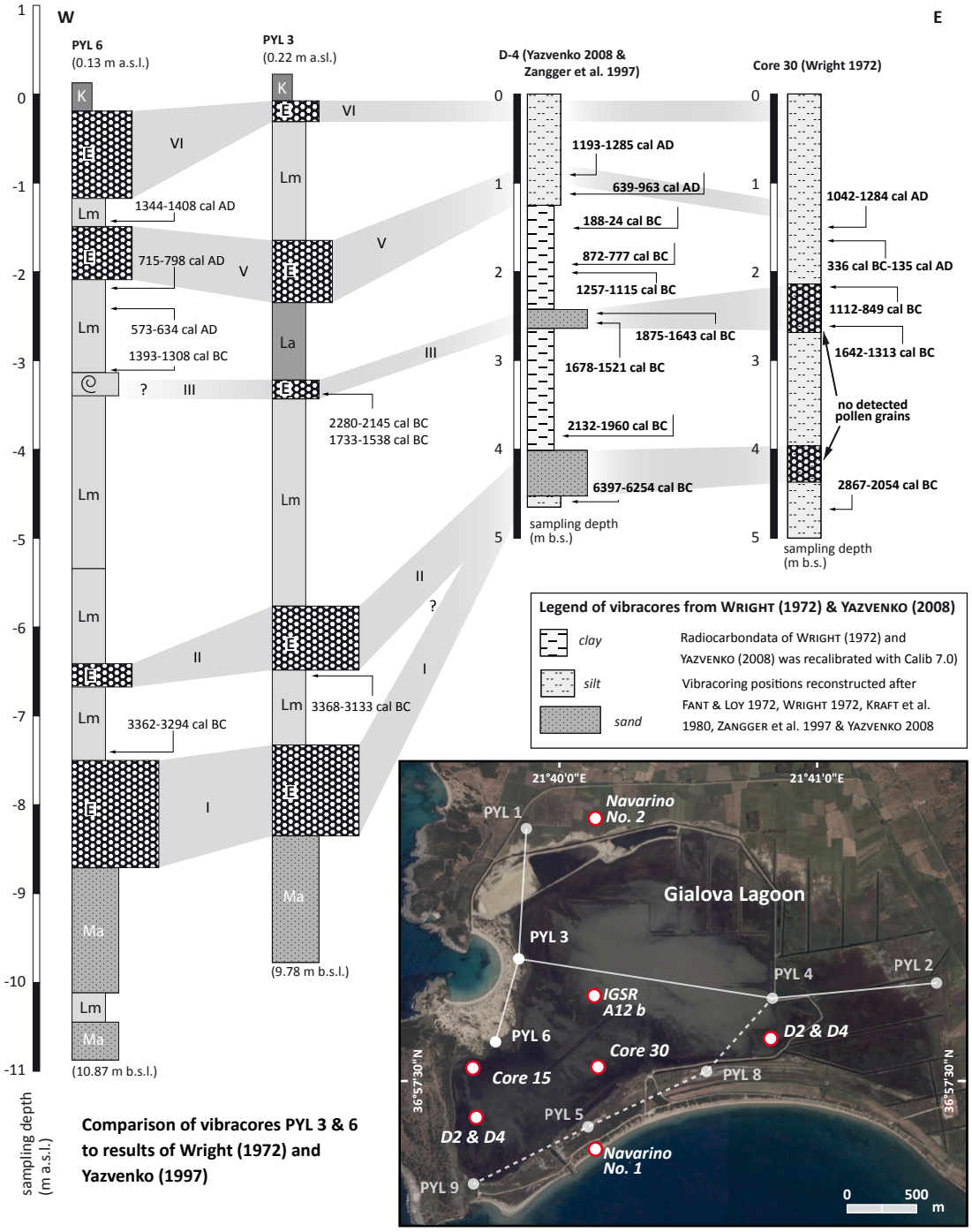

Fig. 4-14: Synoptic stratigraphical view of vibracores PYL 3 and PYL 6 compared with simplified stratigraphies of Core 30 (Wright 1972) and core D2/D4 (Yazvenko 2008) which were recovered as base for Pollen analyses. For radiocarbon stratigraphies of PYL 3 & PYL 6 see Table 4-1. Radiocarbon data of Wright (1972), Zangger et al (1997) & Yazvenko (2008) were re-calibrated by Calib 7.0.

The southward shift of the palaeo-coastline during the Holocene and the evolution of the present barrier accretion spit between the Gialova Lagoon and the Bay of Navarino were dated to the time after around 300-100 cal BC. For the time before, the quiescent embayment reconstructed in vibracore transect I implicates a palaeo-barrier system to the north of the present one; together with the closure of the Voidokilia channel, this barrier guaranteed quiescent sedimentation conditions in the Gialova Lagoon which was considerably smaller at that time. After this barrier was shifted to the present position, the quiescent environment has existed up to present times and has been repeatedly affected by the tsunamigenic input of allochthonous marine-borne sediments intersecting quiescent conditions.

4.5.4 Evidence of tsunami impact in the wider Gialova area - revisiting the ancient Pylos harbour site

North of the Gialova Lagoon, beachrock-type tusnamites already provide evidence of high-energy impact on the coastal area close to Romanou, some 2.5 km north of vibracoring site PYL 1 (Figs. 4.12 & 4.13). Within the Pylos Regional Archaeological Project, the nearby Selas river basin was already subject to geoarchaeological studies by Zangger et al. (1997), aimed at the detection of the ancient Pylos harbour site.

Associated with the artificial diversion of the Selos River from the Gioalova Lagoon to the Romanou area, Zangger et al. (1997) postulate the excavation of an artificial harbour basin, accessible from the Ionian Sea through a narrow and winding entrance channel. The stratigraphical record of the site seems to support a harbour, as a thick layer of clayey sediments on top of the Pleistocene bedrock indicates quiescent sedimentation conditions.

Located some 500 m from the recent coastline and with regard to the topographic constellation, only a minor marine influence can be expected for the harbour basin whereas the water supply of the Selors River implies brackish to freshwater conditions. Postulating a controlled freshwater stream to prevent the basin from siltation and "preventing large amounts of seawater from entering it", Zangger et al. (1997) already exclude marine conditions at the harbour site. Microfossil analyses from the harbour basin thus discovered ostracod species from brackish as well as limnic environments. Zangger et al. 1997 found also a significant numbers of marine planktonic foraminifera like *Globigerina* sp. Autochthonous brackish to limnic is represented by e.g. *Aurilia sp.*, *Ilyocypris* sp., *Darwinula* sp. & *Cypris* sp.

In the light of attested tsunamigenic impact for the Gialova Lagoon, we suggest, that the occurrence of these planktonic marine foraminifera is related to palaeotsunami impact. Furthermore, Zangger et al. (1997) describe the widespread burial of the harbour site by sand and gravel, partly including ceramic fragments. However, the decline of hydraulic structures, as postulated by Zangger et al. (1997) would result in a gradual transition from lagoonal/ limnic to fluvial sedimentary environments. The "apparently unstratified gravel" obviously overlies the harbour facies with a sharp contact that "indicates a sudden and drastic change in the parameters controlling the depositional environment" (Zangger et al. 1997: 621). Present-day alluvial deposits of the Selos river that fill in the remains of the suggested ancient harbour basin only consist of fine-grained sediments. Compared to high-energy event deposits detected in the lagoonal environment of Gialova, sedimentary characteristics of the respective

layer at the Pylos harbour are suggested to rather provide the evidence of tsunamigenic high-energy impact than of fluvial deposition.

We conclude that sedimentary evidence presented by Zangger et al. (1997) for the area of Romanou rather reflects the impact of high-energy events on the Pylos coastal area as already demonstrated for the Gialova Lagoon. Most propably both areas were affected by the same tsunami events.

4.6 Conclusion

We found significant geomorphological, sedimentological, microfaunal, geochemical and geochronological evidence of multiple Holocene tsunami imprint in the stratigraphical record of the Gialova Lagoon and its environs. In general, the Gialova Lagoon sediment trap allowed to discrimintate between high-energy allochthonous and low-energy autochthonous sediments and the corresponding depositional processes. Based on our results the following conclusions can be made.

(i) The stratigraphical sequences recovered from the Gialova Lagoon are generally characterized by fine-grained autochthonous sediments of a lower energetic potential which were deposited under brackish lagoonal to limnic conditions. However, we found several distinct interferences of the stratigraphical records by allochthonous gravelly to sandy high-energy deposits which represent temporary extreme events.

(ii) Numerous findings of beachrock-type deposits along the coastline must not be considered as lithified littoral sediments but rather represent cemented parts of tsunami deposits showing characteristic sedimentary features of high-energy dynamics (Vött et al. 2010).

(iii) Allochthonous coarse-grained high-energy deposits encountered in the Gialova Lagoon stratigraphical record show lamination structures, erosional contacts at the base, fining upward sequences, rip up clasts and embedded stones and ceramic fragments all of which are characteristic for tsunami influence but cannot be explained by recent littoral processes.

(iv) Allochthonous coarse-grained deposits show a high amount of fully marine microfauna (foraminifera, molluscs) and shell debris reflecting that high-energy influence originated from the sea side and even affected areas further offshore. In contrast, autochthonous lagoonal deposits strongly differ in abundance and diversity of encountered species.

(v) Based on the local wind-generated wave climate and storm parameters on the one hand and the sedimentary characteristics of the high-energy deposits as well as the large dimensions of the corresponding geomorphological forms on the other hand, allochthonous coarse-grained deposits found in the environs of the Gialova Lagoon are interpreted as being the result of tsunami impact.

(vi) Event-geochronostratigraphical studies allowed to identify 6 different tsunami generations since the mid-Holocene before around 3300 cal BC (I), between the end of the 4th millennium BC and the end of the 3rd millennium BC (II), at around 1200-1000 cal BC (III), shortly after the 4th to 2nd cent. BC (IV), between the 8th and the 14th/15th cent. AD (V), after the mid-14th to the beginning of the 15th cent. AD (VI)).

(vii) The palaeogeographical evolution starts with an open marine embayment covering large parts of the present Gialova Lagoon. Later, a barrier system was established, separating a quiescent water body with lagoonal and limnic conditions from the Bay of Navarino. The data show that the subsequent shift of this barrier system towards the south, implicating a southward enlargement of the Gialova Lagoon, was mainly controlled by high-energy tsunami impacts most probably induced by earthquake focal mechanisms in the nearby Hellenic Trench subduction zone. The evolution of the barrier accretion spit at its present position was dated to around 300-100 cal BC. The Bay of Voidokilia developed associated to the influence of tsunamigenic impact after around 3300 cal BC. Gradual coastal changes for example by longshore processes seem to be merely responsible for the re-arrangement of sediments after high-energy impacts.

5 Synthesis and conclusions

In order to evaluate the contribution of palaeotsunami studies along the coasts of the eastern Ionian Sea for Holocene coastal and palaeo-event research, chapter 5 provides a synoptic view of the results, obtained for all study sites. The central hypothesis and the aims of the study will be discussed against results from - Cefalonia Island (chapter 2), - the Gulf of Kyparissia with the former Mouria Lagoon and Kato Samiko (chapter 3) and the Gialova Lagoon (chapter 4). Chapter 5.1 presents a synoptic view of the local and regional coastal palaeogeographies and the influence of sea level fluctuations on the long term coastal evolution. With reference to the main hypotheses, chapter 5.2 sheds light on the similarities and differences of the sedimentary signatures deciphered for high-energy impacts. The question of storm or tsunami impact as triggering factor for high-energy wave impact will be discussed in detail. Chapter 5.3 combines the palaeogeographical evolution and the sedimentary findings in a detailed geo-chronology for Holocene tsunami events and palaeogeographies. Finally, a perspective for coastal management and future studies is given in chapter 5.4.

5.1 Palaeogeographies and sea level evolution on Cefalonia and the western Peloponnese

The palaeogeographical evolution and palaeo-environmental reconstructions of the investigated areas are based on the analysis of sediment stratigraphies from Holocene near coast geo-archives. The interpretation of the respective stratigraphical records was realized by a geo-scientific multi-method approach comprising geomorphological mapping, sedimentological and geochemical analysis. Micro-morphological, palynological and microfaunal investigations were combined with data from geophysical and geochronological methods to reconstruct horizontal and vertical distribution patterns of palaeo-facies. The combination and cross checking of multiple geo-scientific methods is the key to get a detailed impression of palaeo-landscapes and is therefore essential for Holocene coastal research.

Geographical, geomorphological and sedimentary distribution patterns of facies are the basis to realize the main study aims which are summarized as the following.

(i) the reconstruction of Holocene coastal palaeogeographies along the coasts of the western Peloponnese and Cefalonia Island,

(ii) the detection and deciphering of event related sedimentary signatures in the stratigraphical record,

(iii) to determine between storm or tsunami as main hydromorphic process,

(iv) establishing a geochronology of tsunami generations in local and supra-regional scales,

(v) to identify relationships or differences between the investigated study sites and their sedimentary similarities and differences in terms of palaeogeographies and tsunami deposits,

(vi) to decipher the influence of high-energy impact on the local and regional coastal evolution and

(vii) to detect relative sea level fluctuations and potential tectonic movement against the palaeogeographical background.

Based on the results and the interpretation of sections 2 to 4, the following statements for the palaeogeographical evolution along the eastern Ionian coasts can be made.

On Cefalonia Island the shores of the inner Gulf of Argostoli and the Bay of Livadi are characterized by marine strata at their sedimentary bases. Along the coastal lowlands of the Paliki peninsula autochthonous shallow marine environments were affected by repeated and abrupt input of mixed gravels, coarse sand and microfaunal remains of allochthonous nature into predominantly autochthonous marine, limnic and semi-terrestrial environments. The re-establishment of marine conditions after significant changes in the hydromorphic energetic environments is evident. The recent autochthonous conditions are characterized by loamy distal alluvial deposits along the Lixouri coastal lowlands whereas the Bay of Livadi at the northernmost end of the Gulf is built up out of massive limnic sequences and semi terrestrial swampy conditions since the mid of the 6th millennium cal BC. Palynological data shows constant conditions of limnic communities and a significant distance to marine influence. In a distance of about 800 m to the recent coast an intersecting sand sheet with a fully marine microfaunal spectrum was found that is subsequently overlain by recent marsh deposits. The present beach barrier at the Livadi bay works as a protective morphological system. Sea level studies at the Livadi bay therefore show that the sea level has never been higher than at present and a mid-Holocene sea level highstand can be excluded. Sea level fluctuations are associated to aseismic and coseismic tectonic crustal movements and singular high-energy wave impacts. The results furthermore show that coastal changes at the Gulf of Argostoli are initiated and controlled by extraordinary strong wave impact from the sea-side; the role of gradual processes seems to be restricted to the re-arrangement of sediments after these extreme wave singularities.

Palaeogeographical studies in the environs of the former Mouria Lagoon show that the area passed multiple phases of environmental change. Stratigraphical data provides evidence of a palaeo-shoreline about 1.8 km further inland at around 5000 cal BC. At the most landward side a semi-terrestrial as well as limnic environment established, whereas marine conditions exist to the sea side. Subsequently, the palaeo-coastline shifted in southwestern direction. Environmental changes are associated by wide-spread limnic conditions and are closely related to high-energy sediment input deciphered from the geological record. High-energy impact is associated to sedimentary characteristics like erosive contacts and/or subsequently rapid shifts from marine to limnic and terrestrial/semi-terrestrial conditions. A progradation of beach ridge generations produced a of limnic and marine influenced palaeo-environments on small scales. The extension and the progradation of the lagoonal system go hand in hand with the deceleration and stagnation of the Holocene sea level rise. However, compared to short-term high-energy impact, the influence of the sea level rise since the mid Holocene seems quite low. The establishment and development of the former Mouria Lagoon rather correlates to short-term interruptions than to gradual changes. Comparable to Cefalonia, the relative sea level evolution was characterized by a constant rising and no indicators are given that it has ever been higher than today.

At the study site of Kato Samiko, the palaeogeographical evolution was characterized by event related sediments at the base that were subsequently overlain by alluvial deposits of low-energy environments. For the time period prior to 4000 cal BC, the basal marine sediments are in

atypical stratigraphic position As seen in the Mouria Lagoon, the sea level during this time period was significantly lower. It must thus be assumed that the deposition occurred above local sea level. In the upper part of the stratigraphical record, an abrupt input of coarse sands mixed with archaeological remains is evident. Geophysical investigations document the existence of channel-like deposition with a distinct seaward extend and thinning landward tendencies of the structure. The channel infill is in strong discrepancy to the energetic conditions of the palaeo-environment as well as the recent distal alluvial environment and thus seems to be of allochthonous high-energetic nature.

In the environment of the Gialova Lagoon, situated at the southwestern Peloponnese, significant landscape changes during the Holocene are evident. Present day geomorphologies of the Gialova Lagoon are characterized by the small sea-channel inlets of Sikia and Voidokilia with its semicircular bay and a distinctive barrier-spit system. Vibracore transects across the Gialova Lagoon show thick autochthonous marine sequences at the sedimentary bases, that implie a palaeo-shoreline some kilometers further north. Around 3300 cal BC, the input of allochthonous gravels and sand is of high-energetic nature. This disturbance most probably goes hand in hand with the evolution of the semi-circular Bay of Voidokilia. The palaeo-conditions rapidly changed into phases of quiescent conditions and resulted in a separation into and coexistence of lagoonal and marine environments. At the northern part of the Gialova Lagoon quiescent conditions predominated whereas the southern part was still under marine influence. The southward shift of the palaeo-coastline during the Holocene and the evolution of the present barrier accretion spit are dated to around 300 cal BC. The quiescent embayment implies a palaeo-barrier system further north, which is responsible in combination with the closure of the Voidokilia channel for quiescent sedimentary conditions. This palaeo-barrier system therefore most probably appears between 3300-300 cal BC further north and built up the enclosure to the south. The geomorphic structure of a washover fan system, reaching into the Gialova Lagoon, is evident and is most possibly of a young age (post 2ndmillennium cal AD) as the radiocarbon datings show.

In conclusion and with regard to the study aims, the results of the palaeogeographical evolution along the coasts of Cefalonia and the western Peloponnese show distinct similarities: (i) The palaeo-coastlines extended further inland until the mid-Holocene caused by the post-glacial transgressive behaviour of the littoral system. (ii) The sedimentary sequences are characterized by a marine base which shifted into stillwater or rather low-energetic environments after strong high-energy impulses. (iii) Shifting and destruction of palaeo-landscapes are frequently linked to significantly strong high-energy impact that seems to be a main triggering factor for the coastal evolution. (iv) Gradual coastal processes are often associated with the post-tsunamigenic re-arrangement of sediments. (v) A decline of the Holocene sea level rise resulted in a progradation of terrestrial and semi-terrestrial conditions directly associated to a regressive behaviour of the littoral system. (vi) The relative local sea level has never been higher than present and a mid-Holocene sea level high stand must be excluded for the study sites.

The evolution of the present-day coastlines are the result of both, long-term gradual coastal evolution and short-term high-magnitude events, and thus formed on different time scales.

In the presented case studies, the initial establishment of lagoonal systems is characterized by short-time geomorphological processes within scales whereas the lagoons exist on longer time scales. Single high-energy events therefore have a great influence on the geomorphological inventory and the long-term response of the coastal system. In a summary view, the investigated study areas are excellent sedimentary archives for the reconstruction of the coastal evolution and palaeogeographies during the Holocene.

5.2 Identification and sedimentary significances of palaeotsunami deposits

The identification of high-energy events was based on sedimentary characteristics that reflect conditions of significantly high-energetic flow conditions which were discussed in detail in chapter 2 to chapter 4. The existence and preservation of layers, depend on the specific characteristics of each geo-archive, and depend on the constant accumulation of sediments and preferably no erosion. Sedimentary sequences at the study sites repeatedly show anomalies within the stratigraphical record along the coast. The presented vibracoring transects and field evidence show several similarities and differences in the sedimentary record of the deciphered high-energy layers.

The investigated study sites are characterized by distinct sedimentary features documenting extraordinary high-energy wave impact from sea side. The encountered high-energy deposits are characterized by (i) coarse grained high-energy sediments, found on top of autochthonous littoral, limnic and semi-terrestrial environments and are (ii) characterized by sharp erosional unconformities, attesting singular strong impact. (iii) Layers of allochthonous coarse grained material, intersecting quiescent lagoonal and limnic conditions, are characterized by distinct fining upward sequences and thinning landward tendencies. (iv) Rip-up clasts, out of eroded underlying sediments, were found frequently within high-energy deposits as well as (v) poor

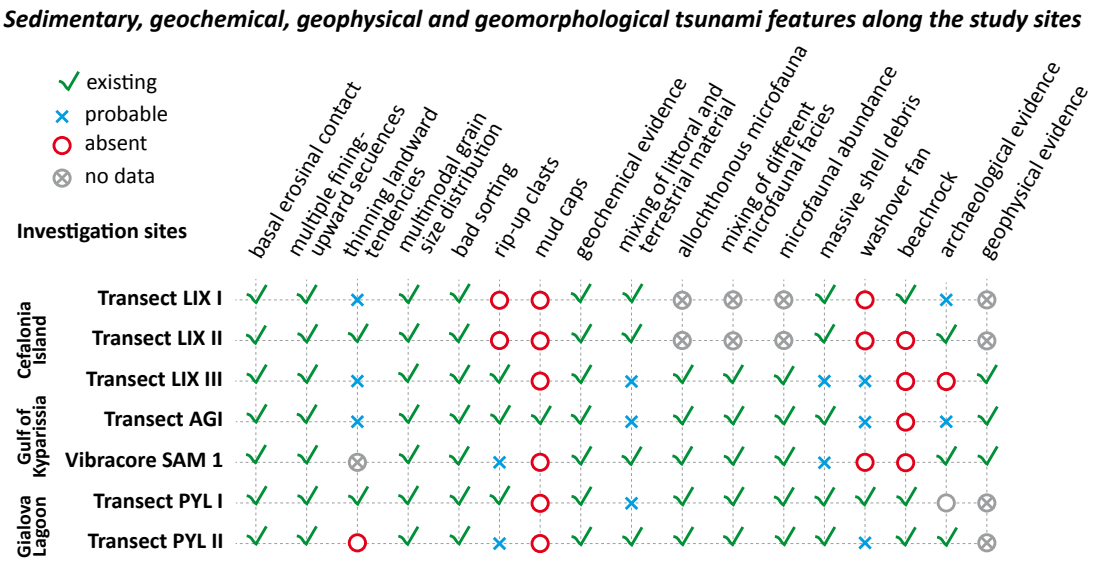

Fig. 5-1: Synopsis of sedimentary, geochemical, geophysical and geomorphological characteristics used for discriminating of palaeo-tsunami deposits along the study sites.

sorting and multimodal grain size distributions and (vi) distinct mud caps or mud drapes. (vii) Macro- and microfaunal analyses document abrupt changes of the faunal assemblage by the massive input of different allochthonous species, partly mixed with species from underlying facies. (viii) The occurrence of massive shell debris in badly sorted event deposits with partly well preserved bivalves besides angular and destroyed molluscs is evident.

Besides sedimentary characteristics geomorphological features documenting high-energy impact were also found on the recent surfaces. These findings were (i) washover fans, (ii) beachrock and beachrock fragments and (iii) archaeological remains mixed with littoral and terrestrial material which were carried out on the individual study sites. The similarities and differences between event deposits from the investigated study areas are shown in detail in Fig. 5-1. Consistent sedimentary characteristics that are evident for all investigated areas comprise (i) the occurrence of basal erosional unconformities, (ii) fining upward sequences, (iii) multimodal grain-size distribution, (iv) bad sorting and (v) characteristic geochemical fingerprints and seem to be an indicator for tsunami impact of supra-regional character.

Sedimentary features like the mixing of different macro- and microfaunal facies, massive shell debris, the input of allochthonous microfaunal remains or the general presence of microfaunal remains were not detected for all study areas and seem to depend on the specific geographical inventory of each site. Also sedimentary characteristics as thinning landward tendencies, the existence of rip-up clasts or mud caps and the mixing of littoral and terrestrial sediments depend on the individual geomorphological and sedimentological inventory of a study area.

Geomorphological surface findings like washover structures and calcarentic beachrock-type tsunamites are linked to local coastal configurations like, for example, an appropriate sediment supply.

General criteria for the detection and differentiation of storm or tsunami events do not exist for fine grained stratigraphies (e.g. Dawson & Shi 2000, Tuttle et al. 2004, Switzer et al. 2005, Morton et al. 2008, Pignatelli et al. 2009, Engel et al. 2011, Etienne et al. 2011, Goff et al. 2010, 2012, Phantuwongraj & Choowong 2012, Scheffers et al. 2013). Geomorphological characteristics, the palaeo-geographical evolution and the recent geographical setting have to be considered in order to distinguish between the hydro-morphological sedimentation processes. The discrimination between storm and tsunamigenic imprint and their influence on long term coastal evolution was realized by site specific strategies and interpretations.

Site specific interpretation of results from Cefalonia Island let us conclude that the high-energy-layers are of tsunamigenic instead of storm borne origin because:

(i) the overall geomorphodynamic potential of storm-wave driven littoral processes in the inner Gulf of Argostoli is limited because of the well sheltered geomorphologies of the gulf against the predominantly west winds.

(ii) Along the shores of the Gulf of Argostoli, high-energy deposits were encountered in consistent stratigraphic positions over distances more than 5 km parallel to the coast and more than 850 m inland.

(iii) Event-stratigraphical characteristics, geochemical fingerprints and microfaunal evidence let us conclude that the high-energy deposits encountered in the study area were caused by tsunami impact. Sedimentary characteristics of typical storm influence as well as superordinate alluvial (torrential) or mass denudation were not found or were beyond the analytical resolution of the methods applied in this study.

(iv) The funnel shape coastline configuration of the Gulf of Argostoli which opens to the south and is directly exposed to the Ionian Sea and the Hellenic Arc is expected to play a major role in tsunami wave propagation inside the gulf. A tsunami triggered in the Ionian Sea and travelling northwards will be accelerated in the funnel shaped coast and is expected to produce highest run up values along the inner Gulf of Argostoli.

Arguments for the interpretation of tsunamigenic impact at the Gulf of Kyparissia can be summarized by the following arguments:

(i) Coastal dynamics along the Gulf of Kyparissia are affected by intense winter storms, however, the observed wave action does merely affect the coastline itself. Here, moderate to strong erosion causes minor cliffs along the continuous dune belt but wave action does not exceed far inland. Both, the vibracore locations along the AGI transect as well as vibracore SAM 1 are located more than 1 km and 2.5 km distant to the recent coastline, respectively.

(ii) The beach barriers along the Gulf of Kyparissia extents about 200 m to 600 m inland providing a massive natural protection, thus, both study areas are by far closed off from storm wave action.

(iii) Computer simulations of tsunami wave inundation scenarios for the Gulf of Kyparissia demonstrate (Röbke et al. 2013), that major tsunami events are well capable of overflowing the protective dune belt along the coastline and inundate far inland.

(iv) Against the respective geomorphological setting, the identified sedimentary structures, geochemical fingerprints and microfossil content of each event-associated layer as well as results from geophysical studies emphasize the tsunamigenic origin of the associated deposits.

In the environs of the Gialova Lagoon the following arguments for our interpretation in the discussion of the main hydromorphic regime which causes the sedimentation of high-energy deposits can be made:

(i) The study area is located directly exposed to the open Ionian Sea, but the investigation site itself is protected by bedrock outcrops. The Bay of Navarino was used as harbour site since the antiquity; it is known to be one of the best protected harbours on the Peloponnese against storm influence.

(ii) The beach barriers extents about 200 m inland providing such a massive natural protection that neither storms or so called Medicanes (tropical storm equivalents for the Mediterranean Sea) are capable to overflow them. Thus, the study area is by far closed off from recent storm wave action.

(iii) In case of the Gialova embayments, the disturbance and destruction of palaeo-environments by extraordinary strong wave action occurred episodically, and left a stratigraphically widespread sediment trap. Storm action is known for high recurrence intervals and a significantly smaller

sedimentary record in the geo-archive.

(iv) The combination of sedimentary signatures of the geological record, surface findings and meso-scale geomorphological structures let us conclude that high-energy deposits encountered at the study site, were deposited most probably by tsunamis and not by storms.

In summary, the reconstruction of palaeo-tsunami events relies on geo-scientific criteria like microfaunal analysis, geomorphological and sedimentological investigations, palaeogeographical evolution, geochemical fingerprints and the geochronology. As mentioned in the aims, it can be verified, that selected investigation sites allow us to parallelize similarities of sedimentary signatures found in all study areas along the Eastern Ionian coasts. All investigated geo archives holds a high potential to conserve tsunami sediments and share common sedimentary characteristics documenting strong tsunamigenic impact.

5.3 Establishing a tsunami geochronology for the eastern Ionian Sea

The establishment of a local as well as supra-regional tsunami geo-chronology was defined as one of the main objectives for the study areas. In this chapter the results of each study are compared to local, regional and supra-regional relationships and correlations. According to the hypothesis, that sedimentary imprints found along the coastlines of the eastern Ionian Sea attest repeated tsunami landfall, a geo-chronology approach is given in in the following chapter to establish intervals and magnitudes of tsunami landfall, this chapter.

Local tsunami chronologies for Cefalonia, the Gulf of Kyparissia and the Gialova Lagoon were established by radiocarbon datings and diagnostic ceramics. Dating strategies were to date terrestrial plant remains from in-situ strata above and below the tsunami deposits if possible (for sandwich dating approach see e.g. Vött et al. 2009b). The dating of well-preserved bivalves out of the tsunami deposit was used to determine *termini ad* or *post quem* for the tsunami event. Based on the dating results of chapter 2, 3 and 4 the following local geo-chronologies can be summarized.

Cefalonia Island was hit by almost 5 tsunami-events, which were dated to 5700 cal BC (I), 4250 cal BC (II), the beginning of the 2nd millennium cal BC (III), 1st millennium cal BC (IV) and 780 cal AD (V).

For the Gulf of Kyparissia we detected 4 generation of tsunamigenic impact. Tsunami landfall was dated to 5th millennium cal BC (I), mid to late 2nd mill. BC (II), Roman times (1st cent. BC to early 4th cent. AD) (III) and most possible one of the well-known 365/521/551 AD historic tsunamis (IV).

Event-geochronostratigraphical studies at the Gialova Lagoon allowed to identify 6 different tsunami generations during the Holocene. Generation I was detected before around 3300 cal BC, II around the end of 4th and the beginning of 3rd millennium BC, III after around 1100 cal BC, IV after 4th to 2nd cent. BC, V between 8th and early 15th cent. AD, VI after mid-14th to beginning of 15th cent. AD.

As defined in the aims, the reconstruction of palaeo-events and the establishment of a geochronology was realized with respect to dating accuracies of selected materials. One of the

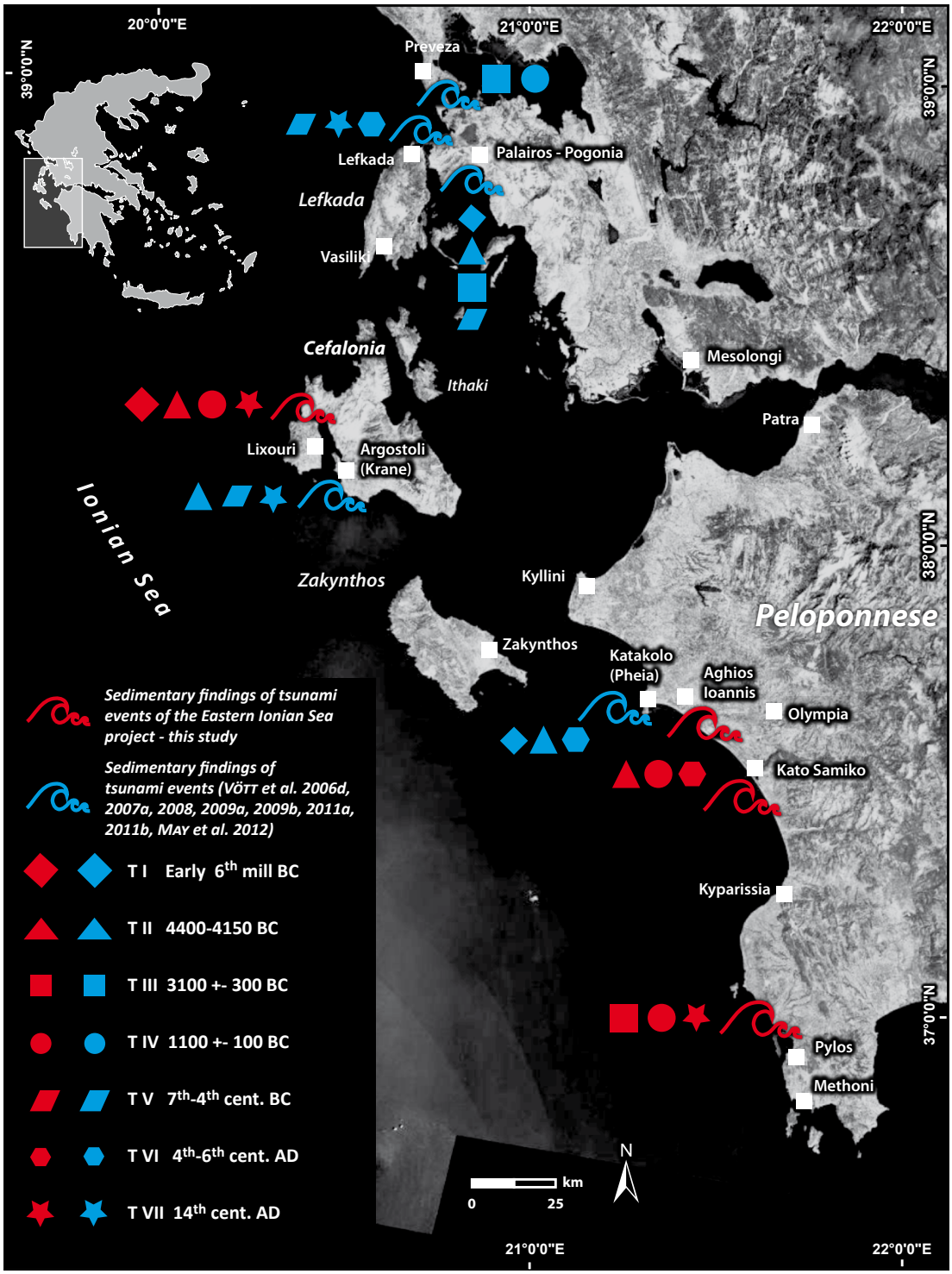

Fig. 5-2: Synpsis of geochronology data and sedimentary palaeo-tsunami evidences along the eastern Ionian Sea (map is modified after Bing aerial maps 2013).

main hypotheses was to date and reconstruct regional and supra-regional effects of tsunami events in the eastern Ionian Sea. In the following the main conclusions of the correlation of local and supra-regional tsunami effects can be made.

Effects on supra-regional scales, that hit the coast along the western Peloponnese, the Ionian Islands and coastal Akarnania, were deciphered by geo-scientific evidences (see Fig. 5-2). Correlating evidence of supra-regiona-tsunami impact is published for the following areas:

(i) In the early 6th millennium cal BC, Cefalonia delivers evidence yielding ages of 5700 cal BC and shares similarities for tsunamigenic impact for nearby coastal Akarnania at around 6000 cal BC (Vött et al. 2011a), the early 6th millennium at the Lake Voulkaria (Vött et al. 2009 b) and the ancient harbor of Pheia (Vött et al. 2011b) which was inundated by a tsunami at the beginning of the 6th millennium.

(ii) Frequent evidence of tsunami impact is also given for the 5th millennium cal BC. On Cefalonia, we deciphered strong tsunami influence at around 4250 cal BC and along the Gulf of Kyparissia our dating approach yields evidence of tsunami impact for the beginning of the 5th millennium BC. Sedimentary findings at the Bay of Palairos – 4400 cal BC (Vött et al. 2011a), Pheia – 4300 cal BC (Vött et al. 2011b) and Krane on Cefalonia – 4150 cal BC (Vött et al. 2013) show strong correlations, considering the dating inaccuracies.

(iii) Along the coasts of eastern Ionian, major tsunami landfall around 3000 cal BC was documented by several geo-scientific investigations. The coastal area of Preveza together with the entrance of the Ambrakian Gulf – 2800 cal BC (Vött et al. 2007a) and the Palairos coastal plain at 3500 cal BC (Vött et al. 2011a) show sedimentary signatures of possibly correlating tsunami impact. Within dating accuracies, the results of the Gialova Lagoon that attest tsunami landfall before around 3300 cal BC fit very well to this timeframe.

(iv) Documented by Vött et al. (2006d, 2007a, 2009a, 2009b, 2011a, 2011b) and May et al. (2012) the time at 1000 cal BC delivers hints of extraordinary strong tsunami impact. On Cefalonia, our results indicate an event for 1st millennium cal BC, as also identified by Vött et al. (2013) for the nearby ancient harbour of Krane, Koutavos Bay. The Lake Voulkaria and the Bay of Palairos were also hit in between 1200-1000 cal BC by strong tsunami influence (Vött et al. 2009a, b). Effects of strong tsunami impact are also given for the Gialova Lagoon at around 1100 cal BC delivering strong correlations of supra-regional scale impact. Not to forget the Santorini/ Thera eruption (Friedrich et al. 2006, 2013) at the beginning of the 17th century cal BC, which correlates to findings along the shores of the Gulf of Kyparissia in the former Mouria Lagoon (generation II).

(v) For the former Mouria Lagoon our results document tsunamigenic impact in the 3rd century cal AD and post 3rd century cal AD, that probably correlates to the nearby ancient harbour of Pheia. Here, Vött et al. (2012) detected tsunami influence in 4th century cal AD and the 6th century cal AD. The distance between the study sites is negligible and the dating approaches are correlating well. A speculative correlation, with respect to dating accuracies, can be made to the effects of the well-known and historical tsunami event of 365 AD.

(vi) Supra-regional tsunami evidence for the time around 1000-1400 cal AD is given for

the Lefkada coastal zone (Vött et al. 2006d) and Krane at around 1000 cal AD (Vött et al. 2013). Correlated time intervals are deciphered for the Bay of Livadi at around 1300 cal AD and the Gialova Lagoon at 1300 cal AD. At the Gulf of Kyparissia we detected an event which took place after the 3rd century AD, and therefore a correlation is highly speculative.

To sum up, almost 6 events between the 6th millennium and medieval times were found in the study sites which were most probably occurred on a supra-regional scale at the eastern Ionian Sea. Geo-scientific findings along the coasts of the Ambrakian Gulf, the Lefkada coastal area, the Bay of Palairos Pogonia, Cefalonia Island as well as the northwestern and southwestern Peloponnese were dated to comparable time spans. It has to be assumed that strongest tsunamigenic influence with wide area effects took place in the early 6th millennium cal BC, around 4300 cal BC, around 3000 cal BC, 1000 cal BC, 365, 521 & 551cal AD and 1300 cal AD.

Regional events, affecting the Ionian Islands and the western Peloponnese, were dated to around 2000 cal BC. On Cefalonia Island we deciphered tsunami influence in the 2nd millennium cal BC which most possibly correlates with an event at Krane around 2000 cal BC described by Vött et al. (2013). The former Mouria Lagoon delivers similarities regarding the geo-chronological investigations, we deciphered a tsunami event yielding to 2000 cal BC.

The effects of the event at 2000 cal BC are seems to be limited on Cefalonia and the Gulf of Kyparissia, but cannot be excluded for other study areas because conservation and dating are depending on the characteristics of the investigated geo-archives, thus erosion or accumulation effects are highly different.

On Cefalonia, the Bay of Koutavos as well as the Bay of Livadi show local signatures of tsunamigenic impact during the first millennium cal BC. Parallels to coastal Akarnania between 500-300 cal BC (Vött et al. 2008, 2009a, 2011a) are even speculative.

Local events are limited to the specific study sites; the correlation to supra-regional impact cannot be verified or may be too speculative. Local evidences and geo-chronologies most possibly are driven by triggering factors of individual geographical character.

In summary, the geo-chronological correlation between supra-regional effects of tsunami imprint in the study areas is given. Sedimentary findings and the time span show distinct similarities and let us come to the conclusion that tsunami events of extraordinary repeatedly scale hit the coasts of the eastern Mediterranean. The possibility of a local, regional and supra-regional tsunami reconstruction is given, with respect to the dating accuracies, as the results show.

5.4 Perspectives

The focus of this project was the identification and characterization of parallels and dating of Holocene tsunami wave deposits and to add valuable information to already existing data of sedimentary findings and historical accounts.

The sedimentary findings at the study sites along the eastern Ionian Sea show strong correlations to recent (e.g. Etienne et al. 2009, Matsumoto et al. 2010, Phantuwongraj & Choowong

2012) and sub-recent tsunami events (e.g. Vött et al. 2006d, 2007a, 2008, 2009a, 2009b, 2011a, 2011b, May et al. 2012, Scheffers et al. 2008, Mastronuzzi et al. 2000, 2007, Smedile et al. 2011). It has been verified that the coasts were frequently affected by strong tsunami imprint that also controlled the long- and short-term coastal evolution. The tsunami risk in the eastern Mediterranean must be categorized as significantly high in frequency and magnitude and therefore holding high risks for human settlements and infrastructure.

Further investigations along the coasts all over the eastern Ionian Sea most probable hold valuable information about the coastal evolution as well as the frequency and magnitude of tsunami imprint. After Hadler et al. (2012) "it is stated that a non-entry of a tsunami event in a catalogue for which geo-scientific traces have been found does not mean at all that the event did not take place". For that reason, further detailed investigations in near coast geo-archives along the Mediterranean coasts have to be carried out to obtain more detailed information to provide a comprehensive data pool suitable for future tsunami risk mitigation.

Sedimentary findings also provide valuable information for the numeric modelling of tsunami events as well as information to verify and to falsify modeling results.

The results presented on this study show that the tsunami hazard in the Mediterranean holds an exceptional high risk. As shown by Synolakis (2008), the public awareness rather tends to earthquakes than to tsunami hazard in the Mediterranean. However, in terms of tsunami vulnerability and risk assessments, eastern Mediterranean coastlines have to be reviewed in a new light as our results show. It is therefore important to further intesify geo-scientific studies on palaeotsunami events in order to call attention to the public awareness of the tsunami hazard and to use these preliminary findings as a basis for risk mitigation strategies to reduce humans risk.

References

Ad-hoc-Arbeitsgruppe Boden der Staatlichen Geologischen Dienste und der Bundesanstalt für Geowissenschaften und Rohstoffe (eds.) (2005): Bodenkundliche Kartieranleitung. – Stuttgart, 438 pp.

Almogi-Labin, A., Siman-Tov, R., Rosenfeld, A. & Debard, E. (1995): Ocurrence and distribution of the foraminifer Ammonia beccarii tepida (Cushman) in water bodies, Recent and Quaternary, of the Dead Sea Rift, Israel. – Marine Micropaleontology **26**: 153-159.

Altinok, Y., Tinti, S., Alpar, B., Yalçiner, A.C., Ersoy, S., Bortolucci, E. & Armigliato, A. (2001): The Tsunami of August 17, 1999 in Izmit Bay, Turkey. – Natural Hazards **24**: 133-146.

Alvarez-Zarikian, C.A., Soter, S. & Katsonopoulou, D. (2008): Recurrent Submergence and Uplift in the Area of Ancient Helike, Gulf of Corinth, Greece: Microfaunal and Archaeological Evidence. – Journal of Coastal Research **1**: 110-125.

Ambraseys, N.N. & Synolakis, C.E. (2010): Tsunami Catalogs for the Eastern Mediterranean, Revisited. – Journal of Earthquake Engineering **14**(3): 309-330.

Andrade, C., Freitas, M.C., Moreno, J. & Craveiro, S.C. (2004): Stratigraphical evidence of Late Holocene barrier breaching and extreme storms in lagoonal sediments of Ria Formosa, Algarve, Portugal. – Marine Geology **210**: 339-362.

Antonopoulos, J. (1979): Catalogue of tsunamis in the Eastern Mediterranean from Antiquity to present times. – Annali die Geofisica **32**: 113-130.

Arvanitides, C., Koutsoubas, D., Dounas, C. & Eleftheriou, A. (1999): Annield fauna of a Mediterranean lagoon (Gialova Lagoon, south-west Greece): community structure in a severely fluctuating environment. – Journal of the Marine Biological Assosiation of the United Kingdom **79**: 849-856.

Bahlburg, H. & Spiske, M. (2012): Sedimentology of tsunami inflow and backflow deposits: key differences revealed in a modern example. – Sedimentology (2012) **59**: 1063-1086.

Barbano, M.S., Pirrotta, C. & Gerardi, F. (2010): Large boulders along the south-eastern Ionian coast of Sicily: Storm or tsunami deposits? – Marine Geology **275**: 140-154.

Barsch, H., Billwitz, K. & Bork, H.-R. (eds.) (2000): Arbeitsmethoden in Physiogeographie und Geoökologie. – Gotha, Stuttgart, 612 pp.

Beug, H.J. (2004): Leitfaden der Pollenbestimmung für Mitteleuropa und angrenzender Gebiete. – München, 542 pp.

Benetatos, C., Kiratzi, A., Papazachos, C. & Karakaisis, G. (2004): Focal mechanisms of shallow and intermediate depth earthquakes along the Hellenic Arc. – Journal of Geodynamics **37**: 253-296.

Bernasconi, M.P., Melis, R. & Stanley, J.D. (2006): Benthic biofacies to interpret Holocene environmental changes and human impact in Alexandria's Eastern Harbour, Egypt. – The Holocene **116** (8): 1163-1176.

Billi, A., Funiciello, R., Minelli, L., Faccenna, C., Neri, G., Orecchio, B. & Presti, D. (2008): On the cause of the 1908 Messina tsunami, southern Italy. – Geophysical Research Letters **35:** 191-212.

Bird, E. (2005): Coastline changes. – In: Schwartz, M.L. (eds.): Encyclopedia of Coastal Science. Springer, Dordrecht: 319-323.

Bird, E. (2008): Coastal Geomorphology – An Introduction. – New York, 411 pp.

Bisbee, H.L. (1937): Samikon. – Hesperia: The Journal of the American School of Classical Studies at Athens **6** (4): 525-538.

Bondevik, S., Mangerud, J., Dawson, S., Dawson, A. & Lohne, Ø. (2005): Evidence for three North Sea tsunamis at the Shetland Islands between 8000 and 1500 years ago. – Quaternary Science Reviews **24**: 1757-1775.

Brückner, H., Kelterbaum, D., Marunchak, O., Porotov, A. & Vött, A. (2010): The Holocene sea level story since 7500 BP – Lessons from the Eastern Mediterranean, the Black and the Azov Seas. – Quaternary International **225** (2): 160-179.

Bruins, H.J., MacGillivray, J.A., Synolakis, C.E., Benjamini, C., Keller, J., Kisch, H.J., Klügel, A. & van der Plicht, J. (2008): Geoarchaeological tsunami deposits at Palaikastro (Crete) and the Late Minoan IA eruption of Santorini. – Journal of Archaeological Science **35**: 191-212.

Bryant, E. (2008): Tsunami – The Underrated Hazard. – Springer, Berlin, 330 pp., 2nd Ed.

Chagué-Goff, C., Schneider, J.C., Goff, J.R., Dominey-Howes, D. & Strotz, L. (2011): Expanding the proxy toolkit to help identify past events - Lessons from the 2004 Indian Ocean Tsunami and the 2009 South Pacific Tsunami. – Earth-Science Reviews **107** (1-2): 107-122.

Cavaleri, L. (2005): The Wind and wave Atlas of the Mediterranean Sea - The Calibration Phase. – Advances in Geosciences **2**: 255-257.

Cimerman, F. & Langer, M.R. (1991): Mediterranen Formaminifera. – Ljubiljana, 118 pp.

Cisternas, M., Atwater, B.F., Torrejon, F., Sawai, Y., Machuca, G., Lagos, M., Eipert, A., Youlton, C., Salgado, I., Kamataki, T., Shishikura, M., Rajendran, C.P., Malik, J.K., Rizal, Y. & Husni, M. (2005): Predecessors of the giant 1960 Chile earthquake. – Nature **437**: 404-407.

Clement, C., Hirn, A., Charvis, P., Sachpazi, M. & Marnelis, F. (2000): Seismic structure and the active Hellenic subduction in the Ionian islands. – Tectonophysics **329**: 141-156.

Clews, J.E. (1989): Structural controls on basin evolution: Neogene to Quaternary of the Ionian zone, Western Greece. – Journal of the Geological Society **146**: 447-457.

Cocard, M., Kahle, H.-G., Peter, Y., Geiger, A., Veis, G., Felekis, S., Paradissis, D. & Billiris, H. (1999): New constraints on the rapid crustal motion of the Aegean region: recent results inferred from GPS measurements (1993–1998) across the West Hellenic Arc, Greece. – Earth and Planetary Science Letters **172**: 39-47.

Crawley, R. (2009): Thucydides. The history of the Peloponnesian War. EBook #7142, Project Gutenberg. – http://www.gutenberg.org/files/7142/7142-h/7142-h.htm#2HCH0011. 01/2012.

Davis, J.L. (2008): Sandy Pylos: An Archaeological History from Nestor to Navarino. – University of Texas Press, Austin, 342 pp., 2nd Ed.

Dawson, A. (1996): The geological significance of tsunamis. – Zeitschrift für Geomorphologie N.F., Suppl.- Vol. **102**: 190-210.

Dawson, A.G. & Shi, S. (2000): Tsunami deposits. – Pure and Applied Geophysics **157**: 875-897.

Dawson, A.G. & Stewart, I. (2007): Tsunami deposits in the geological record. – Sedimentary Geology **200**: 166–183.

Dearing, J.A. (1999): Environmental Magnetic Susceptibility. Using the Bartington MS2 System. – British Library Cataloguing in Publication Data.

Debenay, J.P., Bénéteau, E., Zhang, J., Stouff, V., Geslin, E., Redois, F. & Fernandes-Gonzales, M. (1998): Ammonia beccarii and Ammonia tepida (Foraminifera): morphofunctional arguments for their distinction. – Marine Micrpaleontology **34**: 235-244.

De Martini, P.M., Burrato, P., Pantosti, D., Maramai, A., Graziani, L. & Abramson, H. (2003): Identification of liquefaction features and tsunami deposits in the Gargano area (Italy): paleoseismological implication. – Annals of Geophysics **46**(5): 883-902.

Di Bella, L., Bellotti, P., Frezza, V., Bergamin, L. & Carboni, M.G. (2011): Benthic foraminiferal assemblages of the imperial harbour of claudius (Rome): Further palaeoenvironmental and geoarchaeological evidences. – The Holocene **21** (8): 1245-1259.

Dominey-Howes, D.T.M., Cundy, A. & Croudace, I. (2000): High energy marine flood deposits on Astypalaea Island, Greece: possible evidence for the AD 1956 southern Aegean tsunami. – Marine Geology **163**: 303-315.

Dominey-Howes, D.T.M., Humphreys, G.S. & Hesse, P.P. (2006): Tsunami and palaeotsunami depositional signatures and their potential value in understanding the late-Holocene tsunami record. – The Holocene **16** (8): 1095-1107.

Donato, S.V., Reinhardt, E.G., Boyce, J.I., Rothaus, R. & Vosmer, T. (2008): Identifying tsunami deposits using bivalve shell taphonomy. – Geology **36** (3): 199-202.

Ebeling, C.W., Okal, E.A., Kalligeris, N. & Synolakis, C.E. (2012): Modern seismological reassessment and tsunami simulation of historical Hellenic arc earthquakes. – Tectonophysics **530-531**: 225-239.

Einsele, G. (2000): Sedimentary Basins: Evolution, Facies, and Sediment Budget. – Springer, Berlin, Heidelberg, 792 pp., 2nd Ed.

Elias, N.D. (2010): Pilot Chart 19 1:218 536. Map based on Hydrographic Service of the Hellenic Navy (Greece).

Engel, M., Knipping, M., Brückner, H., Kiderlen, M. & Kraft, J.C. (2009): Reconstructing middle to late Holocene palaeogeographies of the lower Messenian plain (southwestern Peloponnese, Greece): Coastline migration, vegetation history and sea level change. – Palaeogeography, Palaeoclimatology, Palaeoecology **284** (3-4): 257-270.

Engel, M. & Brückner, H. (2011): The identification of Palaeotsunami deposits - a major challenge in coastal sedimentary research. – In: Karius, V., Hadler, H., Deicke, M., Von Eynatten, H., Brückner, H. & Vött, A. (eds.): Dynamische Küsten – Grundlagen, Zusammenhänge und Auswirkungen im Spiegel angewandter Küstenforschung. – Coastline Reports **17**: 65-80.

Erginal, A.E., Kiyak, N.G. & Özcan, H. (2009): Optically Stimulated Luminescence to Date Coastal Dunes and a Possible Tsunami Layer on the Kavak Delta (Saros Gulf, NW Turkey). – Turkish Journal of Earth Sciences **18**: 465-474.

Ernst, J.A. & Matson, M. (1983): Mediterranean tropical storm? – Weather **38**(11): 332-337.

Etienne, S., Buckley, M., Paris, R., Nandasena, A.K., Clark, K., Strotz, L., Chagué-Goff, C., Goff, J. & Richmond, B. (2011): The use of boulders for characterizing past tsunamis: Lessons from the 2004 Indian Ocean and 2009 South Pacific tsunamis. – Earth-Science Reviews **107**: 76-90.

Faegri, K., Kaland, P.E., Krzywinski, K. & Iversen, J. (1989): Textbook of Pollen analysis. – Chichester, 328 pp.

Fairbanks, R.G. (1989): A 17,000-year glacio-eustatic sea level record: influence of glacial melting rates on the Younger Dryas event and deep-ocean circulation. – Nature **342**: 637-642.

Fant, J.E. & Loy, W.G. (1972): Survey and Mapping. – In: Mc Donald, W.A. & Rapp, R. Jr. (eds.): The Minnessota Messenia Expedition. – University of Minnesota Press, Mineapolis: 18-46.

Feldens, P., Schwarzer, K., Sakuna, D., Szczucinski, W. & Sompongchaiyakul, P. (2012): Sediment distribution on the inner continental shelf off Khao Lak (Thailand) after the 2004 Indian Ocean tsunami. – Earth Planets Space **64**: 875-887.

Ferentinos, G. (1992): Recent gravitative mass movements in a highly tectonically active arc system: The Hellenic Arc. – Marine Geology **104**: 93-107.

Fiorini, F. (2004): Benthic foraminiferal associations from Upper Quaternary deposits of south-eastern Po Plain, Italy. – Micropaleontolgy **50** (1): 45-58.

Floth, U., Vött, A., May, S.M., Brückner, H. & Brockmüller, S. (2009): Geo-scientific evidence versus computer models of tsunami landfalls in the Lefkada coastal zone (NW Greece). – Marburger Geographische Schriften **145**: 140-156.

Fokaefs, A., Gerassimos, A. & Papadopoulos, A. (2007): Tsunami hazard in the Eastern Mediterranean: strong earthquakes and tsunamis in Cyprus and the Levantine Sea. – Natural Hazards **40**: 503-526.

Friedrich , W.L., Kromer, B. Friedrich, M., Heinemeier, J., Pfeiffer, T. & Talamo, S. (2006): Santorini Eruption Radiocarbon Dated to 1627-1600 B.C. – Science **312**: 548.

Friedrich, W.L. (2013): The Minoan Eruption of Santorini around 1613 B.C. and its consequences. – In: Meller, H., Bertemes, F., Bork, H.R. & Risch, R. (eds): 1600 – Kultureller Umbruch im Schatten des Thera-Ausbruchs? – Tagungen des Landesmuseums für Vorgeschichte Halle **9**: 37-48

Gelfenbaum, G. & Jaffe, B.E. (2003): Erosion and sedimentation from the 17 July, 1998 Papua New Guinea Tsunami. – Pure and Applied Geophysics **160**: 1969-1999.

Gianfreda, F., Mastronuzzi, G. & Sanso, P. (2001): Impact of historical tsunamis on a sandy coastal barrier: an example from the northern Gargano coast, southern Italy. – Natural Hazards and Earth System Sciences **1:** 213-219.

Goff, J., Chagué-Goff, C. & Nichol, S. (2001): Palaeotsunami deposits: a New Zealand perspective. – Sedimentary Geology **143**: 1-6.

Goff, J., Lane, E. & Arnold, J. (2009): The tsunami geomorphology of coastal dunes. – Natural Hazards and Earth System Sciences **9**(3): 847-854.

Goff, J., Pearce, S., Nichol, S.L., Chagué-Goff, C., Horrocks, M. & Strotz, L. (2010): Multi-proxy records of regionally-sourced tsunamis, New Zealand. – Geomorphology **118**: 369-382.

Goff, J., Chagué-Goff, C., Nichol, S., Jaffe, B. & Dominey-Howes, D.T.M. (2012): Progress in palaeotsunami research. – Sedimentary Geology **243-244**: 70-88.

Goodman-Tchernov, B.N., Dey, H.W., Reinhardt, E.G., McCoy, F. & Mart, Y. (2009): Tsunami waves generated by the Santorini eruption reached Eastern Mediterranean shores. – Geology **37**(10): 943-946.

Gornitz, V. (2005): Natural Hazards. – In: Schwartz, M.L. (eds.), Encyclopedia of Coastal Science. Springer, Dordrecht: 678-684.

Goto, K., Chavanich, S.A., Imamura, F., Kunthasap, P., Matsui, T., Minoura, K., Sugawara, D. & Yanagisawa, H. (2007): Distribution, origin and transport process of boulders deposited by the 2004 Indian Ocean tsunami at Pakarang Cape, Thailand. – Sedimentary Geology **202** (4): 821-837.

Goto, K., Okada, K. & Imamura, F. (2010a): Numerical analysis of boulder transport by the 2004 Indian Ocean tsunami at Pakarang Cape, Thailand. – Marine Geology **268**(1-4): 97-105.

Goto, K, Kawana, T & Imamura, F. (2010b): Historical and geological evidence of boulders deposited by tsunamis, southern Ryukyu Islands, Japan. – Earth Science Reviews **102**: 77-99.

Goto, K., Chagué-Goff, C., Fujino, S., Goff, J., Jaffe, B., Nishimura, Y., Richmond, B., Sugawara, D., Szczuciński, W., Tappin, D.R., Witter, R.C. & Yulianto, E. (2011): New insights of tsunami hazard from the 2011 Tohoku-oki event. – Marine Geology **290**: 46-50.

Guidoboni, E. & Comastri, A. (1997): The large earthquake of 8 August 1303 in Crete: seismic scenario and tsunami in the Mediterranean area. – Journal of Seismology **1**: 55-72.

Guidoboni, E. & Ebel, J.E. (2009): Earthquakes and tsunami in the past. A guide to techniques in historical seismology. – Cambridge, 602 pp.

Gupta, B.K.S. (eds.) (2002): Modern foraminifera. – Kluwer Academic Publisher, Dordrecht, 371 pp.

Hadler, H., Vött, A., Brückner, H., Bareth, G., Ntageretzis, K., Warnecke, H. & Willershäuser, T. (2011a): The harbour of ancient Krane, Kutavos Bay (Cefalonia, Greece) – an excellent geo-archive for palaeo-tsunami research. – In: Karius, V., Hadler, H., Deicke, M., Von Eynatten, H., Brückner, H. & Vött, A. (eds.): Dynamische Küsten – Grundlagen, Zusammenhänge und Auswirkungen im Spiegel angewandter Küstenforschung. – Coastline Reports **17**: 111-122.

Hadler, H., Vött, A., Koster, B., Mathes-Schmidt, M., Mattern, T., Ntagertzis, K., Reicherter, K., Sakellariou, D. & Willershäuser, T. (2011b): Lechaion, the ancient harbour of Corinth (Peloponnese, Greece) destroyed by tsunamigenic impact. – In: Grützner, C., Pérez-López, R., Fernández Steeger, T., Papanikolaou, I., Reicherter, K., Silva, P.G. & Vött, A. (eds.): Earthquake Geology and Archaeology. Science, Society and Critical Facilities. Proceedings Vol. 2, 2nd INQUA-IGCP 567 International Workshop on Active Tectonics, Earthquake Geology, Archaeology and Engineering, 19.-24.09.2011, Corinth (Greece): 70-73.

Hadler, H., Willershäuser, T., Ntageretzis, K., Henning, P. & Vött, A. (2012): Catalogue entries and non-entries of earthquake and tsunami events in the Ionian Sea and the Gulf of Corinth (eastern Mediterranean, Greece) and their interpretation with regard to palaeotsunami research. – Bremer Beiträge zur Geographie und Raumplanung **44**: 1-15.

Hadler, H., Vött, A., Koster, B., Margret Mathes-Schmidt, Mattern, T., Ntageretzis, K., Reicherter, K. & Willershaeuser, T. (2013): Multiple late-Holocene tsunami landfall in the eastern Gulf of Corinth recorded in the palaeotsunami geo-archive at Lechaion, harbour of ancient Corinth (Peloponnese , Greece). – Zeitschrift für Geomorphologie (DOI: 10.1127/0372-8854/2013/S-00138).

Hecht, S. & Fassbinder, J.W.E. (2006): Der Blick in den Untergrund: Magnetometrie und Geoelektrische Tomographie in der Geoarchäologie. – Geographische Rundschau **58**: 38-45.

Hindson, R.A. & Andrade, C. (1999): Sedimentation and hydrodynamic processes associated with the tsunami generated by the 1755 Lisbon earthquake. – Quaternary International **56**: 27-38.

Hinsbergen D.J.J. van, Meer, D.G. van der, Zachariasse, W.J. & Meulenkamp, J.E. (2006): Deformation of western Greece during Neogene clockwise rotation and collision with Apulia. – International Journal of Earth Sciences **96**: 463-490.

Hollenstein, C., Geiger, A., Kahle, H.G. & Veis, G. (2006): CGPS time-series and trajectories of crustal motion along the West Hellenic Arc. – Geophysical Journal International **164** (1): 182-191.

Hollenstein, C., Müller, M.D., Geiger, A. & Kahle, H.G. (2008): Crustal motion and deformation in Greece from a decade of GPS measurements, 1993-2003. – Tectonophysics **449**: 17-40.

Horton, B.P., Rossi, V. & Hawkes, A.D. (2009): The sedimentary record of the 2005 hurricane season from the Mississippi and Alabama coastlines. – Quaternary International **195**: 15-30.

Hottinger, L., Halicz, E. & Reiss, Z. (1993): Recent Foraminferida from the Gulf of Aqaba, Red Sea. – Ljubiljana.

Institute for Geology and Mineral Exploration (IGME 1980a): Geological Map of Greece, 1:50000. – Koroni-Pylos-Skhiza Sheet. Athens.

Institute for Geology and Mineral Exploration (IGME 1980b): Geological Map of Greece, 1:50000. – Pyrgos Sheet. Athens.

Institute for Geology and Mineral Exploration (IGME 1982a): Geological Map of Greece, 1:50000. – Cefalonia-north & Cefalonia south Sheets. Athens.

Institute for Geology and Mineral Exploration (IGME 1982b): Geological Map of Greece, 1:50000. – Olympia Sheet. Athens.

Jahns, S. (1993): On the Holocene vegetation history of the Argivre Plain (Peloponnese, southern Greece). – Vegetational History Archaeobotany **2**: 187-203.

Jahns, S. (2005): The Holocene history of vegetation and settlement at the coastal site of Lake Voulkaria in Acarnania, western Greece. – Vegetational History Archaeobotany **14**(1): 55-66.

Jankaew, K., Atwater, B.F., Sawai, Y., Choowong, M., Charoentitirat, T., Martin, M.E. & Prendergast, A. (2008): Medieval forewarning of the 2004 Indian Ocean tsunami in Thailand. – Nature **455**: 1228-1231.

Jones, H.L. (1927): Strabo Geography Books 8-9. – Harvard University Press, London.

Kahle, H., Cocard, M., Peter, Y., Geiger, A., Reilinger, R., Barka, A. & Veis, G. (2000): GPS-derived strain rate field with the boundary zones of the Eurasian, African and Arabian Plates. – Journal of Geophysical Research **105** (B10): 23353-23370.

Kearey, P., Brooks, M. & Hill, I. (2006): An Introduction to Geophysical Exploration. – Blackwell, 262 pp., 3rd Ed.

Keating, B.H., Wanink, M. & Helsley, C.E. (2008): Introduction to a tsunami-deposits database. – In: Shiki, T., Tsuji, Y., Yamazaki, T. & Minoura, K. (eds.): Tsunamiites – Features and Implications. – Elsevier, Amsterdam: 359-381.

Kelletat, D. (2005): Neue Beobachtungen zu Paläo-Tsunami im Mittelmeergebiet: Mallorca und Bucht von Alanya, türkische Südküste. – Beck, N. (eds.), Neue Ergebnisse der Meeres- und Küstenforschung. Beiträge der 23. Jahrestagung des Arbeitskreises "Geographie der Meere und Küsten" (AMK), Koblenz, 28–30 April 2005. Schriften des Arbeitskreises Landes- und Volkskunde Koblenz (ALV), 4, 1–14.

Kelletat, D. (2013): Physische Geographie der Meere und Küsten. – Gebrüder Bornträger, Stuttgart, 290 pp., 3rd Ed.

Kelletat, D. & Schellmann, G. (2002): Tsunamis on Cyprus: field evidences and 14C dating results. – Zeitschrift für Geomorphologie N.F. Suppl.-Vol. **137**: 19-34.

Kelletat, D., Scheffers, S.R. & Scheffers, A. (2007): Field signatures of the SE-Asian mega-tsunami along the west coast of Thailand compared to Holocene paleo-tsunami from the Atlantic region. – Pure and Applied Geophysics **164**: 413-431.

Kneisel, C. (2003): Electrical resistivity tomography as a tool for geomorphological investigations – some case studies. – Zeitschrift für Geomorphologie Suppl.-Vol. **132**: 37-49.

Kokinou, E., Papadimitriou, E., Karakostas, V., Kamberis, E. & Vallianatos, F. (2006): The Kefalonia Transform Zone (offshore Western Greece) with special emphasis to its prolongation towards the Ionian Abyssal Plain. – Marine Geophysical Research **27**(4): 241-252.

Kontopoulos, N. & Avramidis, P. (2003): A late Holocene record of environmental changes from the Aliki lagoon, Egion, North Peloponnesus, Greece. – Quaternary International **111**: 75-90.

Kortekaas, S. (2002): Tsunamis, storms and earthquakes: Distinguishing coastal flooding events. – Unbublished PhD thesis, Coventry University.

Kortekaas, S. & Dawson, A.G. (2007): Distinguishing tsunami and storm deposits: An example from Martinhal, SW Portugal. – Sedimentary Geology **200**: 208-221.

Koukouvelas, I., Mpresiakas, A., Sokos, E. & Doutsos, T. (1996): The tectonic setting and earthquake ground hazards of the 1993 Pyrgos earthquake, Peloponnese, Greece. – Journal of the Geological Society **153**: 39-49.

Koutsoubas, D., Dounas, C., Arvanitidis, C., Kornilios, S., Petihakis, G.,Triantafyllou, G. & Eleftheriou, A. (2000): Macrobenthic community structure and disturbance assessment in Gialova Lagoon, Ionian Sea. – ICES Journal of Marine Science **57**: 1472-1480.

Kraft, J.C., Rapp, JR.G. & Aschenbrenner, S.E. (1975): Late Holocene Paleogeography of the Coastal Plain of the Gulf of Messenia, Greece, and its Relationships to Archaeological Settings and Coastal Change. – Geological scociety of America Bulletin **86**: 1191-1208.

Kraft, J.C. & Aschenbrenner, S.E. (1977): Paleogeographic Reconstructions in the Methoni Embayment in Greece. – Journal of Field Archaeology **4**: 19-44.

Kraft, J.C., Rapp, JR.G. & Aschenbrenner, S.E. (1980): Late Holocene Palaeogeographic Reconstructions in the Area of the Bay of Navarino: Sandy Pylos. – Journal of Archaeological Science **7**: 187-210.

Kraft, J.C., Kayan, I. & Aschenbrenner, S.E. (1985): Geological Studies of coastal change applied to Archaeological settings. – In: Rapp, JR.G. & Gifford, J.A. (eds.): Archaeological geology: 57-84. – New Haven, 435 pp.

Kraft, J.C., Rapp, JR.G., Gifford, J.A. & Aschenbrenner, S.E. (2005): Coastal change and archaeological settings in Elis. – Hesperia **45** (1): 1-39.

Lagios, E., Sakkas, V., Papadimitriou, P., Parcharidis, I., Damiata, B.N., Chousianitis K. & Vassilopouiou, S. (2007): Crustal deformation in the central Ionian Islands (Greece): Results from DGPS and DInSAR analyses (1995-2006). – Tectonophysics **444** (1-4): 119-145.

Loeblich, A.R. & Tappan, H.N. (1988): Foraminiferal genera and their classification. – Springer US, New York, 970 pp.

Loke, M.H. & Barker, R. (1996): Rapid least-squares inversion of apparent resistivity pseudosections by a quasi-Newton method. – Blackwell Publishing Ltd. **44**: 131-152.

Louvari, E., Kiratzi, A.A. & Papazachos, B.C. (1999): The Cephalonia Transform Fault and its extension to western Lefkada Island (Greece). – Tectonophysics **308**: 223-236.

Loy, W.D. (1967): The land of Nestor – Apysical Geography of the soutwest Peloponnese. – Foreign field research Program sponsored by the office of naval research **34**: 28-70.

Loy, W.D. & Wright, H.E. Jr. (1972): The physical Setting. In: – Mc Donald, W.A. & Rapp, R. Jr. (eds.): The Minnessota Messenia Expedition. – University of Minnesota Press, Mineapolis: 36-46.

Mamo, B., Strotz, L. & Dominey-Howes, D.T.M. (2009): Tsunami sediments and their foraminiferal assemblages. – Earth-Science Reviews **96** (4): 263-278.

Martorana, R., Fiandaca, G., Casas Ponasti, A. & Cosentino, P.L. (2009): Comparative tests on different multi-electrode arrays using models in near-surface geophysics. – Journal of Geophysics and Engineering **6**(1): 1-20.

Mastronuzzi, G. & Sanso, P. (2000): Boulders transport by catastrophic waves along the Ionian coast of Apulia (southern Italy). – Marine Geology **170**: 93-103.

Mastronuzzi, G. & Sanso, P. (2004): Large Boulder accumulations by extreme waves along the Adriatic coast of southern Apulia (Italy). – Quaternary International **120**: 173-184.

Mastronuzzi, G., Pignatelli, C., Sanso, P. & Selleri, G. (2007): Boulder accumulations produced by the 20th of February, 1743 tsunami along the coast of southeastern Salento (Apulia region, Italy). – Marine Geology **242**: 191-205.

Matsumoto, D., Shimamoto, T., Hirose, T., Gunatilake, J., Wickramasooiya, A., DeLile, J., Young, S., Rathnayake, C., Ranasoorya, J. & Murayama, M. (2010): Thickness and grain-size distribution of the 2004 Indian Ocean tsunami deposits in Periya Kalapuwa Lagoon, eastern Sri Lanka. – Sedimentary Geology **230**: 95-104.

May, S.M., Vött, A., Brückner, H. & Brockmüller, S. (2007): Evidence of tsunamigenic impact on Actio headland near Preveza, NW Greece. – Coastline Reports **9**: 115-125.

May, S. M., Vött, A., Brückner, H., Grapmayer, R., Handl, M. & Wennrich, V. (2012): The Lefkada barrier and beachrock system (NW Greece) - controls on coastal evolution and the significance of extreme events. – Geomorphology **139/140**: 330-347.

Medatlas Group 2004 – The Medatlas Group, Wind and wave atlas of the Mediterranean Sea, Western European Union, WEAO Research Cell, 2004.

Minoura, K., Imamura, F., Kuran, U., Nakamura, T., Papadopoulos, G.A., Takahashi, T. & Yalciner, A.C. (2000): Discovery of Minoan tsunami deposits. – Geology **28** (1): 59-62.

Mitsoudis, D.A., Flouri, E.T., Chrysoulakis, N., Kamarianakis, Y., Okal, E.A. & Synolakis, C.E (2012): Tsunami hazard in the southeast Aegean Sea. – Coastal Engineering **60**: 136-148.

Morhange, C., Marriner, N. & Pirazzoli, P.A. (2006): Evidence of Late-Holocene Tsunami Events in Lebanon. Zeitschrift für Geomorphologie N.F. Suppl.-Vol. **146**: 81-95.

Morton, R.A., Gelfenbaum, G. & Jaffe, B.E. (2007): Physical criteria for distinguishing sandy tsunami and storm deposits using modern examples. – Sedimentary Geology **200**: 184-207.

Morton, R.A., Richmond, B.M., Jaffe, B.E. & Gelfenbaum, G. (2008): Coarse-clast ridge complexes of the Caribbean: A preliminary basis for distinguishing tsunami and storm-wave origins. – Journal of Sedimentary Research **78**(9-10): 624-637.

Mullins, C.E. (1977): Magnetic susceptibility of the soil and its significants in soil science – A review. – Journal of Soil Science **28**: 223-246.

Murray, J.W. (1973): Distribution and ecology of living benthic foraminiferids. – Crane/Russak, New York, 274 pp.

Murray, J.W. (1991): Ecology and palaeoecology of benthic foraminifera. – Longman Scientific & Technical, Harlow, 408 pp.

Murray, J.W. (2006): Ecology and Application of Benthic Foraminifera. – Cambridge University Press, Cambridge, 440 pp.

Nicholls, R.J. & Hoozemanns, M.J. (2005): Global vulnerability analysis. – In: Schwartz, M.L. (eds.): Encyclopedia of Coastal Science. – Springer, Dordrecht: 486-491.

Nomikou, P., Alexandri, M., Lykousis, V., Sakkelariou, D. & Ballas, D. (2011): Swath bathymetry and morphological slope analysis of the Corinth Gulf. – In: Grützner, C., Pérez-Lopez, R., Fernández Steeger, T., Papanikolaou, I., Reicherter, K., Silva, P.G., Vött, A. (eds.): Earthquake Geology and Archaeology: Science, Society and Critical facilities. Proceedings of the 2nd INQUA- IGCP 567 International Workshop on Active Tectonics, Earthquake Geology, Archaeology and Engineering, 19-24 September 2011, Corinth (Greece):155-158. ISBN: 978-960-466-093-3.

Okal, E.A. (2011): Tsunamigenic Earthquakes: Past and Present Milestones. – Pure and Applied Geophysics **168**(6-7): 969-995.

Okal, E.A., Borrero, J.C. & Chagué-Goff, C. (2011): Tsunamigenic predecessors to the 2009 Samoa earthquake. – Earth-Science Reviews **107** (1-2): 128-140.

Pantosti, D., Barbano, M.S., Smedile, A., Martini, P.M.D. & Tigano, G. (2008): Geological evidence of paleotsunamis at Torre degli Inglesi (northeast Sicily). – Geophysical Research Letters **35**: L05311.

Papanikolaou, D., Fountoulides, I. & Metaxas, C. (2007): Active faults, deformation rates and Quaternary paleogeography at Kyparissiakos Gulf (SW Greece) deduced from onshore and offshore data. – Quaternatry International **171-172**: 14-30.

Papatheodorou, G., Geraga, M. & Ferentinos, G. (2005): The Navarino Battle Site, Greece – an Integrated Remote-Sensing Survey and a Rational Management Approach. – The International Journal of Nautical Archaeology **34**: 95-109.

Papazachos, B.C. & Dimitriu, P.P. (1991): Tsunamis In and Near Greece and Their Relation to the Earthquake Focal Mechanisms. – Natural Hazards **4**: 161-170.

Papazachos, B.C. & Papazachou, C. (1997): The earthquakes of Greece. – Thessaloniki, 304 pp.

Pasaric, M., Brizuela, B., Graziani, L., Maramai, A. & Orlic, M. (2012): Historical tsunamis in the Adriatic Sea. – Natural Hazards **61**: 281-316.

Perrisoratis, C. & Conispoliatis, N. (2003): The impacts of sea-level changes during latest Pleistocene and Holocene times on the morphology of the Ionian and Aegean Seas (SE Alpine Europe). – Marine Geology **196**: 145-156.

Petihakis, G., Triantafyllou, G., Koutsoubas, D., Allen, I. & Dounas, C. (1999): Medelling the annual cycles of nutrients and phytoplankton in a Mediterranean lagoon (Gialova, Greece). – Marine Environmental Research **48**: 37-58.

Phantuwongraj, S. & Choowong, M. (2012): Tsunami versus storm deposits from Thailand. – Natural Hazards **63**: 31-50.

Pignatelli, C., Sansò, P. & Mastronuzzi, G. (2009): Evaluation of tsunami flooding using geomorphologic evidence. – Marine Geology **260**: 6-18.

Pilarczyk, J.E., Horton, B.P., Witter, R.C., Vane, C.H., Chagué-Goff, C. & Goff, J. (2012): Sedimentary and foraminiferal evidence of the 2011 Tōhoku-oki tsunami on the Sendai coastal plain, Japan. – Sedimentary Geology **282**: 78-89.

Pillay, T.V.R. (1966): A preliminary survey of the lagoon fisheries of the western Peloponnesus, Greece, September 1964. – Economic survey of the western Peloponnesus, Greece. FAO Fishery Circular **108**, Vol. 3. Agriculture. Rome, FAO, FAO/SF8/GRE. Appendix 3, Part 5: 207-224.

Pirazzoli, P.A., Stiros, S.C., Laborel, J., Laborel-Deguen, F., Arnold, M., Papageorgiou, S. & Morhange, C. (1994): Late-Holocene shoreline changes related to paleoseismic events in the Ionian Islands, Greece. – The Holocene **4** (4): 397-405.

Pirazzoli, P.A., Laborel, J. & Stiros, S.C. (1996): Earthquake clustering in the Eastern Mediterranean during historical times. – Journal of Geophysical Research **101**(3): 6083-6097.

Pirazzoli, P.A., Stiros, S.C., Arnold, M., Laborel, J. & Laborel-Deguen, F. (1999): Late Holocene coseismic vertical displacement and tsunami deposits near Kynos, Golf of Euboea, central Greece. – Physics and Chemistry of the Earth **24**(4): 361–367.

Poppe, G.T. & Goto, Y. (1991): European Seashells. Volume I: Scaphopoda, Caudofoveata, Solenogastra, Gastropoda. – Wiesbaden, 352 pp.

Poppe, G.T. & Goto, Y. (2000): European Seashells. Volume II: Scaphopoda, Bivalvia, Cephalopoda. – Hackenheim, 221 pp.

Poulos, S.E., Lykousis, V., Collins, M.B., Rohling, E.J. & Pattiaratchi, C.B. (1999): Sedimentation processes in a tectonically active environment: the Kerkyra-Kefalonia submarine valley system (NE Ionian Sea). – Marine Geology **160** (1-2): 25-44.

Pytharoulis, I., Craig, G.C. & Ballard, S.P. (2000): The hurricane-like Mediterranean cyclone of Januray 1995. – Meteorol. Appl. **7**: 261-279.

Raphael, C.N. (1973): Late Quaternary Changes in Coastal Elis, Greece. – Geographical Review **6**(1): 73-89.

Reimer, P.J. & McCormac, F.G. (2002): Marine Radiocarbon Reservoir Corrections for the Mediterranean and Aegean Seas. – Radiocarbon **44** (1): 159-166.

Reimer, P.J., Baillie, M.G.L., Bard, E., Bayliss, A., Beck, J.W., Blackwell, P.G., Bronk, Ramsey, C., Buck, C.E., Burr, G.S., Edwards, R.L., Friedrich, M., Grootes, P.M., Guilderson, T.P., Hajdas, I., Heaton, T.J., Hogg, A.G., Hughen, K.A., Kaiser, K.F., Kromer, B., McCormac, F.G., Manning, S.W., Reimer, R.W., Richards, D.A., Southon, J.R., Talamo, S., Turney, C.S.M., van der Plicht, J., Weyhenmeyer, C.E., (2009): IntCal09 and Marine09 radiocarbon age calibration curves, 0-50,000 years cal BP. – Radiocarbon **51**: 1111-1150.

Reineck, H.E. & Singh, I.B. (1980): Depositional Sedimentary Environments. – Springer, Berlin, Heidelberg, New York, 551 pp., 2nd Ed.

Reinhardt, E.G., Goodman, B.N., Boyce, J.I., Lopez, G., van Hengstum, P., Rink, W.J., Mart, Y. & Raban, A. (2006): The tsunami of 13 December A.D. 115 and the destruction of Herod the Great's harbor at Caesarea Maritima, Israel. – Geology **34** (12): 1061-1064.

Reynolds, J.M. (1997): An Introduction to Applied and Environmental Geophysics. – Wiley, Chichester, 778 pp.

Richmond, B.R., Buckley, M., Etienne, S., Chagué-Goff, C., Clark, K., Goff, J., Dominey-Howes, D.T.M. & Strotz, L. (2011): Deposits, flow characteristics, and landscape change resulting from the September 2009 South Pacific tsunami in the Samoan islands. – Earth-Science Reviews **107** (1-2): 38-51.

Röbke, B.R., Schüttrumpf, H., Wöffler, Th., Fischer, P., Hadler, H., Ntageretzis, K., Willershäuser, T. & Vött, A. (2013): Tsunami inundation scenarios for the Gulf of Kyparissia (western Peloponnese, Greece) derived from numerical simulations and geo-scientific field evidence. – Zeitschrift für Geomorphologie (DOI: 10.1127/0372-8854/2013/S-00152).

Rohling, E.J., Jorissen, F.J., Vergnaud Grazzini, C. & Zachariasse, W.J. (1993): Northern Levantine and Adriatic Quaternary planktic foraminifera; Reconstruction of palaeoenvironmental gradients. – Marine Micropaleontology **21**: 191-218.

Rohn, C. & Heiden, J. (2009): Neue Forschungen zur antiken Siedlungstopographie Triphyliens. – In: Matthei, A. & Zimmermann, M. (eds.): Stadtbilder im Hellenismus. – Verlag Antike, Die hellenistische Polis als Lebensform **1**: 348-364.

Rönnfeld, W. (2008): Foraminiferen – Ein Katalog typischer Foraminiferen. – Institut für Geowissenschaften der Universität Tübingen. – Tübingen, 146 pp.

Sachpazi, M., Hirn, A., Clément, C., Haslinger, F., Laigle, M., Kissling, E., Charvis, P., Hello, Y., Lépine, J.C., Sapin, M. & Ansorge, J. (2000): Western Hellenic subduction and Cephalonia Transform: local earthquakes and plate transport and strain. – Tectonophysics **319** (4): 301-319.

Sakkelariou, D., Lykoussis, V. & Rousakis, G. (2011): Holocene seafloor faulting in the Gulf of Corinth: The potential for underwater paleoseismology. – In: Grützner, C., Pérez-Lopez, R., Fernández Steeger, T., Papanikolaou, I., Reicherter, K., Silva, P.G., Vött, A. (eds.): Earthquake Geology and Archaeology: Science, Society and Critical facilities. Proceedings of the 2nd INQUA- IGCP 567 International Workshop on Active Tectonics, Earthquake Geology, Archaeology and Engineering, 19-24 September 2011, Corinth (Greece): 218-221. ISBN: 978-960-466-093-3.

Sakuna, D., Szczucinski, W., Feldens, P., Schwarzer, K. & Khokiattiwong, S. (2012): Sedimentary deposits left by the 2004 Indian Ocean tsunami on the inner continental shelf offshore of Khao Lak, Andaman Sea (Thailand). – Earth Planets and Space **64**: 931-943.

Satake, K. & Atwater, B.F. (2007): Long-Term Perspectives on Giant Earthquakes and Tsunamis at Subduction Zones. – Annual Review of Earth and Planetary Sciences **35**(1): 349-374.

Schäfer, A. (2005): Klastische Sedimente. Fazies und Sequenzstratigraphie. – Spektrum Akademischer Verlag, München, 413 pp.

Scheffers, A. & Kelletat, D. (2003): Sedimentologic and geomorphologic tsunami imprints worldwide – a review. – Earth-Science Reviews **63**: 83-92.

Scheffers, A. & Scheffers, S. (2007): Tsunami deposits on the coastline of west Crete (Greece). – Earth and Planetary Science Letters **259**: 613-624.

Scheffers, A., Kelletat, D., Vött, A., May, S.M. & Scheffers, S. (2008): Late Holocene tsunami traces on the western and southern coastlines of the Peloponnesus (Greece). – Earth and Planetary Science Letters **269** (1-2): 271-279.

Scheffers, A., Engel, M., May, S.M., Scheffers, S., Joannes-Bau, R., Hänssler, E., Kennedy, K., Kelletat, D., Brückner, H., Vött, A., Schellmann, G., Schäbitz, F., Radtke, U., Sommer, B., Willershäuser, T. & Felis, T. (2013): Potential and limits of combining studies of coarse- and fine-grained sediments for the coastal event history of a Caibbean carbonate environment. – The Geological Society of London (DOI: 10.1144/SP388.4).

Scheinost, A.C. & Schwertmann, U. (1999): Color Identification of Iron Oxides and Hydroxysulfates: Use and Limitations. – Soil Science Societey of America Journal **63**(5): 1463-1471.

Schielein, P., Zschau, J., Woith, H. & Schellmann, G. (2007): Tsunamigefährdung im Mittelmeer - Eine Analyse geomorphologischer und historischer Zeugnisse. – Bamberger Geographische Schriften **22**: 153-199.

Schrott, L. & Sass, O. (2008): Application of field geophysics in geomorphology: Advances and limitations exemplified by case studies. – Geomorphology **93**(1-2): 55-73.

Scicchitano, G., Monaco, C. & Tortorici, L. (2007): Large boulder deposits by tsunami waves along the Ionian coast of south-eastern Sicily (Italy). – Marine Geology **238**(1-4): 75-91.

Seyfarth, W (1971): Ammianus Marcellinus. Römische Geschichte. Vierter Teil. Buch 26-31. Darmstadt.

Shaw, B., Ambraseys, N.N., England, P.C., Floyd, M.A., Gorman, G.J., Higham, T.F.G., Jackson, J.A., Nocquet, J.M., Pain, C.C. & Piggott, M.D. (2008): Eastern Mediterranean tectonics and tsunami hazard inferred from the AD 365 earthquake. – Nature Geoscience **1** (4): 268-276.

Shaw, B & Jackson, J. (2010): Earthquake mechanisms and active tectonics of the Hellenic subduction zone. – Geophysical Journal International **181**: 966-984.

Shiki, T., Minoura, K., Tsuji, Y. & Yamazaki, T. (2008): Introduction: Why a book on tsunamites. – In: Shiki, T., Tsuji, Y., Yamazaki, T. & Minoura, K. (eds.): Tsunamites – Features and Implications. – Elsevier, Amsterdam: 1-4.

Smedile, A., De Martini, P. M., Pantosti, D., Bellucci, L.G., Del Carlo, P., Gasperini, L., Pirrotta, C., Polonia, A. & Boschi, E. (2011): Possible tsunami signatures from an integrated study in the Augusta Bay offshore (Eastern Sicily-Italy). – Marine Geology **281**: 1-13.

Smid, T.C. (1970): Tsunamis in Greek Literature. – Greece and Rome, Second Series **17** (1): 100-104.

Soloviev, S.L. (1990): Tsunamigenic Zones in the Mediterranean Sea. – Natural Hazards **3**: 183-202.

Soloviev, S.L., Solovieva, O.N., Go, C.N., Kim, K.S. & Shchetnikol, N.A. (2000): Tsunamis in the Mediterranean Sea 2000 BC – 2000 AD. – Dordrecht, 237 pp.

Soukissian, T., Prospathopoulos, A., Hatzinaki, M. & Kabouridou, M. (2008): Assessment of the Wind and Wave Climate of the Hellenic Seas Using 10-Year Hindcast Results. – The Open Ocean Engineering Journal 2008 **1**: 1-12.

Srinivasalu, S., Thangadurai, N., Switzer, A.D., Mohan, V.R. & Ayyamperumal, T. (2007): Erosion and sedimentation in Kalpakkam (N Tamil Nadu, India) from the 26th December 2004 tsunami. – Marine Geology **240**: 65-75.

Srisutam, C. & Wagner, J.F. (2010): Tsunami Sediment Characteristics at the Thai Andaman Coast. – Pure and Applied Geophysics **167**: 215-232.

Stanley, J.-D. & Bernasconi, M.P. (2006): Holocene Depositional Patterns and Evolution in Alexandria's Eastern Harbor, Egypt. – Journal of Coastal Research **22**(2): 283-297.

Stefanakis, M.I. (2006): Natural Catastrophes in the Greek and Roman World: Loss or Gain? Four Cases of Seaquake-Generated Tsunamis. – Mediterranean Archaeology and Archaeometry **6**(1): 61-88.

Stiros, S.C., Pirazzoli, P.A., Laborel, J. & Laborel-Deguen, F. (1994): The 1953 Earthquake in Cephalonia (Western Hellenic Arc): coastal uplift and halotectonic faulting. – Geophysical Journal International **117**: 834-849.

Stiros, S.C. (2010): The 8.5+ magnitude, AD365 earthquake in Crete: Costal uplift, topography changes, archaeological and historical signature. – Quaternary International **216**: 54-63.

Sugawara, D., Goto, K., Imamura, F., Matsumoto, H. & Minoura, K. (2012): Assessing the magnitude of the 869 Jogan tsunami using sedimentary deposits: Prediction and consequence of the 2011 Tohoku-oki tsunami. – Sedimentary Geology **282**: 14-26.

Switzer, A.D., Pucillo, K., Haredy, R.A., Jones, B.G. & Bryant, E.A. (2005): Sea Level, Storm, or Tsunami: Enigmatic Sand Sheet Deposits in a Sheltered Coastal Embayment from Southeastern New South Wales, Australia. – Journal of Coastal Research **21**: 655-663.

Synolakis, C.E. (2008): Europe's Tsunami of Inaction Against Tsunamis. – The Wall Street Journal, November 5th 2008.

Szczuciński, W. (2012): The post-depositional changes of the onshore 2004 tsunami deposits on the Andaman Sea coast of Thailand. – Natural Hazards **60**: 115-133.

Tappin, D.R. (2007): Sedimentary features of tsunami deposits – Their origin, recognition and discrimination: An introduction. – Sedimentary Geology **200**: 151-154.

The United Kingdom Hydrographic Office (UKHO 1992): Greece-West Coast, 1:300 000. Hydrographic Service of the Hellenic Navy (Greece).

Thermo Fischer Scientific (2010): Thermo Scientific Niton Xl3t GOLDD+ XRF Analyzer. – http://www.niton.com/docs/literature/Niton_XL3t_GOLDD_Spec_Sheet.pdf?sfvrsn=2.

Tinti, S. (1991): Assessment of Tsunami Hazard in the Italian Seas. – Natural Hazards **4**: 267-283.

Tinti, S., Maramai, A. & Graziani, L. (2004): The new catalogue of Italian tsunamis. – Natural Hazards **33**: 439-465.

Tinti, S., Manucci, A., Pagnoni, G., Armigliato, A. & Zaniboni, F. (2005): The 30 December 2002 landslide induced tsunamis in Stromboli: sequence of the events reconstructed from eyewitness accounts. – Natural Hazards and Earth System Sciences **5**: 763-775.

Tselentis, G-A, Stavrakakis, G., Sokos, E., Gkika, F. & Serpetsidaki, A. (2010): Tsunami hazard assessment in the Ionian Sea due to potential tsunamogenic sources - results from numerical simulations. – Natural Hazards and Earth System Sciences **10** (5): 1021-1030.

Tuttle, M.P., Ruffman, A., Anderson, T. & Jeter, H. (2004): Distinguishing Tsunami from Storm Deposits in Eastern North America: The 1929 Grand Banks Tsunami versus the 1991 Halloween Storm. – Seismological Research Letters **75**(1): 117-131.

Underhill, J.R. (1989): Late Cenozoic deformation of the Hellenide foreland, western Greece. – Geological Society of America Bulletin 1989 **101**: 613-634.

Vött, A. (2007): Relative sea level changes and regional tectonic evolution of seven coastal areas in NW Greece since the mid-Holocene. – Quaternary Science Reviews **26**: 894-919.

Vött, A., Handl, M. & Brückner, H. (2002): Rekonstruktion holozäner Umweltbedingungen in Akarnanien (Nordwestgriechenland) mittels Diskriminanzanalyse von geochemischen Daten. – Geologica et Palaeontologica **36**: 123-147.

Vött, A., Brückner, H., Handl, M. & Schriever, A. (2006a): Holocene palaeogeographies and the geoarchaeological setting of the Mytikas coastal plain (Akarnania, NW Greece). – Zeitschrift für Geomorphologie N.F. Suppl.-Vol. **142**: 85-108.

Vött, A., Brückner, H., Schriever, A., Luther, J., Handl, M. & Van Der Borg, K. (2006b): Holocene palaeogeographies of the Palairos coastal plain (Akarnania, NW Greece) and their geoarchaeological implications. – Geoarchaeology **21** (7): 649-664.

Vött, A., Brückner, H., Handl, M. & Schriever, A. (2006c): Holocene palaeogeographies of the Astakos coastal plain (Akarnania, NW Greece). – Palaeogeography, Palaeoclimatology, Palaeoecology **239**: 126-146.

Vött, A., May, M., Brückner, H.& Brockmüller, S. (2006d): Sedimentary Evidence of Late Holocene Tsunami Events near Lefkada Island (NW Greece). – Zeitschrift für Geomorphologie N.F. Suppl.-Vol. **146**: 139-172.

Vött, A., Brückner, H., May, M., Lang, F. & Brockmüller, S. (2007a): Late Holocene tsunami imprint at the entrance of the Ambrakian gulf (NW Greece). – Mediterranée **108**: 43-57.

Vött, A., Schriever, A., Handl, M. & Brückner, H. (2007b): Holocene palaeogeographies of the eastern Acheloos River delta and the Lagoon of Etoliko (NW Greece). – Journal of Coastal Research **23**/4: 1042-1066.

Vött, A., Schriever, A., Handl, M. & Brückner, H. (2007c): Holocene palaeogeographies of the central Acheloos River delta (NW Greece) in the vicinity of the ancient seaport Oiniadai. – Geodinamica Acta **20**/4: 241-256.

Vött, A., Brückner, H., May, M., Lang, F., Herd, R. & Brockmüller, S. (2008): Strong tsunami impact on the Bay of Aghios Nikolaos and its environs (NW Greece) during Classical-Hellenistic times. – Quaternary International **181** (1): 105-122.

Vött, A., Brückner, H., Brockmüller, S., Handl, M., May, S.M., Gaki-Papanastassiou, K., Herd, R., Lang, F., Maroukian, H., Nelle, O. & Papanastassiou, D. (2009a): Traces of Holocene tsunamis across the Sound of Lefkada, NW Greece. – Global and Planetary Change **66** (1-2): 112-128.

Vött, A., Brückner, H., May, S.M., Sakellariou, D., Nelle, O., Lang, F., Kapsimalis, V., Jahns, S., Herd, R., Handl, M. & Fountoulis, I. (2009b): The Lake Voulkaria (Akarnania, NW Greece) palaeoenvironmental archive - a sediment trap for multiple tsunami impact since the mid-Holocene. – Zeitschrift für Geomorphologie N.F. **53** (1): 1-37.

Vött, A., Bareth, G., Brückner, H., Curdt, C., Fountoulis, I., Grapmayer, R., Hadler, H., Hoffmeister, D., Klasen, N., Lang, F., Masberg, P., May, S.M., Ntageretzis, K., Sakellariou D. & Willershäuser T. (2010): Beachrock-type calcarenitic tsunamites along the shores of the eastern Ionian Sea (western Greece) - case studies from Akarnania, the Ionian Islands and the western Peloponnese. – Zeitschrift für Geomorphologie N.F. **54** (3): 1-50.

Vött, A., Lang, F., Brückner, H., Gaki-Papanastassiou, K., Maroukian, H., Papanastassiou, D., Giannikos, A., Hadler, H., Handl, M., Ntageretzis, K., Willershäuser, T. & Zander, A. (2011a): Sedimentological and geoarchaeological evidence of multiple tsunamigenic imprint on the Bay of Palairos-Pogonia (Akarnania, NW Greece). – Quaternary International **242** (2011): 213-239.

Vött, A., Bareth, G., Brückner, H., Lang, F., Sakellariou, D., Hadler, H., Ntageretzis, K. & Willershäuser, T. (2011b): Olympia's harbour site Pheia (Elis, western Peloponnese, Greece) destroyed by tsunami impact. – Die Erde **142** 2011 (3): 259-288.

Vött, A., Hadler, H., Willershäuser, T., Ntageretzis, K., Brückner, H., Warnecke, H., Grootes, P.M., Lang, F., Nelle, O. & Sakellariou, D. (2013): Ancient harbours used as tsunami sediment traps – the case study of Krane (Cefalonia Island, Greece). – Byzas (in press).

Wagner, G.A. (1998): Age determination of Young Rocks and Artifacts. – Springer, Berlin, Heidelberg and New York. 411p.

Wang, D.W., Mitchell, D.A., Teague, W.J., Jarosz, E. & Hulbert, M.S. (2005): Extreme waves under Hurricane Ivan. – Science **309**: 896.

Walker, M.J.C. (2005): Quaternary Dating Methods. – Chichester, 286 pp.

Willershäuser, T., Vött, A., Brückner, H., Bareth, G., Hadler, H. & Ntageretzis, K. (2011a). New insights in the Holocene evolution of the Livadi coastal plain, Gulf of Argostoli (Cefalonia, Greece). – In: Karius, V., Hadler, H., Deicke, M., Von Eynatten, H., Brückner, H. & Vött, A. (eds.): Dynamische Küsten – Grundlagen, Zusammenhänge und Auswirkungen im Spiegel angewandter Küstenforschung. – Coastline Reports **17**: 99-110.

Willershäuser, T., Vött, A., Bareth, G., Brückner, H., Hadler, H. & Ntageretzis, K. (2011b): Sedimentary evidence of Holocene tsunami impacts at the Gialova Lagoon (southwestern Peloponnese, Greece). – In: Grützner, C., Pérez-Lopez, R., Fernández Steeger, T., Papanikolaou, I., Reicherter, K., Silva, P.G., Vött, A. (eds.): Earthquake Geology and Archaeology: Science, Society and Critical facilities. Proceedings of the 2nd INQUA- IGCP 567 International Workshop on Active Tectonics, Earthquake Geology, Archaeology and Engineering, 19-24 September 2011, Corinth (Greece): 283-285. ISBN: 978-960-466-093-3.

Willershäuser, T., Vött, A., Hadler, H., Henning, P. & Ntageretzis, K. (2012): Evidence of high-energy impact near Kato Samiko, Gulf of Kyparissia (western Peloponnese), during history. – Bremer Beiträge zur Geographie und Raumplanung **44**: 27-36.

Willershaeuser, T., Vött, A., Brückner, H., Bareth, G., Nelle, O., Nadeau, M.J., Hadler, H. & Ntageretzis, K. (2013): Holocene tsunami landfalls along the shores of the inner Gulf of Argostoli (Cefalonia Island, Greece). – Zeitschrift für Geomorphologie (DOI: 10.1127/0372-8854/2013/S-00149).

Williams, H.F.L. (2009). Stratigraphy, Sedimentology and Microfossil Content of Hurricane Rita Storm Surge Deposits in Southwest Louisiana. – Journal of Coastal Research **25**(4): 1041-1051.

Williams, H. & Hutchinson, I. (2000): Stratigraphic and Microfossil Evidence for Late Holocene Tsunamis at Swantown Marsh, Whidbey Island, Washington. – Quaternary Research **54**: 218-227.

Woodroffe, C. (2003): Coasts: form, processes and evolution. – Cambridge, 623 pp.

Wright, H.R. Jr (1972): Vegetation History. – In: Mc Donald, W.A. & Rapp, R. Jr. (eds.): The Minnessota Messenia Expedition. – University of Minnesota Press, Mineapolis: 188-199.

Yazvenko, S.B. (2008): From Pollen to Plants. – In: Davis, J.L. (ed.): Sandy Pylos: An Archaeological History from Nestor to Navarino. – University of Texas Press, Austin: 14-20.

Zangger, E. (2008): The environmental setting. – In: Davis, J.L. (ed.): Sandy Pylos: An Archaeological History from Nestor to Navarino. – University of Texas Press, Austin: 1-9.

Zangger, E., Timpson, M.E., Sergei, B.Y., Kuhnke, F. & Knauss, J. (1997): The Pylos Regional Archaeological Project: Part II: Landscape Evolution and Site Preservation. – Hesperia **66**(4): 549-641.

Zhu, Y. & Weindorf, D.(2009): Determination of soil calcium using field portable X-ray fluorescence. – Soil Science **174** (3): 151-155.